ANALYTICA CHIMICA ACTA

International monthly devoted to all branches of analytical chemistry
Revue mensuelle internationale consacrée à tous les domaines de la chimie analytique
Internationale Monatsschrift für alle Gebiete der analytischen Chemie

ELSEVIER PUBLISHING COMPANY
AMSTERDAM

Anal. Chim. Acta, Vol. 42, No. 3, 349–556, September 1968
Published monthly
Completing Volume 42

GENERAL INFORMATION

Languages

Papers will be published in English, French or German.

Submission of papers

Papers should be sent to: Prof. PHILIP W. WEST, Coates Chemical Laboratories, College of Chemistry and Physics, Louisiana State University, Baton Rouge 3, La. 70803 (U.S.A.)
or to
Dr. A. M. G. MACDONALD, Department of Chemistry, The University, P.O. Box 363, Birmingham 15 (Great Britain)

Manuscripts

Authors should submit two copies in double-spaced type with adequate margins on pages of uniform size. Acknowledgements, summary and references should be placed at the end of the paper.

Tables should be typed on separate pages and numbered in Roman numerals in the order in which they are mentioned in the text. All Tables should have descriptive titles. The use of chemical formulae and conventional abbreviations is encouraged in Tables and Figures but chemical formulae should not be used in the text unless they are necessary for clarity. Units of weight, volume, etc., when used with numerals should be abbreviated and unpunctuated (*e.g.*, 2%, 2 ml, 2 g, 2 μl, 2 μg, 2 ng, 2 cm, 200 nm).

Figures should be drawn in Indian ink on drawing or tracing paper with all lettering in **thin** pencil. Standard symbols should be used in line drawings; the following are available to the printers:

▼ ▽ ■ □ ● ◎ ■ ◘ ◈ ▣ ▪ + ×

Photographs should be submitted as clear black and white glossy prints. Figures and photographs should be of the same size as the typed pages. Legends for figures should be **typed on a separate page**. Figures should be numbered in Arabic numerals in the order in which they are mentioned in the text.

References should be given at the end of the paper and should be numbered in the order of their appearance in the text (**not** arranged alphabetically). Abbreviations of journal titles should conform to those adopted by the *Chemical Abstracts List of Periodicals*, 1961 Edition and supplements. The recommended form for references to journal papers and books is as follows:

1. J. J. LINGANE AND A. M. HARTLEY, *Anal. Chim. Acta*, 11 (1954) 475.
2. F. FEIGL, *Spot Tests in Organic Analysis*, 7th Ed., Elsevier, Amsterdam, 1966, p. 516.

For multi-author references, **all** authors must be named, and initials given, in the reference list, although the use of, for example, SMITH *et al.*, is desirable in the text.

Summaries are published in English, French and German; authors must always provide a summary in the language of the paper, and are encouraged to supply translations where convenient. No summaries are needed for Short Communications.

Reprints

Fifty reprints will be supplied free of charge. Additional reprints (minimum 100) can be ordered at quoted prices. They must be ordered on order forms which are sent together with the proofs.

Publication

Analytica Chimica Acta has three issues to the volume, and four vols. will appear in 1968. Subscription prices: $ 17.50 or Dfl. 63.— per volume; $70.00 or Dfl. 252.— for 1968, plus postage. Additional cost for copies by airmail available on request. For subscribers in the U.S.A. and Canada, 2nd class postage paid at Jamaica, N.Y. For advertising rates apply to the publishers.

Subscriptions

Subscriptions should be sent to:

ELSEVIER PUBLISHING COMPANY P.O. Box 211, Amsterdam, The Netherlands

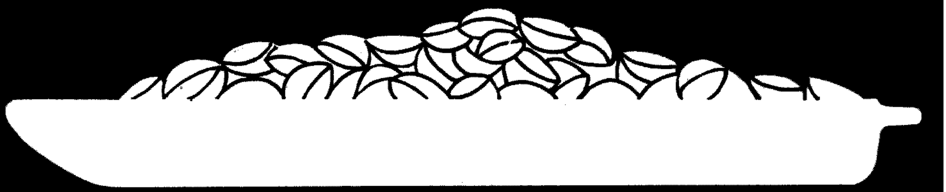

E Merck

SUMMARIES OF PAPERS PUBLISHED IN ANALYTICA CHIMICA ACTA
Vol. 42, No. 3, September 1968

THE ULTRAVIOLET SPECTROPHOTOMETRIC DETERMINATION OF FLUORIDE WITH CERIUM(III)- OR LANTHANUM(III)-ALIZARIN FLUORINE BLUE IN PRESENCE OF DIMETHYLSULFOXIDE

(in French)

A comparative study of the absorption spectra, in the visible and the ultraviolet regions, of the ternary complex cerium(III)–alizarin fluorine blue–fluoride and lanthanum–alizarin fluorine blue–fluoride has been made both in aqueous medium and in media containing 25% dimethylsulfoxide. This solvent very greatly enhances the sensitivity of the reaction in every case; moreover, since it has no important absorption band in the ultraviolet region, it can be used advantageously in exploring the spectra of the above-mentioned fluoride chelates in that region. Determinations of fluorides, with a final spectrophotometric measurement at 625 or 283 nm are described. The interference of 8 ions was studied.

M. HANOCQ AND L. MOLLE,
Anal. Chim. Acta, 42 (1968) 349–356

SECONDARY STANDARDS

PART II. ACETYLACETONATES

The preparation of several acetylacetonates is described, the novel feature being that the organic reagent is added in substoichiometric amount. Several of the compounds are obtainable 99.9% pure or better, and are proposed as secondary standards for the metals they contain or for elementary analysis. These are the copper(II), chromium(III), zinc, cadmium, magnesium, thorium, cobalt(III), iron(II) and calcium compounds. Cobalt(II) and nickel dipyridine acetylacetonates are also proposed. Aluminium and beryllium acetylacetonates are suitable as routine test materials.

R. A. CHALMERS AND M. UMAR,
Anal. Chim. Acta, 42 (1968) 357–364

SIMULTANEOUS DETERMINATION OF TANTALUM AND HAFNIUM IN SILICATES BY NEUTRON ACTIVATION ANALYSIS

A neutron activation procedure suitable for the routine determination of tantalum and hafnium in silicates is described. The irradiated sample is fused with sodium peroxide and leached, and the insoluble hydroxides are dissolved in dilute hydrofluoric acid–hydrochloric acid. After LaF_3 and AgCl scavenges, tantalum and hafnium are separated by anion exchange. Tantalum is obtained radiochemically pure; ^{233}Pa and ^{95}Zr contaminants in the hafnium fraction are resolved by γ-ray spectrometry. The chemical yield of the procedure is determined after counting by re-irradiation. Values for the 8 U.S. Geological Survey standard rocks are reported.

L. P. GREENLAND,
Anal. Chim. Acta, 42 (1968) 365–370

THE DETERMINATION OF IMPURITIES IN ZINC BY NEUTRON ACTIVATION

PART I. THE DETERMINATION OF SILVER AND COBALT IN ZONE-REFINED ZINC

(in French)

A neutron activation method for the determination of cobalt and silver in the microgram range in a matrix of electrolytic zone-refined zinc is described. Silver and cobalt can be separated in a state of high radiochemical purity by means of an anion-exchange resin, silver being eluted by 10 *M* hydrochloric acid and cobalt by 4 *M* hydrochloric acid. The standard deviations are, respectively, 0.1 p.p.m. for silver and 0.01 p.p.m. for cobalt for impurity levels of 1 p.p.m. silver and 0.1 p.p.m. cobalt.

R. Machiroux and F. Mousty,
Anal. Chim. Acta, 42 (1968) 371–378

THE ATOMIC ABSORPTION SPECTROSCOPY OF SELENIUM

Selenium can be determined in aqueous solution by atomic absorption spectroscopy at 1960, 2040, 2063 or 2075 Å; the sensitivities for these lines with a Techtron 10-cm air–acetylene burner are in the ratio of 1:9:60:93. When a Beckman triple-burner (air–hydrogen) and a triple-pass optical system are used, the most sensitive 1960 Å line provides a sensitivity of 0.5 p.p.m. and a detection limit of 1.0 p.p.m. The performance in air–hydrogen and air–acetylene flames is described, and optimum experimental conditions determined. With the Se 1960 Å line and a Techtron 10-cm air–acetylene burner, selenium extracted into methyl isobutyl ketone as its diethyldithiocarbamate complex gives a sensitivity of 0.30 p.p.m., which is a 2.4-fold increase over that found in aqueous solution.

C. L. Chakrabarti,
Anal. Chim. Acta, 42 (1968) 379–387

RAPID DETERMINATION OF DYSPROSIUM IN ROCK SAMPLES BY NEUTRON ACTIVATION ANALYSIS WITH A Ge(Li) DETECTOR AFTER CHEMICAL SEPARATION

A neutron activation method for the rapid determination of dysprosium in rocks, based on simple chemical separation and γ-spectrometry with a lithium-drifted germanium detector, is described. The 94.7-keV photopeak of dysprosium-165 (2.3 h half-life) was measured. Several geochemical standard rocks covering a variety of rock types were analyzed. The detection limit was 0.005 μg of dysprosium. A precision of $\pm 4.7\%$ was obtained on 7 separate analyses of a basalt standard rock. The accuracy of the method is discussed.

K. Tomura, H. Higuchi, N. Onuma and H. Hamaguchi,
Anal. Chim. Acta, 42 (1968) 389–395

THE SIMULTANEOUS DETERMINATION OF VANADIUM, CHROMIUM, MANGANESE, IRON, COBALT, NICKEL, COPPER AND ZINC IN SEA WATER BY X-RAY FLUORESCENCE SPECTROMETRY

A procedure is described for the determination of microgram quantities of the elements vanadium, chromium, manganese, iron, cobalt, nickel, copper and zinc in sea water. Separation and concentration of these elements from a large salt matrix, in order to prevent interferences in the subsequent X-ray fluorescence spectrometry, is achieved by continuous solvent extraction. Ammonium pyrrolidine dithiocarbamate is used as a chelating agent, and the chelated trace elements are quantitatively extracted at a pH of *ca.* 2.5 into methyl isobutyl ketone. Detection limits of 0.14 μg or better are obtained when a 600-sec counting period is used for X-ray fluorescence spectrometry.

A. W. MORRIS,
Anal. Chim. Acta, 42 (1968) 397–406

CATHODE-RAY EXCITED EMISSION SPECTROSCOPIC ANALYSIS FOR TRACE RARE EARTHS

PART II. DETERMINATION OF EUROPIUM

Trace amounts of europium can be determined quantitatively *in situ* by excitation with cathode rays (electrons) and detection of europium transitions. Europium can then be determined from a standard plot of intensity *vs.* concentration. Matrix effects, voltage effects, detection lines, and rare-earth and first-transition-group interferences are discussed. While the detection limit of europium under normal conditions is about 0.1 p.p.m., optimizing the above effects yields an ultimate detection limit, by extrapolation, of about 0.005 p.p.m.

S. LARACH,
Anal. Chim. Acta, 42 (1968) 407–413

SPECTROPHOTOMETRIC DETERMINATION OF YTTRIUM WITH MOLYBDOPHOSPHORIC ACID

A simple sensitive spectrophotometric determination of yttrium, based on the reaction of molybdophosphoric acid with yttrium at pH 4.8, is described. The resulting complex is reduced and the absorbance measured at 695 nm. The method is applicable in the presence of several-fold excesses of lanthanum, cerium, and phosphate.

B. L. MADISON AND J. C. GUYON,
Anal. Chim. Acta, 42 (1968) 415–421

RADIOCHEMICAL PURIFICATION OF MICROGRAM AND SUB-MICROGRAM AMOUNTS OF BERYLLIUM

A method is presented for the separation and radiochemical purification of microgram and tracer amounts of beryllium from solutions. It is a four-stage ion-exchange procedure consisting of (*1*) selective adsorption of the beryllium onto NaDAP resin and its elution with ammonium fluoride, (*2*) adsorption of the fluoroberyllate complex onto an anion-exchange column and elution of the beryllium with hydrochloric acid, (*3*) adsorption and selective elution of the beryllium on a cation-exchange column and (*4*) a pass through an anion-exchange column in concentrated hydrochloric acid. The method is quantitative and requires no carrier. Decontamination factors from most radionuclides tested were greater than 10,000. The method can be used to determine beryllium-10 in environmental materials.

N. R. PIPER,
Anal. Chim. Acta, 42 (1968) 423–429

APPLICATION OF COULOMETRY TO THE STUDY OF COMPLEXES

PART I. INSTRUMENTATION AND APPLICATION TO THE HYDROLYSIS OF BERYLLIUM(II)

(in French)

In order to study complex formation at variable pH values, a constant-current coulometric titration cell is described. The performance of this device was tested by a study of the hydrolysis of beryllium(II).

M. R. PÂRIS AND CL. GREGOIRE,
Anal. Chim. Acta, 42 (1968) 431–437

APPLICATION OF COULOMETRY TO THE STUDY OF COMPLEXES

PART II. COMPLEX FORMATION OF TITANIUM(III) WITH HYDROXIDE OR PICOLINIC ACID

(in French)

The hydrolysis and the complexation of titanium(III) with picolinic acid were studied by coulometric titration of protons. The composition and the stability constants of the species formed are reported.

M. R. PÂRIS AND CL. GREGOIRE,
Anal. Chim. Acta, 42 (1968) 439–444

A POLAROGRAPHIC STUDY OF THE REDOX AND COMPLEX-FORMING REACTIONS OF PENICILLAMINE, N-ACETYLPENICILLAMINE AND COPPER(I) OR (II)

(in French)

Polarographic methods are used to study the redox and complexation reactions between copper(II) or (I) and penicillamine, N-acetylpenicillamine or the oxidation product, dithiobisvaline. The formation of a 1:1 copper(I) complex between penicillamine and copper(I) was proved, and the stability of the complex measured. Copper(II) oxidizes the sulphur compound to the disulphide and the copper(I) formed then forms a complex with the sulphur amino-acid. The greater stability of the non-acetylated copper(I) complex suggests that RSCu(I) contains a chelate ring with participation of the free amino group. The disulphide can only form a complex with copper(II) and the stability of this complex is low. The results suggest that the copper(I) chelate is the form in which copper is eliminated during treatment with penicillamine.

J. J. VALLON AND A. BADINAND,
Anal. Chim. Acta, 42 (1968) 445–454

1-DICARBOXYMETHYLAMINOMETHYL-2-HYDROXY-3-NAPHTHOIC ACID AS A SENSITIVE AND SELECTIVE FLUORIMETRIC REAGENT FOR BERYLLIUM, AND FOR LANTHANUM AND LUTETIUM IN PRESENCE OF THE OTHER LANTHANIDES

1-Dicarboxymethylaminomethyl-2-hydroxy-3-naphthoic acid (DHNA) forms fluorescent complexes with Al, Be, Ga, Hf, In, La, Lu, Mg, Sc, Th, Y and Zr. The Be, La and Lu complexes have a metal : ligand ratio of 1:1. The beryllium complex shows maximal fluorescence at pH 6.8 with excitation-fluorescence maxima at 360 and 450 nm; linear calibration curves are obtained in the range 0.09–1.8 μg Be. In the presence of the calcium–EDTA complex, of 25 cations studied, only $>$100-fold molar ratios of aluminium and $>$10-fold molar ratios of magnesium and scandium caused interference in the determination of 0.1 μmole of beryllium. Amongst 15 anions, $>$ 100-fold molar ratios of phosphate, $>$50-fold molar ratios of arsenate or oxalate and $>$ 10-fold molar ratios of citrate, fluoride and tartrate caused low results. Lanthanum and lutetium can be determined at pH 10 and 370/460 nm in the range 7–28 μg even in the presence of a 3-fold molar ratio of the other lanthanides without interference.

B. Buděšínský and T. S. West,
Anal. Chim. Acta, 42 (1968) 455–465

A POTENTIOMETRIC STUDY OF THE WATER-SOLUBLE SILVER(I) COMPLEXES OF N,N′-BIS(2-HYDROXYETHYL)-DITHIOOXAMIDE

PART III. DETERMINATION OF THE DIFFERENT SPECIES

Silver(I) and N,N′-bis(2-hydroxyethyl)dithiooxamide (H_2X) in acidic solutions, form a series of water-soluble polynuclear complexes. These complexes can be represented by two general formulae: $H_{2q}Ag_pX_q$ and $H_{2q-1}Ag_pX_q$ with $q = 1,2,3$ and $p = q, q-1$.

L. C. van Poucke and M. A. Herman,
Anal. Chim. Acta, 42 (1960) 467–471

STEP-WISE FORMATION OF URANIUM(VI) COMPLEXES WITH SULPHONATED PHENOLIC COMPOUNDS

The metal complexes of uranium(VI) with disodium 2-naphthol-3,6-disulphonate and 7-amino-1-naphthol-3,6-disulphonic acid were studied by the established potentiometric techniques of Bjerrum and Irving and Rossotti. The step-wise protonation constants of the ligands and the step-wise stability constants of the uranyl complexes were determined in 0.1 *M* sodium perchlorate media at 25°.

A. Banerjee and A. K. Dey,
Anal. Chim. Acta, 42 (1968) 473–479

DETERMINATION OF MICROGRAM AMOUNTS OF THE SIX PLATINUM-GROUP METALS IN IRON AND STONY METEORITES

Microgram amounts of the 6 platinum-group metals in 5 stony and 3 iron meteorites were determined spectrophotometrically after perchloric acid decomposition and ion-exchange separation. The accuracy of the determinations of osmium, ruthenium and platinum was improved by the use of more sensitive procedures; arsenazo III was used for the determination of palladium in presence of platinum, rhodium and iridium. The data for platinum-group metals thus obtained are compared with published data obtained by neutron activation and spectrographic methods for the same meteorites or for other meteorites of the same class. With a few exceptions, the agreement between the new data and published data is satisfactory.

J. G. SEN GUPTA,
Anal. Chim. Acta, 42 (1968) 481–488

A COMPARISON OF METHODS FOR THE ANALYSIS OF TIN–SAMARIUM ALLOYS

(in French)

Several methods of analysis for tin–samarium alloys are studied: chemical analysis, X-ray fluorescence and arc spectrography. Their characteristics and the results obtained are compared. The chemical methods are most precise but are insensitive and tedious. X-Ray fluorescence is suitable for routine work and for control of alloy homogeneity. Arc spectrography is by far the most sensitive method. The methods can be applied to alloys of other rare earths with tin.

A. PERCHERON AND M. PINTA,
Anal. Chim. Acta, 42 (1968) 489–502

THE SOLVENT EXTRACTION OF METAL COMPLEXES OF PYRIDINE-2-ALDEHYDE-2′-PYRIDYLHYDRAZONE

The distribution behaviour of the complexes formed between the terdentate ligand, pyridine-2-aldehyde-2′-pyridylhydrazone, and Zn(II), Cd(II), Fe(II), Cu(II), Ni(II), Mn(II) and Pd(II) has been studied between aqueous buffer and chloroform. Results are interpreted in terms of the complexes in the aqueous solution and the loss of a proton from each coordinated ligand to form an uncharged, extractable species. The suitability of PAPHY as a spectrophotometric reagent used in conjunction with a solvent extraction procedure is discussed.

M. A. QUDDUS AND C. F. BELL,
Anal. Chim. Acta, 42 (1968) 504–513

COMPUTER TECHNIQUES FOR THREE-DIMENSIONAL ANALYSIS IN ATOMIC-ABSORPTION FLAME PHOTOMETRY

Flame methods, specifically in atomic-absorption work, have been augmented and enhanced by computer techniques for data reduction and mathematical analysis. Three-dimensional graphic display of experimental results allows for both a realistic and comprehensive approach to atomic-absorption analysis. The computer procedures and the mathematical techniques are described. Their coordination establishes quick, reliable, easily interpreted and useful results. The various equipment used is also described. The use of the remote scope (basically a cathode-ray tube) for immediate on-line display of three-dimensional data representation is explored. Several typical problems and their resulting solutions are presented in detail. Variations of absorbance are studied as a function of analyte concentration and a second variable: height of selection zone, concentration of interferent components, feed rate, slit width, or pressure of combustion gases. Variations of absorbance values are closely related to variations of percentual sensitivity.

J. L. Malakoff, J. Ramírez-Muñoz and W. Z. Scott,
Anal. Chim. Acta, 42 (1968) 515–522

SOME INTERFERENCE EFFECTS OCCURRING IN THE HYDROGEN/ARGON/ENTRAINED-AIR FLAME

An examination was made of the effects of various cations and anions on the determinations of calcium (4227 Å) by flame emission using turbulent hydrogen/argon/entrained-air and hydrogen/oxygen flames. The effects of height of observation and mechanisms of interference are discussed for Cs^+, Rb^+, F^-, Br^-, I^-, NO_3^-, ClO_4^-, SO_4^{2-}, PO_4^{3-}, $P_2O_7^{4-}$, acetate, oxalate, citrate, tartrate and EDTA. Ionization interferences were not detected in the hydrogen/argon/entrained-air flame, but all other types of interference were more serious with this flame than with the hydrogen/oxygen flame. The study also suggests some methods by which the effects of the interferences may be overcome.

R. Smith, C. M. Stafford and J. D. Winefordner,
Anal. Chim. Acta, 42 (1968) 523–531

THE ADSORPTION OF TRACE ELEMENTS IN SEA WATER ON VARIOUS CONTAINER SURFACES

(Short Communication)

D. E. Robertson,
Anal. Chim. Acta, 42 (1968) 533–536

HEATS OF TRANSITIONS AND KINETIC STUDY OF LIQUID CRYSTALS BY DIFFERENTIAL THERMAL ANALYSIS

(Short Communication)

A. V. Santoro and G. I. Spielholtz,

Anal. Chim. Acta, 42 (1968) 537–539

THE ANALYSIS OF CERIUM(IV) PHOSPHATES AND PHOSPHATOSULPHATES

(Short Communication; in German)

K.-H. König, E. Meyn and G. Eckstein,
Anal. Chim. Acta, 42 (1968) 540–542

UV MEASUREMENTS OF HETEROPOLYMOLYBDIC ACIDS

(Short Communication; in French)

M. Jean,
Anal. Chim. Acta, 42 (1968) 543–545

UV MEASUREMENTS OF HETEROPOLYTUNGSTIC ACIDS

(Short Communication; in French)

M. Jean,
Anal. Chim. Acta, 42 (1968) 545–548

ATOMIZATION WITH HEATED AIR FOR SENSITIVITY ENHANCEMENT IN ATOMIC ABSORPTION SPECTROPHOTOMETRY

(Short Communication)

J. P. Riley and D. Taylor,
Anal. Chim. Acta, 42 (1968) 548–549

Analytica Chimica Acta
Elsevier Publishing Company, Amsterdam
Printed in The Netherlands

DOSAGE PAR SPECTROPHOTOMETRIE DANS L'ULTRAVIOLET DE L'ION FLUORURE A L'AIDE DES CHELATES

CERIUM(III)-ALIZARINE COMPLEXON OU LANTHANE(III)-ALIZARINE COMPLEXON, EN PRESENCE DE DIMETHYLSULFOXYDE

M. HANOCQ ET L. MOLLE
Laboratoires de Chimie Analytique et de Chimie Pharmaceutique inorganique, Institut de Pharmacie, Université libre de Bruxelles, Bruxelles (Belgique)

(Reçu le 4 mars, 1968)

Lors d'une étude comparative sur les méthodes de dosage spectrophotométrique de micro-quantités de fluorure, basées sur la formation de complexes avec l'alizarine complexon de cérium(III), de lanthane(III) et de praséodyme(III), BELCHER ET WEST[1] ont montré que le procédé utilisant le réactif au cérium en solution aqueuse à pH 4.3 avec mesure à 610 nm est légèrement plus sensible que celui utilisant le lanthane en solution aqueuse au même pH. Pour des pH supérieurs, la sensibilité de la méthode au lanthane s'accroît, et à pH 5.1 et avec mesure à 620 nm, elle est de 4% supérieure à la première. Ces chercheurs[1], de même que RILEY ET GREENHALGH[2] démontrent aussi qu'on peut augmenter la sensibilité des deux réactifs en opérant à pH 4.3 en présence de 25% d'acétone et en effectuant la mesure à 610 nm environ. En outre, se basant sur la constatation que les spectres des chélates du cérium(III) et du lanthane(III) présentent à 281 nm une bande d'absorption beaucoup plus intense que celle située dans le visible à 610 nm, et après avoir établi des courbes d'étalonnage des chélates formés à cette longueur d'onde, BELCHER ET WEST en concluent que la méthode à base de réactif au lanthane, réalisée *en milieu aqueux* à pH 5.2 avec mesure à 281 nm est deux fois plus sensible que celle utilisant le réactif au cérium, réalisée en milieu aqueux à pH 4.3 avec mesure à 610 nm.

Au cours d'un précédent article[3], nous avons démontré que la sensibilité de la méthode basée sur la formation du complexe cérium(III)–alizarine complexon–fluorure est exaltée au maximum en présence de 25% de diméthylsulfoxyde, le plus polaire de tous les solvants aprotiques, et en opérant à pH 4.1; dans ces conditions, la vitesse de la réaction est aussi nettement accrue. L'étude spectrale des chélates binaire cérium(III)–alizarine complexon et ternaire cérium(III)–alizarine complexon–fluorure, réalisée en explorant le spectre dans le visible de 375 à 780 nm, indique que la longueur d'onde la plus favorable à la mesure de la densité optique est de 625 nm. En opérant de cette manière, il est possible de doser des quantités d'ions fluorures variant de 1 à 25 µg.

Le but de ce présent travail est d'étudier les spectres d'absorption dans l'ultraviolet des complexes cérium(III)–alizarine complexon–fluorure et lanthane(III)–alizarine complexon–fluorure, réalisés soit en milieu aqueux pur, soit en présence de 25% de diméthysulfoxyde afin d'examiner les possibilités d'accroître encore la sensibilité des méthodes décrites précédemment par BELCHER *et al.* et par nous-mêmes.

PARTIE EXPÉRIMENTALE

Appareillage

Spectrophotomètre Cary 15, avec cellule de quartz de 1 cm*.
Spectrophotomètre Zeiss M 4 Q, avec cellule de quartz de 1 cm.
Spectrophotomètre Unicam SP 500, avec cellule de quartz de 1 cm.

Réactifs

Solutions tampons de pH 3.5 et de pH 4.3. Voir l'article précédent[3].

Solution tampon de pH 5.0–5.2[1]. Dissoudre 50 g d'acétate de sodium trihydraté (Merck P.A.) dans environ 400 ml d'eau bidistillée; ajouter ensuite 5.5 ml d'acide acétique cristallisable 99–100% (Merck P.A.) et compléter à 500 ml à l'aide d'eau bidistillée.

Solutions étalonnées d'ions fluorures[3]. A l'aide d'une solution-mère, préparer les solutions dont 1 ml = 10 μg ou 1 μg de F^-.

Solution[3] *d'alizarine complexon (AC) 10^{-3} M.* On prépare une solution d'alizarine complexon (AC) $5 \cdot 10^{-4}$ *M* par dilution de la solution précédente à l'aide d'eau bidistillée.

Solutions de nitrate de cérium(III) 10^{-3} M et de nitrate de lanthane 10^{-3} M et $5 \cdot 10^{-4}$ M. A préparer par dilution de solutions 0.02 *M*, dont le titre exact aura été préalablement déterminé au moyen d'une solution 0.05 *M* d'éthylènediamine tétracétate disodique, en présence de xylénol-orange comme indicateur.

Mode opératoire

Dans un ballon jaugé de 50 ml, on introduit une quantité déterminée de solution contenant de 1 à 25 μg d'ions fluorures. On ajoute alors successivement et en agitant après addition de chaque réactif, 2 ml de la solution tampon à pH 3.5, 5 ml de la solution de nitrate de cérium(III) 10^{-3} *M* ou de nitrate de lanthane(III) 10^{-3} *M*, 25 ml de la solution aqueuse à 50% de diméthylsulfoxyde[3], 5 ml de la solution d'alizarine complexon 10^{-3} *M* et enfin, on complète à 50 ml au moyen d'eau bidistillée. Après 10 min, on mesure l'absorption à 625 nm ou à 283 nm dans une cuvette de quartz de 1 cm d'épaisseur, par comparaison avec une solution contenant les mêmes quantités de réactifs, mais exempte de fluorure.

RÉSULTATS ET DISCUSSION

Etudes spectrales dans le visible et dans l'ultraviolet

Le mécanisme de la réaction entre le fluorure, l'alizarine complexon et le cérium(III) ou le lanthane(III) proposé par LEONARD ET WEST[4] permet de prévoir une absorption importante du complexe ternaire dans la région ultraviolette du spectre. Il en est d'ailleurs bien ainsi comme l'ont démontré BELCHER ET WEST[1] en publiant par la suite une méthode de dosage des ions fluorures *en milieu aqueux* à pH 5.2 et mesure à 281 nm. Cependant, pour pouvoir exploiter plus à fond cette propriété, il y aurait encore intérêt à opérer en présence de solvants renforçant par

---

* Nous adressons nos vifs remerciements à notre collègue, Monsieur le Professeur JEAN BRACHET, d'avoir bien voulu mettre cet appareil à notre disposition.

eux-mêmes la sensibilité de la réaction; pour ce faire, il est indispensable que ces derniers ne présentent pas une absorption trop forte dans la région ultraviolette du spectre, cas présenté précisément par l'acétone (Fig. 1). C'est ce qui explique vraisemblablement pourquoi, malgré un accroissement de sensibilité provoqué par la présence de ce solvant, BELCHER ET WEST[1] ne l'utilisent pas dans leur méthode spectrophotométrique à 281 nm. Par contre, comme le montre nettement le tracé B de la Fig. 1, tel n'est pas le cas du diméthylsulfoxyde dont la bande d'absorption n'apparaît qu'à des longueurs d'onde très inférieures. Ce solvant qui, comme nous l'avons prouvé antérieurement[3], exalte au maximum la sensibilité de la réaction, sera donc aussi avantageusement utilisé pour effectuer les mesures dans la région ultraviolette du spectre.

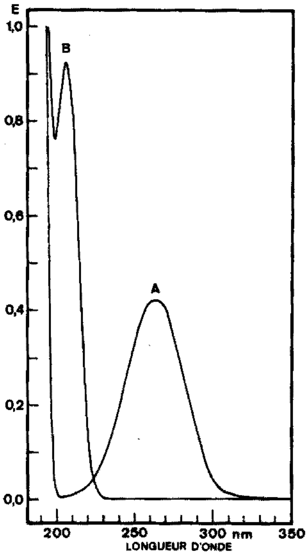

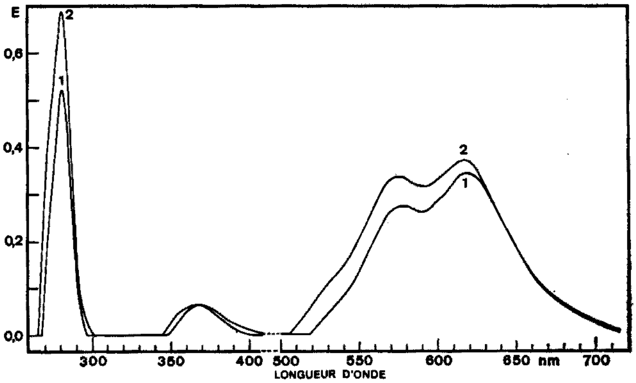

Fig. 1. Spectres d'absorption. (A) Solution aqueuse à 0.2% (v/v) d'acétone; (B) solution aqueuse à 0.005% (v/v) de diméthylsulfoxyde.

Fig. 2. Spectres d'absorption des chélates ternaires réalisés en présence de diméthylsulfoxyde (pH réel=4.1; 20 μg F⁻). (1) Complexe Ce(III)–AC–F⁻; (2) complexe La(III)–AC–F⁻.

En suivant le mode opératoire décrit, et notamment l'utilisation de réactifs 10^{-3} *M* à base soit de cérium(III), soit de lanthane(III) en présence de 25% (v/v) de diméthylsulfoxyde, et en explorant ensuite le spectre de 240 à 750 nm, on obtient les tracés de la Fig. 2 qui montrent deux maxima d'absorption principaux, l'un situé à 283 nm et l'autre à 625 nm. Sans préjuger des résultats qu'on obtiendrait à des pH différents en ce qui concerne le lanthane(III), on peut ainsi constater que la méthode au lanthane est légèrement plus sensible (environ 6%) que celle au cérium(III) dans la région visible mais qu'elle est très nettement plus sensible (environ 34%) dans la région ultraviolette.

Nous avons également tenté de tracer le spectre d'absorption dans l'ultraviolet du complexe ternaire lanthane(III)–alizarine complexon–fluorure, réalisé en opérant en présence de 25% d'acétone et à pH réel de 4.7. Comme le laissait prévoir le comportement de ce solvant dans cette région spectrale, ce tracé est inutilisable en raison de l'intense absorption de l'acétone entre 200 et 300 nm.

Signalons enfin que, dans la méthode que nous préconisons, le maximum d'absorption situé à 283 nm peut être décelé à l'aide du spectrophotomètre Cary 15, mais non en utilisant les spectrophotomètres Zeiss M 4 Q et Unicam SP 500.

Comparaison des diverses méthodes

En vue d'un examen comparatif, nous avons rassemblé dans la Fig. 3, le spectre d'absorption du complexe ternaire cérium(III)–alizarine complexon–fluorure réalisé en présence de diméthylsulfoxyde et celui du complexe lanthane(III)–alizarine complexon–fluorure réalisé en milieu aqueux, dans les conditions prescrites par BELCHER ET WEST[1]. En outre, afin de rendre plus comparables encore les deux réactions utilisées, un troisième tracé a été effectué en utilisant la méthode de BELCHER ET WEST, sauf en ce qui concerne la concentration du réactif au lanthane(III) qui a été augmentée à 10^{-3} *M* (au lieu de $5 \cdot 10^{-4}$ *M*), comme la solution de nitrate de cérium(III) utilisée par ailleurs. De la lecture comparative de ces tracés, il ressort que la sensibilité de la réaction est nettement accrue par la présence de diméthylsulfoxyde, aussi bien dans la région visible qu'ultraviolette, cette dernière étant donc particulièrement favorable aux déterminations de faibles quantités d'ions fluorures.

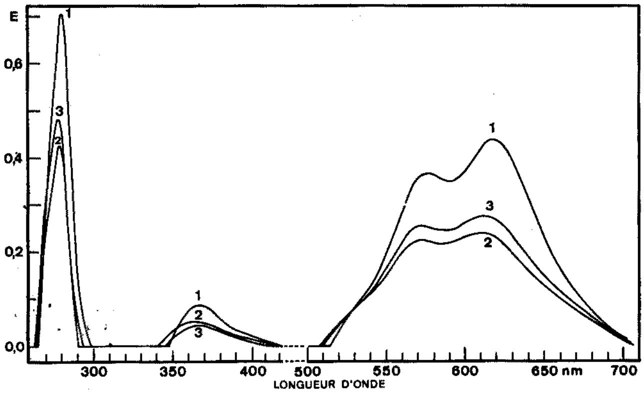

Fig. 3. Etude spectrale des complexes (25 μg F^-). (1) Ce(III)–AC–F^-+25% DMSO (pH réel=4.1); (2) La(III)–AC–F^-: méthode de BELCHER ET WEST (pH réel=5.2); (3) La(III)–AC–F^-: méthode de BELCHER modifiée (pH réel=5.2).

La Fig. 4 rassemble quelques droites d'étalonnage réalisées dans le visible en utilisant soit le réactif au nitrate de cérium(III) 10^{-3} *M*, soit le réactif au nitrate de lanthane(III) 10^{-3} *M*; ces différentes opérations ont été menées aux pH les plus favorables en présence d'eau, d'acétone ou de diméthylsulfoxyde. L'influence éminemment favorable de ce solvant sur la sensibilité de la réaction apparaît clairement, avec un léger avantage pour la méthode à base de nitrate de lanthane(III).

La Fig. 5 permet de comparer les droites d'étalonnage des complexes cérium(III)–alizarine complexon–fluorure et lanthane (III)–alizarine complexon–fluorure en présence de 25% de diméthylsulfoxyde dans la région ultraviolette: la supériorité du réactif à base de lanthane est ainsi nettement démontrée.

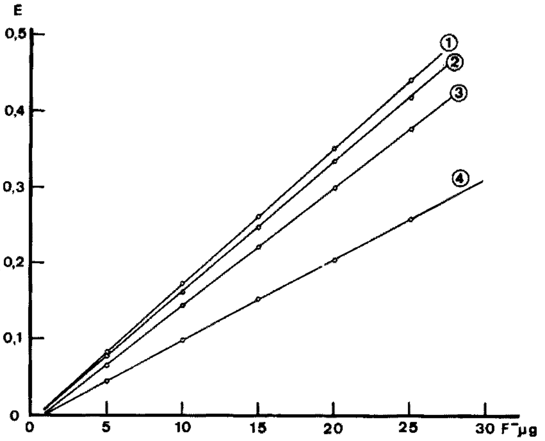

Fig. 4. Courbes d'étalonnage de solutions d'ions fluorures dans la région visible du spectre: (1) La(III)–AC–F^-+25% DMSO (pH réel=4.1); (2) Ce(III)–AC–F^-+25% DMSO (pH réel=4.1); (3) La(III)–AC–F^-+25% acétone (pH réel=4.7); (4) La(III)–AC–F^- (pH réel=5.2).

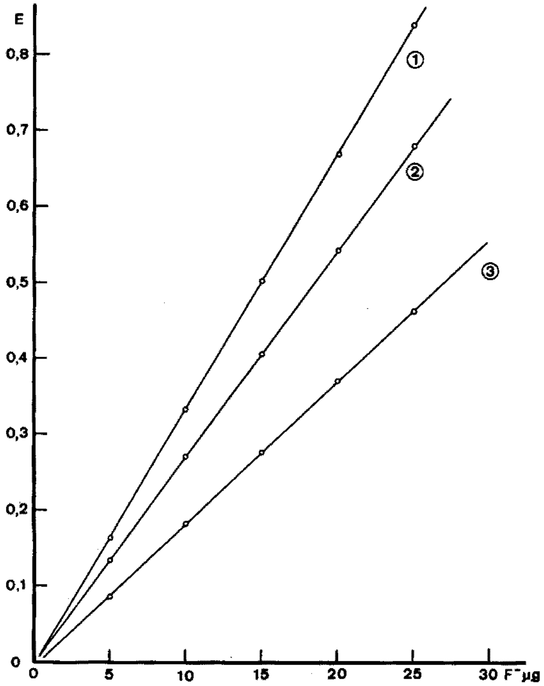

Fig. 5. Courbes d'étalonnage de solutions d'ions fluorures dans la région ultraviolette du spectre: (1) La(III)–AC–F^-+25% DMSO (pH réel=4.1); (2) Ce(III)–AC–F^-+25% DMSO (pH réel=4.1); (3) La(III)–AC–F^- (pH réel=5.2).

Le Tableau I, où sont rassemblés les coefficients d'extinction molaire se rapportant aux diverses méthodes utilisées, permet une comparaison meilleure encore des sensibilités de ces dernières. On peut en conclure que, dans tous les cas, il convient d'opérer en présence de 25% de diméthylsulfoxyde: si les mesures sont

TABLEAU I

COMPARAISON DE LA SENSIBILITÉ DES DIVERSES MÉTHODES

Solvant	*pH final*	*Concentration du réactif (M)*	*Longueur d'onde (nm)*	*ΔE*[a]	*Coefficient d'extinction molaire ($\cdot 10^4$)*
Eau	4.3	Ce 10^{-3}	625	0.0079	0.73
	5.2	La $5 \cdot 10^{-4}$	610	0.0090	0.84
	5.2	La 10^{-3}	610	0.0110	0.98
Eau+acétone 4:1	4.2	Ce 10^{-3}	625	0.0146	1.32
	4.7	La $5 \cdot 10^{-4}$	610	0.0136	1.06
	4.7	La 10^{-3}	610	0.0160	1.44
Eau+DMSO 4:1	4.1	Ce 10^{-3}	625	0.0170	1.54
	4.1	La 10^{-3}	615	0.0183	1.66
Eau	5.2	La $5 \cdot 10^{-4}$	281	0.0166	1.52
	5.2	La 10^{-3}	281	0.0190	1.74
Eau+DMSO 4:1	4.1	Ce 10^{-3}	283	0.0278	2.62
	4.1	La 10^{-3}	281	0.0334	3.19

[a] ΔE = variation de l'extinction qui provoque 1 µg d'ion fluorure.

TABLEAU II

INFLUENCE DE DIVERS IONS SUR LE DOSAGE DES IONS FLUORURES PAR FORMATION DU COMPLEXE Ce(III)–AC–F^- ET MESURES À 625 nm ET 283 nm (pH RÉEL = 4.1)

Ion		*X/F*[a]	*Extinction*		*Interférence (%)*[b]	
Nature	*Quantité ajoutée (mg)*		*625 nm*	*283 nm*	*625 nm*	*283 nm*
—	—	0	0.322	0.545	—	—
Cl^-	30	1500	0.320	0.541	− 0.62	− 0.73
	100	5000	0.313	0.530	− 2.79	− 2.75
SO_4^{2-}	0.5	25	0.320	0.542	− 0.62	− 0.55
	3	150	0.316	0.535	− 1.86	− 1.83
NO_3^-	30	1500	0.321	0.582	− 0.31	+ 6.79
	100	5000	0.312	0.638	− 3.10	+17.06
HCO_3^-	10	500	0.325	0.635	+ 0.93	+16.51
	50	2500	0.347	0.721	+ 7.76	+32.29
	50[c]	2500	0.323	0.554	+ 0.31	+ 1.65
CO_3^{2-}	10	500	0.334	0.652	+ 3.73	+19.63
	50	2500	0.356	0.785	+10.56	+62.38
	50[c]	2500	0.325	0.569	+ 0.93	+ 2.57
Ca^{2+}	5	250	0.318	0.530	− 1.25	− 2.75
	20	1000	0.302	0.475	− 6.21	−12.84
Mg^{2+}	1	50	0.321	0.537	− 0.31	− 1.48
	4	200	0.335	0.469	+ 4.03	−13.94
PO_4^{3-}	0.040	2	0.319	0.540	− 0.93	− 0.91
	0.160	8	0.306	518	− 4.96	− 4.95

[a] X/F représente le rapport entre la quantité d'ions X ajoutés et la quantité d'ions fluorures présents, toutes deux étant exprimées dans les mêmes unités de poids.

[b] L'interférence a été calculée à l'aide de la relation 100 $\Delta E/E_0$ dans laquelle E_0 représente l'extinction correspondant à 20 µg d'ions fluorures et ΔE, la variation d'extinction provoquée par la même quantité d'ions fluorures, additionnée d'ions étrangers.

[c] Echantillon acidifié par HCl 0.1 *N* avant le développement de la coloration.

effectuées dans le visible, il est assez indifférent d'utiliser le réactif au cérium(III) ou au lanthane(III); mais si les mesures sont effectuées dans la région ultraviolette à 283 nm, l'emploi du réactif au nitrate de lanthane(III) s'impose puisqu'il permet un accroissement de sensibilité de 34%.

Influence de divers ions sur les méthodes de dosage proposées

Nous avons envisagé[1] six modes d'interférence par les cations et les anions sur la formation du chélate ternaire. Nous avons étudié ici l'influence de quelques ions en dosant le fluorure suivant la méthode préconisée en effectuant les mesures de la densité optique à 625 nm et à 283 nm. Les solutions à analyser contiennent une quantité constante en ions fluorures (20 μg), à laquelle les cations ont été ajoutés sous forme de chlorures et les anions, sous forme de sels de sodium. Le Tableau II rassemble les résultats de cette étude.

Les anions phosphates gênent d'une manière analogue dans les deux méthodes: en présence d'une quantité 8 fois plus grande en phosphate par rapport au fluorure, l'erreur atteint près de 5% par défaut.

Si, en opérant dans le visible, des concentrations élevées en nitrates apportent des erreurs minimes par défaut, il n'en est pas de même lorsqu'on opère dans l'ultraviolet où les erreurs sont notables et par excès. Ce fait peut s'expliquer par l'importante bande d'absorption présentée par la fonction nitrate vers 270 nm.

Comme nous l'avons déjà noté[3], l'interférence observée aussi bien à 283 nm qu'à 625 nm pour des quantités importantes d'ions hydrogénocarbonates ou carbonates peut être facilement éliminée par acidification préalable des échantillons à analyser à l'aide d'une solution décinormale d'acide chlorhydrique. Soulignons toutefois que cette interférence est plus importante pour les mesures effectuées dans la région ultraviolette du spectre.

Parmi les cations examinés, le calcium et le magnésium provoquent une diminution de l'extinction, notablement plus élevée dans l'ultraviolet que dans le visible.

Après cette étude préliminaire, il semble que la méthode se terminant par une mesure de la densité optique à 625 nm soit, en général, moins sensible aux interférences.

Conclusions

La méthode la plus sensible et la plus spécifique de dosage des ions fluorures est basée sur la formation du complexe lanthane(III)–alizarine complexon–fluorure en présence de 25% de diméthylsulfoxyde, suivie de la mesure de la densité optique à 283 nm. Ce procédé est 0.69 fois plus sensible que celui décrit précédemment par nous utilisant un réactif au cérium(III) et se terminant par une mesure à 625 nm[2]; il est 2.12 fois plus sensible que la méthode décrite originellement par BELCHER ET WEST[1].

RÉSUMÉ

Une étude comparative des spectres d'absorption dans le visible et dans l'ultraviolet des complexes ternaires cérium(III)–alizarine complexon–fluorure et lanthane(III)–alizarine complexon–fluorure, réalisés soit en milieu aqueux pur, soit en présence de 25% de diméthylsulfoxyde a été entreprise. Elle confirme d'abord que ce solvant exalte au maximum la sensibilité de la réaction, dans tous les cas; d'autre part, ne présentant aucune bande d'absorption importante dans l'ultraviolet, celui-ci peut avantageusement être utilisé pour explorer dans cette région les spectres des chélates fluorés ci-dessus. En se basant sur ces constatations, une méthode de dosage des ions fluorures, se terminant par une mesure de la densité optique, soit à 625 nm, soit à 283 nm, a été mise au point. L'interférence éventuelle de 8 ions a été aussi étudiée.

SUMMARY

A comparative study of the absorption spectra, in the visible and the ultraviolet regions, of the ternary complex cerium(III)–alizarin fluorine blue–fluoride and lanthanum–alizarin fluorine blue–fluoride has been made both in aqueous medium and in media containing 25% dimethylsulfoxide. This solvent very greatly enhances the sensitivity of the reaction in every case; moreover, since it has no important absorption band in the ultraviolet region, it can be used advantageously in exploring the spectra of the above-mentioned fluoride chelates in that region. Determinations of fluorides, with a final spectrophotometric measurement at 625 or 283 nm are described. The interference of 8 ions was studied.

ZUSAMMENFASSUNG

Eine vergleichende Untersuchung der Absorptionsspektren der ternären Komplexen von Cer(III)-alizarinfluorinblaufluorid und Lanthan–alizarinfluorinblaufluorid wurde im sichtbaren und im ultravioletten Bereich durchgeführt und zwar sowohl im wässrigen Medium als auch in Medien, die 25% Dimethylsulfoxid enthielten. Dieses Lösungsmittel steigerte in jedem Falle sehr stark die Empfindlichkeit der Reaktion. Darüber hinaus kann es, da es keine wesentliche Absorptionsbande im ultravioletten Bereich besitzt, vorteilhaft bei der Erforschung der Spektren der oben genannten Fluoridchelate verwendet werden. Die Bestimmung von Fluoriden durch spektralphotometrische Messungen bei 625 oder 283 nm wird beschrieben. Der Einfluss von 8 Ionen wurde untersucht.

BIBLIOGRAPHIE

1 R. Belcher et T. S. West, *Talanta*, 8 (1961) 863.
2 J. P. Riley et R. Greenhalgh, *Anal. Chim. Acta*, 25 (1961) 179.
3 M. Hanocq et L. Molle, *Anal. Chim. Acta*, 40 (1968) 13.
4 M. A. Leonard et T. S. West, *J. Chem. Soc.*, (1960) 4477.

Analytica Chimica Acta
Elsevier Publishing Company, Amsterdam
Printed in The Netherlands

SECONDARY STANDARDS

PART II. ACETYLACETONATES

ROBERT A. CHALMERS AND MOHAMMAD UMAR
Chemistry Department, University of Aberdeen, Old Aberdeen (Scotland)

(Received February 24th, 1968)

In the first paper of this series[1] some nickel ammine complexes which could be prepared in 99.9–100.1% purity and used directly as secondary standards, were described. Various other compounds of similar type which were not obtainable in such a high degree of purity, were also reported, and it appeared that it would be unusual to be able to prepare pure co-ordination compounds containing unidentate ligands or mixed ligands. Attention was therefore turned to complexes containing bidentate ligands. Acetylacetone complexes have long been known as readily crystallised compounds, some of which can be sublimed or distilled without decomposition; these were therefore investigated.

A wide range of metal acetylacetonates, prepared commercially, was obtained and analysed for metal content, but the results were very disappointing, many of the products being far from pure. These acetylacetonates were then prepared by the methods recommended in *Inorganic Syntheses* and elsewhere and analysed for metal content. The results were much better, but still not satisfactory for the purpose of providing secondary standards. All the methods of preparation used an excess of acetylacetone, so that the products were probably contaminated with entrained acetylacetone, even after recrystallisation. The preparations were then repeated, but with the metal ion in 5% stoichiometric excess. All the acetylacetone was thus used to form the metal complex, and only the neutral complex species should be soluble in the organic solvents used for purification; the only danger was that mixed ligand neutral species would also be formed, but this was thought to be unlikely, as the ligands to be displaced would almost certainly be water rather than anions. Some of the neutral species were found to be hydrated, with enough water molecules to complete the co-ordination sphere.

The compounds and methods of preparation are described individually, and the analytical results are collected in Tables I and II. The methods of analysis were selected for their reliability and were either gravimetric or titrimetric. The most difficult problem in the analysis was to decompose the samples in such a way as to avoid loss of metal acetylacetonate but to remove the acetylacetone completely so that it could not interfere in the subsequent metal determination. It was found that double evaporation, to near dryness, of a solution of about 0.5 g of the acetylacetonate in 10 ml of 6 *M* hydrochloric acid (3 *M* sulphuric acid for chromium compounds), followed by dissolution in water or dilute acid, fulfilled these conditions.

TABLE I

METAL CONTENT OF ACETYLACETONATES (acac$=C_5H_7O_2$)

Compound	*Metal content (%)*			
	Theory	*Commercial*	*Excess of ligand*	*Excess of metal*
$Mn(acac)_2 \cdot 2H_2O$	18.99	—	18.29–18.36 (6)[a]	18.85–18.89 (7)[a] [18.87][b]
$Mn(acac)_3$	15.59	[labelled $Mn(acac)_2$] 18.41–18.45 (5)[a] 15.22–15.30 (4)[c]	15.68–15.82 (5)	—
$Th(acac)_4$	36.92	36.76–36.78 (4)[a] 36.80 (4)[c]	36.56–35.64 (3)	36.83–36.87 (8) [36.86]
$Co(acac)_3$	16.54	16.03–16.09 (6) 16.39–16.42 (8)[d]	16.28–16.42 (4)	16.48–16.52 (10) [16.50]
$Al(acac)_3$	8.31	8.10–8.13 (3)[d]	8.15–8.27 (4)	8.24–8.32 (11) [8.27]
$Cr(acac)_3$	14.88	14.67 (3)[d]	14.67–14.74 (5)	14.88–14.89 (6) [14.88]
$VO(acac)_2$	19.21	21.14 (4)[f]	19.33–19.37 (4)	—
$V(acac)_3$	14.62	23.35–23.47 (3)[e]	—	—
$MoO_2(acac)_2$	29.42	—	29.72 (4)	—
$Zr(acac)_4 \cdot 10H_2O$	13.65	17.17 (4)		30.08–30.14 (5)
$Zr(acac)_4$	18.70	30.99–31.10 (4)[e]	21.43 (2)	[30.12]
$ZrO(acac)_2$	29.86			
$Be(acac)_2$	4.35	—	—	4.28–4.36 (7) [4.33]
$Cu(acac)_2$	24.27	25.35–25.40 (5) 24.05–24.11 (5)[d]	—	24.20–24.30 (7) [24.24]
$Mg(acac)_2$	10.92	9.45 (3)	—	10.88–10.92 (8)
$Mg(acac)_2 \cdot 2H_2O$	9.42	8.32 (4)[d]		[10.91]
$Fe(acac)_2$	21.98	23.56 (4) 21.67 (3)[d]	—	21.89–21.97 (7) [21.93]
$Fe(acac)_3$	15.81	19.03 (4) 15.55 (4)[e]	—	—
$Ca(acac)_2$	16.81	—	—	16.77–16.80 (8) [16.78]
$Zn(acac)_2$	24.80	28.34 (3) 22.11–22.16 (5)[e]	—	24.77–24.82 (8) [24.80]
$Cd(acac)_2$	36.19	—	—	36.15–36.20 (8) [36.18]
$Ni(acac)_2$	22.85	20.06 (4)	—	—
$Ni(acac)_2 \cdot 2CH_3OH$	18.28	18.22 (4)[d]		

[a] Spread of results; figure in brackets is number of results.
[b] Mean.
[c] Recrystallised from petroleum ether.
[d] Recrystallised from methanol.
[e] Recrystallised from benzene.
[f] Recrystallised from acetone.

The results in Table I show that copper(II), chromium(III), zinc, cadmium and magnesium acetylacetonates can be recommended as secondary standards, and that thorium, cobalt(III), iron(II) and calcium acetylacetonates are almost as good and could certainly be used as test materials for new methods. The compounds listed in Table II appear suitable for use as standards for determination of carbon and hydrogen in organometallic compounds, even though the metal content is not always within 1 part per 1000 of theoretical: this is so because of the greater tolerance allowed on microdeterminations of carbon and hydrogen. These compounds extend the range of acetylacetonates used by GAWARGIOUS AND MACDONALD[2].

TABLE II

CARBON AND HYDROGEN CONTENTS OF ACETYLACETONATES

Compound	*Carbon (%)*		*Hydrogen (%)*	
	Theory	*Found*	*Theory*	*Found*
Cr(acac)$_3$	51.57	51.4	6.05	6.3
Cu(acac)$_2$	45.88	45.7	5.39	5.5
Co(acac)$_3$	50.56	50.9	5.94	6.0
Mn(acac)$_2$·2H$_2$O	41.53	41.5	6.27	6.2
Cd(acac)$_2$	38.66	38.4	4.54	4.7
Ca(acac)$_2$	50.40	50.6	5.92	6.2
Be(acac)$_2$	57.96	57.7	6.80	6.6
Al(acac)$_3$	55.55	55.3	6.52	6.4

Aluminium, beryllium and manganese(II) acetylacetonates were prepared in about 99.5% purity, and in view of the low atomic weight of beryllium and aluminium, the first two could probably be used satisfactorily as test materials. The high value for the zirconium compound could not be accounted for by postulating the presence of hafnium as impurity, and was probably caused by the presence of a small amount of mixed-ligand species. The compound obtained by the modified preparation appeared to be $ZrO(C_5H_7O_2)_2$, whereas that obtained by the use of excess of acetylacetone was of indefinite composition. No evidence was found of the decahydrate $Zr(C_5H_7O_2)_4 \cdot 10H_2O$ reported in the literature[3]. Nickel acetylacetonate crystallises out as the dihydrate, which can be converted into the anhydrous form by heating *in vacuo* at 80°. If the compound is recrystallised from methanol, however, it appears that the water of crystallisation is replaced by methanol (*cf.* HOLM AND COTTON[4]). Similar considerations apply to the cobalt(II) compound. An excess of metal could not be used in the preparation of the vanadium(IV) and molybdenum(VI) compounds.

EXPERIMENTAL

Preparation of acetylacetonates

Thorium acetylacetonate. Dissolve 13.7 g of freshly distilled acetylacetone in 50 ml of water by gentle heating, and add the solution slowly and with stirring to 21.2 g of thorium nitrate hexahydrate dissolved in 200 ml of water. Add concentrated ammonia solution dropwise with stirring until precipitation of thorium acetylacetonate occurs. Filter off the precipitate, wash it with water and dry it in air. Dissolve the dried product in methanol and add 2–3 g of activated charcoal, boil and filter.

Cool the solution and collect the crystals. Recrystallise twice more, and dry the product first in air and then *in vacuo*.

Beryllium acetylacetonate. The procedure is similar to that for thorium, but the quantities are 18.9 g of acetylacetone, and 13.6 g of beryllium carbonate tetrahydrate dissolved in the minimum of 6 M hydrochloric acid necessary and diluted to 100 ml. The charcoal is omitted in the purification.

Aluminium acetylacetonate. Prepare as for the thorium compound, but with 23.3 g of acetylacetone and 36.9 g of aluminium ammonium sulphate dodecahydrate (in 100 ml of water); omit the charcoal.

Chromium(III) acetylacetonate. Dissolve 8.5 g of chromium(III) chloride hexahydrate in 200 ml of water and add 9.1 g of acetylacetone and about 60 g of urea. Heat the solution on a hot-plate for about 4 h to hydrolyse the urea and raise the pH. Filter off the caramel-coloured product on a Buchner funnel, and dry it in air. Recrystallise thrice from methanol (no charcoal), and dry the product first in air and then *in vacuo*.

Cobalt(III) acetylacetonate. Heat 4.3 g of cobalt(II) carbonate and 10.5 g of acetylacetone to 100° in a 125-ml Erlenmeyer flask and slowly add dropwise, with rapid magnetic stirring, 52 ml of 10% hydrogen peroxide solution during 45 min. Chill the intensely green liquid in an ice–salt bath to crystallise out the cobalt(III) acetylacetonate. Wash the crystals with ice-cold water, dry them at 100°, and recrystallise them thrice from methanol. Dry the product in air and then *in vacuo*.

Iron(II) acetylacetonate. Dissolve 11.1 g of ammonium iron(II) sulphate hexahydrate in 100 ml of water and add slowly, with stirring, 6.0 g of acetylacetone dissolved in 10 ml of methanol. Add concentrated ammonia solution dropwise to precipitate the complex. Collect the product, wash it successively with water, small portions of methanol and a small portion of ether, and then dry it at 100° to obtain the anhydrous product. This preparation is different from the others, since it is necessary to use an excess of acetylacetone; attempts to recrystallise the product from organic solvents lead to partial oxidation of the iron, so that an excess of iron(II) cannot be used.

Magnesium acetylacetonate. Dissolve 22.7 g of magnesium sulphate heptahydrate in 100 ml of water and add 100 ml of 16% sodium acetate trihydrate solution. Then add, slowly and with stirring, a solution of 17.6 g of acetylacetone in 30 ml of methanol, followed by concentrated ammonia until the complex is precipitated. Collect and wash the product, dry it in air, and recrystallise it thrice from methanol. Dry the product at 140° to obtain the anhydrous product.

Cadmium acetylacetonate. Prepare as for the magnesium compound, but use 8.8 g of hydrated cadmium sulphate ($3CdSO_4 \cdot 8H_2O$), 6.5 g of acetylacetone and 10% sodium acetate solution. Dry the recrystallised product in air and *in vacuo*.

Calcium acetylacetonate. Proceed as for magnesium, but use 7.0 g of calcium acetate and 8.4 g of acetylacetone, and omit the sodium acetate. Dry the recrystallised product at 100° to obtain the anhydrous complex.

Zinc acetylacetonate. Proceed as for magnesium, but use 22.2 g of zinc sulphate heptahydrate and 14.7 g of acetylacetone. Dry the recrystallised product in air and *in vacuo*. The literature refers to the zinc complex as containing one or two molecules of water of crystallisation (*cf.* GRADDON AND WEEDEN[5]), but the analytical results and a thermogravimetric examination showed that the product obtained as described is anhydrous.

Copper(II) acetylacetonate. Proceed as for magnesium, but use 24.8 g of copper(II) sulphate pentahydrate, 18.9 g of acetylacetone in 40 ml of methanol, and 20% sodium acetate solution. Dry the recrystallised product in air and *in vacuo.*

Manganese(II) acetylacetonate. Proceed as for magnesium, but use 24.8 g of manganese(II) chloride tetrahydrate and 23.9 g of acetylacetone, and avoid exposure of the wet product to air (to prevent aerial oxidation to manganese(III)). The dry product is stable in air. Recrystallise from methanol in an atmosphere of carbon dioxide and dry the light yellow crystals *in vacuo.* The product appears to be the dihydrate $Mn(C_5H_7O_2)_2 \cdot 2H_2O$.

Cobalt and nickel dipyridine acetylacetonates. The difficulty experienced in preparing pure nickel and cobalt acetylacetonates, whether associated with two molecules of water or methanol, led to consideration of other mixed-ligand complexes, in which a more basic second ligand would be used. An obvious choice was pyridine. The compounds with methanol as second ligand were prepared by the method outlined for magnesium acetylacetonate (12 g of nickel chloride hexahydrate and 9.6 g of acetylacetone; 9.4 g of cobalt sulphate heptahydrate and 6.4 g of acetylacetone). The product was suspended in 30 ml of methanol, 60 ml of pyridine were added, and the mixture was warmed until a clear solution was obtained (any insoluble residue was filtered off). The solution was set aside to crystallise. The product (blue for nickel, orange-red for cobalt) was collected and recrystallised twice from pyridine. The nickel compound was dried for 4 h at 90° in an oven, and then *in vacuo* at room temperature. The cobalt compound was dried *in vacuo* at room temperature only, as it showed signs of losing pyridine at temperatures above 60°. Analyses gave 14.17–14.20% Co (8 results, mean 14.19; $Co(acac)_2 \cdot 2py$ requires 14.19%) and 14.10–14.16% Ni (8 results, mean 14.13; $Ni(acac)_2 \cdot 2py$ requires 14.14%). The nitrogen contents were 7.0% for the nickel compound (theory 6.75%) and 6.5% for the cobalt compound (theory 6.75%). These two compounds may therefore be recommended as nickel and cobalt standards and also for use as nitrogen standards for microanalysis of organometallic compounds.

Recrystallisation to obtain anhydrous species

The need to recrystallise to remove water was demonstrated with zinc acetylacetonate. An unrecrystallised specimen contained only 22.48% zinc [theory 24.80 for $Zn(acac)_2$]; one recrystallisation raised the zinc content to 24.49%, and two more raised it to 24.79%.

X-Ray diffraction data

There is comparatively little information in the literature on the X-ray diffraction characteristics of the acetylacetonates, and some of what there is appears to be in conflict. The results obtained with the compounds prepared in this work are reported in Table III. The data for cobalt acetylacetonate dihydrate and copper(II) acetylacetonate agree with those given by HOLM AND COTTON[4] and by SHIBATA[6]. For nickel acetylacetonate dihydrate, the results differ from HOLM AND COTTON's but agree fairly well with SHIBATA's. The data for zinc acetylacetonate are quite different from either SHIBATA's or HOLM AND COTTON's (which do not agree with each other

TABLE III

X-RAY DIFFRACTION DATA

(vvs = very very strong; vs = very strong; s = strong; ms = medium strong; m = medium; mw = medium weak; w = weak; vw = very weak. Lines less intense than very weak are not reported)

d(Å I)	*d(Å I)*	*d(Å I)*	*d(Å I)*
$Th(acac)_4$[a]	$Be(acac)_2$[a]	$Al(acac)_3$[a]	$MoO_2(acac)_2$[a]
10.92 vw	7.76 vw	8.12 vvs	6.24 vvs
8.42 vvs	6.19 vvs	6.97 vvs	5.83 vs
7.97 m	5.79 ms	6.70 vvs	4.11 m
6.81 m	5.28 vw	6.07 w	3.90 vs
5.99 w	5.04 w	5.40 vs	3.51 ms
5.64 vw	4.62 mw	4.98 vw	3.41 vw
4.35 w	4.33 s	4.67 ms	2.84 vw
4.02 mw	3.97 ms	4.35 s	2.67 vw
3.86 w	3.85 ms	4.15 vs	2.63 vw
3.80 w	3.68 vs	3.96 s	2.49 vw
3.51 vw	3.39 w	3.79 vvs	2.46 vw
2.81 w	2.49 vw	3.59 s	2.21 vw
	2.43 vw	3.48 mw	1.95 vw
$ZrO(acac)_2$[a]		3.39 ms	
9.83 vvs	$Mn(acac)_2 \cdot 2H_2O$[a]	3.09 vw	$VO(acac)_2$[a]
7.76 vvs	5.54 vs	2.97 vw	6.81 vvs
7.25 vw	5.47 s	2.51 vw	6.46 vw
7.02 vw	4.90 w	2.44 vw	6.33 vw
5.40 vw	3.59 s	2.23 vw	4.75 vw
4.04 mw	3.48 mw	2.21 vw	4.08 mw
3.83 w	2.73 vw		3.97 vw
3.62 w	2.43 vw	$Mn(acac)_3$[a]	3.53 w
3.52 w	2.41 vw	8.27 vs	3.44 m
2.71 vw	1.86 vw	6.97 ms	3.20 ms
2.26 vw		6.76 m	
2.14 vw	$Ni(acac)_2 \cdot 2CH_3OH$[a]	4.15 w	$Co(acac)_3$[b]
	10.28 vvs	3.83 vw	7.97 vvs
$Co(acac)_2 \cdot 2CH_3OH$[b]	6.61 vs	2.52 vw	7.38 vw
10.47 vvs	6.24 s		6.81 ms
9.72 vw	4.75 w	$Ni(acac)_2 \cdot 2H_2O$[a]	6.51 vvs
5.95 vw	4.19 vw	10.78 vvs	5.37 s
5.40 vvs	3.49 mw	5.47 m	4.86 mw
4.82 vs	3.06 vw	4.93 w	4.51 vw
4.60 s		4.69 vw	4.21 vw
4.15 s	$Fe(acac)_2$[b]	3.88 vw	4.08 ms
3.79 vs	8.19 vs	3.52 ms	3.86 m
3.48 ms	6.92 w	3.45 w	3.69 vs
3.40 s	6.76 vvs	3.09 vw	3.51 m
3.05 ms	6.24 m	2.89 vw	3.30 s
2.96 s	5.22 s	2.44 vw	3.03 w
2.65 ms	4.82 vw		2.44 w
2.56 w	4.33 w	$Mg(acac)_2$[a]	2.33 vw
2.47 w	4.13 s	10.92 vvs	2.15 vw
2.38 mw	4.00 w	6.19 mw	
2.34 mw	3.88 w	5.47 vvs	$Cr(acac)_3$[a]
2.23 mw	3.72 s	4.85 m	8.12 vvs
2.14 vw	3.59 w	4.21 vw	6.96 ms
2.07 w	3.49 m	3.83 ms	6.70 vs
2.02 w	3.12 w	3.53 m	5.40 vw
1.90 mw	2.87 vw	3.45 ms	4.98 vw
1.87 w	2.80 vw	3.07 vw	4.11 vw
1.85 w	2.49 vw	2.70 vw	3.78 mw
	2.23 w	2.40 vw	3.42 vw
	2.15 w	2.37 vw	

TABLE III (continued)

d(Å I)	*d(Å I)*	*d(Å I)*		*d(Å I)*
Cd(acac)$_2$[a]	*Cu(acac)$_2$*[a]	*Zn(acac)$_2$*		*Ni(acac)$_2$·2py*[a]
9.61 vvs	7.90 vvs	10.65[a] vvs		7.90 vvs
8.67 s	7.60 vvs	7.83 w		7.53 vs
6.76 mw	5.75 vs	7.20 mw		6.66 vvs
6.07 vw	5.25 vvs	6.03 w		6.37 s
4.75 mw	4.04 vw	5.50 mw	5.44[b,c] s	5.50 w
4.04 mw	3.62 m	4.90 m	4.85 s	4.82 w
3.97 mw	3.43 m	4.39 m	4.72 m	4.37 mw
3.52 m	3.30 m	4.04 vw	4.35 w	4.21 m
3.45 w	2.96 vw	3.87 vw	3.83 w	4.11 w
3.14 vw	2.86 vw	3.65 m	3.63 ms	3.93 s
3.06 w	2.33 vw	3.53 vs	3.48 vvs	3.83 vw
2.85 w	2.25 vw	3.02 w	3.38 vw	3.80 vw
2.64 vw	2.03 w	2.65 vw	3.35 s	3.49 m
2.34 vw		2.47 vw	2.99 vw	2.47 vw
			2.51 vw	

[a] Phillips PW 1051 X-ray diffractometer, Cu K radiation, Ni filter.
[b] Phillips 1024 powder camera, Co K radiation, Fe filter.
[c] Second preparation.

anyway), and those for manganese(II) acetylacetonate dihydrate differ from those of HOLM AND COTTON. It appears that a thorough investigation of these complexes is urgently required.

Infrared data

Infrared spectra were obtained (Nujol mull, KBr disc window, Perkin-Elmer 225; Nujol mull, NaCl window, Perkin-Elmer 237) and the peaks in the 400–700 cm^{-1} range were compared with those reported in the literature. Agreement was generally satisfactory.

Storage and stability

All the compounds should have a good shelf-life if stored in well-stoppered bottles, though some of the anhydrous compounds (*e.g.* zinc acetylacetonate[7]) may need protection from moist air. The acetylacetonates used by GAWARGIOUS AND MACDONALD[2] had been stored for about 30 years and required only one recrystallisation[8].

DISCUSSION

Acetylacetonates are relatively easy to prepare, and can be obtained in good yield and a fairly high state of purity. Further purification may be achieved by sublimation or by gas chromatography[9] or by zone-refining[10]. The method of preparation used here, with the organic moiety present in substoichiometric amount in the reaction mixture, might be applied with advantage to other preparations of metal chelates. The only drawback to the use of these compounds as standards is that they are insoluble in aqueous media and that their stability constants are sufficiently high to make it necessary to remove the acetylacetone before determining the metal ion or using the compound to check a method. Nevertheless, these compounds provide a useful range of standard materials with reasonably large equivalent weights.

We wish to thank B.D.H. Ltd. for a grant in aid of this work, and the University of Aberdeen for a Research Scholarship awarded to M.U.

SUMMARY

The preparation of several acetylacetonates is described, the novel feature being that the organic reagent is added in substoichiometric amount. Several of the compounds are obtainable 99.9% pure or better, and are proposed as secondary standards for the metals they contain or for elementary analysis. These are the copper(II), chromium(III), zinc, cadmium, magnesium, thorium, cobalt(III), iron(II) and calcium compounds. Cobalt(II) and nickel dipyridine acetylacetonates are also proposed. Aluminium and beryllium acetylacetonates are suitable as routine test materials.

RÉSUMÉ

On décrit une préparation de plusieurs acétylacétonates, avec addition du réactif organique en quantité substoechiométrique. La plupart de ces composés présentent une pureté de 99.9% au moins; ils sont proposés comme étalons pour les métaux ou pour l'analyse élémentaire. Ces métaux sont: cuivre(II), chrome(III), zinc, cadmium, magnésium, thorium, cobalt(III), fer(II) et calcium. Cobalt(II) et nickel dipyridine acétylacétonates sont également proposés. L'aluminium et le béryllium acétylacétonates conviennent à des tests de routine.

ZUSAMMENFASSUNG

Die Darstellung zahlreicher Acetylacetonate wird beschrieben. Das Neue dabei ist, dass das organische Reagenz in substöchiometrischen Mengen zugegeben wird. Zahlreiche Verbindungen werden in 99.9%iger oder besserer Reinheit erhalten und werden als Sekundär-Standards für die darin enthaltenen Metalle oder für die Elementaranalyse vorgeschlagen. Es sind dies Kupfer(II), Chrom(III), Zink, Cadmium, Magnesium, Thorium, Kobalt(III), Eisen(II) und Calcium. Kobalt(II)- und Nickel-Dipyridinacetylacetonat werden ebenfalls empfohlen. Aluminium- und Beryllium-Acetylacetonat sind für Routineuntersuchungen geeignet.

REFERENCES

1 R. A. Chalmers and M. Umar, *Anal. Chim. Acta*, 39 (1967) 521.
2 Y. A. Gawargious and A. M. G. Macdonald, *Anal. Chim. Acta*, 27 (1962) 119.
3 W. Biltz and J. A. Clinch, *Z. Anorg. Allgem. Chem.*, 40 (1904) 218.
4 R. H. Holm and F. A. Cotton, *J. Phys. Chem.*, 65 (1961) 321.
5 D. P. Graddon and D. G. Weeden, *Australian J. Chem.*, 16 (1963) 980.
6 S. Shibata, *Bull. Chem. Soc. Japan*, 30 (1957) 842.
7 G. Rudolph and M. C. Henry, *Inorg. Syn.*, 6 (1967) 74.
8 Y. A. Gawargious and A. M. G. Macdonald, Personal communication.
9 R. Belcher, *Proc. Soc. Anal. Chem.*, 5 (1968) 4.
10 H. Kaneko, H. Kobayashi and K. Ueno, *Talanta*, 14 (1967) 1403.

Analytica Chimica Acta
Elsevier Publishing Company, Amsterdam
Printed in The Netherlands

SIMULTANEOUS DETERMINATION OF TANTALUM AND HAFNIUM IN SILICATES BY NEUTRON ACTIVATION ANALYSIS*

L. PAUL GREENLAND
U.S. Geological Survey, Washington, D.C., 20242 (U.S.A.)

(Received January 31st, 1968)

Tantalum and hafnium are of great geochemical interest in that they represent parts of the chemically coherent pairs: niobium–tantalum and zirconium–hafnium. Although niobium and zirconium can be determined readily by emission spectrography, there has been a need for a simple and accurate method for the determination of tantalum and hafnium. This report describes a procedure for simultaneous determination of tantalum and hafnium for application to geochemical studies of silicate rocks and minerals.

Neutron activation followed by radiochemical separations has been applied to the determination of tantalum[1–3] and hafnium[4–6] in silicates. These procedures require repeated precipitations and solvent extractions which are tedious and time-consuming and hence not suitable for the analysis of large numbers of samples. KIM AND MEINKE[7] have described a rapid method for the determination of tantalum by neutron activation but the sensitivity of their method is inadequate for most silicates. Tantalum and hafnium were not determined simultaneously in these studies.

TABLE I

NUCLEAR DATA FOR THE DETERMINATION OF TANTALUM AND HAFNIUM

	Hf	*Ta*
Atomic number	72	73
Reaction	^{180}Hf (n,γ)^{181}Hf	^{181}Ta (n,γ)^{182}Ta
Parent isotope abundance (%)	35.2	99.99
Thermal neutron cross section (barns)	10	21
Half-life of product (days)	43	115
γ-Energies measured (MeV)	0.48	composite: 1.12, 1.19 1.22, 1.23; and composite: 0.067, 0.100

Data relevant to the determination of tantalum and hafnium by neutron activation are summarized in Table I. Interferences from competing (n,p) and (n,α) reactions on other elements have been considered previously (see references above) and have been shown to be completely negligible for ordinary silicate rocks and minerals. Possible errors from self-shielding in the flux monitors have been avoided by using only microgram amounts of tantalum and hafnium as monitors.

---

*Publication authorized by the Director, U.S. Geological Survey.

The data reported by NELSON *et al.*[8] suggest that tantalum and hafnium can be readily separated from each other and most other elements by anion exchange in hydrofluoric–hydrochloric acid media. The concurrent operation of many ion-exchange columns simplifies procedures and makes possible relatively fast routine analyses; hence an anion-exchange process was used to provide radiochemical purification of tantalum and hafnium after neutron irradiation. The use of hydrofluoric acid media is also advantageous in preventing the well-known problem of hydrolysis of tantalum and hafnium solutions.

EXPERIMENTAL

Counting apparatus

A 2 × 2-in NaI (Tl) detector coupled to a single-channel analyzer was used for counting ^{182}Ta. A similar detector coupled to a 200-channel analyzer was used for counting ^{181}Hf.

Anion-exchange columns

The ion-exchange columns used were cut from a cylinder of Teflon. Dimensions of the column were: 4-in length, 0.25-in I.D. tapering to 0.125 in at the tip; a reservoir 2-in deep and 1-in I.D. was cut at the top of the column. Wide variation from these dimensions is probably permissible if solution volumes are altered accordingly. The tip of the column was plugged with a moistened wad of filter paper pulp and the column loaded with a slurry of Dowex 1-X8 (100–200 mesh) resin in solution A. The column was washed with 20 ml of solution A immediately before use.

Reagents

Tantalum carrier. Dissolve about 2 g of tantalum pentachloride in 30 ml of 1:1 sulfuric acid plus 10 ml of 48% hydrofluoric acid and dilute to 200 ml with water. Standardize this solution by evaporating an aliquot in a platinum crucible, igniting to the oxide and weighing.

Hafnium carrier. Dissolve about 3 g of hafnium oxychloride octahydrate in 30 ml of 1:1 sulfuric acid plus 10 ml of 48% hydrofluoric acid and dilute to 200 ml. Standardize as for tantalum.

Lanthanum carrier. Dissolve about 3 g of lanthanum nitrate hexahydrate in 100 ml of 0.5 *M* nitric acid. The exact concentration is unimportant.

Silver carrier. Dissolve about 3 g of silver nitrate in 200 ml of 0.5 *M* nitric acid. The exact concentration is unimportant.

Solution A. 1 *M* hydrofluoric acid–0.25 *M* hydrochloric acid.

Solution B. 5 *M* hydrofluoric acid–2.5 *M* hydrochloric acid.

Solution C. 2.6 *M* ammonium chloride–1 *M* hydrofluoric acid.

Solution D. 2.6 *M* ammonium chloride–1 *M* hydrofluoric acid adjusted to pH 5.5 with ammonia solution.

Tantalum flux monitor. Dilute 1 ml of the tantalum carrier to 50 ml with water just before use.

Hafnium flux monitor. Dilute 1 ml of the hafnium carrier to 50 ml with water just before use.

Sample and monitor preparation

Approximately 100 mg of silicate samples are sealed into clean 0.5-dram polyethylene vials. Monitors to accompany each batch of samples are prepared by evaporating 1 weighed drop (0.05–0.1 ml) of the flux monitor solution on enough spectrographically pure silica to approximate sample volumes in the irradiation vials.

Neutron irradiation

Samples and monitors were irradiated for two days (7–8 h per day) in the Nuclear Reactor at the Naval Research Laboratory, Washington, D.C. This reactor has a thermal neutron flux of $7 \cdot 10^{12}$ $ncm^{-2}sec^{-1}$. After irradiation the samples were allowed to "cool" for about two weeks to permit decay of short-lived radionuclides.

Procedure for radiochemical separations (samples)

Evaporate 1.0 ml each of the tantalum and hafnium carriers with about 1 g of sodium hydroxide in an iron crucible. Weigh the sample, transfer to the crucible and add about 2 g of sodium peroxide. Fuse the mixture at red heat over a burner for 5 min, occasionally swirling the melt. Quench the melt and transfer the crucible to a beaker.

Add about 30 ml of water to the beaker and heat on a hot plate. Centrifuge the mixture, wash the precipitate once with 20–30 ml of water, and discard the supernate and washing to radioactive waste.

Dissolve the precipitate in about 15 ml of solution A. Add 1 ml each of lanthanum carrier and silver carrier to precipitate rare earth, silver, and halide activities. Filter the solution through a Whatman 42 paper onto the anion-exchange column. Since the drainage rate of the filter paper is faster than the flow rate through the column, this filtration effectively takes no time if the funnel is arranged to drip directly onto the column. After the sample solution has drained through the column, discard the precipitate to radioactive waste. Add 10 ml of solution A to the column. Discard the effluents from these steps to radioactive waste.

Elute hafnium from the column with 10 ml of solution B. Dilute this effluent to 10.0 ml and transfer to a polyethylene counting vial. Seal the vial. Add 10 ml of solution C to the column to elute any remaining activities other than ^{182}Ta. When this has drained through, discard the effluent.

Elute tantalum from the column with 10 ml of solution D. Dilute this effluent to 10.0 ml and transfer to a polyethylene counting vial. Seal the vial.

Procedure for radiochemical separations (monitors)

After completing the radiochemical operations required for the separation of hafnium and tantalum from the sample solutions, wash the outside of the monitor vial with 1 *M* hydrofluoric acid to remove external sources of contamination. Open the vial, transfer its irradiated contents to a platinum dish containing 1.0 ml each of the tantalum and hafnium carriers, 20 ml of 48% hydrofluoric acid and 2 ml of 72% perchloric acid, and then also submerge the emptied monitor vial on its side in the acid solution. Cover with a Teflon disc and warm gently with frequent stirring for 2–3 h. This treatment will not only effect volatilization of silica but will cause solution and leaching of the hafnium and tantalum monitors from the interior of the vial. Remove the vials after adequate but minimal washing with 1 *M* hydrofluoric acid. Evaporate the combined washings and solution to incipient dryness on a hot plate. Dissolve the residue in 15 ml of solution A, add the lanthanum and silver carriers and then follow the same radiochemical separations indicated above for the samples.

Counting of the radioactivity

Count the γ-emission of the tantalum fraction with a single-channel analyzer, using a window set to encompass the 0.067-MeV and 0.10-MeV γ-peaks. Then, recount the sample radioactivity with the window set to cover the composite peaks at 1.12 and 1.22 MeV. The ratio of these two counts should be the same in all samples and monitors, the constancy of this ratio being a substantiation of the radiochemical purity of ^{182}Ta.

Count the hafnium fraction with a multichannel analyzer. Determine the ^{181}Hf activity by integrating the area under the 0.48 MeV peak using the method described by COVELL[9].

Yield determination

After counting, open the vials and weigh 3–4 drops on to a clean 0.5-dram polyethylene irradiation vial. Seal the vial. Irradiate the hafnium yield samples for 1 min and the tantalum yield samples for 2 min. After cooling for 2–3 days, determine yields by counting each with the single-channel analyzer. Integral counting may be used, as only hafnium or tantalum activities will be present.

Calculation of results

Let: A = The activity determined from the sample counting rate.
A' = The activity determined from the yield counting rate.
W = The weight of original sample (g).
W' = The weight of solution used for the yield determination.
M = The weight of Ta and Hf originally taken for the flux monitor (μg).
C = The concentration of Ta or Hf in the original sample

$$\text{Then } C = \left(\frac{A}{W}\,\frac{W'}{A'}\right)_{\mathrm{s}} \left(\frac{M}{A}\,\frac{A'}{W'}\right)_{\mathrm{m}}$$

where the subscript s refers to the sample and the subscript m to the monitor.

DISCUSSION AND RESULTS

The radiochemical purity of the tantalum separated by this procedure was checked by examination of the γ-spectra of several samples with a multichannel analyzer. No activity other than that of ^{182}Ta was observed. A further routinely performed check of the purity was to count the sample with the single-channel analyzer window set first to cover the 0.067- and 0.01-MeV peaks, then with the window covering the composite peak at 1.2 MeV; the ratio of these two counts was always found to be the same in monitors and samples.

The separated hafnium fraction was not radiochemically pure. Activity from 65-day ^{95}Zr and to 27.4-day ^{233}Pa (formed by β^- decay of ^{233}Th) was routinely observed. Nevertheless, the 0.48-MeV γ-peak of ^{181}Hf was free of interference and reliable analyses could be obtained by using a multichannel analyzer. The radioactive decay of several samples containing abundant ^{233}Pa contamination was followed for three months; the 0.48-MeV peak in these samples decayed with the 43-day half-life of ^{181}Hf, further demonstrating that ^{233}Pa does not interfere with the hafnium determination.

The sensitivity of this method depends on the sample size, irradiation conditions, and counter background. Under the conditions described here, 0.1 p.p.m. of tantalum and 0.02 p.p.m. of hafnium could be reliably determined.

The analytical precision obtained with this method was estimated from 8 replicate analyses of a natural silicate glass. The use of a natural glass (a pulverized and blended tektite in this case) minimizes sampling problems of a normal rock analysis. Thus, the analyses given in Table II should provide a valid indication of the analytical precision. These results yield standard deviations, expressed as percent of the median, of 8.7 and 7.6% for tantalum and hafnium respectively. This precision is adequate for most geochemical purposes.

The accuracy of this procedure is more difficult to evaluate. Analyses of the 8 U.S. Geological Survey standard rock samples are given in Table III. Currently, comparison with other analyses of these rocks is possible for only G-1 and W-1. The results quoted by Fleischer[10] for tantalum and hafnium in G-1 and W-1 are also shown in Table III. This comparison shows reasonably good agreement of the tantalum values; the hafnium values found here are slightly, but probably not significantly, lower. This comparison demonstrates the absence of gross error in the pro-

TABLE II

PRECISION OF SIMULTANEOUS DETERMINATION OF TANTALUM AND HAFNIUM IN A TEKTITE (Po-300) FROM THE ORTIGAS SITE NEAR MANILA, PHILLIPPINES

(8 replicate determinations)

	Ta (p.p.m.)			*Hf (p.p.m.)*		
	1.5	1.3	1.6	5.8	5.3	6.2
	1.5	1.4	1.7	5.8	5.4	6.5
	1.5	1.4		6.1	5.5	
Median	1.5			5.8		
Standard deviation	0.13			0.44		
Coefficient of variation (%)	8.7			7.6		

TABLE III

DETERMINATION OF TANTALUM AND HAFNIUM IN U.S. GEOLOGICAL SURVEY STANDARD ROCK SAMPLES

Sample	*Split-position*[a]	*This study*		*Other results*[b]	
		Ta (p.p.m.)	*Hf (p.p.m.)*	*Ta (p.p.m.)*	*Hf (p.p.m.)*
G-1 Granite	—	2.0	4.5	1.6	5, 5.2, 7.6
W-1 Diabase	—	0.55	1.4	0.7	1.5, 2
AGV-1 Andesite	74–32	0.32	3.7		
G-2 Granite	1–22	0.82	6.1		
GSP-1 Granodiorite	66–6	0.77	11		
BCR-1 Basalt	6–28	0.86	3.3		
PCC-1 Peridotite	38–19	<0.1	0.05		
DTS-1 Dunite	49–21	<0.1	0.03		

[a] Data about preparation of samples is given by Flanagan[11].

[b] Cited by Fleischer[10].

posed method but a small bias cannot be precluded until other analyses of the standard rocks are published.

SUMMARY

A neutron activation procedure suitable for the routine determination of tantalum and hafnium in silicates is described. The irradiated sample is fused with sodium peroxide and leached, and the insoluble hydroxides are dissolved in dilute hydrofluoric acid–hydrochloric acid. After LaF_3 and AgCl scavenges, tantalum and hafnium are separated by anion exchange. Tantalum is obtained radiochemically pure; ^{233}Pa and ^{95}Zr contaminants in the hafnium fraction are resolved by γ-ray spectrometry. The chemical yield of the procedure is detemined after counting by re-irradiation. Values for the 8 U.S. Geological Survey standard rocks are reported.

RÉSUMÉ

On décrit un procédé par activation au moyen de neutrons pour le dosage de routine du tantale et de l'hafnium dans des silicates. L'échantillon irradié est fondu avec du peroxyde de sodium; l'hydroxyde formé est dissous dans un mélange acide fluorhydrique–acide chlorhydrique. Après élimination de LaF_3 et AgCl, tantale et hafnium sont séparés par échangeurs d'anions. Le tantale est obtenu radiochimiquement pur, les contaminants ^{233}Pa et ^{95}Zr dans la fraction hafnium sont résolus par spectrométrie-γ. Le rendement chimique de ce procédé est déterminé après comptage par re-irradiation. On indique les valeurs obtenues pour 8 roches étalons de l' "U.S. Geological Survey".

ZUSAMMENFASSUNG

Ein geeignetes Verfahren zur routinemässigen, gleichzeitigen Bestimmung von Tantal und Hafnium in Silikaten mit Hilfe der Neutronenaktivierungsanalyse wird beschrieben. Die bestrahlten Proben werden mit Natriumperoxid geschmolzen, ausgelaugt und die unlöslichen Hydroxide in einem Gemisch aus verdünnter Fluorwasserstoff- und Salzsäure gelöst. Nachdem so LaF_3 und AgCl abgetrennt sind, werden Tantal und Hafnium an einem Ionenaustauscher getrennt. Tantal wird radiochemisch rein erhalten. Kontaminierungen der Hafniumfraktion durch ^{233}Pa und ^{95}Zr werden durch γ-Spektrometrie eliminiert. Die chemische Ausbeute des Verfahrens wird durch Zählen nach erneuter Bestrahlung bestimmt. Werte für 8 Standardgesteine werden angegeben.

REFERENCES

1 D. H. F. ATKINS AND A. A. SMALES, *Anal. Chim. Acta*, 22 (1960) 462.
2 D. F. C. MORRIS AND A. OLYA, *Talanta*, 4 (1960) 194.
3 W. D. EHMANN, *Geochim. Cosmochim. Acta*, 29 (1965) 43.
4 E. MERZ, *Geochim. Cosmochim. Acta*, 26 (1962) 347.
5 J. J. SETZER AND W. D. EHMANN, *Geochim. Cosmochim. Acta*, 28 (1964) 764.
6 J. R. BUTLER AND A. J. THOMPSON, *Geochim. Cosmochim. Acta*, 29 (1965) 167.
7 C. K. KIM AND W. W. MEINKE, *Anal. Chem.*, 35 (1963) 2135.
8 F. NELSON, R. M. RUSH AND K. A. KRAUS, *J. Am. Chem. Soc.*, 82 (1960) 339.
9 D. F. COVELL, *Anal. Chem.*, 31 (1959) 1785.
10 M. FLEISCHER, *Geochim. Cosmochim. Acta*, 29 (1965) 1263.
11 F. J. FLANAGAN, *Geochim. Cosmochim. Acta*, 31 (1967) 289.

Analytica Chimica Acta
Elsevier Publishing Company, Amsterdam
Printed in The Netherlands

DOSAGE DES IMPURETES DANS LE ZINC PAR ACTIVATION NEUTRONIQUE

I. DOSAGE DE L'ARGENT ET DU COBALT DANS UN ZINC RAFFINÉ PAR FUSION ZONALE

R. MACHIROUX ET F. MOUSTY*
Laboratoires de Chimie Analytique, Université de Liège, Liège (Belgique)

(Reçu le 18 février, 1968)

L'analyse des métaux de haute pureté ($\geqslant$99.9999%) par les méthodes usuelles conduit souvent à des résultats assez décevants pour de nombreuses raisons. L'analyse par activation, par contre, constitue une méthode de choix dont la sensibilité extrême n'est pas la moindre qualité. Toutefois, dans le cas du zinc, l'existence des isotopes 69m et 65 émetteurs gamma de périodes respectives de 13.8 heures et de 245 jours, ne permet pas de réaliser des analyses non destructives. Il est indispensable de mettre en oeuvre des méthodes de séparation très sélectives d'une part et aussi rapides et simples que possible, d'autre part, pour ne pas soumettre l'opérateur aux radiations émises par la matrice très active.

Il est bien établi que le zinc contient des impuretés comme le plomb, l'argent, le cadmium, le cuivre, le fer, le cobalt, l'indium, le thallium, l'étain, le nickel, l'antimoine et le germanium, et, dans ces conditions, il nous a paru que la séparation chromatographique sur échangeur anionique avec élution à l'acide chlorhydrique pourrait constituer une méthode élégante de séparation d'un certain nombre de ces impuretés; en effet, d'après les données de KRAUS ET NELSON[1] on peut s'attendre aux résultats suivants:

(*a*) Cr(III), Ti(III), Ni(II) ne sont pas retenus par l'échangeur en milieu HCl 12 *N*.

(*b*) Ag(I), Mn(II), Co(II), Cu(II), Fe(III), Ga(III), Sb(III) peuvent être élués successivement en réduisant progressivement la concentration de la solution éluante de 12 *N* à 0.5 *N*.

(*c*) Zn(II) peut être élué avec HCl 0.005 *N*.

(*d*) Hg(II), In(III), Bi(III), Au(III), Tl(III) restent fixés sur la colonne après élution du zinc.

Sans doute, ces données ont été obtenues dans des conditions différentes de celles que nous allons rencontrer dans l'analyse du zinc; mais il semble qu'elles soient capables de servir de base au dosage d'un certain nombre d'impuretés. Dans cette première publication, nous présentons quelques détails concernant la méthode adoptée et nous donnons les résultats de dosage de l'argent et du cobalt dans une série d'échantillons de zinc électrolytique et de zinc raffiné par fusion zonale.

---

* Chercheur à l'Institut Interuniversitaire des Sciences Nucléaires.

TABLEAU I

CARACTÉRISTIQUES NUCLÉAIRES DU ZINC, DE L'ARGENT ET DU COBALT[2,3]

Isotopes stables	*Abond. isotopique (%)*	*Type de réaction*	*σ (barns)*	$T_{\frac{1}{2}}$	*β (MeV)*	*γ (MeV)*
^{64}Zn	48.89	(n,γ) ^{65}Zn	0.44 b	245 j	E.C.	0.511; 1.119
		(n,p) ^{64}Cu	10 μb	12.8 h	0.571; 0.657; E.C.	1.34
		(n,α) ^{61}Ni	—	Stable	—	—
^{66}Zn	27.81	(n,α) ^{63}Ni	20 μb	80 a	0.067	—
^{67}Zn	4.11	(n,p) ^{67}Cu	1.3 mb	58.5 h	0.38; 0.57	0.182; 0.092; 0.296
		(n,α) ^{64}Ni	6 μb	Stable	—	—
^{68}Zn	18.56	(n,γ) ^{69m}Zn	97 mb	13.8 h	—	0.438
		(n,α) ^{65}Ni	20 μb	2.56 h	2.10; 1.01; 0.60	1.49; 1.12; 0.37
^{70}Zn	0.62	(n,γ) ^{71m}Zn	85 mb	3 h	1.5	Multiples
		^{71}Zn		2.2 m	2.4	Multiples
^{107}Ag	51.4	(n,γ) ^{108}Ag	30 b	2.3 m	1.8	0.43
^{109}Ag	48.6	(n,γ) ^{110}Ag	96 b	24.2 s	2.84; 2.16	Divers
		^{110m}Ag	2.3 b	253 j	0.536; 0.086	0.656 (100%) 0.880 (75%) 0.93 (25%) 0.76 (24%) 1.38 (20%) etc
^{59}Co	100	(n,γ) ^{60}Co	22.5 b	5.3 a	0.312	1.17; 1.33
		^{60m}Co	16 b	10.1 m	1.56	0.059

Caractéristiques nucléaires du zinc, de l'argent et du cobalt (Tableau I)

Les réactions parasites ^{110}Cd (n,p) ^{110m}Ag, ^{113}In (n,α) ^{110m}Ag et ^{60}Ni (n,p) ^{60}Co, ont dans ce cas particulier du zinc très pur, des incidences négligeables sur le dosage de l'argent et du cobalt.

Comme on peut déjà le remarquer à l'examen du Tableau I, le dosage du cuivre et du nickel soulèvera des difficultés particulières à cause de l'existence de réactions parasites (n,p) et (n,α) sur le zinc et à cause de la courte période des isotopes utilisés (12.8 et 2.56 h). Ce problème fera l'objet d'une étude particulière.

PARTIE EXPÉRIMENTALE

Echantillonnage

Quelle que soit la qualité du zinc utilisé (électrolytique ou raffiné par zone) nous avons accordé un soin tout particulier à la préparation des échantillons. Pour éliminer les risques de contamination, les échantillons ont été préparés en atmosphère filtrée, dans une boite à gants munie de filtres absolus et maintenue en légère surpression pendant toutes les opérations. Les outils utilisés pour débiter les échantillons sont recouverts de polythène. Les échantillons dont le poids varie entre 0.2 et 1.5 g ont été pesés et emballés dans du papier d'aluminium.

Etalons

Les étalons d'argent et de cobalt ont été préparés à partir de solutions de $AgNO_3$ et $CoSO_4$ (p.a.) dans l'eau tridistillée; on dépose une goutte de solution de densité et de concentration connues dans un tube en quartz préalablement nettoyé et taré. La connaissance de son poids permet le calcul du poids de l'étalon prélevé.

Après évaporation à sec de la solution, les tubes de quartz sont scellés et ils subissent à nouveau un nettoyage au mélange sulfonitrique. Après irradiation, les tubes sont rayés au diamant puis cassés dans une solution contenant un poids connu d'entraîneur La solution et les eaux de rinçage sont transvasées dans un jaugé dont on complète le volume; on fait trois prises d'essai en vue de la mesure de l'activité spécifique et du contrôle de la pureté radiochimique par spectrométrie-γ.

Irradiation

Les tubes contenant les échantillons de zinc et les étalons ont été irradiés dans des flux de $8 \cdot 10^{12}$ (BR2, Mol) et $1.6 \cdot 10^{13}$ (Saclay) n/sec·cm^2 pendant 4 jours. Il s'est écoulé en général 40 à 50 h entre la sortie du réacteur et le traitement du premier échantillon.

Traitement des échantillons

Attaque. L'échantillon de zinc débarrassé de son enveloppe d'aluminium est attaqué par 5 ml d'acide chlorhydrique 12 N contaminé par 0.16 mg/ml de Sb_2O_3 destiné à accélérer l'attaque. Nous avons placé à la sortie du récipient d'attaque des barboteurs contenant une solution de $AgNO_3$ pour retenir SbH_3 formé; le précipité d'argent métallique formé par réduction par SbH_3 et de AgCl est filtré, lavé et mesuré au spectromètre-γ (Fig. 1). La solution d'attaque et les fractions de rinçage (2 × 5 ml HCl 12 N) du ballon d'attaque sont versées sur la colonne chromatographique où va se faire la séparation.

Séparation. Nous avons utilisé des colonnes de 2 cm de diamètre et de 25 cm de hauteur remplies de résine anionique Dowex 1-X8, 100–200 ou 200–400 mesh (environ 40 g de résine sèche). La résine a subi les traitements préliminaires usuels que nous avons complétés par une décarbonatation par une solution à 10% de NaCl. Avant la fixation de la solution active, la colonne a été équilibrée avec HCl 12 N de

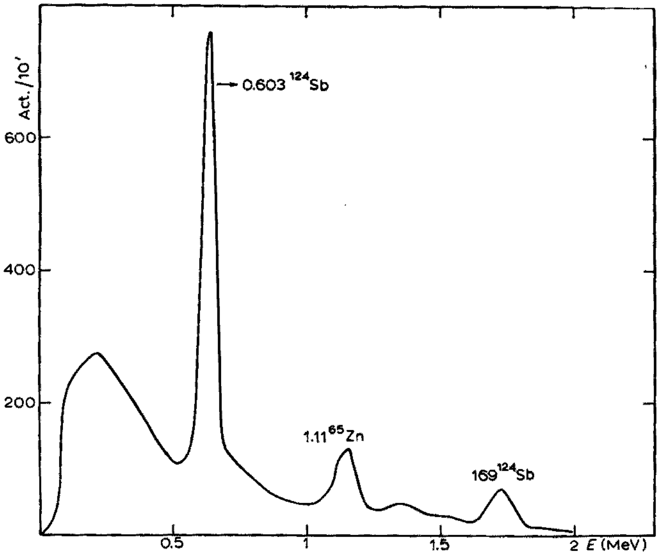

Fig. 1. Spectre du précipité Ag–AgCl.

manière très progressive par passage de fractions de 100 ml d'acide de concentrations croissantes (de 0.2 à 8 N), le conditionnement n'étant achevé qu'au moment de l'emploi. Nous avons pu constater au cours des expériences, qu'il était indispensable de procéder de la sorte pour conserver intact le tassement des couches de résine. Les séparations ont été réalisées grâce à l'élution par des solutions successives d'acide chlorhydrique de normalité décroissante (de 12 N à 0.1 N; vitesse d'élution 0.3 ml/cm^2·min). Les changements d'éluant ont été effectués au moyen d'un appareil automatique dont la description détaillée fera l'objet d'une note séparée. En résumé, celui-ci consiste en un robinet à huit entrées permettant d'amener sur la colonne huit éluants différents. Le robinet est actionné par un moteur dont la mise en marche est assurée par des interrupteurs et des cames portées par le plateau du collecteur de fractions. Nous avons récolté dans des tubes en plexiglas des volumes de 10 ml au moyen d'un siphon automatique. La radioactivité a été mesurée à l'aide d'une échelle Baird-Atomic munie d'un détecteur à scintillation avec cristal à puits NaI(Tl). Les identifications ont été effectuées au moyen d'un spectromètre R.I.D.L. (cristal NaI(Tl) 7.5 × 7.5 cm) à 400 canaux, dans la région de 0 à 2 MeV.

RÉSULTATS QUALITATIFS

La Fig. 2 montre la courbe d'élution obtenue avec un échantillon de zinc raffiné par zone. Jusqu'à présent, nous avons mis en évidence les isotopes suivants:

fractions en milieu HCl 12 N ^{51}Cr, ^{24}Na
10 N ^{110m}Ag
4 N ^{60}Co
2.5 N ^{64}Cu, ^{67}Cu
0.5 N ^{59}Fe

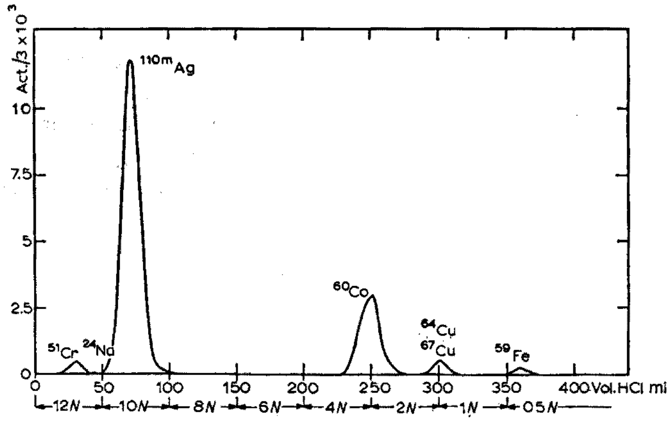

Fig. 2. Courbe d'élution d'un échantillon de zinc raffiné par zone.

Il est bien connu que le zinc contient un certain nombre d'autres impuretés. Si elles n'apparaissent pas dans ce chromatogramme, c'est pour l'une des raisons suivantes:

(*a*) Après leur sortie du réacteur, les échantillons subissent un "refroidissement" de 24 h avant d'être expédiés. Ceci porte à 40 h environ la durée qui s'écoule entre la fin de l'irradiation et l'enregistrement des premiers résultats. Tous les isotopes de période égale ou inférieure à 6 h (^{65}Ni, ^{56}Mn...) échappent par conséquent à la mesure.

(*b*) De nombreux éléments (Cd, In, Sn, Au, Hg...) sont fortement fixés sur la colonne et ils sont élués après le zinc dans nos conditions opératoires. Leur détection s'avère particulièrement malaisée. Parmi ceux-ci, nous avons pu déceler le ^{203}Hg après lavage de la colonne au moyen de Complexon III 10^{-2} M à pH = 8 et électrolyse de l'éluat acidifié par l'acide sulfurique entre anode de graphite et cathode de platine.

RÉSULTATS QUANTITATIFS

Nous avons commencé par examiner systématiquement le dosage de l'argent et du cobalt. Le dosage du fer semble pouvoir se réaliser aisément mais un certain

TABLEAU II

ANALYSE D'UN ZINC ÉLECTROLYTIQUE

Série[a]	*No. de l'échant.*	*Poids (g)*	*Ag (p.p.m.)*	*Co (p.p.m.)*
I	1	0.8884	1.41	0.13
	2	0.5955	1.49	0.12
	3	0.2512	1.45	0.08
	4	0.6007	1.51	0.12
	Moyenne		1.46	0.113
	σ (p.p.m.)		0.04	0.02
	σ (%)		3	17
II	1	1.2593	1.33	0.13
	2	0.6596	1.46	0.13
	3	1.7669	1.15	0.15
	4	1.6496	1.28	0.17
	Moyenne		1.30	0.145
	σ (p.p.m.)		0.12	0.019
	σ (%)		9	13

[a] Série I = irradiation = 4 jours au flux de $9 \cdot 10^{12}$ n/cm^2·sec (BR2).
Série II = irradiation = 4 jours au flux de $8 \cdot 10^{12}$ n/cm^2·sec (Mol).

TABLEAU III

ANALYSE D'UN ZINC AVANT RAFFINAGE PAR ZONE: SERIE III[a]

No. de l'échant.	*Poids (g)*	*Ag (p.p.m.)*	*Co (p.p.m.)*
1	0.2708	1.50	0.34
2	1.0827	1.62	0.37
3	1.3459	1.63	0.38
4	0.6566	1.60	0.38
5[b]	0.2411	—	0.29
Moyenne		1.59	0.37
σ (p.p.m.)		0.06	0.02
σ (%)		4	5

[a] Irradiation = 4 jours au flux de $1.6 \cdot 10^{13}$ n/sec·cm^2 (EL3, Saclay).
[b] Les résultats de l'échantillon 5 n'ont pas été pris en considération pour le calcul de la moyenne et du σ parce qu'obtenus dans des conditions de comptage peu sûres (installation défectueuse).

TABLEAU IV

ANALYSE DU ZINC APRÈS RAFFINAGE PAR ZONE

Série[a]	*No. de l'échant.*	*Poids (g)*	*Ag (p.p.m.)*	*Co (p.p.m.)*
IVa	1	0.6898	1.52	
	2	0.8734	1.84	
	3	0.9838	1.87	
	4	0.7981	1.53	
	5	1.8547	1.43	
	Moyenne		1.69	
	σ (p.p.m.)		0.19	
	σ (%)		11	
IVb	1	1.8295	1.73	
	2	0.3740	1.76	
	3	0.2544	1.72	
	4	0.6798	1.70	
	Moyenne		1.73	
	σ (p.p.m.)		0.025	
	σ (%)		1.5	
	Moyenne (IVa + IVb)		1.71	
	σ (p.p.m.)		0.127	
	σ (%)		7	
V	1	0.5807	1.56	0.16
	2	0.8072	1.46	0.16
	3	0.3078	1.62	0.19
	4	0.2472	1.72	0.19
	5	0.1680	1.41	0.18
	6	0.5969	1.43	0.13
	7	0.1256	1.77	0.16
	8	0.7271	1.40	0.14
	9	0.1340	1.88	0.19
	Moyenne		1.58	0.166
	σ (p.p.m.)		0.17	0.022
	σ (%)		11	13
VI	1	0.1299	1.94	0.17
	2	0.1453	1.76	0.16
	3	0.7025	1.87	0.15
	4	0.7739	1.97	0.16
	5	0.8404	1.88	0.15
	Moyenne		1.88	0.16
	σ (p.p.m.)		0.08	0.007
	σ (%)		4	3

[a] Série IVa (échant. sciés) = irradiation 4 jours au flux $8 \cdot 10^{12}$ n/sec·cm^2 (BR2, Mol).
Série IVb (échant. cassés) = irradiation 4 jours au flux $8 \cdot 10^{12}$ n/sec·cm^2 (BR2, Mol).
Série V = irradiation 84 heures au flux $8 \cdot 10^{12}$ n/sec·cm^2 (BR2).
Série VI = irradiation 4 jours au flux $1.6 \cdot 10^{13}$ n/sec·cm^2 (EL3, Saclay).

manque de reproductibilité nous a incités à attendre de plus amples informations avant de publier nos résultats. Les premiers dosages ont été réalisés sur des échantillons de zinc électrolytique (Tableau II), par la suite nous avons analysé un zinc électrolytique avant (Tableau III) et après (Tableau IV) raffinage par fusion zonale.

DISCUSSION

Il faut tout d'abord noter que les résultats que nous avons obtenus jusqu'à présent confirment le fait que la méthode chromatographique sur résine anionique s'avère être extrêmement intéressante pour le dosage d'un certain nombre d'impuretés dans le zinc par activation neutronique; celles-ci peuvent être éluées directement dans un état de pureté radiochimique suffisant pour le dosage; il est assez remarquable que, en une seule opération, les fractions contenant les différents pics d'élution ne permettent plus de mettre en évidence d'activité due au zinc.

ABLEAU V

BLEAU RÉCAPITULATIF DES RÉSULTATS

rie	*I*		*II*		*III*		*IV*		*V*		*VI*	
	Moyenne (p.p.m.)	*σ (%)*	*Moyenne (p.p.m.)*	*σ (%)*	*Moyenne (p.p.m.)*	*σ (%)*	*Moyenne (p.p.m.)*	*σ (%)*	*Moyenne (p.p.m.)*	*σ (%)*	*Moyenne (p.p.m.)*	*σ (%)*
g	1.46	3	1.30	9	1.59	4	1.71	7	1.58	11	1.88	4
o	0.11_3	17	0.14_5	13	0.37	5	—	—	0.16_6	13	0.16_5	3

Les résultats particuliers que nous avons obtenus pour l'argent et pour le cobalt montrent que la méthode est particulièrement commode, sensible et précise. Notons à ce propos dans le Tableau V que les écarts types sont nettement plus faibles dans les séries III et VI correspondant aux échantillons irradiés à Saclay; cela veut-il dire que le flux dans ce réacteur est plus homogène que dans le BR2 de Mol ou bien s'agit-il d'une pure coïncidence et que la raison doit être cherchée dans l'hétérogénéité de l'échantillon. Il est difficile de trancher à l'heure actuelle.

Nous désirons remercier Monsieur le Professeur G. DUYCKAERTS, pour la constante sollicitude qu'il a bien voulu manifester à notre égard tout au long de l'accomplissement de cette recherche. Notre gratitude va également à l'Institut Interuniversitaire des Sciences Nucléaires, qui a subsidié une partie de ce travail.

RÉSUMÉ

Une méthode de dosage par activation neutronique de traces d'argent et de cobalt dans le zinc électrolytique raffiné par fusion zonale a été mise au point; l'argent et le cobalt peuvent être obtenus successivement dans un état de pureté radiochimique suffisant pour le dosage en faisant passer la solution d'attaque chlorhydrique du zinc sur une résine échangeuse d'ions et en éluant l'argent par l'acide chlorhydrique 10 *N* et le cobalt par HCl 4 *N*. Des teneurs en argent de l'ordre du p.p.m. peuvent être dosées avec un écart type de l'ordre de 0.1 p.p.m.; le cobalt donne un écart type de l'ordre de 0.01 p.p.m. pour des teneurs de l'ordre de 0.1 p.p.m.

SUMMARY

A neutron activation method for the determination of cobalt and silver in the microgram range in a matrix of electrolytic zone-refined zinc is described. Silver and cobalt can be separated in a state of high radiochemical purity by means of an anion-exchange resin, silver being eluted by 10 *M* hydrochloric acid and cobalt by 4 *M* hydrochloric acid. The standard deviations are, respectively, 0.1 p.p.m. for silver and 0.01 p.p.m. for cobalt for impurity levels of 1 p.p.m. silver and 0.1 p.p.m. cobalt.

ZUSAMMENFASSUNG

Die Bestimmung von Mikrogrammen Kobalt und Silber in elektrolytischem, zonengereinigten Zink mit Hilfe der Neutronenaktivierungsanalyse wird beschrieben. Silber und Kobalt können mit einem Anionenaustauscher in hoher radiochemischer Reinheit abgetrennt werden. Silber wird dabei mit 10 *M* und Kobalt mit 4 *M* Salzsäure eluiert. Im Bereich von 1 p.p.m. Silber und 0.1 p.p.m. Kobalt betragen die Standardabweichungen 0.1 p.p.m. für Silber und 0.01 p.p.m. für Kobalt.

BIBLIOGRAPHIE

1 K. A. KRAUS ET F. NELSON, *Proc. Intern. Conf. Peaceful Uses At. Energy, Genève, 1955*, 7 (1956) 113–125.
2 J. M. HOLLANDER, I. PERLMAN ET G. T. SEABORG, Table of Isotopes, *Rev. Mod. Phys.*, 25 (2) (1953) 469–651.
3 R. C. KOCH, *Activation Analysis Handbook*, Academic Press, New York, 1960.

Analytica Chimica Acta
Elsevier Publishing Company, Amsterdam
Printed in The Netherlands

THE ATOMIC ABSORPTION SPECTROSCOPY OF SELENIUM*

CHUNI L. CHAKRABARTI
Department of Chemistry, Carleton University, Ottawa 1, Ontario (Canada)

(Received January 25th, 1968)

Some aspects of the determination of selenium by atomic absorption spectroscopy have been reported in the literature[1-4], but there are many other aspects of the atomic absorption spectroscopy of selenium including that of the behaviour of selenium complexes in organic solvents which have not been described. In the present paper, the sensitivities possible at different wavelengths in air–acetylene flames are discussed. The effect of organic solvents has been studied and a sensitive extraction procedure has been developed.

EXPERIMENTAL

Apparatus

Two different atomic absorption spectrophotometers were used. One was a Jarrell-Ash atomic absorption flame spectrometer, fitted with a multipass optical system, a Beckman "total-consumption" triple-burner (air–hydrogen) system, and a R-106 photomultiplier, sensitive at low wavelengths. The other was a Techtron Model AA3 atomic absorption spectrophotometer, fitted with a 10-cm long-path premix burner (air–acetylene or air–hydrogen) giving a laminar flow, and a R-106 photomultiplier. A Westinghouse selenium hollow-cathode tube (standard) was used with both instruments.

A meter readout and a Brown recorder were used with the Jarrell-Ash instrument, and a meter readout and a Sargent recorder model SRL with the Techtron instrument.

Selenium absorption lines

Table I shows the sensitivity of 4 selenium lines at 1960, 2040, 2063 and 2075 Å, in air–hydrogen and air–acetylene flames; in the latter flame, the sensitivities for these lines are in the ratio of 1:9:60:93. Although the sensitivities of the selenium lines vary widely in these flames, the ratio of the sensitivities of any of these lines in these two flames remains nearly the same. The significance of this is that the various broadening effects, especially self-absorption, Doppler, resonance and pressure broadening, have roughly the same relative effect on these lines in air–hydrogen (2100°)[5] and air–acetylene (2200°)[5] flames. The Se 1960 Å line is the most sensitive in both flames. The air–acetylene flame is more sensitive than the air–hydrogen for

---

* This paper was presented at the 49th Canadian Chemical Conference held in Saskatoon on June 5–8, 1966.

TABLE I

SENSITIVITY OF SELENIUM LINES

(Techtron AA3 spectrophotometer. Techtron 10-cm burner. Aqueous solution of selenium contains 10% (v/v) nitric acid)

State	*Energy levels (K)*	*Absorption lines (Å)*	*Sensitivity (p.p.m./1% absorption)*		*Ratio of (a):(b)*
			Air–hydrogen flame (a)	*Air–acetylene flame (b)*	
$^3P_2$	0–50997	1960.26	1.0	0.72	1:1.4
$^3P_2$	0–48142	2074.79	110.0	66.7	1:1.6
$^3P_0$	2534–50997	2062.79	68.8	43.1	1:1.6
$^3P_1$	1989–50997	2039.85	10.0	6.3	1:1.6

all the lines mentioned. With a Beckman triple-burner (air–hydrogen) and a triple-pass optical system, the Se 1960 Å line gives a sensitivity of 0.5 p.p.m. and a detection limit of 1.0 p.p.m. Since Se 1960 Å is the most sensitive line, the work described below was done with this line.

Absorption of the Se 1960 Å line by flame gases and air

Figure 1 shows that the Se 1960 Å line is strongly absorbed by the gases of air–hydrogen and air–acetylene flames. It can be seen from Fig. 1 that over 90% of this line is absorbed at flow rates of acetylene exceeding 2 l/min. The Se 1960 Å line is also strongly absorbed by atmospheric oxygen even in the absence of a flame.

Sensitivities and calibration curves at various acetylene flow rates

Figure 2 shows the sensitivities of air–hydrogen and air–acetylene flames. It can be seen that the highest sensitivity with an air–acetylene flame is obtained with

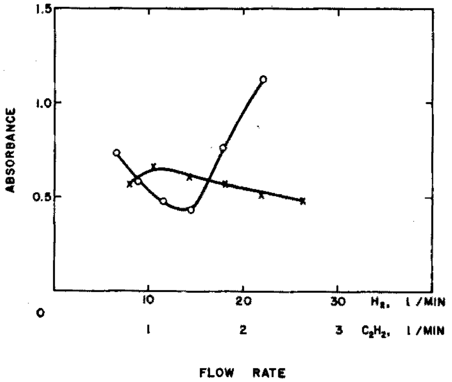

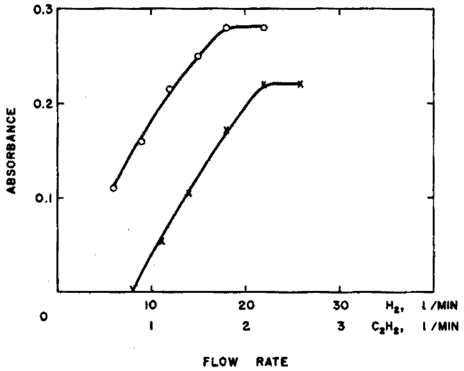

Fig. 1. The absorbance of the Se 1960 Å line by flame gases alone as a function of the flow rate of acetylene and hydrogen (Techtron). Air flow rate kept constant at 4.5 l/min. Lamp current 13 mA. Spectral band-width 9.9 Å. (○) C_2H_2; (×) H_2.

Fig. 2. The sensitivity of the Se 1960 Å line in air–acetylene and air–hydrogen flames as a function of the flow rate of acetylene and hydrogen. Conditions as for Fig. 1; 50 p.p.m. Se aqueous solution containing 10% (v/v) nitric acid. (○) C_2H_2; (×) H_2.

an acetylene flow rate of 1.8 l/min and that the sensitivity remains constant above that flow rate. The sensitivity with an air–hydrogen flame is highest for a hydrogen flow of 22 l/min, above which the sensitivity again remains constant. In both cases the air flow rate was held constant at 4.5 l/min. Thus, for the highest sensitivity, both flames must be strongly reducing. Figure 3 shows the sensitivity of Se 1960 Å line as a function of acetylene flow rate at the constant flow rate of air 4.5 l/min for an aqueous 100-p.p.m. selenium solution.

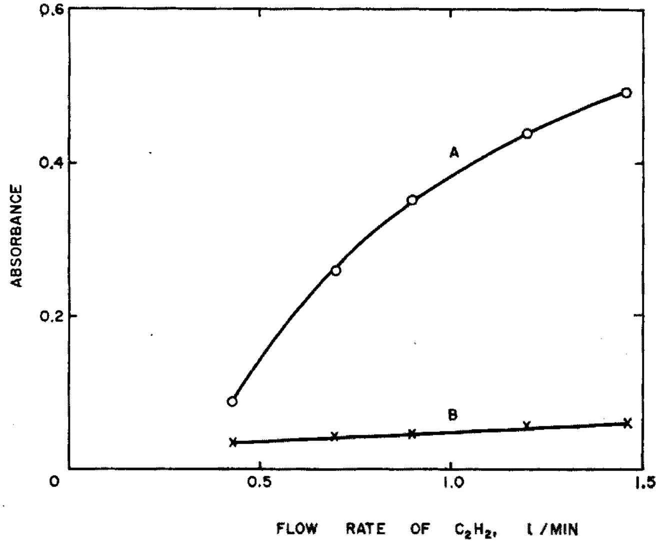

Fig. 3. The sensitivity of the Se 1960 Å line in an air–acetylene flame as a function of the flow rate of acetylene. Conditions as for Fig. 1 except that the lamp current was 7.5 mA. (A) 100 p.p.m. Se aqueous solution containing 10% (v/v) nitric acid; (B) flame + distilled water.

Figure 4 shows calibration curves for selenium in aqueous solution with an air–acetylene flame at various flow rates of acetylene. It can be seen all curves bend towards the concentration axis with increasing concentration of selenium. This curvature is due to the resonance broadening of the absorption line at high concentrations of selenium, and to the formation of selenium dioxide which is not completely dissociated. It will be seen later that at the lamp current used (7.5 mA) the hollow-cathode lamp does not show any self-absorption of the line.

Absorbance and noise at various lamp currents

The absorbance of the line as a function of lamp current decreases with increasing lamp current starting from about 8 mA. This decrease in absorbance is due to self-absorption broadening and increasing Doppler broadening (caused by higher temperature) of the emission line. It is therefore advisable to work with a low lamp current if the highest sensitivity is desired.

A study of the signal-to-noise ratio (obtained with an aqueous solution of selenium 10^{-3} *M*) as a function of the lamp current showed that this ratio increases about 2.4-fold (from 9.8:1 to 23.5:1) when the lamp current is increased from 7 to 13 mA, and then remains constant up to 15 mA. Since the detection limit of an

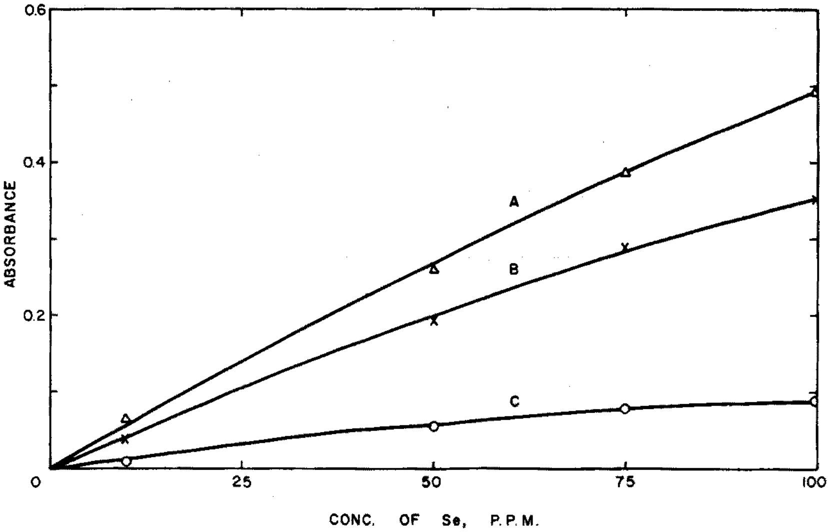

Fig. 4. Calibration curves for the Se 1960 Å line in an air–acetylene flame using various flow rates of acetylene. Conditions as for Fig. 3. Se in aqueous solution containing 10% (v/v) nitric acid. (A) flow rate 1.5 l/min; (B) flow rate 0.9 l/min; (C) flow rate 0.4 l/min.

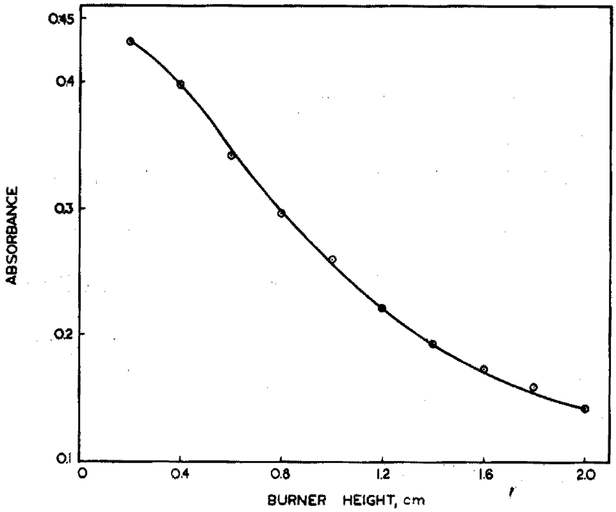

Fig. 5. The absorbance-height profile. Se 1960 Å. 10^{-3} M Se in aqueous solution containing 10% (v/v) nitric acid. Spectral band-width 9.9 Å. Lamp current 15 mA. Techtron 10-cm air–acetylene burner. C_2H_2 at 1.5 l/min; air at 4.5 l/min.

element is set by the signal-to-noise ratio rather than by the magnitude of the signal[6,7], in actual analysis near the detection limit of an element, it may be advantageous to work with a rather high lamp current although it will mean a slight sacrifice in sensitivity.

Flame profile

Figure 5 shows the absorbance-height profile of an aqueous solution of selenium in an air–acetylene flame produced by a 10-cm Techtron burner. The rapid fall-off in absorbance above the height of 0.2 cm is caused by recombination of selenium with oxygen in the flame ($Se + O_2 \rightleftarrows SeO_2$) and by dilution of the selenium concentration by the thermal expansion of flame gases and by surrounding air.

Absorbance as a function of time

Figure 6 shows the absorbance as a function of the time elapsed after the Techtron 10-cm air–acetylene burner is lit. It can be seen that the absorbance decreased gradually for about 30 min and then remained constant; insulating the monochromator slightly reduced this effect. The hollow-cathode lamp was pre-warmed for 30 min and was then tested and found to give a constant signal after a further 30 min. The spectrophotometer remained switched on continuously and the signal stability was excellent. Nevertheless, effects similar to those shown in Fig. 6 were observed with the hollow-cathode lamp even when the zero time was taken at 1-, 1.5- or 2-h intervals after the time of starting the warm-up of the hollow-cathode lamp.

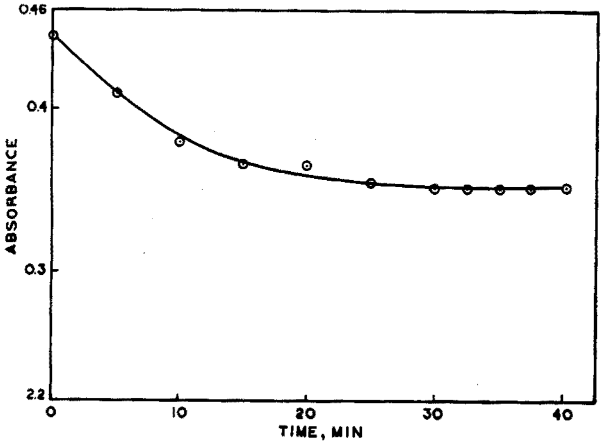

Fig. 6. The absorbance as a function of the time elapsed after the burner is lit. Techtron 10-cm burner, cold at time = 0. Other conditions as in Fig. 5.

Absorbance as a function of spectral band-width

The absorbance as a function of the spectral band-width shows that the highest absorbance is obtained with the narrowest spectral band-width; the absorbance decreases slightly from 3.3 Å to 6.6 Å, and then falls off more rapidly from 6.6 Å to 9.9 Å. The radiation from a spectral band-width less than about 3 Å is inadequate for satisfactory measurement.

Cationic and anionic interferences

Many cations and anions interfere with the absorbance of selenium; Tables II and III respectively show the effects of 1000-fold amounts of various cations and anions. In all cases, the ion was added to a 10^{-3} *M* selenium solution containing 10% (v/v) nitric acid. Interference is regarded as a deviation greater than twice the

TABLE II

CATIONIC INTERFERENCES

(Techtron AA3 spectrophotometer with 10-cm air–acetylene burner. Lamp current 15 mA. Air 4.5 l/min. Acetylene 1.5 l/min. Se 1960 Å. 10^{-3} *M* selenium solution)

Compound added	*Concn. of cation (M)*	*Molar ratio of cation to Se*	*Absorbance*	*Δ Absorbance*	*Interference*
	Nil	Nil	0.323^a	Nil^a	
$NaNO_3$	1	1000	0.349	+0.026	+
KNO_3	0.5	500	0.352	+0.029	+
$Ca(NO_3)_2$	1	1000	0.343	+0.020	+
$Mg(NO_3)_2$	1	1000	0.359	+0.036	+
$Fe(NO_3)_3$	1	1000	0.288	−0.035	−
$Al(NO_3)_3$	0.5	500	0.332	+0.009	Nil
$Cu(NO_3)_2$	1	1000	0.347	+0.024	+
$Cd(NO_3)_2$	1	1000	0.340	+0.017	Nil
Te^b	0.1	100	0.372	+0.049	+
$Zn(NO_3)_2$	1	1000	0.340	+0.017	Nil
$Bi(NO_3)_3$	0.5	500	0.356	+0.033	+
$Cr(NO_3)_3$	0.5	500	0.347	+0.024	+
$Hg(NO_3)_2$	1	1000	0.349	+0.026	+
$SnCl_4$	1	1000	0.339	+0.016	Nil
$(NH_4)_6Mo_7O_{24}$	1	1000	0.358	+0.035	+
K_3AsO_3	1	1000	0.348	+0.025	+

[a] The standard deviation was 0.009; deviations of less than 0.018 are therefore considered as non-interferences.

[b] Te was prepared in aqueous solution containing 10% (v/v) nitric acid.

standard deviation (0.009 absorbance units). Even 1000-fold amounts of the ions tested did not change the rate of aspiration from that obtained with the selenium solution alone. It was found that the standard deviations for the samples of selenium plus interfering ion were of the same magnitude as that obtained for pure selenium solutions; deviations exceeding twice the standard deviation can thus be attributed to interference. It may be pointed out that in normal samples, the amounts of foreign ions present are usually of much lower magnitude than shown in the Tables, and that in many cases the interference noted may decrease or even disappear. The nature and the mechanism of interference with elements including selenium is now under study, and the results will be published separately.

Determination of selenium in p.p.m. level in aqueous samples

Selenium in some aqueous samples from metallurgical processes cannot be determined satisfactorily by means of the calibration curves obtained with aqueous solution of selenium. For example, aqueous samples containing very high concentrations of foreign cations and anions such as large amounts of copper, nitrates, and free nitric acid, cannot be accurately determined unless the sample and standard solutions are similar in physical, and also, as far as possible, chemical characteristics. This can be accomplished in many cases by diluting the aqueous samples suitably with distilled water; Table IV shows the results of analyses done in this way. The alternative is to prepare the standards so as to simulate the samples.

TABLE III

ANIONIC INTERFERENCES

(Conditions as for Table II)

Compound added	*Concn. of anion (M)*	*Molar ratio anion to Se*	*Absorbance*	*Δ Absorbance*	*Interference*
	Nil	Nil	0.323[a]	Nil	
NH_4NO_3	1	1000	0.355	+0.032	+
HNO_3	1	1000	0.324	+0.001	Nil
NH_4Cl	1	1000	0.353	+0.030	+
HCl	1	1000	0.316	−0.007	Nil
$(NH_4)_3PO_4$	1	1000	0.336	+0.013	Nil
H_3PO_4	1	1000	0.324	+0.001	Nil
$(NH_4)_2SO_4$	1	1000	0.345	+0.022	+
H_2SO_4	1	1000	0.378	+0.055	+
NH_4F	1	1000	0.345	+0.022	+
NH_4Br	1	1000	0.346	+0.023	+
NH_4VO_3	0.1	100	0.342	+0.019	+
Na_2WO_4	0.1	100	0.316	−0.007	Nil
$Na_2B_4O_7$	0.1	100	0.055	+0.032	+
$(NH_4)_6Mo_7O_{24}$	0.1	100	0.339	+0.016	Nil
$KClO_3$	0.5	500	0.304	−0.019	—
$KClO_4$	1	1000	0.345	+0.022	+
$(NH_4)_2Cr_2O_7$	1	1000	0.395	+0.072	+
$K_3Fe(CN)_6$	0.8	800	0.281	−0.042	—
$K_3Fe(CN)_6$	0.4	400	0.324	+0.001	Nil
$K_4Fe(CN)_6$	0.5	500	0.314	−0.009	Nil
$K_4Fe(CN)_6$	0.25	250	0.319	−0.004	Nil
KIO_3	0.2	200	0.362	+0.029	+
$(NH_4)_2S_2O_8$	1	1000	0.361	+0.038	+

[a] See footnote to Table II.

TABLE IV

SELENIUM IN PRESSURE LEACHED ACID LIQUOR SAMPLES

(Jarrell-Ash spectrometer with Beckman triple-burner (air–H_2) and a triple-pass optical system. Se 1960 Å.
The samples contained Cu (50–80 g/l), H_2SO_4 ~ 20 g/l, Te ~ 15–20 g/l, As ~ 0–1 g/l, Pb (saturated), Ni ~ 0.3 g/l, Sn ~ 0.1 g/l. The samples were diluted 10–20 fold with distilled water before measurement; the calibration curve was prepared with an aqueous solution of selenium alone in 10% (v/v) nitric acid)

Sample no.	*Se (g/l)*	
	Atomic absorption spectroscopy	*Standard method*
1	0.64	0.65
2	1.32	1.33
3	0.30	0.34
4	0.014	----
5	0.015	----

Selenium complexes in organic solvents

Selenium can be quantitatively extracted[8] from an aqueous solution at pH 4–6.2; the selenium diethyldithiocarbamate complex is formed by adding a freshly prepared aqueous 2% (v/v) solution of sodium diethyldithiocarbamate, and is extracted into methyl isobutyl ketone. Other elements which are co-extracted as their diethyldithiocarbamate complexes do not interfere with the atomic absorption spectroscopy of selenium, hence rigid pH control is unnecessary. Figure 7 shows the calibration curves in air–acetylene and air–hydrogen flames in which the experimental conditions were optimized in each case. With the Techtron spectrophotometer, a 10-cm burner, the Se 1960 Å line, and an air–hydrogen flame, the sensitivities (in p.p.m./1% absorption) for the selenium diethyldithiocarbamate complex in methyl isobutyl ketone, and of an aqueous solution of selenium containing 10% (v/v) nitric acid, were 0.70 and 1.0 respectively; thus the extraction gave a 1.5-fold enhancement in sensitivity. With an air–acetylene flame, the corresponding sensitivities were 0.30 and 0.72 respectively, *i.e.*, the extraction gave a 2.4-fold enhancement in sensitivity. The throughput ratio of methyl isobutyl ketone to distilled water was 1.4:1. For the extraction procedure, the air–acetylene flame gives not only a higher sensitivity but also a smaller blank absorbance than the air–hydrogen flame.

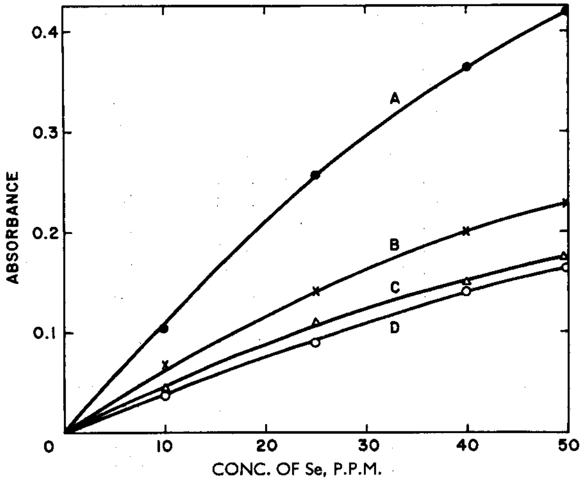

Fig. 7. Calibration curves for selenium in aqueous and organic solvents with air–hydrogen and air–acetylene flames. Air flow rate 4.5 l/min. Se 1960 Å. Lamp current 13 mA. Spectral band-width 9.9 Å. (A) Se(DDTC)$_4$ complex in methyl isobutyl ketone (MIBK) with acetylene at 0.9 l/min; (B) Se(DDTC)$_4$ complex in MIBK with hydrogen at 24 l/min; (C) selenium in aqueous solution containing 10% (v/v) nitric acid with acetylene at 2 l/min; (D) selenium in aqueous solution containing 10% (v/v) nitric acid with hydrogen at 24 l/min.

The author is indebted to the National Research Council of Canada for an operating grant and a major equipment grant. The author also thanks Dr. S. P. SINGHAL and Mr. D. E. WILLIS for technical assistance.

SUMMARY

Selenium can be determined in aqueous solution by atomic absorption spectroscopy at 1960, 2040, 2063 or 2075 Å; the sensitivities for these lines with a Techtron 10-cm air–acetylene burner are in the ratio of 1:9:60:93. When a Beckman triple-burner (air–hydrogen) and a triple-pass optical system are used, the most sensitive

1960 Å line provides a sensitivity of 0.5 p.p.m. and a detection limit of 1.0 p.p.m. The performance in air–hydrogen and air–acetylene flames is described, and optimum experimental conditions determined. With the Se 1960 Å line and a Techtron 10-cm air–acetylene burner, selenium extracted into methyl isobutyl ketone as its diethyldithiocarbamate complex gives a sensitivity of 0.30 p.p.m., which is a 2.4-fold increase over that found in aqueous solution.

RÉSUMÉ

Le sélénium peut être dosé en solution aqueuse par spectroscopie par absorption atomique à 1960, 2040, 2063 ou 2075 Å; les sensibilités de ces raies, avec un brûleur Techtron de 10 cm air/acétylène sont dans un rapport 1:9:60:93. Si l'on utilise un triple brûleur Beckman (air–hydrogène) et un système optique à triple passe la raie la plus sensible à 1960 Å fournit une sensibilité de 0.5 p.p.m. et une limite de détection de 1.0 p.p.m. Avec la raie du sélénium à 1960 Å et un brûleur Techtron 10-cm air–acétylène le sélénium extrait dans la méthylisobutylcétone sous forme de complexe diéthyldithiocarbamate donne une sensibilité de 0.3 p.p.m. correspondant à 2.4 fois celle obtenue en solution aqueuse.

ZUSAMMENFASSUNG

Selen kann in wässriger Lösung mit der Flammenabsorptionsanalyse bei 1960, 2040, 2063 oder 2075 Å bestimmt werden. Die Empfindlichkeiten dieser Linien mit einem Techtronbrenner, der Luft und Acetylen verwendet, stehen im Verhältnis von 1:9:60:93. Wenn ein Beckman-Dreifachbrenner (Luft–Wasserstoff) und ein dreifach durchgängiges optisches System verwendet werden, besitzt die empfindlichste Linie eine Empfindlichkeit von 0.5 p.p.m. und eine Nachweisgrenze von 1.0 p.p.m. Die Flammen werden beschrieben und die optimalen experimentellen Bedingungen bestimmt. Wird Selen mit Methylisobutylketon als Diäthyldithiocarbamat extrahiert, so ergibt sich ein Anstieg der Empfindlichkeit um das 2.4fache gegenüber Wasser.

REFERENCES

1 J. E. Allan, *Spectrochim. Acta*, 18 (1962) 259.
2 J. E. Allan, *4th Australian Spectroscopy Conference, Canberra, 1963*.
3 S. Sprague, D. C. Manning and W. Slavin, *Perkin-Elmer Atomic Absorption Newsletter*, No. 20, May, 1964.
4 C. S. Rann and A. N. Hambly, *Anal. Chim. Acta*, 32 (1965) 346.
5 J. A. Dean, *Flame Photometry*, McGraw-Hill, New York, 1960, p. 17.
6 J. D. Winefordner and T. J. Vickers, *Anal. Chem.*, 36 (1964) 1939.
7 J. D. Winefordner and T. J. Vickers, *Anal. Chem.*, 36 (1964) 1947.
8 C. L. Luke, *Anal. Chem.*, 31 (1959) 572.

Analytica Chimica Acta
Elsevier Publishing Company, Amsterdam
Printed in The Netherlands

RAPID DETERMINATION OF DYSPROSIUM IN ROCK SAMPLES BY NEUTRON ACTIVATION ANALYSIS WITH A Ge(Li) DETECTOR AFTER CHEMICAL SEPARATION

KENJI TOMURA AND HIDEO HIGUCHI
The Institute for Atomic Energy, Rikkyo University, Yokosuka (Japan)
NAOKI ONUMA AND HIROSHI HAMAGUCHI
Department of Chemistry, Faculty of Science, University of Tokyo, Hongo, Tokyo (Japan)

(Received April 15th, 1968)

Simple, convenient and sensitive analytical methods for lanthanides in rock samples are important in geochemical studies, because the chondrite-normalized lanthanide pattern (the ratio of each rare earth abundance to the abundance of the same element in chondritic meteorites) is helpful in the interpretation of the evolution of various types of rocks[1]. In recent years, high-resolution lithium-drifted germanium detectors (Ge(Li) detector) have been applied to neutron activation analysis for the lanthanides in rock samples by several authors[2-4].

However, the determination of dysprosium by non-destructive neutron activation using Ge(Li) γ-ray spectrometry was not successful because the 95-keV ^{165}Dy peak was obscured by the presence of the Bremstrahlung and Compton background from ^{56}Mn and ^{24}Na as pointed out by COBB[2] and by GORDON *et al.*[3]. In the analytical method involving a Ge(Li) detector and chemical group separation reported from this laboratory[4], the simultaneous measurement of ^{165}Dy (2.3 h) together with the other lanthanide nuclides was difficult because of the contribution of activities from the other rare earth nuclides due to long irradiation.

In the present paper, a procedure is described for the determination of dysprosium in rock samples with a Ge(Li) detector after a short sample irradiation and rapid chemical separation by conventional precipitation.

EXPERIMENTAL

Nuclear data for the determination of dysprosium are as follows: ^{164}Dy (28.2%) (n_{th},γ) ^{165}Dy; effective cross section for this reaction, 2700 b; half-life of ^{165}Dy, 2.32 h; energies and intensities of γ-rays emitted by ^{165}Dy, 94.7 keV (15%), 279.8 keV (0.6%), 361.7 keV (1.1%), 633.5 keV (0.7%), and 715 keV (0.7%).

The Ge(Li) detector used was made in this Institute and the active volume of the detector was estimated to be approximately 9.6 ml. The detector was operated in a vacuum at 77°K with a bias voltage of 1080 V. The output signal from the detector was fed into an ORTEC Model 118A preamplifier and an ORTEC Model 410 linear amplifier. The resultant pulse was then analyzed by an RCL 400-channel pulse-height analyzer. Resolution for the ^{57}Co 122-keV peak was 2.5 keV.

The samples employed in this study are described in Table I.

Samples (500 mg each) were sealed in polyethylene ampoules. A 10-μl aliquot of the reference standard solution of dysprosium (0.22 mg Dy/ml) was pipetted onto an aluminium foil, evaporated under a heat lamp and wrapped in an aluminium foil. The samples and the reference standard were irradiated in the TRIGA MARK-II reactor of Rikkyo University for 5 min at a neutron flux of $1.5 \cdot 10^{12}$ n/cm²/sec.

TABLE I

DESCRIPTION OF SAMPLES ANALYZED

Name	*Source*[a]
G-1	Westerly Granite, R.I.
W-1	Diabase from Centerville, Va.
G-2	Westerly Granite, from Sullivan Quarry, Bradford, R.I. Split 54, Position 10
GSP-1	Granodiorite, from Silver Plume, Colo. Split 13, Position 22
AGV-1	Andesite, from Guano Valley, Lak County, Ore. Split 26, Position 3
BCR-1	Basalt, Columbia River Group, from the Bridal Veil Flow Quarry (Wash-Ore.). Split 39, Position 20
JG-1	Granodiorite, from Sori, Ahio, Tochigi, Japan

[a] G-1 and W-1 were received from MICHAEL FLEISHER of the U.S. Geological Survey, G-2, GSP-1, AGV-1, BCR-1 from FRANCIS J. FLANAGAN of U.S. Geological Survey, JG-1 from ATSUSHI ANDO of Japan Geological Survey, respectively.

After cooling for 20 min, the irradiated sample was decomposed by sodium peroxide fusion in a nickel crucible containing lanthanum and manganese carriers (16.6 mg La and 10 mg Mn). The melt was dissolved with water and minimum amounts of concentrated hydrochloric acid to ensure complete sample decomposition. To the clear solution obtained was added concentrated ammonia solution to precipitate the hydroxides. This step was repeated twice (if necessary, undissolved silica was separated from the acidic solution by centrifuge). The hydroxides were dissolved in concentrated nitric acid and subjected to a conventional fluoride–hydroxide cycle (twice repeated). Finally, the lanthanum hydroxide containing the dysprosium activities was centrifuged in a 1-cm diameter polyethylene tube and transferred to the Ge(Li) detector for γ-counting. The irradiated reference standard was dissolved in a small amount of concentrated nitric acid in the presence of the lanthanum and manganese carriers and treated by the chemical procedure stated above so as to obtain the same counting geometry as the samples.

The 94.7-keV photopeak of ^{165}Dy was used for the determination. The half-life of the peak was checked by counting for 4 half-lives at suitable intervals.

After the counting measurements, the chemical yield of dysprosium was obtained by a simple re-activation technique. The lanthanum carriers recovered were irradiated at the neutron flux of $5 \cdot 10^{11}$ n/cm²/sec for 5 min and the 1600-keV peak areas of ^{140}La from the samples and the reference standard were measured.

The time required for the chemical separation was 2.5 h for 7 samples and the chemical yields were *ca.* 80%.

RESULTS AND DISCUSSION

Figure 1 shows the spectra of γ-rays from the samples obtained by the present chemical separation. The 94.7-keV ^{165}Dy, 103-keV ^{153}Sm, and 122-keV ^{152}Eu peaks stand clearly above the background level. The intense photopeak of the 847-keV

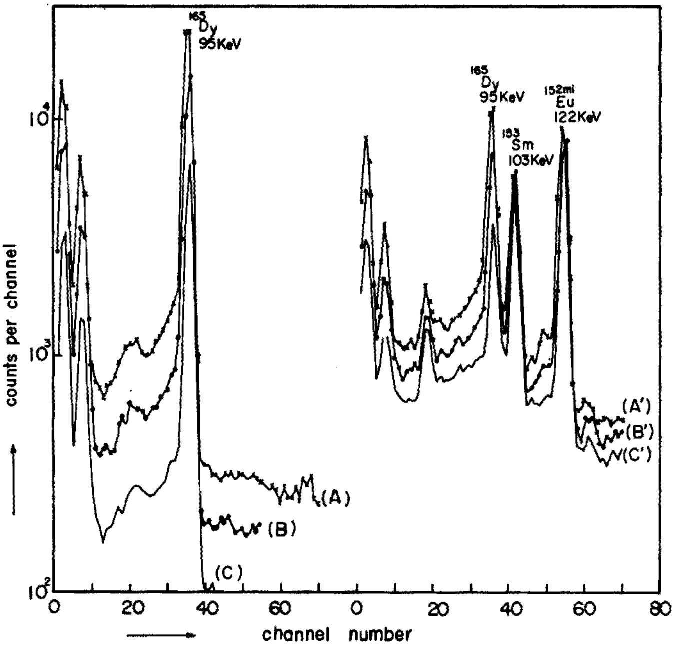

Fig. 1. γ-spectra from the sample G-1 and the reference standard (left: Dy std, right: G-1; (A) (A'), (B) (B'), and (C) (C') correspond to the time elapsed 3, 5 and 8 h after EOB).

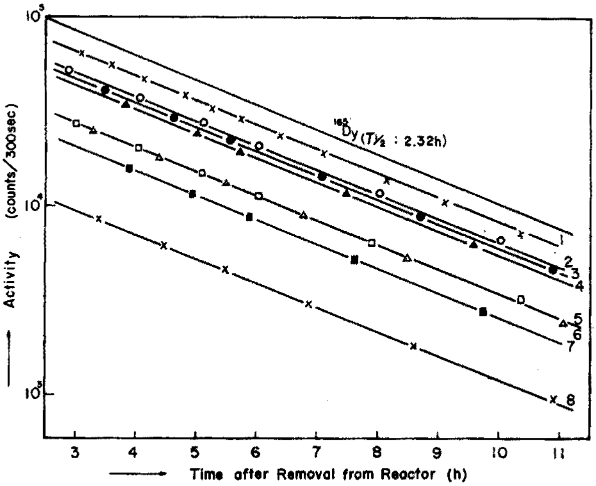

Fig. 2. Decay curves from the various samples and the reference standard. (1) Dy std, (2) BCR-1 (3) GSP-1, (4) BCR-1, (5) W-1, (6) G-1, (7) G-2, (8) AGV-1.

^{56}Mn and Compton tails from the high-energy γ-rays from ^{56}Mn, ^{24}Na etc. did not appear. Figure 2 indicates that the 94.7-keV ^{165}Dy peak decayed with a 2.3-h half-life. The lower limit for dysprosium detection in rock samples was 0.005 μg Dy, the activity corresponded to 200 times the background level.

The reasons for the use of lanthanum carrier instead of dysprosium are as follows: when the simple re-activation technique is used for the determination of the chemical yield of dysprosium, the use of dysprosium carrier is inadequate because of the self-shielding effect due to a large atomic absorption cross-section of dysprosium (n_{th}: 1500 b); no self-shielding effect on the mg-amounts of lanthanum was found (Fig. 3). Moreover, the use of the 1600-keV peak of ^{140}La is quite adequate for the γ-ray counting.

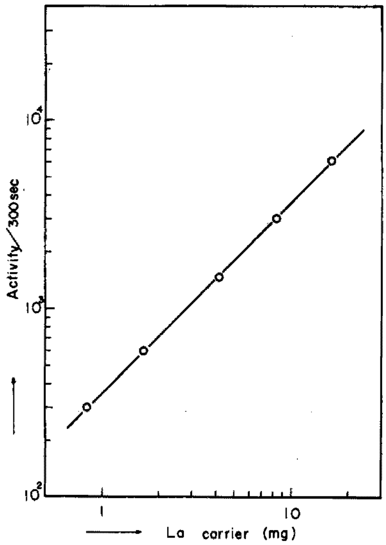

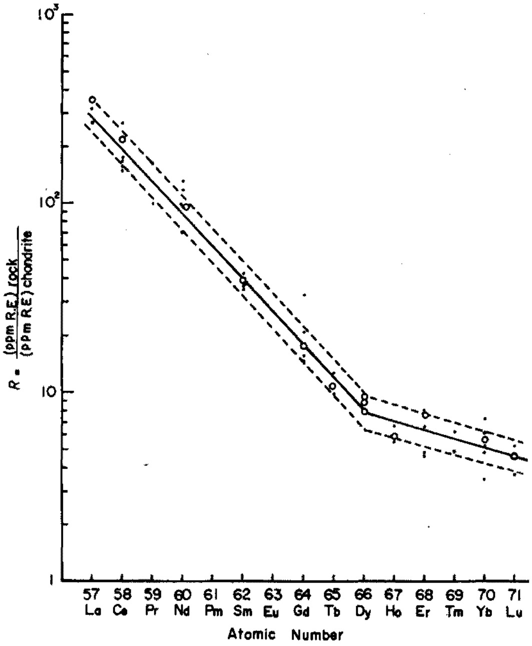

Fig. 3. Calibration curve for the determination of chemical yield.

Fig. 4. Chondrite-normalized pattern for the standard rock G-1. (o) This work, (·) previous work.

TABLE II

CONCENTRATIONS OF DYSPROSIUM IN SEVERAL GEOCHEMICAL STANDARD ROCKS

Sample	*p.p.m. Dy*	*av. p.p.m. Dy*
G-1 (Granite)	2.40, 2.67, 2.82	2.63
W-1 (Diabase)	3.67, 3.56, 3.77	3.67
G-2 (Granite)	1.98, 2.11	2.05
GSP-1 (Granodiorite)	5.66, 5.66	5.66
AGV-1 (Andesite)	3.28, 3.63	3.46
BCR-1 (Basalt)	6.01, 6.89, 6.28 6.27, 6.25, 5.98, 6.10	6.25
JG-1 (Granodiorite)	4.96, 4.35	4.66

Dysprosium abundances found in the geochemical standard rocks, G-1, W-1, G-2, GSP-1, AGV-1, BCR-1, and JG-1 are summarized in Table II.

The precision of ±4.7% (as standard deviation) for this procedure was estimated from a statistical treatment of the seven separate analyses of BCR-1.

The accuracy of the present method can be assessed by comparison with the reported values on two geochemical standard rocks, G-1 and W-1. Table III gives a comparison of the present results with those of other workers. As shown in Table III, there are many conflicting values for the dysprosium concentrations in the standard rocks G-1 and W-1. To examine these discrepancies, the chondrite-normalized patterns (the ratio of each lanthanide abundance in p.p.m. to the abundance of the same element in chondrite) for the standard rocks G-1 and W-1 are shown in Figs. 4 and 5. These data are cited from SCHMITT *et al.* (av. chondrite abundances)[13,14], HASKIN

TABLE III

COMPARISON OF DYSPROSIUM CONCENTRATIONS IN THE STANDARD ROCKS G-1 AND W-1 (p.p.m)

G-1	*W-1*	*Method*	*Reference*
5	5	Spark source mass Spectrographic	BROWN AND WOLSTENHOLME (1964)[5]
4.5	2.3	Spark source mass Spectrographic	TAYLOR (1965)[6]
—	3.89	Spark source mass Spectrographic	NICHOLLS *et al.* (1967)[7]
5.5	3.8	X-ray fluorescence	ALEKSIEV AND BOYADJIEVA (1966)[8]
2.52 (av. of 2)	3.97 (av. of 3)	Mass spectrometric isotope dilution	SCHNETZLER *et al.*(1967)[9]
1.33	3.3	Neutron activation	MADDOCK AND MEINKE (1962)[10]
2.51 (av. of 2)	7.7	Neutron activation	CHASE *et al.* (1963)[11]
2.52	4.38	Neutron activation	TOWELL *et al.* (1965)[12]
2.1	2.7	Neutron activation	COBB (1967)[2]
2.63 (av. of 3)	3.67 (av. of 3)	Neutron activation	This work (1968)

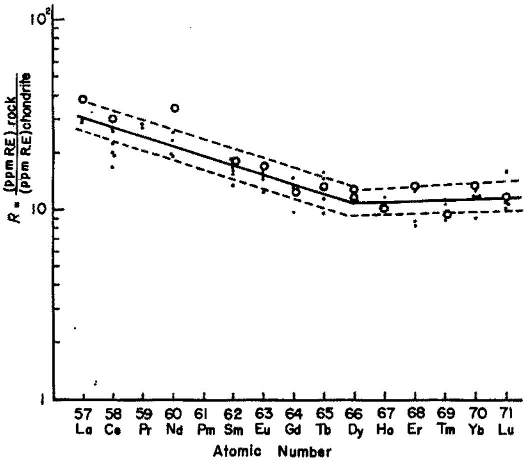

Fig. 5. Chondrite-normalized pattern for the standard rock W-1, (o) This work, (·) previous work.

AND GEHL[15], TOWELL *et al.*[12], SCHNETZLER *et al.*[9], COBB[2], GORDON *et al.*[3], NICHOLLS *et al.*[7], ALEKSIEV AND BOYADJIEVA[8] and our group (this work and unpublished data).

The logarithm of normalized abundance decreases linearly (except europium) with Z over the range between lanthanum and dysprosium, and there is a clear inflection point at dysprosium in G-1 (see Fig. 4). While TOWELL *et al.*[12] pointed out that all lanthanides in W-1 appear to exhibit a smooth abundance pattern approximated by a straight line from lanthanum to lutetium, there seems to exist also an inflection point at dysprosium for W-1 as shown in Fig. 5. Both upper and lower lines in Figs. 4 and 5 correspond to the scattering range obtained statistically. The existence of these ranges, arising from both the experimental error and sample inhomogeneity, makes it difficult to obtain best values for dysprosium in the standard rocks. Anyhow, judging from the lines in these figures and adopting a value of 0.30 p.p.m. dysprosium in chondrites[13,14], the best values are estimated to lie between 1.9 and 3.0 for G-1, and 2.6 and 3.9 p.p.m. for W-1, respectively. All of our data for dysprosium fell within these ranges.

The authors are very grateful to Messrs. M. HATTORI and T. NAGAHARA of the Institute for Atomic Energy, Rikkyo University, for allowing us to use their high resolution Ge(Li) detector. The authors are also indebted to the operators of the Rikkyo Reactor for their cooperation in carrying out our experiments.

SUMMARY

A neutron activation method for the rapid determination of dysprosium in rocks, based on simple chemical separation and γ-spectrometry with a lithium-drifted germanium detector, is described. The 94.7-keV photopeak of dysprosium-165 (2.3 h half-life) was measured. Several geochemical standard rocks covering a variety of rock types were analyzed. The detection limit was 0.005 μg of dysprosium. A precision of $\pm 4.7\%$ was obtained on 7 separate analyses of a basalt standard rock. The accuracy of the method is discussed.

RÉSUMÉ

On décrit une méthode de dosage rapide du dysprosium dans des roches par spectrométrie gamma à l'aide d'un détecteur Ge(Li), après séparation chimique. On mesure le photopic du dysprosium-165 94.7-keV (période de 2.3 h). On a analysé ainsi plusieurs standards géochimiques. On arrive à une limite de détection de 0.005 μg de dysprosium. Une précision de $\pm$ 4.7% est obtenue avec 7 analyses séparées d'une roche standard.

ZUSAMMENFASSUNG

Es wird eine neutronenaktivierungsanalytische Methode zur schnellen Bestimmung von Dysprosium in Gesteinen beschrieben. Dabei wird der 94.7-keV Photopeak des Dyprosium-165 (2.3 h) γ-spektrometrisch mit einem Lithium-gedrifteten Germanium-Detektor gemessen. Zahlreiche verschiedene geochemische Standardgesteine werden analysiert. Die Genauigkeit der Methode wird diskutiert. Ihre

Reproduzierbarkeit beträgt ±4.7%. Als Nachweisgrenze ergab sich 0.005 μg Dysprosium.

REFERENCES

1 A. Masuda and Y. Matsui, *Geochim. Cosmochim. Acta*, 30 (1966) 239.
2 J. C. Cobb, *Anal. Chem.*, 39 (1967) 127.
3 G. E. Gordon, K. Ranale, G. G. Goles, J. B. Corliss, M. H. Beeson and S. S. Oxley, *Geochim. Cosmochim. Acta*, in press.
4 K. Tomura, H. Higuchi, N. Miyaji, N. Onuma and H. Hamaguchi, *Anal. Chim. Acta*, 41 (1968) 217.
5 R. Brown and W. A. Wolstenholme, *Nature*, 201 (1964) 598.
6 S. R. Taylor, *Nature*, 205 (1965) 34.
7 G. D. Nicholls, A. L. Graham, E. Williams and M. Wood, *Anal. Chem.*, 39 (1967) 584.
8 E. Aleksiev and R. Boyadjieva, *Geochim. Cosmochim. Acta*, 30 (1966) 511.
9 C. C. Schnetzler, H. H. Thomas and J. A. Philpotts, *Anal. Chem.*, 39 (1967) 1888.
10 R. S. Maddock and W. W. Meinke, private communication to M. Fleischer (1962) cited in *Geochim. Cosmochim. Acta*, 29 (1965) 1263.
11 J. W. Chase, J. W. Winchester and C. D. Coryell, *J. Geophys. Res.*, 68 (1963) 567.
12 D. G. Towell, R. Volfovsky and J. W. Winchester, *Geochim. Cosmochim. Acta*, 29 (1965) 569.
13 R. A. Schmitt, R. H. Smith, J. E. Lasch, A. W. Mosen, D. A. Olehy and J. Vasilevskis, *Geochim. Cosmochim. Acta*, 27 (1963) 577.
14 R. A. Schmitt, R. H. Smith and D. A. Olehy, *Geochim. Cosmochim. Acta*, 28 (1964) 67.
15 L. Haskin and M. A. Gehl, *J. Geophys. Res.*, 68 (1963) 2037.

Analytica Chimica Acta
Elsevier Publishing Company, Amsterdam
Printed in The Netherlands

THE SIMULTANEOUS DETERMINATION OF VANADIUM, CHROMIUM, MANGANESE, IRON, COBALT, NICKEL, COPPER AND ZINC IN SEA WATER BY X-RAY FLUORESCENCE SPECTROMETRY

A. W. MORRIS
Marine Science Laboratories, Menai Bridge, Anglesey, North Wales (United Kingdom)

(Received January 29th, 1968)

Accurate determination of the concentration in sea water of the transition elements is essential to the study of the marine geochemical and biochemical process in which they take part. These elements are normally present in sea water within the concentration range 0–20 μg/l, although considerable seasonal and geographical variations occur.

RILEY[1] has fully reviewed the analytical methods which have been used for the determination of trace elements in sea water. Except when radioactivation analysis or possibly, atomic absorption spectrophotometry[2] is used, the low concentrations and the interferences in the analytical procedures arising from the presence of relatively overwhelming amounts of other elements necessitate a preliminary separation and concentration.

Very few analytical methods allow the determination of several elements in microgram amounts in a single concentrate from a sea water sample. Neutron activation analysis can be used but the precision is rather poor. SCHUTZ AND TUREKIAN[3] obtained coefficients of variation of 17.6% for cobalt and 21.2% for nickel in sea water. Emission spectrographic analysis permits the simultaneous determination of a large number of elements, but even when an internal standardization technique is used, a precision of better than ±5% is difficult to obtain.

The non-destructive X-ray fluorescence spectrometric method has seldom been applied to the determination of trace elements in sea water. With this method, maximum sensitivity is obtained for elements of atomic number around 28 with detection limits of better than 1 p.p.m. Therefore a preliminary concentration by a factor of 1000 to 5000 is required for the determination of the transition elements in sea water.

NATELSON *et al.*[4] have described a procedure for the determination of the elements chromium to zinc, inclusive, in sea water. The trace elements were separated from the major constituents of evaporated sea water salts by dissolution in glacial acetic acid. The solution was subsequently spotted onto filter paper using a ring-oven technique to obtain a coherent spot suitable for X-ray fluorescence spectrometry. No quantitative evaluation of this procedure was given.

The present paper describes an X-ray fluorescence spectrometric technique for the determination of the dissolved ionic forms of the elements vanadium to zinc, inclusive, in sea water after a preliminary separation and concentration using a continuous solvent extraction procedure. These trace elements exist in sea water associated with particulate matter, as colloidal particles and in true solution. Dissolved material is conventionally defined as that which will pass through a 0.5-μ pore-sized membrane filter. Cobalt, nickel, copper and zinc are predominantly in the free divalent cationic form. "Soluble" iron consists mainly of colloidal iron(III) hydroxide and iron(III) phosphate which are solubilized in acid solution to give iron(III)[5]. Although the manganese(II) is thermodynamically unstable in natural sea water, manganese universally occurs as dissolved divalent cations[6].

The speciation of chromium and vanadium in sea water is still in some doubt. FUKAI[7] suggested that the hexavalent chromate species is the thermodynamically stable state but he invariably detected the trivalent form in Mediterranean waters, where it at times predominated. On the contrary, CHUECAS AND RILEY[8] were unable to detect chromium(VI) in a number of unspecified samples of sea water.

According to DUCRET[9], vanadium should be present in sea water almost entirely as the pentavalent vanadate species but KALK[10] has detected vanadyl cations representing about 1% of the total vanadium present.

Together with the inorganic species, transition elements may also occur as dissolved organically complexed species, although DUURSMA AND SEVENHUYSEN[11] were unable to demonstrate experimentally that such complexes are formed in natural sea water.

Solvent extraction of chelated trace elements

MALISSA AND SCHOFFMANN[12] have described the chelating properties of substituted dithiocarbamates for many elements and the complexes formed have been utilized in several determinations of trace elements in sea water. For example, copper[5,13], manganese and zinc[14] can be extracted with sodium diethyldithiocarbamate and zinc can be determined turbidimetrically[15].

Ammonium pyrrolidine dithiocarbamate (APDC) forms stable chelates with all the transition elements over a wide pH range. This reagent has therefore become popular for the determination of trace elements in a variety of materials because of the rapid, often quantitative extraction of microgram amounts of chelated trace elements from aqueous solution into high-boiling ketones which are suitable for subsequent atomic absorption analysis. A typical example is the determination of copper in sea water[16]. Despite the possibility of ensuring complete extraction, continuous extraction procedures have not been used to any great extent for sea water analysis, although BROOKS[17] has applied liquid/liquid discontinuous countercurrent extraction to the transfer of copper, molybdenum and zinc from sea water into a 1% solution of 8-quinolinol in chloroform.

Preliminary experiments on the pH dependence of the extraction of copper and manganese from 500 ml of sea water to which varying amounts of APDC had been added, were carried out. The chelated elements in a sea water sample alone, and in a sample of the same sea water to which 10 μg each of copper and manganese had been added, were extracted into 10 ml of *n*-amyl methyl ketone by vigorous mechanical shaking for a period of 30 min. The organic phase was then separated and excess of ketone was evaporated off, without boiling, by warming on a hot-plate. The residue was dissolved in 2 ml of concentrated nitric acid and the solution was again evaporated to dryness. The resultant residue was finally dissolved in 1.00 ml of concentrated nitric acid and 9.00 ml of distilled water. The amounts of copper and manganese in the extracts were determined by atomic absorption spectrophotometry. The results were compared with those obtained from standards prepared by evaporating solutions containing 10 μg each of copper and manganese to dryness and then repeating the dissolution procedure.

Maximum yield (*ca.* 90%) of copper was obtained in the pH range 1.0–5.5 and was largely independent of APDC concentrations greater than 0.2 g per 500 ml of sea water. For manganese, maximum yield was obtained in the pH range 3.0–7.0, but this yield exceeded 80% only when APDC concentrations greater than 1.0 g per 500 ml of sea water were used.

A continuous extraction procedure was then attempted. A standard Quickfit upward displacement liquid/liquid extraction unit of nominal capacity 1 l was used; this equipment was modified by shortening the upper piece of the extractor unit by 30 cm and the inner distribution column was correspondingly shortened. This modification increased the rate of passage of solvent through the aqueous phase by reducing the amount of condensation of solvent vapour on the extractor walls. Further improvement was obtained by lagging the shortened piece.

The actual volume of water which could be extracted was 800 ml and *ca.* 75 ml of organic solvent were required for efficient operation of the extraction unit. When *n*-amyl methyl ketone was used as the organic phase, difficulties arose due to the instability of the organic solvent–water interface because of the high boiling point (148°) of the solvent. Methyl isobutyl ketone (b.p. 111°) was found to be a satisfactory substitute and was used in all subsequent experiments. With the atomic absorption technique, it was found that 10 μg each of copper and manganese could be quantitatively extracted from 800 ml of sea water at pH values between 2.0 and 3.5 to which 2 g of APDC had been added, during an extraction period of less than 3 h. pH values less than 2.0 reduced the solubility of APDC in the sea water to too great an extent; pH values greater than 3.5 gave rise to excessively long extraction periods. From these results, it seemed likely that the other transition elements could also be quantitatively extracted under similar conditions. This was subsequently found to be so.

Preparation of extracts for analysis

The extracted trace elements are obtained as chelated compounds dissolved in *ca.* 30 ml of ketone and are free from the large amounts of elements which would cause matrix interferences during X-ray fluorescence analysis. Further concentration is readily obtained by evaporating off excess of solvent.

The use of this organic solution for direct analysis was not attempted because of the difficulties which arise due to evaporation and convection of liquid samples when irradiated close to a hot X-ray tube. Other methods of sample mounting include spotting of the solution onto filter paper, adsorption of the trace elements onto cation-exchange membranes and incorporation of the solution into a non-interfering matrix such as powdered cellulose.

In the spotting technique, the production of a reproducibly sized coherent spot is essential for quantitative analysis and this necessitates the use of sophisticated methods such as the ring-oven technique described by NATELSON *et al.*[4]. The adsorption of microgram traces of cations from solution onto cation-exchange membranes has been investigated by LUKE[18]. It was found that continuous stirring for 2–3 h was required for the attainment of equilibrium and, even then, quantitative uptake was not always obtained.

Absorption of a small volume of solution into powdered cellulose offers a simple, rapid procedure for the preparation of extracts for analysis. The following procedure was adopted.

Most of the ketone was removed by distillation to leave *ca.* 5 ml of solution. This solution was quantitatively transferred to a 50-ml platinum dish and the removal of organic solvent was completed by evaporation, without boiling, on a warm hot-plate, leaving a dark-brown partially decomposed residue. Some partially decomposed residue remained in the extraction flask. This was dissolved in 3 ml of hot nitric acid, and the nitric acid solution was transferred with washings to the dish. Organic material was destroyed by adding a further 2 ml of nitric acid and evaporating to dryness. The nitric acid fuming was twice repeated leaving a brown-yellow residue. On cooling, the residue was finally dissolved in 0.6 ml of 25% nitric acid; 300.0 mg of Whatman standard grade powdered cellulose were added and the resulting pulp was thoroughly mixed with a teflon rod. After the pulp had been dried at 80°, as much of it as possible was scraped into an agate mortar and ground to a fine powder. The powder was pressed into a 1-in diameter stainless steel X-ray fluorescence sample holder under a pressure of 4000 lb/in^2. In order to give mechanical strength to the paper pellet, a further 500 mg of cellulose powder was pressed into the sample holder under the same pressure.

The reproducibility of this process was assessed. Ten 5-ml portions of a standard solution containing 1 μg/ml each of cobalt, nickel, copper and zinc were pipetted into 50-ml beakers and evaporated to dryness. The nitric acid fuming and pellet-making procedures were then carried out. The coefficient of variation about the mean number of counts (N) obtained during a 600-sec counting period (uncorrected for background) using X-ray fluorescence spectrometry of the first order Kα lines of the elements, with pulse height discrimination, are present in Table I. A 0.0045-in thick titanium filter was used to remove tungsten Lα lines, arising from the X-ray tube, which would otherwise interfere in the determination. The coefficients of variation of the counts obtained from the ten samples are compared with the theoretical standard counting error ($\sqrt{N}$, expressed as a percentage)[19], which represents the optimum value which can be obtained under ideal conditions for repetitive counting of a single sample. Although this ideal is not obtained, coefficients of variation of 2.0% or less illustrate the excellent reproducibility of the sample preparation technique.

TABLE I

REPRODUCIBILITY OF SAMPLE PREPARATION; PRACTICAL AND THEORETICAL COUNTING CONDITIONS

Element (5 µg)	*K$\alpha_{1,2}$ line (°2θ)*	*Number of samples*	*Mean count per 600 sec (N) sample and background*	*Coefficient of variation (%)*	*Theoretical standard counting error ($\sqrt{N}/N \cdot 100$) (%)*
Co	52.78	10	8756	2.0	1.1
Ni	48.64	10	14861	1.3	0.82
Cu	44.99	10	17644	1.1	0.75
Zn	41.77	10	20012	1.8	0.71

X-ray fluorescence analysis

Fluorescent excitation of the transition elements was achieved using the X-radiation from a tungsten target X-ray tube operated at a voltage of 50 kV and a current of 20 mA. The fluorescent emission from the sample was resolved using a lithium fluoride crystal, with a fine 0.16-mm collimator between the sample and the crystal. The spectrometer was evacuated to a pressure of less than 1 mm Hg. In order to minimise instrumental drift during analysis, the instrument was switched on for a period of 6 h before use. The diffracted radiation at each characteristic angle was measured using a gas-flow proportional counter operated at 1450 V with pulse-height selection. P-10 gas (90% argon, 10% methane) was passed through the counter at a rate of 35 ml/min.

The unresolved first order $K\alpha_1$ and $K\alpha_2$ lines of the elements were used for quantitative analysis. However, under the conditions described above, the intense first-order tungsten $L\alpha_1$ line at 42.99° and the $L\alpha_2$ line at 43.44° emitted by the X-ray tube completely swamped the $K\alpha_{1,2}$ emission of 5-p.p.m. amounts of zinc, copper and nickel at 41.77, 44.99 and 48.64°, respectively. It has been demonstrated[4] that this tungsten radiation is removed by interposing a titanium sheet between the X-ray tube window and the sample. In the present study, a 0.0045-in thick titanium filter was found to be the minimum thickness required to eliminate the tungsten radiation, but this thickness seriously reduced the emission intensity for the required elements. A thinner filter (0.0026 in) did not eliminate the interfering tungsten lines, but their intensity was reduced to such an extent that they were completely resolved from the required zinc, copper and nickel analytical lines.

A quantitative evaluation of the analysis of the transition metals from vanadium to zinc is presented in Table II. Despite the favourable decrease in background count rates, it can be seen that the use of the titanium filter results in such a decrease in sensitivity that the standard counting error for a given sample is increased. It was therefore decided to analyse for the elements vanadium to cobalt without the titanium filter and to use the minimum thickness of filter required to completely resolve the tungsten lines (0.0026 in) when analysing for the elements nickel, copper and zinc. The relatively high background count for iron arises from the presence of iron in the cellulose powder used for preparing the standard pellets.

A further complication in the X-ray fluorescent determination of the transition elements in the presence of one another arises from the proximity of the first order $K\beta_1$ emissions of the transition elements to the first order $K\alpha$ lines of the next element in order of increasing atomic number. Thus, the LiF crystal and associated collimators used in the present work will not resolve the $K\beta_1$ line of vanadium at 69.12° from the $K\alpha$ lines of chromium at 69.29° and 69.43°. In addition, the $K\beta_1$ lines of chromium and manganese are only partially resolved from the $K\alpha$ lines of manganese and iron, respectively. Contrary to the statement of NATELSON *et al.*[4], it is not possible to remove the interfering $K\beta_1$ lines by pulse-height selection. The magnitude of the interferences was therefore investigated.

Standard paper pellets containing 10 µg each of chromium, manganese, iron, and cobalt, both alone and with varying amounts of the interfering elements were analysed under the conditions described above. The results (Table III) show that appreciable interferences may arise in the determination of chromium and manganese in the presence of vanadium and chromium, respectively. However, a correction for

TABLE II

THE DETERMINATION OF TRACE ELEMENTS BY X-RAY FLUORESCENCE SPECTROMETRY

Element $K\alpha_{1,2}$ emission (°2θ)	*Background count (600 sec)*	*Net count per µg (600 sec)*	*Detection limit (µg)*	*Standard counting error (%) 2-µg sample*
No filter				
V 76.91	20724	5958	0.07	1.9
Cr 69.34	79803	10922	0.08	2.0
Mn 62.94	81004	15108	0.06	1.4
Fe 57.49	387142	19811	0.09	2.3
Co 52.78	304508	24610	0.06	1.5
Ni 48.64	—	—	—	—
Cu 44.99	—	—	—	—
Zn 41.77	—	—	—	—
0.0026-in Ti filter				
V 76.91	—	—	—	—
Cr 69.34	4021	1545	0.12	3.4
Mn 62.94	2516	1985	0.08	2.4
Fe 57.49	56440	2299	0.31	7.5
Co 52.78	2363	2550	0.06	1.9
Ni 48.64	13334	2821	0.12	3.2
Cu 44.99	22060	3087	0.14	3.6
Zn 41.77	22462	3364	0.13	3.4
0.0045-in Ti filter				
V 76.91	—	—	—	—
Cr 69.34	790	262	0.32	8.8
Mn 62.94	732	400	0.20	5.9
Fe 57.49	12871	612	0.55	13
Co 52.78	1031	731	0.13	4.0
Ni 48.64	5760	850	0.27	6.8
Cu 44.99	6735	1012	0.24	6.0
Zn 41.77	7342	1231	0.21	5.3

TABLE III

INTER-ELEMENT INTERFERENCES DURING X-RAY FLUORESCENCE ANALYSIS

Analytical $K\alpha_{1,2}$ emission (°2θ)	*Interfering $K\beta_1$ emission (°2θ)*	*Net count per µg per 600 sec*			*Count per 600 sec per µg interfering element*
		No interfering element	*10 µg interfering element*	*20 µg interfering element*	
Cr 69.34	V 69.12	10922	18182	25506	728
Mn 62.94	Cr 62.35	15108	17330	19598	223
Fe 57.49	Mn 56.61	19811	19606	19925	0
Co 52.78	Fe 51.72	24610	24587	24499	0

these interferences can be readily determined by measuring the count rates of standards containing known amounts of the interfering elements at the 2θ angle of the required element. Interferences in the determination of iron and cobalt arising from the presence of manganese and iron, respectively, are only appreciable in the presence of relative concentrations of the interfering elements much in excess of those typically found in sea water.

The theoretical detection limits, calculated as the concentrations of each element required to give a count equivalent to 3 times the standard deviation of the background count, for a counting period of 600 sec are shown in Table II, together with the corresponding theoretical counting error for the determination of a 2-μg sample. Improved values for these parameters can be obtained either by increasing the total counting period or by increasing the sample size. Longer counting times, however, increase the possibility of errors arising from long-term instrumental instability. This possibility can be reduced by using a sequential system of counting between standards and samples, *e.g.* by counting each for 100-sec intervals in turn.

If optimum precision is not required, a more rapid analysis can be carried out by scanning samples and standards over the 2θ range from 40° to 77° at a scanning rate of 1°/min. Linear calibration curves of element concentration against peak height at the characteristic 2θ angle are obtained. Coefficients of variation of *ca.* ±15% were obtained by this procedure at the 5-μg level.

EXPERIMENTAL

Apparatus

A Quickfit upward displacement liquid/liquid extraction unit (catalogue No. 1L RDLUS) was used for continuous extraction of chelated trace metals (see p. 398). X-Ray fluorescence spectrometry measurements were made using a Philips PW 1540 instrument. All glassware must be thoroughly washed with hot nitric acid before use.

Standard metal solutions

Stock solutions containing 1 mg/ml were prepared using analytical-grade reagents and de-ionised water. The following compounds were used. Vanadium(V): 2.295 g/l ammonium metavanadate. Chromium(III): 9.602 g/l chromium potassium sulphate (24 H_2O). Chromium(VI): 3.734 g/l potassium chromate. Manganese: 3.602 g/l manganese chloride tetrahydrate. Iron: 4.979 g/l (in 1 *N* HCl) iron(II) sulphate heptahydrate. Cobalt: 4.939 g/l cobalt nitrate hexahydrate. Copper: 3.929 g/l copper(II) sulphate pentahydrate. Zinc: 4.398 g/l zinc sulphate heptahydrate.

Working standard solutions containing 1 μg/ml were prepared from these solutions by dilution.

Procedure

Filter 800 ml of sea water through a membrane filter (pore size 0.5 μ) and place it in the extractor unit. Stir 2 g of ammonium pyrrolidine dithiocarbamate into a slurry with 5 ml of the filtered sea water, add this to the sea water in the extractor unit and mix well by stirring. Adjust the pH of the solution to 2–3 (indicator paper) by dropwise addition of 5 *N* hydrochloric acid (A.R.). Introduce the solvent distributor column into the solution and attach the extraction flask. Pour previously redistilled methyl isobutyl ketone down the extractor column and allow the ketone to run over into the extraction flask until it contains *ca.* 30 ml of solvent. Add the upper piece of the extraction unit and condenser and lag the upper piece.

Boil the ketone and allow the circulation to continue for 3 h. After cooling, remove the extraction flask and distil off the excess ketone from it, leaving *ca.* 5 ml of solution. Carry out the nitric acid fuming, pellet making and X-ray fluorescent spectrometry as described in the previous sections. Samples and standards must be prepared with an identical volume of nitric acid in order to obviate contamination from this reagent. It is advisable to use electronic-grade nitric acid, which contains less iron than the analytical-grade acid.

Prepare calibration curves for each of the elements to be determined over the range 0–25 μg, from pellets prepared in the same manner from suitable evaporated portions of the diluted standard solutions. Separate standard pellets must be prepared containing vanadium or chromium alone in order to determine the correction which must be applied for their contribution to the count obtained when measured at the chromium and manganese $K\alpha_{1,2}$ peaks, respectively.

TABLE IV

RECOVERY OF TRACE ELEMENTS ADDED TO SEA WATER

Element	*Concentration ($\mu g/l$)*							
	Sea water alone	*Mean*	*Sea water + 2 $\mu g/l$ added*		*Sea water + 4 $\mu g/l$ added*		*Sea water + 6 $\mu g/l$ added*	
			Expected	*Found*	*Expected*	*Found*	*Expected*	*Found*
V	0.85 1.05 0.79 0.74	0.86 ± 0.14	2.86	2.59	4.86	4.45	6.86	6.81
Cr	0.31 0.38 0.27 0.20	0.29 ± 0.07	2.29	2.14	4.29	4.56	6.29	6.45
Mn	1.99 1.84 1.84 1.75	1.86 ± 0.10	3.86	3.93	5.86	5.64	7.86	8.00
Fe	4.93 4.56 4.62 4.81	4.73 ± 0.17	6.73	6.80	8.73	8.72	10.7	9.61
Co	0.04 0.07 0.05 0.10	0.07 ± 0.03	2.07	2.29	4.07	4.14	6.07	6.27
Ni	1.81 1.72 2.19 2.00	1.93 ± 0.21	3.93	4.11	5.93	6.12	7.93	8.11
Cu	11.8 11.2 12.2 11.4	11.7 ± 0.4	13.7	13.3	15.7	14.8	17.7	17.0
Zn	25.8 25.4 24.7 24.8	25.2 ± 0.5	27.2	28.0	29.2	28.5	31.2	32.4

RESULTS

Some preliminary experiments were carried out in order to determine whether the extraction procedure would discriminate between trivalent and hexavalent chromium. Determination of the chromium content of 800-ml portions of a sea water sample both alone and to which 5 μg of either chromium(III) (as chromic potassium sulphate) or chromium(VI) (as potassium chromate) had been added gave recoveries of 102% and 106%, respectively, of the added species. This result is surprising since the extraction of chromium(III) as its APDC complex has not been reported in the literature.

As a test of the method, a series of 800-ml portions of sea water from the Menai Straits was analysed both alone and when spiked with 2, 4 and 6 μg/l amounts of the trace elements. For chromium and cobalt, which were present at a concentration of less than 1 μg/l, greater accuracy was obtained by counting combined evaporated extracts from three 800-ml portions of sea water. The results, including quadruplicate analyses of the sea water alone, which are shown in Table IV, indicate that the analytical process has a satisfactory accuracy.

SUMMARY

A procedure is described for the determination of microgram quantities of the elements vanadium, chromium, manganese, iron, cobalt, nickel, copper and zinc in sea water. Separation and concentration of these elements from a large salt matrix, in order to prevent interferences in the subsequent X-ray fluorescence spectrometry, is achieved by continuous solvent extraction. Ammonium pyrrolidine dithiocarbamate is used as a chelating agent, and the chelated trace elements are quantitatively extracted at a pH of *ca.* 2.5 into methyl isobutyl ketone. Detection limits of 0.14 μg or better are obtained when a 600-sec counting period is used for X-ray fluorescence spectrometry.

RÉSUMÉ

Un procédé est décrit pour le dosage par spectrométrie de fluorescence aux rayons-X de microquantités des éléments: vanadium, chrome, manganèse, fer, cobalt, nickel, cuivre et zinc dans l'eau de mer. On sépare et on concentre ces éléments d'avec la matrice de sel, pour éviter des interférences spectrométriques, par extraction continue dans un solvant. Le dithiocarbamate d'ammonium pyrrolidine est utilisé comme agent chélatant; les chélates obtenus avec les traces de métaux sont quantitativement extraits à un pH d'environ 2.5 dans la méthylisobutylcétone. Limites de détection: 0.14 μg ou mieux, avec une période de comptage de 600 sec pour la spectrométrie de fluorescence aux rayons-X.

ZUSAMMENFASSUNG

Die gleichzeitige Bestimmung von Mikrogrammen der Elemente Vanadin, Chrom, Mangan, Eisen, Kobalt, Nickel, Kufper und Zink in Seewasser mit Hilfe der Röntgenfluoreszenzanalyse wird beschrieben. Um Störungen bei der Spektralanalyse

zu vermeiden, werden diese Elemente aus einer grossen Salzmatrix mit Hilfe kontinuierlicher Flüssigextraktion abgetrennt und angereichert. Die Spurenelemente werden dabei quantitativ als Pyrrolidindithiocarbamate bei einem pH-Wert von etwa 2.5 mit Methylisobutylketon extrahiert. Bei einer Zählzeit von 600 sec wurden Nachweisgrenzen von 0.14 μg oder besser erhalten.

REFERENCES

1 J. P. Riley, in *Chemical Oceanography*, Vol. 2, Academic Press, New York, 1965, pp. 323–362.
2 B. P. Fabricand, R. R. Sawyer, S. G. Ungar and S. Adler, *Geochim. Cosmochim. Acta*, 26 (1962) 1023.
3 D. F. Schutz and K. K. Turekian, *Geochim. Cosmochim. Acta*, 29 (1965) 259.
4 S. Natelson, D. R. Leighton and C. Calas, *Microchem. J.*, 6 (1962) 539.
5 J. D. H. Strickland and T. R. Parsons, *Bull. Fisheries Res. Board Can.*, No. 125 (1960) 185 pp.
6 E. D. Goldberg, in M. Hill, *The Sea*, Vol. 2, Interscience, New York, p. 7.
7 R. Fukai, *Nature*, 213 (1967) 901.
8 L. Chuecas and J. P. Riley, *Anal. Chim. Acta*, 35 (1966) 240.
9 L. P. Ducret, *Ann. Chem.*, 6 (1951) 705.
10 M. Kalk, *Nature*, 198 (1963) 1010.
11 E. K. Duursma and W. Sevenhuysen, *Neth. J. Sea Res.*, 3 (1966) 95.
12 H. Malissa and E. Schoffmann, *Mikrochim. Acta*, (1955) 187.
13 T. J. Chow and T. G. Thompson, *J. Marine Res. (Sears Found. Marine Res.)*, 11 (1952) 124.
14 E. Rona, D. W. Hood, L. Muse and B. Buglio, *Limnol. Oceanog.*, 7 (1962) 201.
15 W. R. G. Atkins, *J. Marine Biol. Assoc. U.K.*, 20 (1936) 625.
16 R. R. Brooks, B. J. Presley and J. R. Kaplan, *Anal. Chim. Acta*, 38 (1967) 321.
17 R. R. Brooks, *Geochim. Cosmochim. Acta*, 29 (1965) 1369.
18 C. L. Luke, *Anal. Chem.*, 36 (1964) 318.
19 H. A. Liebhafsky, H. C. Pfeiffer, F. H. Winslow and D. D. Zemany, *X-ray Absorption and Emission in Analytical Chemistry*, John Wiley, New York, 1960, 357 pp.

Analytica Chimica Acta
Elsevier Publishing Company, Amsterdam
Printed in The Netherlands

CATHODE-RAY-EXCITED EMISSION SPECTROSCOPIC ANALYSIS FOR TRACE RARE EARTHS

PART II. DETERMINATION OF EUROPIUM

SIMON LARACH
RCA Laboratories, Princeton, N. J. 08540 (U.S.A.)

(Received February 9th, 1968)

The concept of utilizing cathode-ray-excited emission spectroscopy for the detection of rare earths was discussed in a previous paper[1]. The trace rare earths were excited by cathode rays to emit their characteristic *f–f* luminescence emission, and a *hauptlinien* spectrum and table of sensitivities were derived for each of the pertinent rare earths. From these, it can be seen that, in an yttrium oxide matrix, the 611-nm emission line is most sensitive for europium, and this emission ($^5D_0 \rightarrow {}^7F_2$) was chosen for one of the detection lines for the determination of trace amounts of europium. For a second line, the 533-nm emission ($^5D_1 \rightarrow {}^7F_1$) was selected.

EXPERIMENTAL

Sample preparation

Ultrapure (99.9999% purity with respect to rare earths) yttrium oxide was used as the primary matrix material. Series of yttrium oxide samples containing amounts of europium (sulfate) from $5 \cdot 10^{-4}\%$ to 0.1% were prepared in quadruplicate, by the firing procedures described previously[1]. "Blanks" were prepared in identical fashion. Similar procedures were used also in preparing known trace amounts of europium in a gadolinium oxide matrix.

Measurements

A demountable cathode-ray equipment was used for the measurements as described previously[1], in conjunction with a grating spectroradiometer and RCA 1P21 multiplier phototube (S4 surface); the detection wavelength was 611 nm or 533 nm. All samples were placed together on the metal disk, and were measured successively.

RESULTS AND DISCUSSION

Figure 1 shows the relative cathodoluminescence emission intensity at 611 nm as a function of concentration of europium(III) in the Y_2O_3 matrix. These data were obtained at an acceleration potential of 8000 V and a beam current of 1 μA. The "blank" reading of a sample determined as part of the same run indicated a residual emission at 611 nm which was equivalent to 0.25 p.p.m. of europium. This blank was subtracted from the values of the series containing europium. In Fig. 1, linearity is present between roughly 0.5 p.p.m. and 100 p.p.m.; at 500 p.p.m. (and beyond) the intensity–concentration curve becomes non-linear. This is in approximate agreement with BROWN *et al.*[2] who found rare earth ion–ion interactions appearing at about 1000 p.p.m.

Matrix effects

Whereas Fig. 1 summarizes the data for europium in yttrium oxide, the results for europium in a gadolinium oxide matrix are shown in Fig. 2. Again, non-linearity of the intensity *vs.* concentration curve occurred above 100 p.p.m. As was mentioned previously[1], a change in the matrix can have beneficial results; in the present case, the intensity of the 611-nm emission from europium in Gd_2O_3 was about seven times greater than that in Y_2O_3.

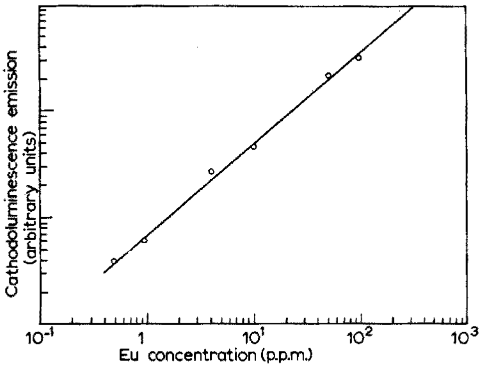

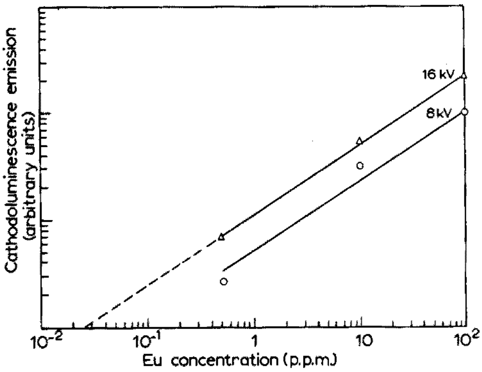

Fig. 1. Cathodoluminescence emission intensity at 611 nm as a function of europium concentration in Y_2O_3 matrix at 8 kV.

Fig. 2. Cathodoluminescence emission intensity at 611 nm for two accelerating potentials as a function of europium concentration in Gd_2O_3 matrix.

Voltage effects

The cathodoluminescence emission intensity varies directly with the potential through which the primary electrons are accelerated[1]. This relationship can be utilized to increase the emission intensity, particularly where very small traces ($<$ 1 p.p.m.) of europium are involved. Cautions to be observed include (*1*) measuring the "blank" sample under the higher voltage condition, and (*2*) measuring an entire run under these conditions*.

The data for curve (b) of Fig. 2 were obtained with 16 keV electrons, while curve (a) shows data for 8 keV electrons. Clearly, the linear relationship also exists at 16 kV, the slope being the same as that of the 8-kV curve; the 1000 p.p.m. material showed signs of saturation, again presumably due to ion–ion interactions.

---

* Samples in a particular series should be analyzed at the same beam voltage and current. Results for one matrix do not necessarily duplicate these of another matrix, particularly at high voltages, where differences in secondary emission may take place.

Detection wavelength

All measurements for Figs. 1 and 2 were taken at a detection wavelength of 611 nm, the most sensitive europium line, as indicated by the *hauptlinien* spectrum[1]. This line is due to the transition $^5D_0 \rightarrow {}^7F_2$ in europium(III). It is of interest to test other transitions, and the $^5D_1 \rightarrow {}^7F_1$ transition at 533 nm, was chosen for this. Figure 3 summarizes the effects found in utilizing this detection wavelength for europium in Gd_2O_3. It is of interest to note the change in slopes when 533 nm was used as the detection wavelength. Thus, for europium in gadolinium oxide, the slope remained fairly constant, at about 0.4, for each condition of voltage and detection wavelength. However, for europium in yttrium oxide, the slope changed from 0.8 for detection at 611 nm, to 0.45 for detection at 533 nm.

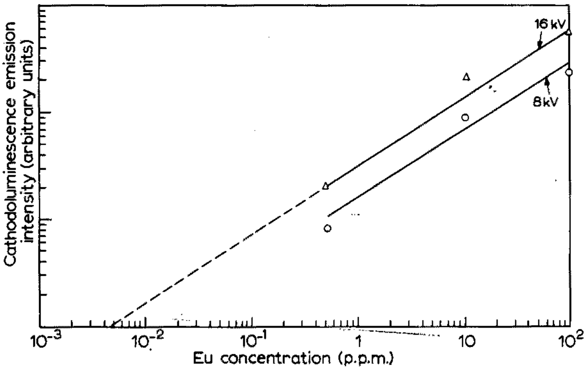

Fig. 3. Cathodoluminescence emission intensity at 533 nm for two accelerating potentials as a function of europium concentration in Gd_2O_3 matrix.

Interferences

It is well known that different species of rare earth ions in the same matrix may interact, and in doing so, affect the luminescence emission intensity. Such interactions have been shown to be dependent on (*a*) ion type, (*b*) concentration, and (*c*) matrix type[3]. However, in general, such interactions are not taken as applying to any large extent where the concentration of the trace ion is much less than about 0.1%. In the general cathode-ray-excited emission method being described in the present series of papers, interferences can manifest themselves in either or both of two ways. Type I interfering ions may emit spectrally in a region which overlaps the emission from the desired ion, thereby reinforcing the emission by increasing the number of photons available to the detector and giving rise to a positive error. The Type II interfering ion can interact with the ion under investigation in such a way that the number of radiative transitions of the latter ion is effectively *decreased* thereby yielding a negative error.

In the absence of large amounts of interfering ions, the possibilities of spectral reinforcement can be avoided by making use of a secondary line for the rare earth, as shown in the *hauptlinien* spectrum shown previously[1].

Examples of the two types of interference can be seen in the following experiments. As can be seen from the *hauptlinien* spectrum of rare earths in yttria[1], the 611-nm emission from europium is flanked by the 607-nm and 617-nm emissions from samarium, while the closest samarium line to the europium 533-nm line is at 565 nm. A series of samples was prepared, with yttrium oxide as the matrix, containing 5 p.p.m. of europium(III), together with various amounts of samarium. The results are shown in Table I.

TABLE I

RELATIVE CATHODOLUMINESCENCE EMISSION INTENSITIES AT 611 nm AND AT 533 nm

Material	*611 nm*	*533 nm*
(a) Y_2O_3:Eu (5 p.p.m.)	100	100
Y_2O_3:Eu (5 p.p.m.):Sm (10 p.p.m.)	187	100
Y_2O_3:Eu (5 p.p.m.):Sm (10^2 p.p.m.)	800	67
:Sm (10^3 p.p.m.)	1400	45
(b) Y_2O_3:Eu (100 p.p.m.)	100	100
Y_2O_3:Eu (100 p.p.m.):Sm (10^2 p.p.m.)	107	96
:Sm (10^3 p.p.m.)	60	32
(c) Y_2O_3:Eu (1000 p.p.m.)	100	100
Y_2O_3:Eu (1000 p.p.m.):Sm (10^3 p.p.m.)	47	46
(d) Y_2O_3:Eu (5 p.p.m.)	100	100
Y_2O_3:Eu (5 p.p.m.):Dy (10 p.p.m.)	100	85
:Dy (10^2 p.p.m.)	—	62
:Dy (10^3 p.p.m.)	69	32
(e) Y_2O_3:Eu (100 p.p.m.)	100	100
Y_2O_3:Eu (100 p.p.m.):Dy (10^2 p.p.m.)	78	75
:Dy (10^3 p.p.m.)	9	13

As can be seen in Table I (a), Type I spectral reinforcement by samarium of the europium 611-nm emission can lead to very large errors in the true reading of this line, particularly as the interfering samarium content is increased to 10^3 p.p.m. However, the 533-nm line of europium is unaffected by small (*ca.* 10 p.p.m.) amounts of samarium, and only slightly affected by larger amounts; even 10^3 p.p.m. of samarium yields an error of only 55% as against the enormous error at the 611-nm line. It can also be seen from Table I (b) that increasing the amount of europium to 100 p.p.m., although this gives greater tolerance to the amount of samarium interference, still shows spectral reinforcement of the 611-nm line, compared to the 533-nm emission. In Table I (c), the large concentration of rare earths would indicate that Type II interference (ion–ion interaction) would be expected to predominate over spectral reinforcement; that this is the case is shown by the identical intensity readings of the 611-nm and 533-nm lines of europium.

As another Type II interfering ion, dysprosium was chosen, since this showed the highest cathode-ray excited intensity[1]. The results for dysprosium given in Table I (d–e), bear out the conclusions arrived at with the Type I interfering ion, samarium, namely that when the interfering trace is low (*i.e.*, of the same magnitude as the europium trace, both being less than 100 p.p.m.), the intensity of the lines will give a valid reading.

Detection limits and analyses

Europium, in a pure yttrium oxide matrix, can be detected to a level of about

0.1 p.p.m., when the 611-nm emission line is used. However, by taking advantage of matrix effects, and by increasing the electron beam accelerating potential, the detection limit can be made lower. Thus, for a matrix of gadolinium oxide, if excitation with 16-keV electrons is used, and the 533-nm emission is measured, the detection limit for europium, *by extrapolation*, is about 0.005 p.p.m. Extension of this method of analysis to "sub-traces" in the p.p.b. range will be reported on more thoroughly in future papers.

Typical analyses were carried out by adding various amounts of europium to pure yttrium oxide; the results, calculated from the standard curve of Fig. 1 are shown in Table II.

TABLE II

ANALYSES OF Y_2O_3:Eu (x p.p.m.) AT 611 nm

Eu added (p.p.m.)	0.70	2.3	14	60
Eu found (p.p.m.)	0.67	2.2	13	57

TABLE III

CATHODOLUMINESCENCE EMISSION INTENSITIES AT 611 nm AND AT 533 nm FOR Y_2O_3:Eu, DOPED WITH IRON, NICKEL AND MANGANESE

Material	*Intensity at 611 nm*	*Intensity at 533 nm*
Y_2O_3:Eu (100 p.p.m.)	100	100
Y_2O_3:Eu (100 p.p.m.):Fe (100 p.p.m.)	88	92
Y_2O_3:Eu (100 p.p.m.):Mn(100 p.p.m.)	77	80
Y_2O_3:Eu (100 p.p.m.):Ni (100 p.p.m.)	97	92

It is also of interest to consider interferences of the first transition group, and for this purpose, samples of Y_2O_3:Eu (100 p.p.m.) were prepared with 100 p.p.m. each of iron, manganese and nickel. The results are shown in Table III. It is evident that ions of the first transition group can interfere in this determination of europium, which indicates the possibility of coupling between $4f$ and $5d$ electrons. Manganese, the ion showing the largest interference effect on europium, can itself be "poisoned", luminescence-wise, by iron and by nickel in group II–group VI compounds[4].

Discussion

As was pointed out previously[1], the cathode-ray-excited emission method of spectroscopic analysis is not limited to a single matrix; any matrix can be utilized which incorporates the rare earth, and supports cathodoluminescence. As has been shown[1], the matrix can affect the particular *f–f* emission line in the *hauptlinien* spectrum, and as demonstrated in the present paper, the sensitivity and ultimate detection limit, are also a function of the matrix and of the transition. Thus, for europium in yttrium oxide, the slope of the intensity–concentration curves reported by WALTERS *et al.*[5] and by LINARES *et al.*[6] for analyses of europium in yttrium oxide by the X-ray excitation method was about 0.8. However, as shown in the present work, by using the 533-nm line as a detection line with the ($^5D_1 \rightarrow {}^7F_1$) transition instead of the 611-nm transition ($^5D_0 \rightarrow {}^7F_2$), the slope becomes 0.45, with the result that smaller amounts of europium can be detected. Even lower detection limits can be obtained by increasing the electron acceleration potential, resulting in greatly increased intensity, with the slope remaining at 0.45. Thus, by optimizing matrix and electron beam potential, this technique can yield a detection limit for europium in the p.p.b. range.

As in any other analytical method, interferences can be a grave source of error. AXE AND WELLER[7] have investigated the effect of rare earth co-dopants on the $^5D_0 \rightarrow {}^7F_2$ fluorescence (611 nm) of rather large amounts of europium (1%) in yttrium oxide, by means of optical excitation. With the exception of gadolinium, which had no effect, all other rare earths caused a decrease in luminescence, neodymium having the most pronounced effect. They accounted for this as being due to nonradiative resonant energy transfer, with overlap of near zone quadrupolar fields. VAN UITERT *et al.*[8] have also discussed energy transfer between rare earth ions.

With respect to interference with small amounts of europium, WALTERS *et al.*[5], using X-ray excitation of Y_2O_3:Eu (100 p.p.m.), investigated the effect of 100 p.p.m. of other rare earths, and reported the europium emission intensity to be independent of the rare earth co-dopant. The present paper, however, shows that although europium is relatively unaffected by trace amounts of samarium, dysprosium can interfere, even in small amounts, depending on the europium content. Interferences between europium and ions of the first transition group should also be avoided. Reliable analyses for europium in materials containing such impurities are quite feasible if the co-dopants are known, and if the standard curve is prepared from measurements of matrices containing europium and the co-dopants. That some co-dopants can exert an "intensifier" action on europium has been disclosed recently by THOMPSON[9]; again, the effects of such ions can be taken into account in the standard samples.

The aid of R. A. KAUFFUNGER in preparation of materials and of Dr. W. H. FONGER in the measurements is gratefully acknowledged.

SUMMARY

Trace amounts of europium can be determined quantitatively *in situ* by excitation with cathode rays (electrons) and detection of europium transitions. Europium can then be determined from a standard plot of intensity *vs.* concentration. Matrix effects, voltage effects, detection lines, and rare-earth and first-transition-group interferences are discussed. While the detection limit of europium under normal conditions is about 0.1 p.p.m., optimizing the above effects yields an ultimate detection limit, by extrapolation, of about 0.005 p.p.m.

RÉSUMÉ

Il est possible de doser l'europium à l'état de traces par excitation à rayons cathodiques (électrons) et détection des transitions europium. On examine l'influence des matrices, de la tension, des lignes de détection et des interférences des terres rares et du premier groupe de transition. Bien que la limite de détection de l'europium dans les conditions normales soit d'environ 0.1 p.p.m. on peut arriver à une limite d'environ 0.005 p.p.m. par extrapolation.

ZUSAMMENFASSUNG

Spuren von Europium können im Ausgangsmaterial quantitativ durch Anregung mit Kathodenstrahlen und Nachweis der Europium-Übergänge bestimmt werden. Es werden Einflüsse der Matrix und der Spannung, die Nachweislinien und Störungen durch andere Seltene Erden und Elemente der ersten Übergangsgruppe diskutiert. Während unter normalen Bedingungen die Nachweisgrenze für Europium 0.1 p.p.m. beträgt, kann man durch Optimalisierung der oben genannten Effekte durch Extrapolation eine Nachweisgrenze von etwa 0.005 p.p.m. erreichen.

REFERENCES

1 S. Larach, *Anal. Chim. Acta*, 41 (1968) 189.
2 M. R. Brown, J. S. S. Whiting and W. A. Shand, *J. Chem. Phys.*, 43 (1965) 1.
3 L. G. Van Uitert and R. R. Soden, *J. Chem. Phys.*, 36 (1962) 1289.
4 R. H. Bube, S. Larach and R. E. Shrader, *Phys. Rev.*, 92 (1953) 1135.
5 R. M. Walters, J. F. Cosgrove and D. J. Bracco, *Symposium on Trace Charac., Gaithesburg, Md., October 1966*, p. 174–180.
6 R. C. Linares, J. B. Schroeder and L. A. Hurlbut, *Spectrochim. Acta*, 21 (1965) 1915.
7 J. D. Axe and P. F. Weller, *J. Chem. Phys.*, 40 (1964) 3066.
8 L. G. Van Uitert and L. F. Johnson, *J. Chem. Phys.*, 44 (1966) 3514.
9 G. L. Thompson, *U.S. Patent 3,322,682*, May 30, 1967.

Analytica Chimica Acta
Elsevier Publishing Company, Amsterdam
Printed in The Netherlands

SPECTROPHOTOMETRIC DETERMINATION OF YTTRIUM WITH MOLYBDOPHOSPHORIC ACID

BRYAN L. MADISON AND JOHN C. GUYON
Department of Chemistry, University of Missouri, Columbia, Mo. 65201 (U.S.A.)

(Received February 7th, 1968)

Although many chromogenic reagents have been utilized for the spectrophotometric measurement of yttrium, there appears to be no reference to a heteropoly acid technique. During an investigation into the use of molybdophosphoric acid for the determination of thorium[1], yttrium was observed to produce a positive interference with the reagent. The purpose of this investigation was to examine the possibility of developing a heteropoly acid method for the determination of yttrium, and to gain information concerning the complex formed between molybdophosphoric acid and yttrium.

EXPERIMENTAL

Apparatus

All spectrophotometric measurements were made on a Cary Model 12 recording spectrophotometer using 1.000±0.002 cm quartz cells. Measurements of pH were made with a Beckman Zeromatic pH meter.

Reagents

Standard yttrium solution. A solution containing 10 mg of yttrium per ml was prepared by dissolving 3.175 g of Y_2O_3 (99.9%) in 30 ml of concentrated nitric acid and diluting the resulting solution to 250 ml. The solution was subsequently standardized gravimetrically. Appropriate dilutions of this solution were made with 1 *M* nitric acid to obtain standard yttrium solutions.

Sodium molybdate–potassium phosphate solution. An 8:1 molybdate–phosphate solution was prepared by dissolving 387.168 g of sodium molybdate dihydrate and 27.218 g of potassium dihydrogen phosphate in water and diluting to 1 l. This gave a solution 1.6 *M* in molybdate and 0.2 *M* in phosphate.

Tin(II) chloride solution. A 0.5% solution was prepared by dissolving 0.595 g of tin(II) chloride dihydrate in 2 ml of concentrated hydrochloric acid and diluting to 100 ml with water. This solution was prepared fresh daily.

Recommended procedure

Based on preliminary experiments and a study of the effect of variables the following recommended procedure was developed. To a solution containing 0.2–8 p.p.m. of yttrium were added 5 ml of 1:10 sulfuric acid and 10 ml of 8:1 molybdate–phosphate reagent, and the volume was adjusted to *ca.* 25 ml. The pH was adjusted to 4.8 with dilute sulfuric acid or sodium hydroxide and a stopwatch started. After *ca.* 5 min, 20 ml of aqueous 25% sodium citrate dihydrate was added and exactly 5 sec later, 2 ml of the tin(II) solution was added by means of a hypodermic syringe. The resulting blue solution was transferred to a 100-ml volumetric flask and diluted to the mark. The absorbance was measured at 695 nm approximately 20 min after the reduction, in 1-cm cells with distilled water as a reference.

STUDY OF VARIABLES

Stability

It was obvious early in the study that the reaction between yttrium and molybdophosphoric acid resulted in a somewhat unstable species. When the reagents were mixed and the pH was adjusted, the yellow color of the unreduced ternary complex formed almost immediately. The absorption spectrum of this species is given in Fig. 1. This yellow color disappeared immediately in moderate or high concentrations of acid, but reasonable stability of the ternary species was found in the presence of dicarboxylic and α-hydroxycarboxylic acids. Of the acids tested, citrate was found to have very little effect on the ternary complex, but was effective in destroying the binary molybdophosphoric acid. Citrate thus provided a means of removing excess molybdophosphoric acid, and of achieving a low blank reading.

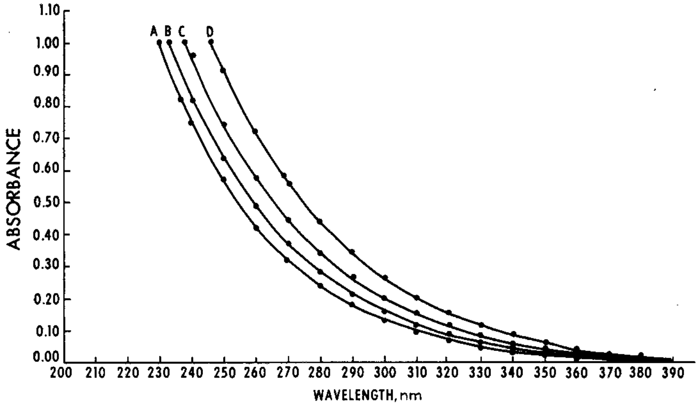

Fig. 1. Absorption spectra of unreduced Mo–P–Y complex. (A) 0.00; (B) 0.25; (C) 0.50; (D) 1.00 mg Y.

Upon addition of the chlorostannous acid the blue color of the reduced complex was fully developed in 5 min, and remained stable for about 90 min. The absorption spectrum of the reduced species showed a broad band between 600 and 800 nm, with a maximum at 695 nm.

Effect of pH

Solutions containing 5 p.p.m. of yttrium were treated as in the recommended procedure except that the pH was varied. The results of this study are shown in Fig. 2. A pH of 4.8 was chosen and it is apparent that the extent of complex formation, and hence the absorbance of the final solution, is highly dependent upon the pH of the solution. Several acids were investigated. Hydrochloric acid gave slightly higher absorbances, but the resulting blue color was unstable. Sulfuric acid was chosen because it gave a quite stable blue color with excellent sensitivity.

Effect of reagent concentrations, time and temperature

Effect of molybdate–phosphate concentration. Solutions containing 2.5 p.p.m. of yttrium were treated as in the recommended procedure except that the concentration of the 8:1 molybdate–phosphate concentration was varied. The results of this study are given in Table I. A volume of 10 ml of the 8:1 molybdate–phosphate reagent was chosen for subsequent work.

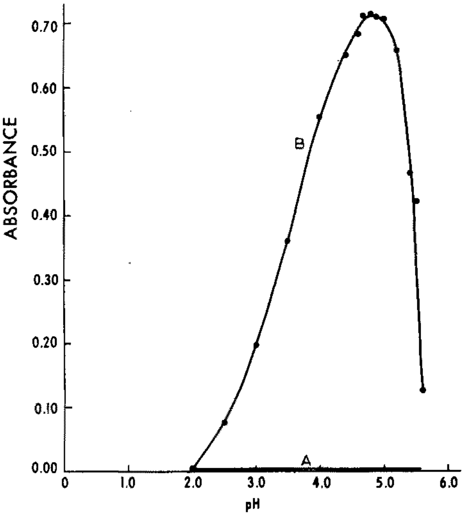

Fig. 2. Effect of pH. (A) reagent blank; (B) 0.5 mg Y.

TABLE I

EFFECT OF 8:1 MOLYBDATE–PHOSPHATE CONCENTRATION

(0.25 mg Y/100 ml solution)

Reagent added (ml)	*Absorbance (695 nm)*	*Reagent added (ml)*	*Absorbance (695 nm)*
0.5	0.123	6.0	0.625
1.0	0.291	8.0	0.626
1.5	0.443	10.0	0.631
2.0	0.523	14.0	0.627
3.0	0.580	16.0	0.629
4.0	0.612	20.0	0.628

Effect of time on complex formation. Solutions containing 5 p.p.m. of yttrium were treated as in the recommended procedure, allowed to stand for different periods of time and then reduced as described. The absorbance of the reduction product was taken as a measure of completeness of complex formation. The absorbance measurements showed that complex formation was nearly instantaneous. To facilitate easy handling of samples, a time of 5 min was selected.

Effect of temperature. Temperature had little effect on the degree or rapidity of complex formation, but elevated temperatures accelerated the interaction between citrate and the ternary species. It was decided to perform subsequent experiments at room temperature.

Effect of sodium citrate concentration. Citrate ion was necessary in the determination to prevent reduction of excess of molybdophosphoric acid. Citrate ion interacts with the molybdate aggregate and forms a non-reducible complex. Solutions containing 2.5 p.p.m. of yttrium were treated as in the recommended procedure except that the concentration of the 25% sodium citrate was varied. The results of this study are shown in Fig. 3; 20 ml of 25% sodium citrate was chosen for further work.

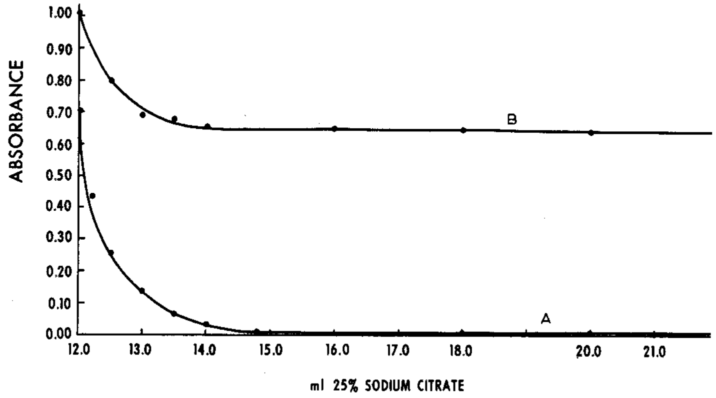

Fig. 3. Effect of sodium citrate concentration. (A) reagent blank; (B) 0.25 mg Y.

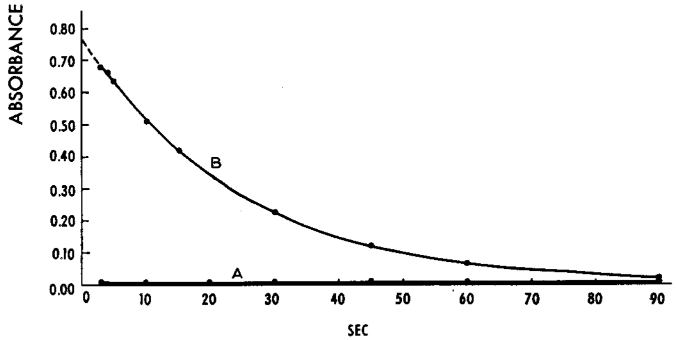

Fig. 4. Time between addition of citrate and reductant. (A) reagent blank; (B) 0.25 mg Y.

Choice and handling of reductant. If given sufficient time, citrate ion decomposes the complex before reduction. To avoid partial complex decomposition, a reductant was required which would give instantaneous color development. Chlorostannous acid gave faster and greater enhancements than other reductants tested.

The time between addition of the citrate and addition of the reductant was studied. The absorbance data (Fig. 4) show that the reductant must be added rapidly to avoid partial complex decomposition. A hypodermic syringe was therefore used to add the reductant exactly 5 sec after the addition of citrate; 5 sec was as fast as was compatible with reproducible results.

Effect of tin(II) concentration. Solutions containing 2.5 p.p.m. of yttrium were treated as in the recommended procedure except that the concentration of tin(II) was varied. The absorbance at 695 nm increased as the added volume of 0.5% tin(II) chloride solution was increased to 1.5 ml and then remained constant up to an addition of 5.0 ml; an addition of 2.0 ml was chosen for subsequent work.

Effect of volume on complex formation. Solutions containing 2.5 p.p.m. of yttrium were treated as in the recommended procedure except that the volume was adjusted to different values by adding water and then adjusting the pH of the solution to 4.8. The data showed a substantial decrease in absorbance with increasing volume. To insure completeness of reaction and eliminate concentration effects, it was necessary to maintain the volume at 25 ml or less.

Effect of molybdate–phosphate ratio. This variable was investigated on solutions containing 2.5 p.p.m. of yttrium. The phosphate concentration of the reagent was maintained at 0.2 *M* and the molybdate concentration varied to give ratios of MoO_4 to PO_4 from 1 to 12. The absorbance increased up to a ratio of 3:1 with no further change at higher ratios. The 8:1 ratio was maintained as used in the previous studies.

Conformity to Beer's law, sensitivity and accuracy

A straight line calibration curve showed conformity to Beer's law for the concentration range studied (0–8 μgY/ml). The molar absorptivity was calculated to be 24,000 and the mean sensitivity (Sandell method) is 0.0035 $\mu g/cm^2$. The range of the method can be varied widely by proper choice of size of sample and cells.

TABLE II

ACCURACY OF THE METHOD

Y (p.p.m.)		*Rel. error (%)*	*Std. dev. (p.p.m.)*
Added	*Found*[a]		
7.90	7.91	0.13	0.02
2.50	2.52	0.80	0.02
5.00	4.96	0.80	0.03
0.50	0.48	4.00	0.04

[a] Mean of 3 determinations.

TABLE III

EFFECT OF DIVERSE IONS

(0.25 mg Y/100 ml solution)

Ion	*Added as*	*Amount permitted (mg)*	*Ion*	*Added as*	*Amount permitted (mg)*
NO_3^-	$NaNO_3$	10	Cd^{2+}	$Cd(NO_3)_2$	10
Cl^-	NaCl	10	UO_2^{2+}	$UO_2(NO_3)_2$	10
SO_4^{2-}	Na_2SO_4	10	Mg^{2+}	$MgCl_2$	10
PO_4^{3-}	NaH_2PO_4	10	IO_3^-	KIO_3	5
SCN^-	KSCN	10	$C_2H_3O_2^-$	$NaC_2H_3O_2$	10
Co^{2+}	$Co(NO_3)_2$	2	Br^-	KBr	10

The accuracy of the method developed was evaluated by carrying known amounts of added yttrium through the recommended procedure and studying its recovery. The results of this study are presented in Table II.

Effects of diverse ions

Solutions containing 2.5 p.p.m. of yttrium were treated as in the recommended procedure, and in addition, 10 mg of various ions were added. A 2% error in the determination of yttrium was considered tolerable. Silver(I), lead(II) and barium(II) formed insoluble precipitates. The following ions interfered seriously: Th^{4+}, As^{3+}, Fe^{2+}, Fe^{3+}, Al^{3+}, VO_3^-, WO_4^{2-}, Ni^{2+}, Ti^{4+}, Zr^{4+}. The rare earths also interfere. The ions listed in Table III can be tolerated in the concentration range reported.

DISCUSSION

Studies are being conducted in an effort to explain the chemistry of the system. Ultraviolet spectra (Fig. 1) show bathochromic shifts with increasing yttrium concentration and this furnishes evidence of an yttrium interaction with molybdophosphoric acid.

A yellow pyridine adduct of the unreduced complex can be prepared. A blue pyridine adduct of the reduced complex has also been prepared. Spectrographic analysis indicates that these materials contain only yttrium, phosphorus and molybdenum in major amounts. Efforts are being made to characterize these substances more completely.

Conventional spectrophotometric techniques for determining complex ion ratios failed to provide conclusive evidence on the nature of the species in solution probably because of the high concentration of molybdophosphoric acid necessary for complex formation (Table I). The adduct studies, which are in progress, should give considerable information as to the nature of the ternary species.

The spectrophotometric method presented here is simple and sensitive but subject to various interferences. Perhaps its chief advantage is that several-fold excesses of lanthanum and cerium do not interfere. Since phosphate is a necessary reagent in this procedure, the method will have a distinct advantage over previous methods reported because no insoluble precipitate is formed. The method should be especially useful in chemical yield studies of fission products separated on an ion-exchange column.

SUMMARY

A simple sensitive spectrophotometric determination of yttrium, based on the reaction of molybdophosphoric acid with yttrium at pH 4.8, is described. The resulting complex is reduced and the absorbance measured at 695 nm. The method is applicable in the presence of several-fold excesses of lanthanum, cerium, and phosphate.

RÉSUMÉ

On décrit un dosage spectrophotométrique simple et sensible de l'yttrium basé sur la réaction de l'acide molybdophosphorique au pH de 4.8. Le complexe formé est réduit; l'absorption est mesurée à 695 nm. Cette méthode est applicable à l'analyse de l'yttrium en présence d'excès, de plusieurs fois, de lanthane, cérium et phosphate.

ZUSAMMENFASSUNG

Eine einfache, empfindliche, spektralphotometrische Bestimmung von Yttrium, die auf der Reaktion von Molybdophosphorsäure mit Yttrium beim pH 4.8 beruht, wird beschrieben. Der resultierende Komplex wird reduziert und die Absorption bei 695 nm gemessen. Die Methode ist anwendbar in Gegenwart eines mehrfachen Überschusses von Lanthan, Cer und Phosphat.

REFERENCE

1 B. L. Madison and J. C. Guyon, *Anal. Chem.*, 39 (1967) 1706.

Analytica Chimica Acta
Elsevier Publishing Company, Amsterdam
Printed in The Netherlands

RADIOCHEMICAL PURIFICATION OF MICROGRAM AND SUB-MICROGRAM AMOUNTS OF BERYLLIUM

N. R. PIPER
Australian Atomic Energy Commission Research Establishment, Lucas Heights, N.S.W. (Australia)

(Received March 20th, 1968)

Current methods for the isolation and radiochemical purification of beryllium[1] used for the determination of beryllium-10 produced by cosmic rays in environmental materials, have several practical disadvantages. Firstly, they depend on procedures for purification of macro-quantities of beryllium from spectrographic or high-activity levels of impurities and are not efficient enough to achieve the extreme radiochemical purity required for measurement of low beryllium activities in the environment. This is shown by the fact that recycling often reduces the apparent specific activity of the beryllium as a result of further decontamination. Most of these procedures also require the addition of stable carrier since gravimetric steps such as the precipitation of beryllium hydroxide from ammoniacal EDTA solution would be impracticable with microgram amounts of beryllium. In addition, the end-product is often beryllium oxide which must be quantitatively transferred to a source tray as a slurry.

Apart from the chemical problems, these methods must introduce some means of measuring the recovery of beryllium. The most common approach is to add stable beryllium carrier and weigh the recovered beryllium oxide. However, the thickness of the source thus prepared results in significant absorption of the weak beryllium-10 β-emission with consequent loss of counting efficiency, an important factor when the activity of the sample is already generally very low.

MERRILL *et al.*[2] discussed the use of beryllium-10 to date deep-sea sediments and suggested that variation of ^{10}Be/^{9}Be ratios within the different levels of the sediment would be a more accurate measure of age than relating beryllium-10 decay to depth of sediment. This would make a carrier-free method essential. Pure γ-emitting beryllium-7 cannot be added to an actual beryllium-10 determination as tracer, since low-level β-counters of the type used to count beryllium-10 have a small efficiency for γ-radiation and would register a spurious count rate.

GOEL *et al.*[3] determined experimental recoveries on a number of artificial and actual sediments using beryllium-7 tracer, establishing an average recovery which was then assumed in all subsequent beryllium-10 analyses. The experimental recovery was 80 ± 10% which introduced a significant error into the overall determination; but a far greater uncertainty arises from the inability to guarantee that the sample has undergone precisely the same procedure and conditions as the trial samples and thus that the recovery of beryllium falls within these limits at all.

The most desirable procedure is one which can be reproduced exactly each time and will give a quantitative recovery of beryllium, eliminating the need for a determination of the recovery and making a greater activity of beryllium available for counting. Such a procedure should have high (at least 10^3 and preferably 10^4) decontamination factors for all artificial and natural activities likely to be present. A method that meets these specifications is now described.

Description of method

KENNEDY AND WHEELER[4] found that polymerised sodium diallyl phosphate (NaDAP) could separate beryllium quantitatively from a wide range of impurities. It was felt that this resin could be used both to isolate the beryllium from large quantities of other elements and to provide an extensive general decontamination, since uranium is the only element reported to interfere. Beryllium is adsorbed on the resin from a solution containing excess of EDTA at a pH of 4.0. All other elements likely to adsorb on the resin are complexed by EDTA with the exception of uranium. Cerium carrier is added to facilitate the removal of cerium which is difficult at tracer levels. Elution of the beryllium is achieved with ammonium fluoride solution. To separate the beryllium from the ammonium fluoride and to achieve further decontamination, the fluoroberyllate is adsorbed onto an anion-exchange resin from dilute fluoride solution. Beryllium is then eluted with 0.5 *M* hydrochloric acid and fluoride removed by fuming to dryness with hydrochloric acid.

To remove thorium contamination, and to obtain further decontamination from rare earths, zirconium and radium, the beryllium is then adsorbed onto a cation-exchange resin from 0.2 *M* hydrochloric acid, and eluted with 1.2 *M* hydrochloric acid which removes beryllium cleanly while the above-mentioned impurities are retained on the resin.

Uranium, protactinium, polonium, iron and a number of other remaining impurities are removed by passing the beryllium through an anion-exchange resin in concentrated hydrochloric acid. Beryllium passes cleanly through in the effluent while the other elements are strongly adsorbed on the resin.

The resulting beryllium solution can be vacuum-evaporated onto planchets for β-counting, placed in pill-packs for γ-counting for beryllium-7 in a well-scintillation counter, or analysed for stable beryllium by spectrophotometric methods.

EXPERIMENTAL

Ion-exchange resins

The sodium diallyl phosphate resin was prepared from triallyl phosphate as described by KENNEDY[5]. The yield of resin was 30 g and it had a capacity for beryllium of 3.1 meq/g of dry resin; 1 g of dry resin produced a wet volume of 2.9 ml. For these experiments, 1 g of resin was used in each experiment, giving an 8-cm column height in a 0.7-cm diameter ion-exchange column. The resin was conditioned by passing 50 ml of 2 *M* sodium chloride solution through it, and washed with 50 ml of water.

The column for the adsorption of the fluoroberyllate consisted of a 13 × 1 cm diameter column of Dowex 1 (8% D.V.B., 30–60 mesh) prepared in the chloride form by washing with 8 *M* hydrochloric acid followed by a water wash.

The cation-exchange column was a 1-cm diameter column filled to a height of 9 cm with Dowex 50 (8% D.V.B., 50–100 mesh) prepared in the hydrogen form by washing with 8 *M* hydrochloric acid followed by a water wash.

The anion-exchange column was a 3 × 1 cm diameter column of Dowex 1

(8% D.V.B., 30–60 mesh) washed with 10 *M* hydrochloric acid just before the decontamination pass.

All flow rates for this work were adjusted to 1 drop/3–6 sec.

Reagents

Cerium carrier solution (10 mg Ce/ml). Dissolve 2.37 g of anhydrous cerium(IV) sulphate in demineralised water, add 10 ml of hydrochloric acid and dilute to 100 ml with demineralised water.

Procedure

The method presupposes that the sample has been brought fully into a dilute acid solution. The method is unaffected by the presence of sulphate, nitrate or perchlorate, although this work was carried out in hydrochloric acid.

To the solution add 10 mg of cerium(IV) carrier. Adjust the pH to *ca.* 4 with ammonia solution. Make the solution 2.5% in EDTA by addition of 10% EDTA solution. If a large amount of ions capable of complexing with EDTA is present, then sufficient EDTA must be added to complex them fully and the solution made 2.5% in excess EDTA. Adjust the pH to 4.0 and pass the solution through the NaDAP column. Wash the column with 40 ml of 2.5% EDTA solution adjusted to pH 4.0, and then with 40 ml of water. Elute the beryllium with 60 ml of 1 *M* ammonium fluoride and dilute the solution to 300 ml.

Pass the solution through the water-washed Dowex 1 column and wash the column with 60 ml of water. Elute the beryllium with 60 ml of 0.5 *M* hydrochloric acid, and fume the solution twice to dryness with hydrochloric acid.

Dissolve the residue in 5 ml of 2 *M* hydrochloric acid and dilute to 50 ml with water. Pass the solution through the Dowex-50 column and wash the column with 50 ml of water. Elute the beryllium with 70 ml of 1.2 *M* hydrochloric acid and evaporate the solution to *ca.* 5 ml.

Dilute the solution to 20 ml with 10 *M* hydrochloric acid and pass through the acid-conditioned Dowex-1 column. Wash the beaker with 10 ml of 10 *M* hydrochloric acid and pass through the column. Wash the column with a further 10 ml of 10 *M* acid. Collect the effluent and washings and evaporate the bulk of the acid. The solution is ready for counting or for chemical analysis of the beryllium.

RESULTS AND DISCUSSION

Isolation and recovery of beryllium

To determine the efficiency of the recovery of beryllium by this procedure and the minimum volumes required for each elution, two series of runs were carried out with beryllium-7 tracer, one being carrier-free and the other containing 1 μg of beryllium carrier, in order to test the adsorption and elution behaviour of tracer and microgram levels of beryllium.

NaDAP stage

After adsorption, no beryllium-7 was detected in the effluent. Both series were eluted with 70 ml of 1 *M* ammonium fluoride and the eluant was collected in 5-ml fractions in polythene pill-packs which were counted in a well-scintillation counter against a beryllium-7 standard. The added carrier produced a slightly greater initial elution rate of beryllium-7 but in both series, 60 ml of ammonium fluoride was required to elute more than 99.5% of the beryllium.

Anion exchange of fluoroberyllate

The fractions from each series were recombined and each solution passed through the resin. The eluant was collected in 5-ml fractions and counted. Again, 60 ml of acid was required to remove more than 99.5% of the beryllium in both cases, although the carrier-free series had a faster initial elution rate.

Cation exchange

From the values for adsorption coefficients on cation-exchange resin published by STRELOW[6], the distribution ratio of beryllium drops to 10 in 1.2 *M* hydrochloric acid. Other distribution ratios for this acid concentration are:

Zr^{4+} 4,000; Th^{4+} ~1000; Ce^{4+} 150; Cs^{+} 60; Sr^{2+} ~44.

This concentration was therefore chosen to give maximum decontamination in a reasonable volume of eluant. No beryllium was detected in the effluent from the column. The elution of the beryllium was more than 99.5% with 65 ml of acid for both the carrier and carrier-free series.

Anion exchange in hydrochloric acid

Beryllium is not adsorbed at all in this step and 100% was recovered in the effluent.

Decontamination of beryllium

A series of runs was made with additions of various expected natural and artificial contaminants. Where possible, γ-emitting isotopes of the elements were used. Decontamination factors were determined at constant geometry with a Li–Ge solid-state detector and a 1024-channel Nuclear Data analyser, by simply measuring the reduction in the height of each γ-peak over the Compton continuum against a standard source equivalent to the original addition. This method gave ± 5–10% accuracy for measurable peaks. Where there was no detectable peak, even over a 1000-min counting time, the mean deviation in the Compton continuum was taken as the maximum peak height. Where no γ-emitting isotopes were available, standard additions of milligram quantities of stable elements were used and decontamination factors were determined chemically.

In each case, the one solution was used to determine decontamination factors through both the NaDAP exchange and the subsequent fluoroberyllate step, since the adsorption solution for the second step must be the fluoride solution from the first. Values for the decontamination from the first step and the overall decontamination could thus be determined on the γ-emitters; the stable isotopes were analysed after the second step and overall decontamination factors only are available.

For each of the other two ion-exchange steps, solutions identical to those used for the NaDAP run were used without addition of further cerium carrier. All of the decontamination factors are listed in Table I.

Details of the individual decontamination runs are set out below.

Fresh fission products (100 days old). This solution contained easily detectable amounts of ^{144}Ce, ^{141}Ce, ^{95}Zr, ^{95}Nb, ^{97m}Tc with a poorly-defined ^{106}Ru peak; 25 mg of each of uranium and thorium, and 5 μg of beryllium were also added. The behaviour of tracer levels of fission-product cerium is unpredictable and so 10 mg of cerium(IV) carrier was added to the solution before the NaDAP stage. Differences in the decontamination factors for ^{144}Ce and ^{141}Ce arise from the fact that their γ-spectra overlap slightly and are located on a steep part of the continuum, making the measurement of their heights difficult. The 0.72-MeV peak of ^{95}Zr was easily separated from the other γ-peaks, but the 0.75-MeV peak of ^{95}Zr and the ^{95}Nb peak overlapped considerably and made estimation of the ^{95}Nb decontamination difficult. Minimum decontaminations only could be estimated for the poor ^{106}Ru/^{106}Rh peak. Technetium was generally not detectable above the very steep continuum slope. The recovery of beryllium was 100%.

Radiocesium. Cesium-137 tracer was used. Peak heights were measured with a 5″ sodium iodide crystal and 512-channel Nuclear Data analyser.

Radium, radiostrontium and lead. Tracers of radium-226 and strontium-85 were added to each run, with 25 mg of lead carrier. Decontamination of the radium was determined from the 0.187-MeV peak of radium only.

Aged fission product solution. Only the ruthenium-106 decontamination was determined.

Polonium, protactinium, bismuth and potassium. These were not determined. Polonium and protactinium are more strongly adsorbed during the 10 M hydrochloric acid pass through anion-exchange resin than is the uranium, and decontamination in that stage must be in excess of 25,000 for each of them. The only bismuth isotope with a significant half-life is ^{207}Bi and since it does not occur naturally or as the product of nuclear blasts, it was ignored. Potassium closely follows the ^{137}Cs through the procedure and its greater concentration should ensure a clean separation from beryllium.

Decontamination by acetylacetone extraction

The method was compared with the acetylacetone extraction procedure in common use by extracting the beryllium from a solution identical to that used in the fresh fission product run. The procedure followed was that of SILL AND WILLIS[7]. The recovery of beryllium was 98 ± 2%. The decontamination factors are listed in Table I.

Conclusion

The method gives consistent quantitative recovery of the beryllium at microgram and tracer levels, and the upper limit of the amount of beryllium recoverable would only be the capacity of the resin columns used. The final solution can be readily analysed for stable beryllium, counted for beryllium-7 in a well-scintillation γ-counter or vacuum-evaporated onto steel, aluminium or plastic planchets for β-counting of the beryllium-10. Decontamination factors are extremely high for most of the nuclides tested, although good determination could not be obtained for technetium-97m and radioruthenium. Actual decontamination factors for these two are likely to be much higher than the conservative values listed. If necessary, further decontamination from them would be achieved by fuming with perchloric acid.

The author thanks Dr. J. W. MORGAN for helpful discussion on the scope of the work, and Albright and Wilson, Ltd., England, for the gift of 200 g of triallyl phosphate for the manufacture of the NaDAP resin.

TABLE I

DECONTAMINATION FACTORS OF VARIOUS NUCLIDES FOR ION-EXCHANGE AND SOLVENT EXTRACTION PROCESSES

Nuclide	*NaDAP exchange*	*Fluoroberyllate exchange*	*Combined D.F. for NaDAP/BeF$_4^{2-}$*	*Cation exchange*	*Anion-exchange pass*	*Overall decontamination factor*	*Acetylacetone extraction in chloroform*
^{144}Ce	380	1.6	595	980	1	$\sim 6 \cdot 10^5$	820
^{141}Ce	340	1.5	515	>500	1	$> 2.6 \cdot 10^5$	720
^{106}Ru/^{106}Rh	> 20	—[a]	> 90	> 4	1	>360	—
	~ 30	—	—	—	—	> 30	—
^{95}Zr	50	1.5	74	>400	150	$> 4.5 \cdot 10^6$	60
^{95}Nb	48	14.5	695	3.3	390	$9.0 \cdot 10^5$	210
^{97m}Tc	135	—	—	—	1	>135	—
U	—	—	1.25	1	>25,000	$> 3 \cdot 10^4$	~ 6
Th	—	—	30	>500	1	$> 1.5 \cdot 10^4$	>500
^{137}Cs	480	> 2,000	>960,000	1.4	1	$> 1.3 \cdot 10^6$	—
^{226}Ra	720	~ 10	~ 7,100	2,480	1	$1.8 \cdot 10^7$	—
^{85}Sr	4,800	~ 8	~ 37,500	2,100	1	$7.9 \cdot 10^7$	—
Pb	—	—	> 5,000	~ 1	1	>5,000	—

[a] A dash indicates that this value was not determined.

SUMMARY

A method is presented for the separation and radiochemical purification of microgram and tracer amounts of beryllium from solutions. It is a four-stage ion-exchange procedure consisting of (*1*) selective adsorption of the beryllium onto NaDAP resin and its elution with ammonium fluoride, (*2*) adsorption of the fluoroberyllate complex onto an anion-exchange column and elution of the beryllium with hydrochloric acid, (*3*) adsorption and selective elution of the beryllium on a cation-exchange column and (*4*) a pass through an anion-exchange column in concentrated hydrochloric acid. The method is quantitative and requires no carrier. Decontamination factors from most radionuclides tested were greater than 10,000. The method can be used to determine beryllium-10 in environmental materials.

RÉSUMÉ

Une méthode est proposée pour la séparation et la purification radiochimique du béryllium en solution, à l'échelle micro et à l'état de traceurs. Ce procédé se fait en 4 étapes: (*1*) adsorption sélective du béryllium sur résine NaDAP et élution à l'aide de fluorure d'ammonium, (*2*) adsorption du complexe fluobéryllate sur colonne échangeuse d'anions et élution du béryllium à l'aide d'acide chlorhydrique, (*3*) adsorption et élution sélective du béryllium sur colonne échangeuse de cations et (*4*) passage à travers une colonne échangeuse d'anions dans l'acide chlorhydrique concentré. La méthode est quantitative et ne nécessite aucun entraîneur. Les facteurs de décontamination de la plupart des radionuclides testés sont plus élevés que 10,000. Ce procédé permet de doser le béryllium-10 en présence de métaux voisins.

ZUSAMMENFASSUNG

Es wird eine Methode zur Abtrennung und radiochemischen Reinigung von Mikrogramm- und Tracer-Mengen von Beryllium aus Lösungen angegeben. Es handelt sich um ein Ionenaustauschverfahren mit folgenden 4 Schritten: (*1*) Selektive Adsorption von Beryllium an NaDAP und seine Eluierung mit Ammoniumfluorid, (*2*) Adsorption des Fluoroberyllatkomplexes an einer Anionenaustauscherkolonne und Eluierung des Berylliums mit Salzsäure, (*3*) Adsorption und selektive Eluierung des Berylliums an einer Kationenaustauscherkolonne und (*4*) Durchlaufen durch eine Anionenaustauscherkolonne in konzentrierter Salzsäure. Die Methode ist quantitativ und benötigt keinen Träger. Die Dekontaminationsfaktoren von den meisten untersuchten Radionukliden war grösser als 10000. Die Methode kann zur Bestimmung von Beryllium-10 in Umgebungsmaterialien verwendet werden.

REFERENCES

1. A. W. Fairhall, *Natl. Acad. Sci. Natl. Res. Council Rept. NAS-NS 3013*.
2 J. R. Merrill, M. Honda and J. R. Arnold, *Proc. U. N. Intern. Conf. Peaceful Uses At. Energy, Geneva, 1958*, A/CONF. 15/1, P/412.
3 P. S. Goel, D. P. Kharkar, D. Lal, N. Narsappaya, B. Peters and V. Yatirajam, *Deep-Sea Res.*, 4 (1957) 202.
4 J. Kennedy and V. J. Wheeler, *Anal. Chim. Acta*, 20 (1959) 412.
5 J. Kennedy, *U.K. Patent 777, 248*.
6 F. W. E. Strelow, *Anal. Chem.*, 32 (1960) 1185.
7 C. W. Sill and C. P. Willis, *Anal. Chem.*, 31 (1959) 598.

Analytica Chimica Acta
Elsevier Publishing Company, Amsterdam
Printed in The Netherlands

APPLICATION DE LA COULOMETRIE À L'ETUDE DES COMPLEXES

I. APPAREILLAGE ET APPLICATION À L'HYDROLYSE DE L'ION BÉRYLLIUM(II)

M. R. PÂRIS ET CL. GREGOIRE
Chaire de Chimie Minérale, Faculté des Sciences de Lyon, Villeurbanne (France)

(Reçu le 10 février, 1968)

Habituellement, pour étudier la formation d'un complexe métal–coordinat, on suit la variation du pH au cours d'un titrage acide–base qui consiste à déplacer, par une base forte, les protons associés au coordinat basique; on ajoute, par exemple, de la soude titrée à la solution initialement acide contenant l'ion métallique à complexer et le coordinat protoné. Il en résulte une dilution des réactifs souvent gênante pour l'exploitation des mesures, en particulier lorsque la méthode de calcul (celle de SILLÉN par exemple) implique la constance de concentration de l'un des réactifs. Pour pallier cet inconvénient on peut compenser la dilution par addition supplémentaire, au moyen d'une burette, du réactif dont la concentration doit demeurer constante, ce qui est délicat, voire même impossible avec certains composés instables; on peut aussi effectuer le titrage par une base concentrée dont on n'ajoutera qu'un faible volume au moyen d'une microburette (type seringue). Si ce dernier artifice ne provoque effectivement qu'une dilution négligeable, il présente cependant l'inconvénient de produire localement une forte concentration de base qui peut entraîner la formation irréversible d'espèces hydroxydées modifiant ainsi le système étudié.

La méthode que nous proposons consiste à modifier graduellement le pH d'une solution, non plus en ajoutant des ions OH^- mais en faisant disparaître les ions H^+ par réduction coulométrique de ces derniers sur cathode de platine. N'entrainant aucune variation de volume en cours de titrage, un tel mode opératoire dispense en outre de préparer un réactif titrant à une concentration puisque l'intensité du courant, réglable à volonté au cours d'un même titrage, s'identifie au titre de la base tandis que le chronomètre interrupteur fait office de robinet de burette.

Dans le présent Mémoire nous décrirons le dispositif expérimental utilisé et nous en illustrerons son application à un système complexe ayant donné lieu à de nombreuses publications concordantes[1–3]: l'hydrolyse de l'ion béryllium(II).

Un deuxième Mémoire sera consacré à l'étude de la complexation du titane(III) par les ions OH^- et par l'acide picolique (carboxy-2-pyridine)—systèmes dont il importait de reprendre l'étude.

DISPOSITIF COULOMÉTRIQUE

Cellule

La littérature fait état de nombreuses publications[4–8] dont certaines très récentes relatives au dosage des acides par coulométrie à intensité constante. Trois impératifs essentiels conditionnent la réalisation des montages: l'obtention d'un rendement de 100% en courant, la mise en évidence de la fin de la réaction et la détermination précise de l'intensité de courant utilisée. La cellule coulométrique que nous proposons (Fig. 1) répond à ces conditions.

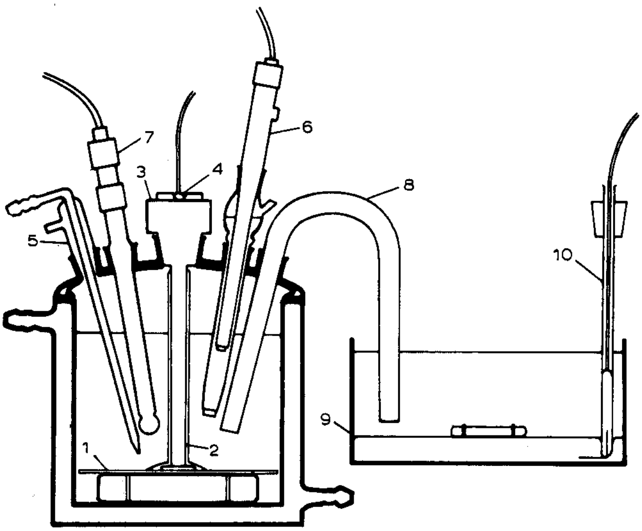

Fig. 1. Cellule de titrage coulométrique.

La réduction coulométrique des protons se fait sur une électrode de platine poli (1) constituée par un disque de platine (⌀ =7.5 cm, épaisseur 0.1 cm) suspendu dans la cellule par une tige rigide (2) recouverte d'une résine isolante à base de téflon.

Cette tige peut tourner librement dans un palier comportant un roulement à billes (3) s'adaptant sur un rodage ménagé dans le couvercle de la cellule et permettant d'assurer l'étanchéité. Un alésage central (4) rempli de mercure permet d'assurer le contact électrique de l'électrode. Enfin, un agitateur magnétique communique un mouvement de rotation à l'électrode par l'intermédiaire d'un barreau aimanté enrobé de téflon et fixé sous le disque de platine.

Ce dispositif permet d'agiter la solution et d'éliminer les bulles d'hydrogène adhérant sur la cathode: de ce fait, la surface de l'électrode reste constante et la réduction se fait ainsi toujours avec 100% de rendement.

Le compartiment anodique est relié à la cellule par un pont d'agar-agar (8) au KCl (pour béryllium(II)) ou au KBr (pour titane(III)). L'anode (9) est constituée par une nappe de mercure recouverte d'une solution saturée de KCl ou KBr. Le mercure est agité en permanence de façon à renouveler continuellement la surface libre. Un fil de platine isolé (10) assure le contact électrique avec la source de tension. Les rodages (6) et (7) supportent les électrodes indicatrices de pH (électrode au calomel et électrode en verre); une tubulure latérale (5) permet en outre de travailler sous courant d'azote purifié par barbotage dans une solution commerciale de titane(III). Enfin, la température est maintenue à 25° par circulation d'eau thermostatée dans la double enveloppe.

La source de courant stabilisé est un coulomètre Tacussel type ASC 3 C permet-

tant de travailler à des intensités variant entre 0.2 et 250 mA. Nous avons choisi la valeur de 100 mA pour effectuer les titrages coulométriques. Les temps d'électrolyse sont mesurés à l'aide d'un chronomètre électronique Tacussel (type CE) placé en série dans le circuit coulométrique.
Enfin, les mesures de pH sont faites grâce à un compensateur Metrohm E 388 à 0.2 mV près.

Etalonnages

Etalonnage du pH. Les conditions d'étude nous ont conduit à déterminer des pH dans une région d'assez forte acidité (jusqu'à environ 130 mM dans le cas de l'hydrolyse de titane(III)), où les mesures sont toujours délicates. Aussi nous ne pouvions effectuer l'étalonnage classique au moyen de solutions tampons.

Le couple d'électrodes a donc été étalonné au moyen d'un titrage "acide sans base", c'est à dire en ajoutant une solution d'acide et de sel neutre à la force ionique μ dans une quantité donnée de sel neutre à la même force ionique. Nous avons pu vérifier que les variations de la force électromotrice E lue sont liées aux variations de pH par la relation

$$E = E_0 + (RT/F) \log h$$

h = concentration des ions hydrogène libre. On a constaté que la valeur de la constante E_0 variait très peu d'un jour à l'autre (de l'ordre de 0.2 à 0.3 mV) et de façon irrégulière.

Etalonnage de l'intensité du courant coulométrique. Par des dosages préliminaires d'acide de titre connu dans les conditions de travail, nous avons vérifié la bonne reproductibilité de nos mesures et déterminé de façon rigoureuse la quantité d'électricité débitée par le circuit générateur. L'étalonnage coulométrique à intensité constante effectué après un étalonnage classique "acide sans base" doivent en effet donner les mêmes valeurs des constantes E_0, indiquant une excellente correspondance entre les protons réduits par coulométrie et les protons ajoutés au cours du titrage "acide sans base".

HYDROLYSE DU BÉRYLLIUM

L'hydrolyse des ions béryllium(II) nous a servi à tester notre méthode de titrage coulométrique puisqu'il s'agissait d'un phénomène déjà bien étudié[1-3]. En représentant, en fonction du pH, le nombre moyen Z d'ion hydroxyde par atome métallique, nous obtenons l'ensemble des courbes de la Fig. 2 où nos résultats sont comparés à ceux de nos prédécesseurs.

Pour déterminer les constantes d'hydrolyse, nous avons fait appel à trois méthodes.

Méthode analytique

En supposant qu'il se forme seulement l'espèce $Be_3(OH)_3^{3+}$, nous en calculons la constante de formation pour des valeurs de Z appartenant à l'intervalle [0.2–0.6]. Nous avons:

$$3\ Be^{2+} + 3\ H_2O \rightleftharpoons Be_3(OH)_3^{3+} + 3\ H^+$$

$$B = b + 3[Be_3(OH)_3] \qquad (1)$$

B est la concentration totale de l'ion béryllium, et b est la concentration de l'ion béryllium libre.

$$ZB = 3[Be_3(OH)_3] \tag{2}$$

$$\beta_{33} = [Be_3(OH)_3]h^3 b^{-3} \tag{3}$$

En éliminant b et après simplification

$$\beta_{33} = 1/3\ (1-Z)^{-3}\, Z\, h^3\, B^{-2} \tag{4}$$

ou encore

$$\log \beta_{33} = \log Z - 3 \log (1-Z) - 3\ \text{pH} - 2 \log B - \log 3 \tag{5}$$

Légèrement modifiée l'éqn. (5) permet de calculer les courbes théoriques $Z(\log h)_B$ correspondant à ce seul complexe formé. En effet:

$$X_{33} = \log (1-Z) - 0.33 \log Z = \log h - 0.33 \log (3\beta_{33}\, B^2) \tag{6}$$

Cette équation permet ainsi de tracer un réseau de courbes et on constate une divergence assez sensible pour les faibles valeurs de Z.

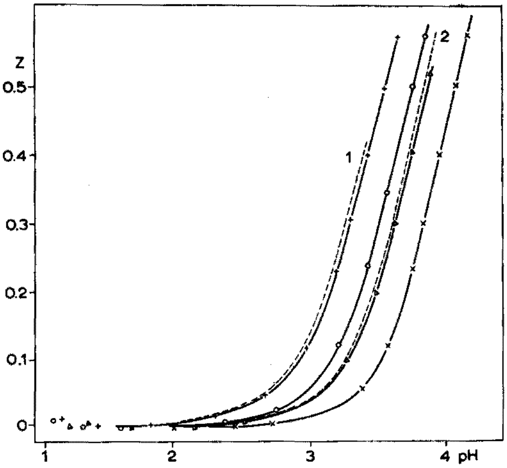

Fig. 2. Hydrolyse du béryllium. — Nos résultats: + B = 174 mM, ○ B = 87 mM, △ B = 58 mM, × B = 29 mM. 1 ----- Résultats tirés de KAKIHANA ET SILLÉN[3]; 2 ----- Résultats tirés de CARELL ET OLIN[2].

Méthode de Sillén

Cette méthode permet de caractériser d'abord l'espèce polynucléaire qui se forme, elle fournit ensuite la constante correspondant à cette dernière. Puisque les courbes $Z(\log h)_B$ ne sont pas confondues, il y a donc formation d'une ou plusieurs espèces polynucléaires de formule générale

$$Be[Be(OH)_t]_n$$

La valeur de t s'obtient à partir de l'écart entre deux courbes quelconques $Z(\log h)_B$ dans leur domaine de parallélisme. Nous trouvons ici $t \sim 1.5$.

S'il ne se forme pas d'autres espèces, les points expérimentaux doivent alors se placer sur une courbe singulière $y(x)$ telle que:

$$y = Z/1.5 \tag{7}$$

$$x = \log B + 1.5 \text{ pH} \tag{8}$$

C'est ce que nos résultats vérifient (Fig. 3).

L'analyse directe de cette courbe $y(x)$ doit fournir alors tous les autres renseignements.

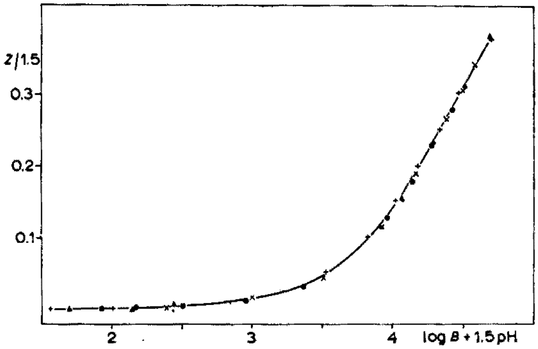

Fig. 3. Hydrolyse du béryllium. $Z/1.5 = f(\log B + 1.5)$. + $B = 174$ mM, × $B = 87$ mM, △ $B = 58$ mM, ○ $B = 29$ mM.

La valeur précédente de n détermine en particulier la formule complète du complexe polynucléaire. Nous allons prendre ici $n = 2$. D'où l'espèce $Be_3(OH)_3^{3+}$.

La valeur de la constante correspondante β_{33} s'obtient alors à partir de l'équation

$$\log \beta_{33} = \log g - 2 \log u \tag{9}$$

Les résultats que nous obtenons ainsi sont médiocres du fait que nous avons effectué ce travail dans un domaine de pH limité. En particulier, l'intégrale $\int_{-\infty}^{x} y \, dx$ calculée à partir de la courbe $y(x)$ en prenant $x = 2$ comme borne inférieure, dépend beaucoup dans notre cas ($y \leqslant 0.35$) des incertitudes sur le tracé de $y(x)$ pour les faibles valeurs de y[7].

Aussi, comme le font d'ailleurs KAKIHANA ET SILLÉN[3] il faut supposer l'existence d'un résidu d'intégration $\delta = \int_{-\infty}^{2} y \, dx$.

Nous avons donc en plus effectué les calculs correspondants à $\delta = -0.02$ et $\delta = -0.03$ qui donnent des valeurs nettement meilleures pour $\log \beta_{33}$ et n. Le sens ($\delta < 0$) et l'existence de cette correction se vérifie d'ailleurs très précisément puisqu'il a été prouvé l'existence d'une autre espèce polynucléaire $Be_2(OH)^{3+}$, prédominante aux faibles valeurs de Z.

Courbes normalisées

C'est cette méthode directe qui convient le mieux à notre cas. Nous nous bornerons à en donner les lignes essentielles (*cf.* CARELL ET OLIN)[2]. En admettant en plus l'existence de l'espèce $Be_2(OH)^{3+}$, il est possible d'écrire:

$$B = b + 2\beta_{12} b^2 h^{-1} + 3\beta_{33} b^3 h^{-3} \tag{10}$$

$$BZ = \beta_{12} b^2 h^{-1} + 3\beta_{33} b^3 h^{-3} \tag{11}$$

En éliminant b et en introduisant la variable et paramètre auxiliaires w et L, nous obtenons l'équation de la famille de courbes normalisées $Z(-\log w)$

$$w = 4\,B\beta_{12}h^{-1} \tag{12}$$

$$L = 3\beta_{33}/(8B\beta_{12}^{3}) \tag{13}$$

$$Z = w^{-1}(\sqrt{1+w(1-Z)}-1)^2 + L(\sqrt{1+w(1-Z)}-1)^3 \tag{14}$$

Si deux courbes appartenant à des réseaux différents coïncident, il vient alors

$$\log \beta_{12} = \log w + \log h - \log\,(4B) \tag{15}$$

$$\log \beta_{33} = \log L + 3\,\log\beta_{12} + \log\,(8B/3) \tag{16}$$

Les résultats obtenus par cette méthode et les courbes $Z(-\log w)_L$ choisies sont représentées sur la Fig. 4.

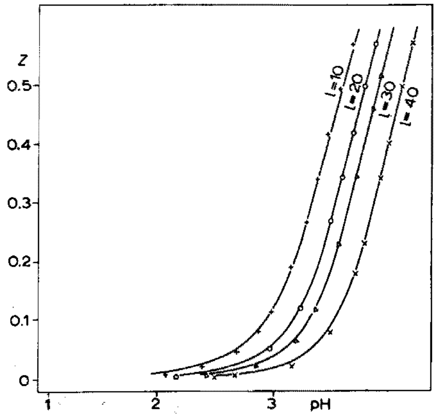

Fig. 4. Courbes normalisées: $Z(-\log w)_1$ (éqn. (14)). — Courbes théoriques; + o △ × Points expérimentaux. + B = 174 mM, o B = 87 mM, △ B = 58 mM, × B = 29 mM.

RÉSULTATS

Les valeurs des constantes que nous avons obtenues par ces trois méthodes sont respectivement:

Méthode analytique—$\log \beta_{33} = -8.93$
Méthode de SILLÉN—$\log \beta_{33} = -8.88$ ($\delta = -0.02$)
$\log \beta_{33} = -8.95$ ($\delta = -0.03$)
Courbes normalisées—$\log \beta_{33} = -8.88$
$\log \beta_{12} = -3.18$

Sur la Fig. 2, nous avons tracé une courbe obtenue par KAKIHANA ET SILLÉN et une autre par CARELL ET OLIN. La bonne concordance de nos résultats avec ceux de la littérature (*cf.* Tableau I) dans la mesure où nous pouvons les comparer (milieux ioniques différents) permet d'affirmer que le titrage coulométrique utilisé ici est tout à fait approprié aux études d'hydrolyse des ions métalliques lorsqu'ils ne sont pas susceptibles d'être réduits à la cathode.

TABLEAU I

COMPARAISON DE NOS VALEURS DE CONSTANTES AVEC LES DONNÉES DE LA LITTÉRATURE

Complexes	*Ref. 3* *$NaClO_4$ 3 M*	*Ref. 2* *$NaClO_4$ 3 M*	*Ref. 1* *$NaClO_4$ 0.5 M*	*Nos valeurs* *KCl 3 M*
$Be_3(OH)_3$	−8.66	−8.66	−8.81	−8.91
$Be_2(OH)$	−3.24	−3.22	−3.20	−3.18

Le procédé est très commode puisqu'il ne provoque pas de variation de volume au cours du titrage. Dès lors, il n'est plus nécessaire de faire des approximations ou bien de faire appel à des burettes supplémentaires afin de maintenir constante la concentration de l'ion métallique.

Il est curieux de constater que l'intérêt d'un tel procédé d'étude ait échappé jusqu'à présent aux auteurs de travaux sur l'hydrolyse puisque la seule communication[8] dont nous avons eu connaissance alors que notre travail était déjà très avancé, est relative à une étude sur la constante de dissociation de l'acide silicique par une technique coulométrique très analogue.

RÉSUMÉ

Les auteurs décrivent une cellule de titrage coulométrique à intensité constante pour suivre la formation des complexes en fonction du pH. Le bon fonctionnement de ce montage est vérifié par l'étude de l'hydrolyse de l'ion béryllium(II).

SUMMARY

In order to study complex formation at variable pH values, a constant-current coulometric titration cell is described. The performance of this device was tested by a study of the hydrolysis of beryllium(II).

ZUSAMMENFASSUNG

Um die Komplexbildung in Abhängigkeit von pH zu untersuchen, beschreiben die Authoren eine konstanter Stromstärke coulometrische Zelle. Diese Vorrichtung ist durch der Be(II) Hydrolyse Untersuchung geprüft.

BIBLIOGRAPHIE

1 F. BERTIN, G. THOMAS ET J.-C. MERLIN, *Bull. Soc. Chim. France*, 7 (1967) 2393.
2 B. CARELL ET A. OLIN, *Acta Chem. Scand.*, 15 (1961) 1875.
3 H. KAKIHANA ET L. G. SILLÉN, *Acta Chem. Scand.*, 10 (1956) 985.
4 J. BADOZ-LAMBLING, *Anal. Chim. Acta*, 36 (1954) 291.
5 F. A. COOPER ET J. C. QUAYLE, *Analyst*, 61 (1966) 363.
6 J. EPSTEIN, H. SEBER ET S. SILVER, *J. Am. Chem. Soc.*, 19 (1947) 675.
7 J. K. TAYLOR ET S. W. SMITH, *J. Res. Natl. Bur. Std.*, 63A (1959) 153.
8 H. BILINSKI ET N. INGRI, *Proc. 9th I.C.C.C. St. Moritz, 1966* (publié par Helv. Chim. Acta).

Analytica Chimica Acta
Elsevier Publishing Company, Amsterdam
Printed in The Netherlands

APPLICATION DE LA COULOMETRIE A L'ETUDE DES COMPLEXES

II. COMPLEXATION DU TITANE(III) PAR LES IONS HYDROXYDE ET L'ACIDE PICOLIQUE

M. R. PÂRIS ET CL. GREGOIRE
Chaire de Chimie Minérale, Faculté des Sciences de Lyon, Villeurbanne (France)

(Reçu le 10 février, 1968)

Ayant montré précédemment[1] que la méthode de titrage coulométrique permettait, dans le cas de l'hydrolyse du béryllium, de retrouver les résultats antérieurs, nous pouvions, en toute confiance, utiliser le même procédé pour étudier un problème encore plus exploré, celui de l'hydrolyse du titane(III) et de sa complexation avec la carboxy-2-pyridine ou acide picolique.

La seule étude relative à l'hydrolyse de l'ion titaneux est due à PECSOK ET FLETCHER[2]. Au moyen de titrages potentiométriques, ces auteurs ont mis en évidence l'existence de l'espèce mononucléaire $Ti(OH)^{2+}$ et ont proposé comme constante d'hydrolyse $\log K_1 = 11.8$ à 25° et force ionique nulle. Ils ont également suggéré la formation possible de composés polynucléaires hydroxydés au delà de pH 4. D'autre part, l'un de nous[3] avait déjà étudié la chélation du titane(III) par l'acide picolique. La potentiométrie et la spectrophotométrie avaient pu révéler l'existence de trois complexes successifs TiL, TiL_2 et TiL_3 mais seule la constante globale avait pu être évaluée. Aussi était-il intéressant de reprendre ces deux études au moyen de notre dispositif coulométrique qui présentait l'avantage de ne pas avoir à réaliser une burette parfaitement étanche contenant une solution titrée du titane(III) exempte du titane(IV).

TECHNIQUES EXPÉRIMENTALES

La manipulation de l'ion titaneux nécessite un appareillage spécial permettant d'éviter à tout instant l'oxydation par l'oxygène de l'air. Nous avons donc effectué toutes les opérations de préparation, de conservation, de dosages et de prélèvements dans une boîte à gants en atmosphère d'azote. Les solutions prêtes à l'emploi étaient introduites dans la cellule coulométrique étanche[1] à l'intérieur de l'enceinte inerte; puis par l'intermédiaire d'un sas à vide le récipient était extrait et placé sur le banc de titrage.

Les solutions de titane(III) étaient obtenues par attaque directe du titane métallique sous forme d'éponge par l'acide bromhydrique dans un récipient opaque muni d'une soupape à mercure qui maintient au-dessus de la solution une atmosphère réductrice d'hydrogène. L'attaque est assez lente en milieu bromhydrique (environ 3 semaines à la température ambiante pour préparer une solution 0.5 *M* en titane(III)). Cette méthode conduit cependant à des solutions dans lesquelles il est très facile de régler les titres respectifs de H^+ et de Ti^{3+} par le choix judicieux des concentrations initiales de réactifs.

L'acide picolique a été préparé par la méthode de BLACK, DEPP ET CORSON[4] avec purification par recristallisation dans le benzène.

Les solutions de titane ont été dosées de la façon suivante:

titre du titane(III): oxydation par l'iode en excès et dosage ampérométrique en retour de cet excès par l'arsenic(III);

titre du titane(IV): passage de la solution de titane(III) sur amalgame de zinc et dosage du titane "total" comme précédemment. La différence avec le titre du titane(III) conduit au titre du titane(IV). Signalons que pour les solutions étudiées, ce dernier a atteint au maximum la valeur de 3%;

titre de l'ion bromure $(Br)_t$: dosage potentiométrique par le nitrate d'argent après élimination du titane(III) par passage sur résine cationique (Amberlite I.R. 120);

titre de l'acide initial. La méthode classique de GRAN[5] n'est ici plus valable car l'ion titaneux hydrolyse en milieu très acide et la droite d'extrapolation conduit à un point d'équivalence erroné.

Si l'on fait le bilan des charges nous obtenons:

$$H = [Br]_t - 3[Ti^{3+}] - 4[Ti^{4+}] \qquad (1)$$

On obtient ainsi pour chaque solution une valeur de l'acidité libre, valeur approchée du fait de l'incertitude des dosages par différence. Si l'on se place dans un domaine d'acidité où l'ion métallique n'a pas encore subi d'hydrolyse, il se trouve alors uniquement sous forme hydratée et la quantité

$$S = h - H + OH^- \qquad (2)$$

doit être nulle. Or en utilisant la valeur approchée de H déterminée par (1), la quantité S demeure bien constante mais se trouve légèrement négative en général pour un assez grand nombre de points au début de chaque titrage. Il suffit alors de modifier la valeur de H d'une quantité δ de façon à annuler S dans cette zône où l'hydrolyse n'a pas encore lieu. Cet artifice n'est pas arbitraire puisque nous vérifions pour plusieurs courbes, correspondant à des prises de titane croissant en progression arithmétique, que la correction δ suit cette même progression.

Signalons enfin que les étalonnages et les mesures de pH été conduits de la même façon que précédemment[1]. Nous avons travaillé à 25° et en milieu KBr 3 M.

Hydrolyse de l'ion Ti^{3+}

Les titrages ayant été effectués dans les conditions déjà indiquées[1], nous avons obtenu des courbes d'hydrolyse très régulières. Chacune des courbes, exploitée ultérieurement, représente la moyenne d'au moins deux titrages réalisés dans les mêmes conditions. Ces courbes permettent de tracer les variations Z(pH) pour différentes concentrations en titane(III) (Fig. 1).

Le déplacement de ces courbes vers les pH acides lorsque la cencontration du titane augmente, est caractéristique de l'existence d'une espèce hydroxydée polynucléaire qu'il serait logique d'étudier par la méthode classique de SILLÉN fondée sur la mesure de l'écart entre les courbes, c'est à dire $t = (\Delta \log B / \Delta \log h)_Z$. Or la quantité H a une influence très importante sur cet écart qui oscille entre les valeurs 3 et 4; de ce fait dans le domaine d'acidité très élevée où nous travaillons, on ne peut accorder beaucoup de crédit à une telle détermination.

C'est pourquoi nous avons dû exploiter les mesures différemment, comme le proposent HIETANEN ET SILLÉN[6,7] pour l'hydrolyse de thorium(IV) et PAJDOWSKI[8] pour l'hydrolyse de vanadium(III); la méthode consiste à comparer les courbes $Z(\log h)_B$ expérimentales avec un faisceau de courbes $X(\log h)_B$ calculées correspondant chacune à une seule espèce hydroxydée. Comme les valeurs expérimentales de Z laissent présager l'existence de complexes ayant au plus 2 OH par atome de Ti, nous nous sommes limités au calcul des courbes théoriques relatives aux espèces: $Ti_2(OH)$, $Ti(OH)$, $Ti_2(OH)_2$ et $Ti(OH)_2$. On constate alors par coïncidence, que les courbes expérimentales révèlent l'existence des deux espèces $Ti(OH)$ et $Ti_2(OH)_2$.

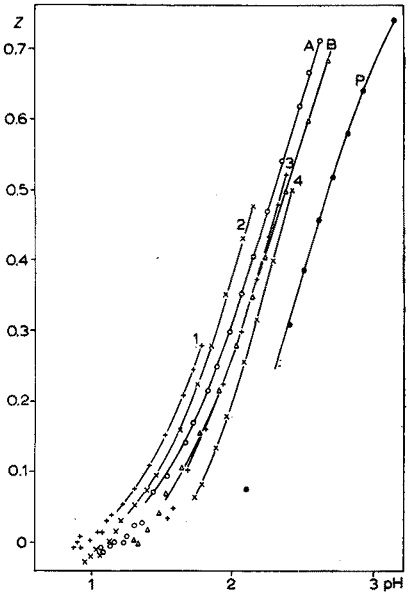

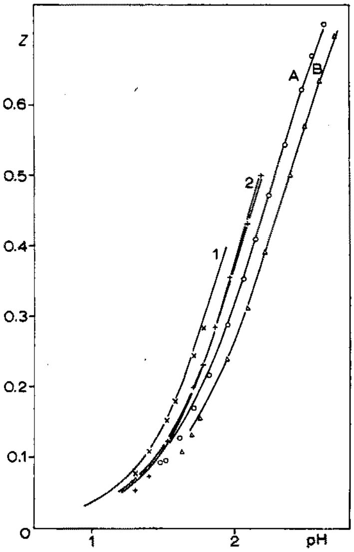

Fig. 1. Hydrolyse de Ti(III). Z=f(pH). (1,2,3,4) titrage coulométrique ($[Ti]_t$=9.615, 25.64, 49.02 96.15 mM); (A, B) titrage par KOH ($[Ti]_t$=9.805, 19.61 mM); (P) courbe d'après réf. 2.

Fig. 2. Hydrolyse de Ti(III). —— courbes calculées; + × points expérimentaux (titrage coulométrique); ○ △ points expérimentaux (titrage par KOH).

On ne peut étudier séparement ces deux complexes en choisissant des conditions expérimentales telles que l'une au moins prédomine (en dessous du mur mononucléaire pour $Ti(OH)$ ou à très forte concentration en Ti(III) pour $Ti_2(OH)_2$) car dans le premier cas les mesures sont très peu précises et dans le second cas la force ionique ne peut être maintenue à 3. C'est pourquoi nous avons travaillé dans le domaine de concentrations intermédiaires en calculant les valeurs β_{11} et β_{22} par approximations successives jusqu'à obtenir le meilleur jeu de constantes. C'est ainsi que l'on a obtenu:

$$\log \beta_{11} = -2.55$$

$$\log \beta_{22} = -3.30$$

Pour apprécier l'exactitude de ces valeurs, nous avons comparé sur la Fig. 2 les points expérimentaux $Z(\log h)_B$ avec les courbes calculées à partir des constantes proposées. Cette comparaison laisse apparaître une assez nette divergence pour $Z < 0.1$ correspondant aux résultats obtenus en milieu très acide. Dans ce domaine, le calcul de Z par la relation $Z = h - H/B$ est très peu précis car $h \sim H$: la différence de deux quantités élevées est très faible. L'imprécision provient essentiellement de la mesure de h car le calcul montre que le fait de modifier légèrement H ne fait subir aux courbes $Z(\log h)_B$ qu'une translation, l'écart entre deux courbes ainsi déplacées étant conservé.

Par contre, au dessus de $Z \sim 0.1$, la concordance est bonne, ce qui permet de conclure au bien fondé des hypothèses et des valeurs des constantes trouvèes.

Système acide picolique–titane (III)

Les études précédentes d'hydrolyse, réalisées par coulométrie nous ayant donné satisfaction, nous avons pensé qu'il pouvait être avantageux d'étendre cette technique à la complexation du titane par un autre coordinat que l'ion hydroxyde: l'anion picolate.

Nous avons dû redéterminer les deux constantes de dissociation de l'acide picolique pour les conditions de travail adoptées: 25° et KBr 3 *M*. En exploitant des courbes de titrages protométriques par les méthodes habituelles, nous avons obtenu

$$pK_1^H = 1.36 \text{ et } pK_2^H = 5.80$$

Pour étudier le système acide picolique–titane(III), nous avons appliqué la méthode classique de BJERRUM[9] à une série de courbes de neutralisation de mélanges $[L]_t$, $[Ti^3]_t$ et H. Dans un premier temps, cette neutralisation a été effectuée par la soude selon le procédé courant. On obtient alors des courbes de formation $\bar{n}(pL)$ qui se déplacent plus ou moins régulièrement vers les faibles pL lorsque le rapport $[L]_t/[Ti^{3+}]_t$ augmente. C'est là un phénomène assez fréquemment observé avec certains complexes de l'acide picolique[3,10,11]. Ce déplacement ne doit pas être attribué à l'hydrolyse de titane, réaction parasite qui perturberait la formation des complexes TiL_n, car il a été observé avec le picolate de cuivre(II)[10], c'est à dire avec un cation beaucoup moins hydrolysable que l'ion titaneux. Nous pensons que l'addition d'une base forte entraîne une concentration locale d'ions OH^- qui provoquerait la formation d'espèces hydroxydées ne redonnant pas reversiblement les espèces TiL_n[12] seules prises en considération dans la méthode de BJERRUM.

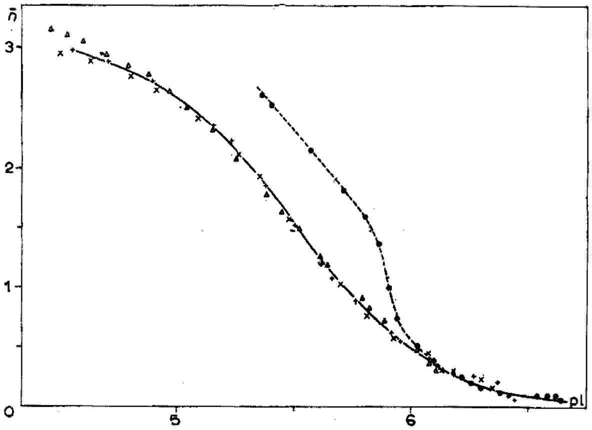

Fig. 3. Courbe de formation du picolate de Ti(III). L_t/B = ●3; +4.5; ×6; △9; o points recalculés.

Il apparaissait donc particulièrement avantageux de pouvoir modifier le pH du mélange non plus en ajoutant des ions OH^- mais en faisant disparaître les ions H^+ par coulométrie.

Quatre mélanges, à divers rapports $[L]_t/[Ti]_t$ ont donc été titrés par la méthode coulométrique. Les données traitées par la méthode de calcul de BJERRUM conduisent alors aux courbes de formation de la Fig. 3: toutes ces courbes sont confondues, exceptée celle qui correspond à une faible concentration en $[L]_t$ ($[L]_t/[Ti]_t=3$) et qui est nettement perturbée par l'hydrolyse.

On peut dès lors être certain que l'hypothèse des complexes successifs mononucléaires TiL, TiL_2 et TiL_3 est vérifiée. On peut en outre déterminer les constantes de stabilité de ces trois espèces en utilisant la méthode de "curve fitting" de ROSSOTTI[13,14]. Le calcul conduit alors à

$\log \beta_1 = 5.62$ $\log K_1 = 5.62$

$\log \beta_2 = 11.10$ $\log K_2 = 5.48$

$\log \beta_3 = 16.58$ $\log K_3 = 5.48$

Afin de vérifier ces valeurs, nous avons comparé la courbe de formation expérimentale avec une courbe de formation théorique calculée à partir de ce jeu de constantes.

La courbe de formation théorique (points o sur la Fig. 3) coïncide exactement avec la courbe expérimentale.

CONCLUSION

L'étude de ces deux systèmes montre que le procédé de titrage coulométrique est des plus intéressants. Certes il ne peut prétendre être d'application aussi générale que les titrages classiques par addition de base. Il est évidemment limité aux cas de mélanges où seuls les protons sont réductibles sur cathode de platine ce qui élimine impérativement un certain nombre de cations et d'agents complexants.

En dehors de ces limitations, nous pensons que cette méthode de titrage présente des avantages certains, notamment lorsqu'on veut réaliser des titrages à concentration constante en ion métallique comme c'est le cas de la plupart des méthodes d'étude des composés de coordination. L'artifice consistant à ajouter au cours du titrage par une base forte une solution d'ion métallique pour compenser les effets de dilution présente des complications d'appareillage lorsqu'on s'adresse à des cations très sensibles à l'oxydation. De plus si l'addition d'une base forte peut provoquer des concentrations locales de base conduisant à la formation d'espèces complexes irréversibles, le fait de réduire coulométriquement des protons pour augmenter le pH est un procédé beaucoup plus progressif qui conduit à de biens meilleures courbes de formation. Nous en avons apprécié l'avantage lors de l'étude du picolate de titane. Il convient également de souligner la souplesse d'emploi d'un tel procédé de titrage qui évite de préparer le réactif titrant à une concentration donnée puisque l'intensité du courant, réglable à volonté au cours d'un même titrage, s'identifie au titre de la base tandis que le chronomètre interrupteur fait office de robinet de burette.

Nous pensons ainsi avoir mis au point un procédé de titrage convenant à l'étude de nombreux cations non réductibles (Be^{2+}, Al^{3+} etc.) ou à leurs valences inférieures, dans la mesure toutefois où le platine de l'électrode ne catalyse pas l'oxydation de l'ion réducteur par les protons (cas du Cr^{2+}).

RÉSUMÉ

Un procédé de titrage coulométrique des protons permet d'étudier l'hydrolyse de l'ion titane(III) et sa complexation par l'acide picolique. Les compositions et les constantes de stabilité des espèces formées sont données.

SUMMARY

The hydrolysis and the complexation of titanium(III) with picolinic acid were studied by coulometric titration of protons. The composition and the stability constants of the species formed are reported.

ZUSAMMENFASSUNG

Die Hydrolyse und die Komplexbildung des Ti(III) Ions mit picolinic Säure ist durch coulometrische Titration der Wasserstoff Ionen durchgeführt. Die Zusammensetzung und die Stabilitätkonstanten der Komplexen sind gegeben.

BIBLIOGRAPHIE

1 M. R. Pâris et Cl. Gregoire, Mémoire précédent.
2 R. L. Pecsok et A. N. Fletcher, *Inorg. Chem.*, 1 (1962) 155.
3 M. R. Pâris, *Thèse*, Lyon, 1963.
4 G. Black, E. Depp et B. B. Corson, *J. Org. Chem.*, 14 (1949) 14.
5 G. Gran, *Analyst*, 77 (1952) 661.
6 S. Hietanen et L. G. Sillén, *Acta Chem. Scand.*, 13 (1959) 533.
7 S. Hietanen et L. G. Sillén, *Acta Chem. Scand.*, 13 (1959) 1828.
8 L. Pajdowski, *Ann. Soc. Chim. Polonorum*, 37 (1963) 1351.
9 J. Bjerrum, *Metal Ammine Formation in Aqueous Solutions*, P. Haase and Son, Copenhagen, 1957.
10 G. Thomas, *Thèse*, Lyon, 1960.
11 R. C. Mercier, *Thèse*, Lyon, 1966.
12 B. O. Hedstrom, *Arkiv Kemi*, 6 (1953) 1.
13 F. J. C. Rossotti, H. S. Rossotti et L. G. Sillén, *Acta Chem. Scand.*, 10 (1956) 203.
14 F. J. C. Rossotti et H. S. Rossotti, *The Determination of Stability Constants*, McGraw Hill, 1961.

Analytica Chimica Acta
Elsevier Publishing Company, Amsterdam
Printed in The Netherlands

ETUDE POLAROGRAPHIQUE DES REACTIONS D'OXYDO-REDUCTION ET DE COMPLEXATION DONNEES PAR LA PENICILLAMINE, LA N-ACETYLPENICILLAMINE ET LES IONS CUIVRE(I) ET (II)

J. J. VALLON ET A. BADINAND
Laboratoire de Chimie Analytique, Faculté Mixte de Médecine et de Pharmacie, Lyon (France)

(Reçu le 29 janvier, 1968)

L'intérêt thérapeutique de la pénicillamine (β,β-diméthylcystéine) pour le traitement des intoxications par le cuivre, le plomb, le mercure et d'autres métaux, a été signalé il y a une dizaine d'années[1-5]. Les stabilités des complexes métalliques formés ont été mesurées[6] à l'exception de celles relatives aux complexes du cuivre pour lesquelles aucune mesure potentiométrique n'a été possible[7]: des phénomènes d'oxydo-réduction entre métal et coordinat ont été rendus responsables du manque de reproductibilité des courbes potentiométriques[7].

La polarographie, permettant l'étude simultanée de l'oxydo-réduction et de la complexation, nous a semblé plus adaptée au problème posé. Nous donnons ici les résultats fournis par l'étude des réactions entre le cuivre(I) et la pénicillamine (RSH), puis de celles entre le cuivre(II) et la pénicillamine ou son dérivé N-acétylé (NARSH). La technique utilisée s'inspire de celle employée par STRICKS ET KOLTHOFF pour le système cuivre–cystéine[8].

APPAREILLAGE ET RÉACTIFS

Appareillage

pH-mètre Tacussel TS4. Polarographe Radiometer type PO4: essais faits sous courant d'azote, à 25°, après barbotage dans un tampon ammoniacal de concentration identique à celle utilisée dans l'essai. Potentiels mesurés par rapport à l'électrode au calomel à KCl saturé. Caractéristiques de l'électrode à goutte de mercure: $m = 4.299$ mg sec^{-1}. $m^{2/3}\, t^{1/6} = 3.09$ mg$^{2/3}$ sec$^{-1/2}$.

Réactifs

Chlorhydrates de pénicillamine et de N-acétylpénicillamine (Laboratoire NBC): solutions dans l'eau distillée conservées sous azote.

Solution de cuivre(I): préparée par dissolution de chlorure cuivreux Merck dans une solution de sulfite disodique de sorte que la concentration finale soit 10 fois supérieure à celle du métal. Un barbotage de SO_2 est ensuite poursuivi 30 min pour assurer la transformation totale en bisulfite et la dissolution complète du sel métallique. Les concentrations finales étaient 0.01 *M* en Cu(I) et 0.2 *M* en bisulfite.

Solution de cuivre(II): préparée par dissolution de $CuSO_4 \cdot 5\,H_2O$ (R.P. Prolabo) dans l'eau.

Solutions d'ammoniaque et de chlorure d'ammonium 5 *M* servant à tamponner le milieu et, dans l'étude avec Cu(I), à convertir extemporanément le complexe sulfitique en ammine cuivreuse.

Du bisulfite de sodium 0.2 *M* et du nitrate de sodium 5 *M* ont servi au maintien d'une concentration constante en SO_3^{2-} ou au maintien de la force ionique.

ÉTUDE DE LA RÉACTION Cu(I)–PÉNICILLAMINE

Etude qualitative

Des additions successives de Cu(I) 0.01 *M* à 50 ml de pénicillamine 0.001 *M* en solution dans le tampon ammoniaque–chlorure d'ammonium 0.1 *M* et en présence de 0.005% de gélatine ont été réalisées. Vingt minutes après chaque addition les polarogrammes ont été enregistrés.

Le coordinat libre (RSH, Fig. 1) présente une vague anodique vers −0.5 V (par rapport à l'électrode au calomel). L'addition de cuivre(I) l'abaisse progressivement et fait apparaître une vague cathodique vers −0.8 V, due à la réduction d'un complexe Cu(I)–RSH en amalgame de cuivre et RSH (courbes B,C,D). Lorsque le coordinat libre a disparu de la solution (courbe B) la vague du complexe atteint un maximum. L'addition ultérieure de cuivre(I) fait apparaître vers −0.4 V, une vague de réduction de l'ammine cuivreuse $Cu(NH_3)_2^+$ en excès, qui se superpose à la précédente. Les positions relatives des vagues de l'ammine et du complexe soufré indiquent la plus grande stabilité de ce dernier.

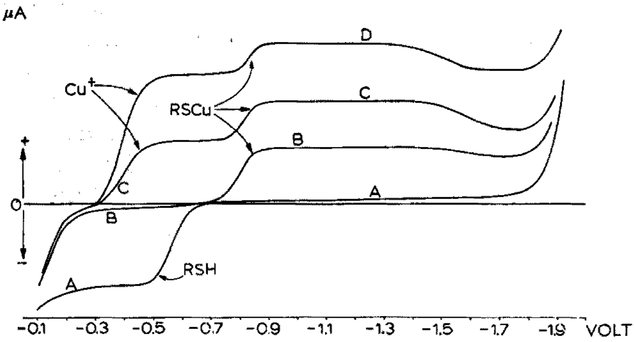

Fig. 1. Polarogrammes obtenus lors du titrage de 50 ml de pénicillamine 10^{-3} *M* par l'ammine cuivreuse 10^{-2} *M*. (RSH) coordinat pur (A), après addition de 5 ml (B), 8.5 ml (C), 11.5 ml (D) de solution de Cu(I).

Nous avons tracé (Fig. 2) les variations des courants limites de diffusion de chaque espèce électroactive au cours de la titration par le cuivre(I). La disparition de RSH libre lorsque le rapport Cu(I)/RSH atteint la valeur 1 correspond au maximum de la courbe du complexe soufré: la structure de celui-ci est du type 1–1(RSCu(I)). Lorsqu'un excès de métal apparaît dans la solution, les courants de diffusion de RSCu(I) diminuent et la courbe de l'ammine cuivreuse se trouve abaissée par rapport à la théorie: ce phénomène traduit la présence de complexes secondaires du type $Cu(RSCu)_x^+$ déjà signalés par STRICKS ET KOLTHOFF[8]. On remarque parallèlement un déplacement de la vague de RSCu(I) vers des potentiels plus négatifs.

Détermination de la constante de dissociation du complexe RSCu(I)

Six essais ont été effectués en présence d'un excès de coordinat pour rendre réversible la réduction de RSCu(I) à l'électrode. La réversibilité a été vérifiée en mesurant la différence $E_{3/4}-E_{1/4}$ qui doit garder la valeur $-0.056/n$. Dans tous les essais, la concentration en ion sulfite a été maintenue à 0.04 *M*, pour que la formation du complexe bisulfitique du cuivre(I) soit négligeable devant celle de l'ammine ($K_{\mathrm{Cu(NH_3)_2^+}} = 10^{-10.87}$; $K_{\mathrm{Cu(SO_3)_2^{3-}}} = 10^{-8.5}$). Le Tableau I donne les concentrations de chaque constituant dans les essais.

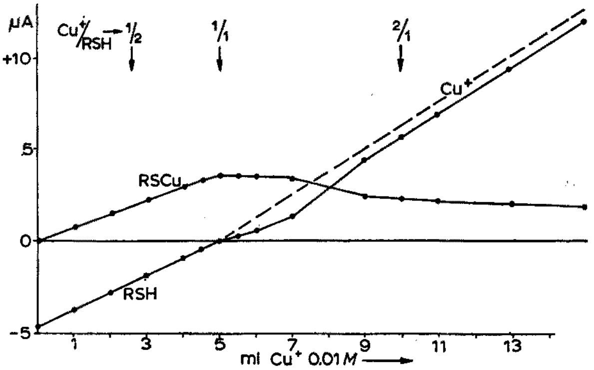

Fig. 2. Titration lente de 50 ml de pénicillamine 10^{-3} *M* par l'ammine cuivreuse 10^{-2} *M*. Variations du courant de diffusion du coordinat (RSH), du complexe (RSCu(I)) et du métal (Cu(I)) en fonction des ml de métal ajoutés.

TABLEAU I

MESURE DE LA CONSTANTE DE STABILITÉ DE RSCu(I)

($2\cdot10^{-3}$ *M* Cu(I), 1.0 *M* NH_4Cl)

Essai	*(RSH)*	*Réversibilité* $E_{3/4}-E_{1/4}$	*pH*	i_d/c	$E_{1/2}$	*n*	$K_{RSCu(I)}$
A	0	—	9.45	6.90	−0.519	0.86	—
B	0.04	−0.055	9.44	5.05	−0.893	1.08	$1.64\cdot10^{-20}$
C	0.04[a]	−0.060	10.30	4.45	−0.931	1.11	$2.38\cdot10^{-20}$
D	0.015	−0.055	9.40	4.35	−0.870	1.20	$1.11\cdot10^{-20}$
E	0.015[b]	−0.060	9.40	6.00	−0.850	1.12	$3.64\cdot10^{-20}$
F	0.04[b]	−0.060	9.39	8.20	−0.870	1.05	$6.07\cdot10^{-20}$

[a] NH_4Cl 0.05 *M*, $NaNO_3$ 0.95 *M*.
[b] Cu(I) $5\cdot10^{-4}$ *M*.

Les courbes log $\{(i_d-i)/i\}=f(Eeg)$ ont permis de déterminer $E_{1/2}$ pour log $(i_d-i)/i=0$. Le nombre d'électrons *n* échangés à l'électrode a été obtenu en mesurant la pente de chaque droite égale à $0.0591/n$ comme le montre l'équation:

$$Eeg = E_{1/2} + (0.0591/n)\log\{(i_d-i)/i\}$$

Les valeurs obtenues ont montré que la réaction met en jeu un seul électron (Tableau I).

La constante de dissociation du complexe RSCu(I) a été calculée pour chaque essai avec la formule de STRICKS ET KOLTHOFF[8]:

$$\log K_{\mathrm{RSCu}} = \frac{E_{1/2\mathrm{RSCu}} - E_{1/2\mathrm{Cu(NH_3)_2^+}}}{0.059} - \log \frac{k_{\mathrm{Cu(NH_3)_2^+}}}{k'_{\mathrm{RSCu}}} + (\mathrm{pH} - \mathrm{p}K_{\mathrm{RSH}})$$
$$+ \log C_{\mathrm{RSH}} + \log K_{\mathrm{Cu(NH_3)_2^+}}$$

Dans cette formule K_{RSCu} est la constante de dissociation du complexe RSCu, $E_{1/2}$ les potentiels de demi-vague; k/k' rapport des constantes de diffusion de l'ammine et du complexe soufré, est égal au rapport entre les courants de diffusion qu'ils donnent pour une concentration identique dans le milieu. pK_{RSH} est le pK du groupe SH de la pénicillamine, trouvé égal à *10.46* par KUCHINSKAS ET ROSEN[6]. Les dissociations des groupes NH_2 et COOH peuvent être négligées dans la zone de pH étudiée. C_{RSH} est la concentration analytique du coordinat libre (concentration mise au départ diminuée de la concentration entrant dans le complexe considéré exactement 1–1). $K_{\mathrm{Cu(NH_3)_2^+}}$ est la constante de dissociation de l'ammine, trouvée égale à $1.35 \cdot 10^{-11}$ par BJERRUM[9].

La valeur moyenne de la constante de dissociation a été trouvée à $2.97 \cdot 10^{-20}$. Dans deux autres séries d'essais, elle était de $2.84 \cdot 10^{-20}$ et $3.07 \cdot 10^{-20}$, soit une valeur moyenne de $2.96 \cdot 10^{-20}$. L'énergie libre de formation du complexe a pour valeur: $\Delta F = -RT \ln K = -26.6$ kcal; la constante de dissociation du complexe Cu(I)–cystéine calculée par KOLTHOFF était de $6.5 \cdot 10^{-20}$ avec une énergie de formation de -26.2 kcal. Nous avons essayé dans les mêmes conditions la forme D et la forme DL de la pénicillamine: les mêmes valeurs ont été enregistrées dans les deux cas.

L'étude des valeurs de i_d/c montre que celles-ci augmentent lorsque l'excès de coordinat par rapport au complexe s'accroît. Ce phénomène, non observé avec la cystéine, pourrait être dû à une modification de structure du complexe, mais son interprètation reste délicate.

ÉTUDE DE LA RÉACTION Cu(II)–PÉNICILLAMINE

50 ml de coordinat 10^{-3} M en solution dans le tampon ammoniacal ($NH_4OH = NH_4Cl = 10^{-1}$ M) ont été titrés par la solution 10^{-2} M de Cu(II) en présence de 0.005% de gélatine. Les enregistrements polarographiques ont été effectués 20 min après chaque addition de métal.

La vague de RSH libre ($E_{1/2} = -0.53$ V) baisse progressivement lors de l'addition de Cu(II) et il apparaît parallèlement la vague cathodique du complexe RSCu(I) ($E_{1/2} = -0.78$ V). Lorsque le rapport RSH/Cu(II) atteint la valeur 2 (point équivalent), la vague de RSH disparaît. Pour des valeurs toujours plus faibles de ce rapport, l'excès de métal, existant alors dans la solution, donne lieu à une double vague cathodique qui correspond à la réduction en deux étapes du complexe amminé (Cu(II)→Cu(I) puis Cu(I)→Cu(0)), phénomène classique en milieu ammoniacal.

Les variations des courants de diffusion de chaque espèce électroactive au cours du titrage par le cuivre(II) (Fig. 3) rendent compte de la disparition progressive de la forme libre RSH au profit du complexe RSCu(I).

Avant le point équivalent (RSH/Cu(II) = 2) on peut considérer que deux réactions ont lieu: une réduction du métal jusqu'au degré un puis une complexation de

Cu(I) par l'excès de coordinat présent:

$$2\,\mathrm{RS^-} + 2\,\mathrm{Cu^{2+}} \rightarrow 2\,\mathrm{Cu^+} + \mathrm{RSSR} \tag{1}$$

$$2\,\mathrm{RS^-} + 2\,\mathrm{Cu^+} \rightarrow 2\,\mathrm{RSCu(I)} \tag{2}$$

La réaction globale s'écrit:

$$4\,\mathrm{RS^-} + 2\,\mathrm{Cu^{2+}} \rightarrow 2\,\mathrm{RSCu(I)} + \mathrm{RSSR} \tag{3}$$

Le disulfure formé est la dithiobisvaline et la réaction globale rend compte du rapport stoechiométrique trouvé (RSH/Cu(II) = 2). Des réactions identiques avaient été observées par KOLTHOFF ET STRICKS[10] entre la cystéine et le cuivre(II); mais, alors que la vague cathodique de la cystine est facilement mise en évidence vers −1.2 V, celle de la dithiobisvaline se situe vers −2 V, c'est-à-dire au potentiel de réduction du solvant, ce qui rend impossible la mesure de courant de diffusion.

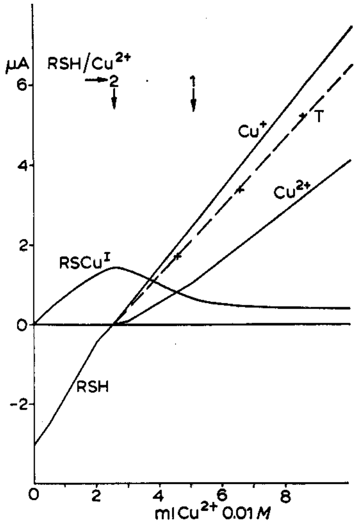

Fig. 3. Titration lente de 50 ml de pénicillamine 10^{-3} M dans NH_3 0.1 N par Cu(II) 10^{-2} M. Variations du courant limite du coordinat (RSH), du complexe cuivreux (RSCu(I)), et du métal (Cu^+ et Cu^{2+}) en fonction des ml de solution cuivrique ajoutés (après corrections de volume). (T) courbe témoin du métal en l'absence de coordinat (courbes Cu^+ et Cu^{2+} identiques).

Après le point équivalent, le cuivre(II) en excès donne les deux courbes de réduction en deux étapes, mais leurs pentes, bien que devant être théoriquement identiques, diffèrent: Cu(II) est abaissée, Cu(I) augmentée (Fig. 3). KOLTHOFF a montré que ce phénomène était dû à une oxydation partielle du complexe par le cuivre(II) selon:

$$2\,\mathrm{RSCu(I)} + 2\,\mathrm{Cu^{2+}} \rightarrow \mathrm{RSSR} + 4\,\mathrm{Cu^+}$$

La réaction consomme Cu^{2+} et RSCu(I) et fournit Cu(I). Elle est plus intense pour les rapports RSH/Cu(II) compris entre 2 et 1 que pour ceux inférieurs à 1.

ÉTUDE DE LA RÉACTION Cu(II)–N-ACÉTYLPÉNICILLAMINE

Les essais ont été conduits dans les mêmes conditions expérimentales que précédemment:

Les polarogrammes (Fig. 4) sont analogues à ceux obtenus avec RSH. Le potentiel de demi-vague du coordinat est à −0.51 V. L'addition de Cu(II) forme un complexe cuivreux NARSCu(I) donnant une vague de réduction en cuivre amalgamé ($E_{1/2} = -0.70$ V) qui se déplace vers les valeurs négatives lorsque la concentration de Cu(II) augmente. Lorsque le métal est en excès, une double vague de réduction en deux étapes se superpose à la précédente.

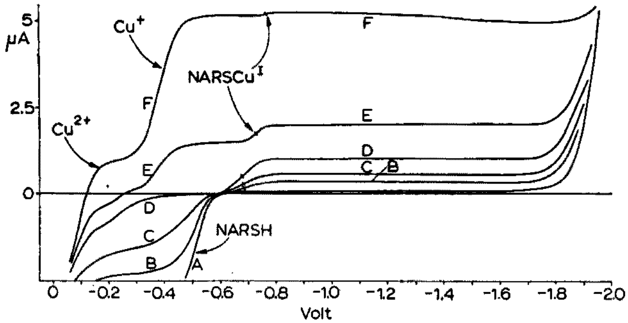

Fig. 4. Titrage de 50 ml de NARSH 10^{-3} M dans NH_3 0.1 N, par l'ammine cuivrique 10^{-2} M. (NARSH) N-acétylpénicillamine en solution pure (A), additionnée de 0.5 ml (B), 1 ml (C), 2.5 ml (D), 3 ml (E), 5 ml (F) de solution cuivrique. (NARSCu(I)) vague du complexe cuivreux.

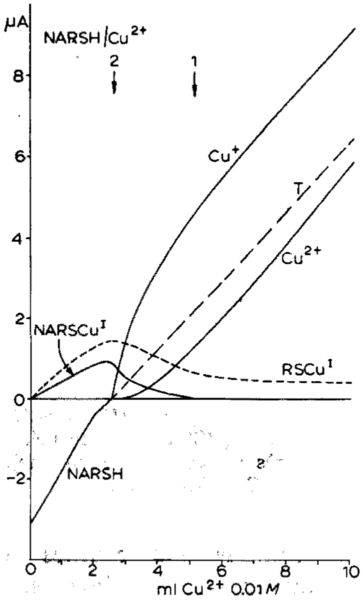

Fig. 5. Titration lente de 50 ml de N-acétylpénicillamine dans NH_3 0.1 N par Cu^{2+} 10^{-2} M. (NARSH) coordinat libre. (NARSCu(I)) complexe cuivreux. (Cu^{+} et Cu^{2+}) ammines cuivreuse et cuivrique. (T) métal en l'absence de coordinat (courbes Cu^{+} et Cu^{2+} identiques).

NARSCu(I) se comporte donc différemment de RSCu(I) après le point équivalent (NARSH/Cu(II) = 2); sa vague polarographique est non seulement déplacée vers des valeurs négatives, mais elle disparaît totalement lorsque le rapport stoéchiométrique atteint la valeur 1. Ceci indique la destruction totale du complexe par Cu(II) en excès, suivant une réaction déjà vue. Le complexe N-acetylé apparaît bien plus instable que RSCu(I).

L'étude des variations des courants de diffusion au cours du titrage offre un intérêt particulier pour comparer les stabilités des complexes en présence d'un excès de métal au degré II (Fig. 5).

La formation de NARSCu(I) est maximum au point équivalent, mais les courants de diffusion sont très inférieurs à ceux de RSCu(I). Avant le point équivalent, les mêmes réactions d'oxydo-réduction et de complexation qu'avec RSH ont lieu et, comme précédemment, la vague de réduction du disulfure n'est pas visible, car probablement située au delà de -2 V. Après le point équivalent, la courbe de NARSCu(I) s'annule vite, tandis que celle de Cu(I) croît beaucoup plus vite qu'en présence de RSH. La courbe Cu(I) est située très au-dessus de la courbe théorique (T) bien que de même pente qu'elle; son prolongement passe par l'origine (0 μA; 0 ml) ce qui confirme que la destruction de NARSCu(I) est totale en présence d'excès de Cu(II), Cu(I) étant alors converti en ammine cuivreuse.

Le complexe cuivreux acétylé manifeste donc une stabilité très inférieure à celle du complexe de la pénicillamine. Ce fait suggère une participation importante du groupe NH_2 dans la complexation; une structure cyclique pentagonale serait responsable de la stabilité du complexe.

RECHERCHE D'UN POUVOIR COMPLEXANT DE LA BISTHIOVALINE

Les essais précédents n'ayant pas permis d'observer la formation d'un complexe entre l'amino-acide et le cuivre(II), il était intéressant de vérifier la possibilité d'une complexation des ions cuivriques par les disulfures formés au cours des oxydo-réductions précédentes (bisthiovaline (RSSR) ou son dérivé N-acétylé).

Des titrages de la bisthiovaline (RSSR) 10^{-3} M par Cu(II) 10^{-2} M, en tampon ammoniacal 10^{-1} M, fournissent des polarogrammes ayant les caractéristiques suivantes: une double vague de réduction de l'ammine cuivrique en deux étapes, et une vague cathodique due à RSCu(I) ($E_{1/2}$ voisin de -0.76 V) qui apparaît lorsque le rapport RSSR/Cu(II) possède des valeurs supérieures à 1. Ce complexe résulte de la réaction à l'électrode:

$$\mathrm{RSSR} + 4\,\mathrm{Cu}^{+} \rightleftarrows 2\,\mathrm{RSCu(I)} + 2\,\mathrm{Cu}^{2+}$$

Comme la présence d'ammoniac 0.1 M pouvait masquer la formation d'un complexe de faible stabilité avec le disulfure, d'autres essais ont été effectués dans du nitrate de sodium molaire. Les polarogrammes ont alors montré une seule vague de réduction de l'aquocomplexe cuivrique et deux vagues cathodiques dues à RSSR et à RSCu(I). Aucun indice de complexation de Cu(II) par RSSR n'a été obtenu.

Par contre, par l' emploi de solutions plus diluées de tampon ammoniacal, nous avons pu mettre en évidence un faible pouvoir complexant de RSSR vis à vis de Cu(II). Dans le tampon ammoniaque–chlorure d'ammonium 0.02 M, le disulfure (RSSR) est réduit vers -1.70 V (Fig. 6). L'addition du cuivre(II) fait apparaître les deux vagues cathodiques des ammines métalliques déplacées de 0.10 V vers les potentiels négatifs par rapport aux potentiels théoriques. Ce déplacement traduit l'existence d'un complexe avec RSSR.

Après le point équivalent (courbes D et E), la vague relative à la première étape de la réduction (Cu^{2+}) reprend sa position théorique ($E_{1/2}$ voisin de -0.05 V), l'autre (Cu^{+}) restant stationnaire. On peut donc attribuer la vague à -0.14 V à un complexe RSSRCu(II) de faible stabilité.

Les données précédentes se trouvent confirmées par l'étude des variations des courants de diffusion au cours du titrage (Fig. 7). La vague cathodique à -0.14 V (RSSRCu(II)) atteint un maximum pour la valeur 1 du rapport coordinat–métal.

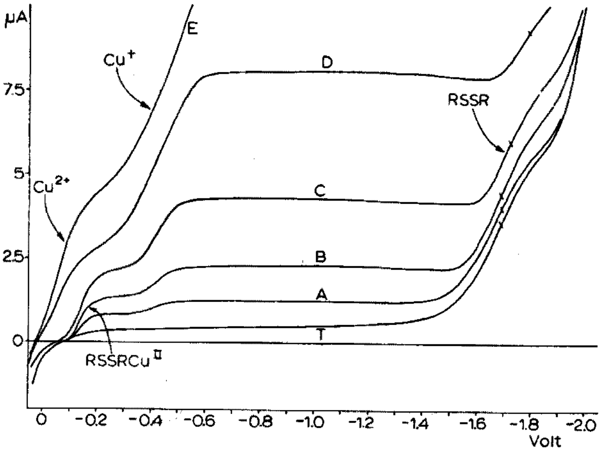

Fig. 6. Polarogrammes obtenus lors du titrage de 50 ml de dithiobisvaline (RSSR) 10^{-3} M dans NH_3 0.02 M par l'ammine cuivrique 10^{-2} M. RSSR coordinat pur (T) en présence de 1 ml (A), 2 ml (B), 4 ml (C), 7.5 ml (D), 10 ml (E) du métal.

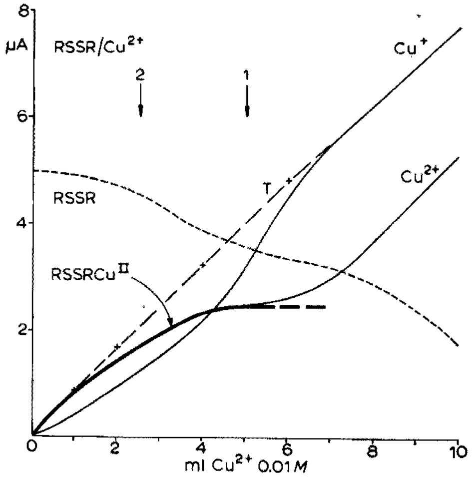

Fig. 7. Titration lente de 50 ml de RSSR 10^{-3} M dans NH_3 0.02 M par Cu^{2+} 10^{-2} M. (RSSR) coordinat libre. (Cu^{2+}) première vague cathodique du métal ($E_{1/2} = -0.07$ V). (Cu^{+}) deuxième vague cathodique du métal ($E_{1/2} = -0.42$ V). (RSSRCu(II)) complexe cuivrique ($E_{1/2} = -0.15$ V).

Avec l'excès de Cu(II), le potentiel de la vague augmente ($E_{1/2}$ voisin de -0.07 V) sans qu'il soit possible de différencier celle-ci de la précédente. Les variations du courant cathodique global (Fig. 7) permettent cependant d'observer la superposition des deux vagues: celle du complexe RSSRCu(II) et celle de l'ammine (Cu^{2+}).

La vague cathodique due à la deuxième étape de la réduction ($E_{1/2} = -0.42$ V) (Cu^+), donne une courbe ampérométrique confondue avec la courbe théorique (T) après le point équivalent mais inférieure à elle au début du titrage. On peut interprèter ce phénomène par une oxydation partielle de Cu(I) par RSSR au niveau de l'électrode. La réaction n'a lieu que lorsque le coordinat est en excès, par rapport à Cu(II).

Au cours du titrage, les courants de diffusion de RSSR s'abaissent. Leur variation irrégulière est due à une transformation à la fois en RSCu(I) et en RSSRCu-(II).

La dithiobisvaline apparaît donc douée de faibles propriétés complexantes vis à vis de Cu(II).

CONCLUSION

L'étude systématique des réactions pouvant avoir lieu entre le cuivre sous ses deux degrés d'oxydation et la pénicillamine ou son dérivé N-acétylé nous permet de préciser les faits suivants:

(*1*) Cu(I) donne avec la pénicillamine un complexe deux fois plus stable que celui de la cystéine.

(*2*) L'acétylation du groupe NH_2 de la pénicillamine diminue considérablement son pouvoir complexant ce qui permet de penser que le complexe cuivreux possède une structure chélatée pentagonale où le métal est en liaison avec l'atome de soufre et l'atome d'azote aminé. Une coordinence reste libre sur le métal et permet probablement la fixation d'une autre molécule donneuse de doublet (NH_3 ou OH_2).

(*3*) Cu(II), mis en présence du coordinat, l'oxyde partiellement et Cu(I) formé donne avec l'autre partie le complexe cuivreux.

(*4*) La recherche de la formation d'un complexe entre Cu(II) et le produit d'oxydation, la dithiobisvaline, a montré que le disulfure ne possède qu'un faible pouvoir complexant, et vis à vis de Cu(II) seulement.

Ces résultats suggèrent que le mécanisme de l'action détoxicante de la pénicillamine vis à vis du cuivre pourrait être le suivant: réduction *in situ* des ions Cu^{2+} fixés dans les tissus, puis complexation de Cu^+ ainsi formé et élimination urinaire du chélate RSCu(I). La forme d'élimination serait donc le métal sous le degré d'oxydation un, stabilisé par chélation.

Des recherches sont entreprises pour tenter d'identifier le complexe cuivreux dans les urines de malades en cours de détoxication.

RÉSUMÉ

Les auteurs ont entrepris une étude polarographique des réactions d'oxydoréduction et de complexation données par les ions Cu^{2+} et Cu^+ en présence de pénicillamine, de N-acétylpénicillamine, et d'un des produits d'oxydation, la dithiobisvaline. La formation d'un complexe cuivreux 1:1 avec la pénicillamine et Cu(I) a été mise en évidence et la stabilité du complexe a été mesurée. Le cuivre(II) oxyde le sulfure en disulfure et Cu(I) formé peut ensuite être complexé par l'amino-acide soufré. La plus grande stabilité du complexe cuivreux non acétylé suggère pour RSCu(I) l'existence d'un cycle chélaté auquel participe le groupe NH_2 libre. Les ions Cu^{2+} ne forment de complexe qu'avec le disulfure et sa stabilité est faible. Ces résultats laissent supposer que le chélate cuivreux est la forme d'élimination du cuivre au cours d'une détoxication par la pénicillamine.

SUMMARY

Polarographic methods are used to study the redox and complexation reactions between copper(II) or (I) and penicillamine, N-acetylpenicillamine or the oxidation product, dithiobisvaline. The formation of a 1:1 copper(I) complex between penicillamine and copper(I) was proved, and the stability of the complex measured. Copper(II) oxidizes the sulphur compound to the disulphide and the copper(I) formed then forms a complex with the sulphur amino-acid. The greater stability of the non-acetylated copper(I) complex suggests that RSCu(I) contains a chelate ring with participation of the free amino group. The disulphide can only form a complex with copper(II) and the stability of this complex is low. The results suggest that the copper(I) chelate is the form in which copper is eliminated during treatment with penicillamine.

ZUSAMMENFASSUNG

Polarographische Methoden werden verwendet, um die Redox- und Komplex-Reaktionen zwischen Kupfer(II) oder Kupfer(I) und Penicillamin, N-Acetylpenicillamin oder dem Oxydationsprodukt Dithio-bis-valin zu untersuchen. Die Bildung eines 1:1-Kupfer(I)-Komplexes zwischen Penicillamin und Kupfer(I) wurde bestätigt und die Stabilität dieses Komplexes gemessen. Kupfer(II) oxydiert die Schwefelverbindung zu Disulfid und das entstandene Kupfer(I) bildet dann einen Komplex mit der Schwefelaminosäure. Die grössere Stabilität des nichtacetylierten Kupfer(I)-Komplexes lässt vermuten, dass RSCu(I) einen Chelatring mit den freien Aminogruppen enthält. Das Disulfid kann nur einen Komplex mit Kupfer(II) bilden, und die Stabilität dieses Komplexes ist gering. Die Ergebnisse lassen vermuten, dass das Kupfer(I)-Chelat die Form ist, in der Kupfer während der Behandlung mit Penicillamin eliminiert wird.

BIBLIOGRAPHIE

1 J. M. Walshe, *Lancet*, 1 (1960) 188.
2 J. M. Walshe, *Am. J. Med.*, 21 (1956) 487.
3 P. Monnet, J. Gauthier, J. Cotte, J. J. Vallon, A. Nicolas et Ruitton-Uggliengo, *Pédiatrie*, XVI, 6 (1961) 565.
4 J. E. Boulding et R. A. Baker, *Lancet*, 273 (1957) 985.
5 H. V. Aposhian, *Science*, 128 (1958) 93.
6 E. J. Kuchinskas et Y. Rosen, *Arch. Biochem. Biophys.*, 97 (1962) 370.
7 D. A. Doornbos et J. S. Faber, *Pharm. Weekblad*, 99 (1964) 289.
8 W. Stricks et I. M. Kolthoff, *J. Am. Chem. Soc.*, 73 (1951) 1723.
9 J. Bjerrum, *Kgl. Danske Videnskab. Selskab, Mat. Fys. Medd.*, 11 (1931) 5; 11 (1932) 10; 12 (1934) 15.
10 I. M. Kolthoff et W. Stricks, *J. Am. Chem. Soc.*, 73 (1951) 1728.

Analytica Chimica Acta
Elsevier Publishing Company, Amsterdam
Printed in The Netherlands

1-DICARBOXYMETHYLAMINOMETHYL-2-HYDROXY-3-NAPHTHOIC ACID AS A SENSITIVE AND SELECTIVE FLUORIMETRIC REAGENT FOR BERYLLIUM, AND FOR LANTHANUM AND LUTETIUM IN PRESENCE OF THE OTHER LANTHANIDES

B. BUDĚŠÍNSKÝ* AND T. S. WEST
Chemistry Department, Imperial College, London S.W.7 (England)

(Received April 10th, 1968)

2-Hydroxy-3-naphthoic acid has been described as a spectrofluorimetric reagent for the detection and determination of aluminium and beryllium[1–4]. Several examples [5,6] of the introduction of an aminomethyldicarboxymethyl group into the molecule of a fluorescent reagent have shown a good combination of fluorescent and complexing properties. For these reasons, a reagent of this type based on 2-hydroxy-3-naphthoic acid was prepared, *viz.* 1-dicarboxymethylaminomethyl-2-hydroxy-3-naphthoic acid (DHNA) and the fluorescence properties of its metal complexes were investigated.

EXPERIMENTAL

Apparatus

Fluorescence measurements were made with a double monochromating spectrofluorimeter (Farrand Optical Co., Cat. No. 104244) fitted with a 150-W Xenon arc lamp (Hanovia Division, Cat. No. 901 C-1) and RCA IP 28 photomultiplier, and equipped with a Honeywell-Brown Recorder. Fused quartz cells (10 × 20 × 50 mm) were used throughout. To obtain the maximum sensitivity compatible with good definition of maxima, 10-nm band-width slits were used in both the exciting and analysing monochromators. Fluorescence was measured at right angles to the incident light such that the mean solution path-length of exciting radiation was 5 mm and of the fluorescent emission, 10 mm.

The pH was measured with a Vibron pH meter, model 39A (Electronic Instruments, Ltd., England).

Preparation of the reagent

Iminodiacetic acid, disodium salt (1.95 g, 0.01 *M*) was dissolved by warming to 50–60° in glacial acetic acid (50 ml). Then 38% aqueous formaldehyde (1.0 ml) was added, the flask was stoppered and shaken for 5 min, and 2-hydroxy-3-naphthoic acid (1.88 g, 0.01 *M*) was added. Although the latter dissolved very quickly, the shaking was continued for 5–10 min, whereupon a white crystalline product began to precipitate from the solution. The mixture was heated at 60–70° for 5 h. It was then cooled to normal temperature and the precipitate was collected by suction on a glass-sinter (No. 4) and washed with absolute ethanol (200 ml). The precipitate was dried for 3 h at

---

* Present address: Nuclear Research Institute, Czechoslovak Academy of Sciences, Řež u Prahy (Czechoslovakia).

100° (yield of crude product, 2.68 g) and then suspended in boiling aqueous 20% sodium acetate solution (50 ml). The hot suspension was filtered by suction and the pure product, as a disodium salt, was obtained after several days of free crystallization under normal conditions. It was collected by suction on a glass-filter (No. 3 or 4), washed with absolute ethanol (50 ml), and dried for 6 h at 100°. The yield was 1.18 g.

The product was analyzed with the following results: 51.21%C, 3.22%H, 3.60% N; required for $C_{16}H_{13}NO_7Na_2$, 50.94% C, 3.47% H, 3.71% N.

Reagents

1.00·10⁻³ M and 1.00·10⁻⁴ M DHNA solutions and analytical-grade salts of metal ions.

0.2 M Calcium–EDTA. Prepared by mixing equal volumes of 0.4 *M* calcium chloride and 0.4 *M* disodium ethylenediaminetetraacetate.

pH adjusting solutions. 9.35 *M* perchloric acid (for acidities of 5.00 to 0.50 *M*); 0.50 *M* perchloric acid + 1.00 *M* hexamine + 0.50 *M* sodium perchlorate (pH 1.10 to 7.44); 1.00 *M* hexamine + 0.50 *M* sodium perchlorate + 0.50 *M* sodium hydroxide (pH 7.44 to 13.00); 10.00 *M* sodium hydroxide (pH 13.00 to 15.80). The ionic strength was kept constant (0.10) in the pH range 1.10 to 13.00 throughout these experiments.

Determination of beryllium with DHNA

Add 5 ml of 0.2 *M* calcium–EDTA to a sample solution containing 0.01–0.20 μmole of beryllium. Adjust, by use of 0.5 *M* perchloric acid and 0.5 *M* sodium hydroxide, to pH 4–7. Add 5.00 ml of $1.00 \cdot 10^{-4}$ *M* DHNA, and 5.00 ml of the hexamine–perchloric acid–perchlorate solution. Dilute to 25 ml in a volumetric flask with water and mix. After 20 min, measure the fluorescence at 450 nm with the excitation monochromator set at 360 nm. Construct the calibration curve for the given range of beryllium amounts under the same conditions. A straight line should be obtained.

Determination of lanthanum and lutetium

Adjust the pH of a solution containing 0.05–0.20 μmole of lanthanum or lutetium to 4–7. Add 5.00 ml of the $1.00 \cdot 10^{-3}$ *M* solution of DHNA reagent, 4.00 ml of the hexamine–perchloric acid–perchlorate solution and 0.2 ml of 0.50 *M* sodium hydroxide. Dilute to 25 ml with water in a volumetric flask and mix well. After 20 min, measure the fluorescence at 460 nm with the excitation monochromator set at 370 nm. Construct the calibration curve for the given range of lanthanum or lutetium in the usual way. A straight line should be obtained in each case.

RESULTS AND DISCUSSION

Sensitivity of determination

To counteract variations in the intensity of the xenon arc source and the sensitivity of the photomultiplier with wavelength, all fluorescence intensities were expressed as the ratio of the fluorescence of a freshly prepared standard quinine sulphate solution ($8 \cdot 10^{-4}$ g of quinine per litre in 10^{-3} *M* sulphuric acid) measured at 450 nm with the excitation monochromator set at 350 nm in the same cell. Relative molar fluorescence, according to the molar absorptivity, was expressed as the ratio of fluorescence of a 1 *M* sample solution (metal concentration) to that of a 1 *M* quinine solution (in $10^{-3}M$ sulphuric acid); see Table V.

The DHNA was found to be three times more sensitive than 2-hydroxy-3-naphthoic acid for the determination of beryllium, six times more sensitive for lanthanum and lutetium, and ten times more sensitive for aluminium.

Spectral characteristics

The spectral characteristics of the lamp and photomultiplier used have been described previously[1,7]. The excitation and emission spectra of the beryllium, lanthanum and lutetium complexes are plotted in Fig. 1. These are uncorrected for the variations in spectral response referred to above. It will be seen that the fluorescence characteristics are those of the fluorophore rather than of the metal ions involved.

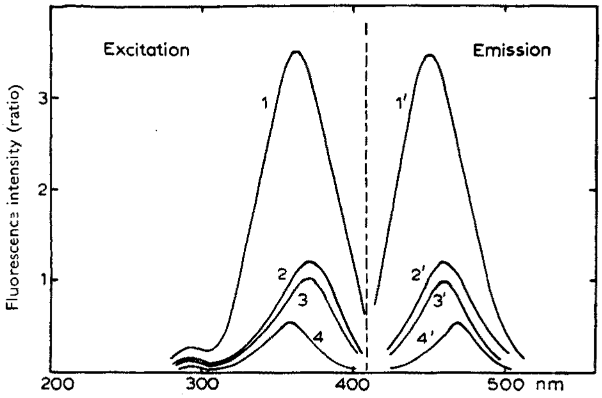

Fig. 1. Excitation and emission spectra of beryllium (1,1'), lutetium (2,2') and lanthanum (3,3') complexes with DHNA, and of DHNA alone (4,4'). 1,1'—pH 6.8; 2,2', 3,3', 4,4'—pH 10.0; $C_L = C_{Be} = C_{Lu} = C_{La} = 2.00 \cdot 10^{-5}$ *M*.

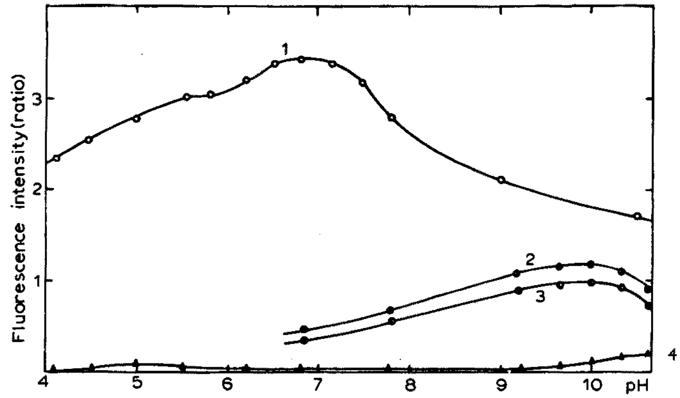

Fig. 2. pH dependence of fluorescence of beryllium (1), lutetium (2) and lanthanum (3) complexes; (4) reagent alone. 1—excitation 360 nm, emission 450 nm; 2,3,4—excitation 370 nm, emission 460 nm. $C_L = C_{Be} = C_{Lu} = C_{La} = 2.00 \cdot 10^{-5}$ *M*.

Influence of pH and adherence to Lambert–Beer law

The dependence of the fluorescence intensity of the reagent and its beryllium, lanthanum and lutetium complexes on pH is given in Fig. 2. The maximum fluorescence of the beryllium complex is at pH 6.8 and that of the lanthanum and lutetium complexes at pH 10.0. The fluorescence of the reagent is negligible at pH 6.8 and only very slight at pH 10. Excitation and fluorescence maxima for the reagent occur at 360/470 nm. Figure 3 shows that the Lambert–Beer law is obeyed for beryllium in the concentration range up to $10^{-5}M$, and for lutetium and lanthanum up to $1.5 \cdot 10^{-5}$ M.

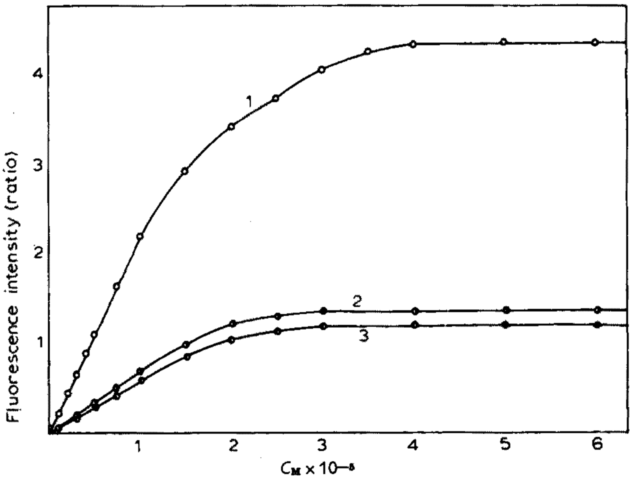

Fig. 3. Dependence of fluorescence on the concentration of metal ion (C_M).
(1) beryllium, pH 6.8, excitation 360 nm, emission 450 nm;
(2) lutetium, pH 10.0, excitation 370 nm, emission 460 nm;
(3) lanthanum, pH 10.0, excitation 370 nm, emission 460 nm, $C_L = 2.00 \cdot 10^{-5}$ M throughout.

Influence of time and temperature

No change of fluorescence was observed during the period 20–60 min after preparation of the solutions for measuring; more prolonged studies were not made. In all experiments, the temperature was 20° ± 3°. No significant variation of fluorescence with temperature of development was noted within this range.

Effect of foreign ions on the determination of beryllium

The effects of 25 cations and 15 anions on the beryllium determination were investigated. The limiting value of the concentration of a foreign ion was taken as that which caused an error of ± 5% in the determination of 0.1 μmole of beryllium. The results obtained are summarized in Table I. Interfering ions (in μmole) are: aluminium (0.5), scandium (1.0), magnesium (1.0), phosphate (10.0), fluoride (1.0), arsenate (5.0), tartrate (1.0), citrate (1.0), and oxalate (5.0). These results were obtained in the presence of the Ca-EDTA masking solution; otherwise, many of the other ions caused complete quenching of the fluorescence or yielded their own fluorescence effect.

Many foreign ions in amounts higher than 0.5 μmole interfere seriously with the determination of lanthanum and lutetium. A preliminary separation of lanthanum from other elements therefore appears to be necessary. Ion exchange, with Dowex 1 or

TABLE I

ANALYSIS OF BERYLLIUM SOLUTIONS TREATED AS UNKNOWN SAMPLES

Beryllium (μmole)		*Foreign ions present (μmole)*	*Beryllium (μmole)*		*Foreign ions present (μmole)*
Present	*Found*		*Present*	*Found*	
0.010	0.010	—	0.100	0.096	Nd (5.0), Yb (5.0)
0.050	0.051	—	0.100	0.095	Pb(II) (5.0), Co(II) (2.0)
0.100	0.098	—	0.200	0.195	AcO^- (10.0), Cl^- (1000.0)
0.150	0.152	—	0.200	0.197	NO_3^-(1000.0), ClO_4^-(10000.0)
0.200	0.195	—	0.200	0.193	PO_4^{3-} (2.0)
0.100	0.099	Al (0.1)	0.200	0.187	PO_4^{3-} (10.0)
0.100	0.095	Al (0.2)	0.200	0.192	F^- (0.5)
0.100	0.091	Al (0.5)	0.200	0.184	F^- (1.0)
0.100	0.102	Sc (0.1)	0.200	0.195	SO_4^{2-} (2.0)
0.100	0.098	Sc (0.3)	0.200	0.186	SO_4^{2-} (20.0)
0.100	0.096	Sc (0.5)	0.200	0.197	Br^-(1000.0), I^-(1000.0)
0.100	0.095	Sc (1.0)	0.200	0.192	AsO_4^{3-} (2.0)
0.200	0.205	Cu(II) (1.0), Hg(II) (1.0)	0.200	0.185	AsO_4^{3-} (5.0)
0.200	0.192	Zr (2.0), Y (2.0)	0.200	0.194	Tartrate (0.5)
0.200	0.196	La (2.0), Hf (2.0)	0.200	0.186	Tartrate (1.0)
0.200	0.197	Ga (2.0), In (2.0)	0.200	0.195	Citrate (0.5)
0.200	0.198	Ca (5.0), Ba (10.0)	0.200	0.185	Citrate (1.0)
0.200	0.195	Th (10.0), Ni (2.0)	0.200	0.197	Oxalate (1.0)
0.200	0.207	Mg (0.5)	0.200	0.188	Oxalate (5.0)
0.200	0.212	Mg (1.0)	0.200	0.196	CN^- (10.0)
0.200	0.205	Lu (2.0), Fe(III) (2.0)	0.200	0.193	CN^- (100.0)
0.200	0.202	Zn (20.0), Cd (10.0)	0.200	0.196	SCN^- (100.0)
0.100	0.098	Ti(IV) (2.0)	0.200	0.192	SCN^- (1000.0)
0.100	0.097	Bi (1.0)			

TABLE II

ANALYSIS OF LANTHANUM AND LUTETIUM SOLUTION IN THE PRESENCE OF OTHER LANTHANONS

Taken (μmole)	*Found (μmole)*	*Foreign ions present (μmole)*	*Taken (μmole)*	*Found (μmole)*	*Foreign ions present (μmole)*
La 0.050	0.052	—	Lu 0.050	0.048	—
0.100	0.099	—	0.100	0.097	—
0.150	0.151	—	0.150	0.155	—
0.200	0.193	—	0.200	0.193	—
0.150	0.152	Ce(III) (0.1), Pr(0.1), Nd(0.1)	0.150	0.144	Tb(0.2), Dy(0.1), Ho(0.1)
0.150	0.145	Yb(III) (0.1), Tm(0.1), Er(0.1)	0.150	0.140	Ce(III)(0.2), Pr(0.2), Nd(0.2)
0.150	0.143	Sm(0.1), Eu(III) (0.1), Ho(0.1)	0.150	0.145	Er(0.1), Tm(0.2), Yb(0.1)
0.150	0.157	Gd (0.1)	0.150	0.156	Gd (0.1)
0.150	0.163	Gd (0.3)	0.150	0.160	Gd (0.3)

2 in a hydrochloric acid medium[8], or extraction with tri-iso-octylamine in xylene[9], from the same medium, should be convenient for such a purpose. The main importance of the proposed method is the possibility of directly determining lutetium and lanthanum in the presence of the other lanthanons. Several typical examples of this determination are given in Table II. The unusual selectivity of this reaction towards the first and last members of the lanthanide series is discussed further on p. 463.

Precision data

These were obtained by multiple analyses of a series of solutions containing

0.1 μmole of beryllium, lanthanum or lutetium. The precision of the fluorescence intensity measurements for beryllium is ± 2.0% (relative standard deviation), corresponding to 0.002 μmole of Be; for lanthanum it is ± 3.5%, corresponding to 0.0035 μmole of La; and for lutetium it is ±2.8%, corresponding to 0.0028 μmole of Lu.

Structure of complexes

The ratio of metal to ligand in the complexes formed was investigated by the method of continuous variation in isomolar solutions. The corrected curves are given in Fig. 4. A ratio of 1:1 was found in all cases; the same constant molar ratio of the complexes formed was found in the whole pH range 4–10. According to the structure of the reagent, a mononuclear composition of the complexes seems probable.

The stability constants of the proton complexes of the DHNA ligand were determined in the acidity range from $H^0 = -4$ (Hammett function) to pH 16 by ultraviolet spectrophotometry at 240 nm and 250 nm (see ref. 10). The values found are given in Table III.

The composition and overall stability constants of the three metal complexes were determined by the method of BUDĚŠÍNSKÝ AND HAAS[10,11], the side-reactions

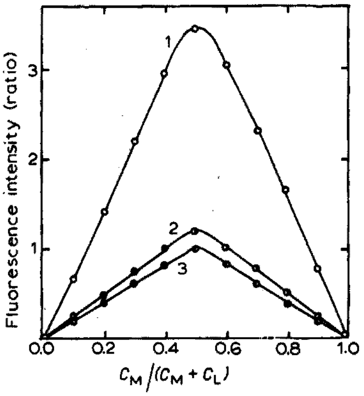

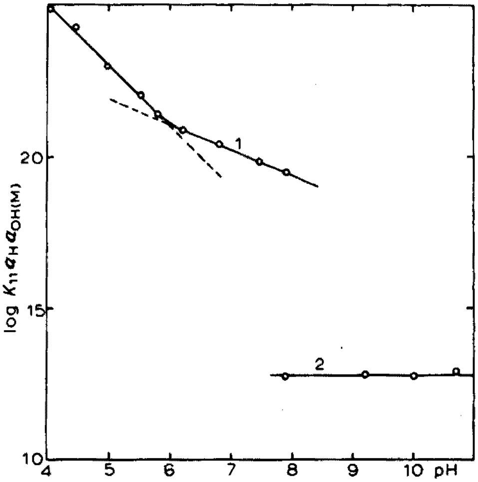

Fig. 4. Continuous variation in isomolar solution.
(1) beryllium, pH 6.8, excitation 360 nm, emission 450 nm;
(2) lutetium, pH 10.0, excitation 370 nm, emission 460 nm;
(3) lanthanum, pH 10.0, excitation 370 nm, emission 460 nm.
$C_M + C_L = 4.00 \cdot 10^{-5}$ throughout.

Fig. 5. Dependence of log $K_{11}\alpha_H\alpha_{OH(M)}$ on pH. (1) beryllium complex, (2) lanthanum complex.

TABLE III

STABILITY CONSTANTS[a] OF PROTON COMPLEXES OF THE LIGAND OF 1-DICARBOXYMETHYLAMINOMETHYL-2-HYDROXY-3-NAPHTHOIC ACID

log K_{11}	*log* K_{21}	*log* K_{31}	*log* K_{41}	*log* K_{51}
13.8	9.7	8.5	2.7	0.7

[a] $K_{a1} = [H_aL]\,[H_{a-1}L]^{-1}\,[H]^{-1}$.

of the ligand with hydrogen ion and of the metal ion with hydroxyl ion[12] being taken into consideration. The conditional formation constants K_{mn} were determined by the method of proportional absorbances; their values are given in Table IV. The calculated dependence of log $K_{mn}\alpha_{H}\alpha_{OH(M)}$ on pH is plotted graphically in Fig. 5. The total analytical concentration of metal ion [M] was 10^{-5} M in all cases. The data on hydrolytic constants of beryllium were taken from HIETANEN AND SILLÉN[13], and the data on hydrolytic constants of lanthanum from BIEDERMANN AND CIAVATTA[14]. The curves plotted in Fig. 5 indicate a complex of composition BeH_2L at pH 4.0–5.5, and a complex of composition BeHL at pH 6.1–8.0. For lanthanum a complex of composition LaL was found in the pH range 7.8–10.7. The corresponding overall stability constants are given in Table IV. The composition of the lutetium complex was not determined since the hydrolytic constants of lutetium are not known, but the composition is probably similar to that of lanthanum since the behaviour of the complexes is exactly similar.

TABLE IV

CONDITIONAL FORMATION CONSTANTS AND OVERALL STABILITY CONSTANTS OF BERYLLIUM AND LANTHANUM DHNA COMPLEXES

Complex composition	*pH*	A_1/A_2[a]	*log* K_{11}	*log* α_H	*log* $\alpha_{OH(M)}$[b]	*log* β_{11J1}[c]
	4.06	2.57	5.0	19.9	0.0	33.0
	4.47	2.32	5.5	18.7	0.0	33.1
BeH_2L	5.00	2.18	5.9	17.0	0.1	33.0
	5.54	2.13_7	6.1	15.4	0.5	33.1
	5.80	2.18	5.9	14.7	0.8	33.0
	6.20	2.21	5.8	13.6	1.5	27.1
BeHL	6.80	2.13_7	6.1	11.6	2.7	27.2
	7.43	2.27	5.6	9.8	4.4	27.2
	7.89	2.37	5.4	8.8	5.3	27.3
	10.68	3.34	4.0	3.2	5.7	12.9
LaL	10.01	2.01_7	8.4	4.1	0.3	12.8
	9.20	2.03	7.3	5.5	0.0	12.8
	7.89	3.06	4.2	8.5	0.0	12.7

[a] Fluorescence proportions.

[b] Stability constants for hydrolytic complexes of beryllium[13]: log $K_{12}^* = -3.22$, log $K_{21}^* = -10.84$, log $K_{33}^* = -8.66$; of lanthanum[14]: log $K_{11}^* = -10.1$, log $K_{12}^* = -9.95$, log $K_{95}^* = -71.4$.

[c] log β_{11J1}, ... = log $K_{11}\alpha_{H}\alpha_{OH(M)} + (1-J)pH + pK_{H_2O}^{J}$

The structure of the beryllium complexes formed may be similar to that suggested previously for its 2-hydroxy-3-naphthoic acid complex and may possibly be of the following forms.

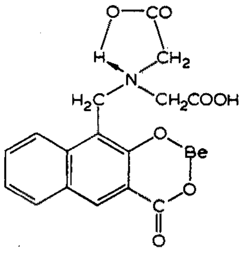

BeH_2L

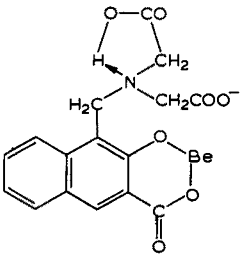

BeHL

Whilst it is known that beryllium tends to form complexes with aminomethyldicarboxymethyl groups, the tendency is slight. This, taken together with the smaller spectral shifts involved upon complex formation with beryllium than with any other metal ion (Table V), suggests that the complexan group plays little part in the formulation of the complex. Most other metals, including lutetium and lanthanum, have a more pronounced tendency to react with aminomethyldicarboxymethyl groups. In these instances, it is much more probable that the latter group is involved; this is borne out by the almost invariable values of 360 nm for excitation and 460 nm for fluorescence observed for the other metal ions (Table V).

It seems probable, therefore, on the evidence of the present observations that the lanthanum and lutetium complexes have the following composition

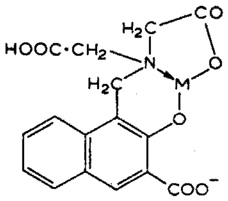

where M represents the lanthanide metal ion.

TABLE V

RELATIVE MOLAR FLUORESCENCE OF SEVERAL METAL COMPLEXES OF DHNA

Metal ion	*pH optimum*	*Molar ratio metal/ligand*	*Emission wavelength (nm)*[a]	*Relative molar fluorescence*[b]
Be	6.8	1:1	450	0.64
Mg	12.0	1:1	470	0.55
Ca	12.0	—	470	<0.01
Zn	10.0	—	460	0.02
Al	6.7	1:2	450	1.02
Ga	6.7	1:2	460	0.89
In	6.7	1:2	460	0.69
Sc	6.2	1:1	460	0.69
Y	9.5	1:1	460	0.61
La	10.0	1:1	460	0.18
Ce(III)	10.0	—	460	<0.01
Pr	10.0	—	460	<0.01
Nd	10.0	—	460	<0.01
Sm	10.0	—	460	<0.01
Eu(III)	10.0	—	460	<0.01
Gd	10.0	1:1	460	0.08
Tb	10.0	—	460	<0.01
Dy	10.0	—	460	<0.01
Ho	10.0	—	460	<0.01
Er	10.0	—	460	<0.01
Tm	10.0	—	460	<0.01
Yb	10.0	—	460	<0.01
Lu	10.0	1:1	460	0.20
Zr	4.9	—	465	0.54
Hf	5.2	—	465	0.36
Th		—	465	0.18

[a] The excitation wavelength was 370 nm in all cases except for beryllium when it was 360 nm.
[b] Relative to quinine sulphate.

Fluorescence of other metal ion complexes

DHNA gives fluorescent complexes with several other ions. This property of the reagent is summarised in Table V, which also shows the optimal pH values for each fluorescence, and gives their intensities relative to that of a quinine sulphate solution of equal molarity. It will be observed that the fluorescence of metals capable of forming complexes which involve two molecules of DHNA per ion, is particularly strong, *e.g.* Al, Ga and In. Thus as an analytical reagent, DHNA, would be particularly sensitive for these metals. The sensitivity towards the other trivalent metals which, however, form 1:1 complexes, *e.g.* Sc and Y, is also noteworthy. Table V suggests that the reagent may have distinct utility as a reagent for the fluorimetric determination of magnesium in the presence of calcium, but this is vitiated by the high background fluorescence of the reagent at this pH.

However, the outstanding behaviour of DHNA as a reagent is undoubtedly its selectivity within the lanthanide contraction for lanthanum, the first member, and lutetium, the last one. There appears to be a close connection between this fluorescent property and the occupation of the $4f$ electron shell in these metals, lanthanum $4f^0$ and lutetium $4f^{14}$. It is also remarkable that there is a slight fluorescence for the half-filled shell in gadolinium, $4f^7$.

Lastly, it is perhaps pertinent to make some comparison between DHNA and 2-hydroxy-3-naphthoic acid, the parent compound. The latter has been used chiefly as a reagent for beryllium and aluminium, and has been shown to be considerably more sensitive for beryllium than for aluminium and to form a 1:1 metal–ligand complex. On the other hand, DHNA is more sensitive towards aluminium (Table V) than to beryllium and forms a 1:2 Al–DHNA complex. In this instance, there is little doubt that the aluminium ions react also with the complexan group present in the latter molecule. In addition, many more ions form fluorescent complexes with DHNA than with the parent compound. This is undoubtedly due to the ability of DHNA to bind these ions across the complexan grouping with subsequent rearrangements of electronic dispositions within the reagent to permit fluorescence phenomena to be observed. It would appear, therefore, that one of the benefits which may accrue from the introduction of a complexan group into a metallofluorescent reagent is that its range of application may be extended and sensitized. It is, however, noticeable that, as usual, only diamagnetic complex-forming ions yield fluorescence behaviour.

We are grateful to the Czechoslovak Academy of Sciences for granting study leave to one of us (B.B.) and to the Science Research Council for a grant for the purchase of the fluorimeter used in these studies.

SUMMARY

1-Dicarboxymethylaminomethyl-2-hydroxy-3-naphthoic acid (DHNA) forms fluorescent complexes with Al, Be, Ga, Hf, In, La, Lu, Mg, Sc, Th, Y, and Zr. The Be, La and Lu complexes have a metal : ligand ratio of 1:1. The beryllium complex shows maximal fluorescence at pH 6.8 with excitation-fluorescence maxima at 360 and 450 nm; linear calibration curves are obtained in the range 0.09–1.8 μg Be. In the presence of the calcium–EDTA complex, of 25 cations studied, only > 100-fold molar ratios of aluminium and > 10-fold molar ratios of magnesium and scandium caused interference in the determination of 0.1 μmole of beryllium. Amongst 15 anions, >100-fold molar ratios of phosphate, >50-fold molar ratios of arsenate or oxalate and >10-fold molar ratios of citrate, fluoride and tartrate caused low results. Lanthanum and lutetium can be determined at pH 10 and 370/460 nm in the range 7–28 μg even in the presence of a 3-fold molar ratio of the other lanthanides without interference.

RÉSUMÉ

L'acide 1-dicarboxyméthylaminométhyl-2-hydroxy-3-naphtoïque (DHNA) donne des complexes fluorescents avec Al, Be, Ga, Hf, In, La, Lu, Mg, Sc, Th, Y et Zr. Les complexes de Be, La et Lu sont dans un rapport métal: ligand de 1:1. Le complexe du béryllium offre une fluorescence maximale à pH 6.8 avec un maximum excitation-fluorescence à 360 et 450 nm; des courbes d'étalonnage linéaires sont obtenues pour des teneurs en béryllium de 0.09–1.8 μg. En présence du complexe calcium–EDTA, parmi 25 cations examinés seuls l'aluminium (en rapport molaire de 100 fois), le magnésium et le scandium (en rapport molaire de 10 fois) causent des interférences pour le dosage de 0.1 μmole de béryllium. Parmi 15 anions, les phosphates (rapport molaire de 100 fois), les arséniates ou les oxalates (rapport de 50 fois), les citrates, les fluorures et les tartrates (rapport de 10 fois) donnent des résultats faibles. Le lanthane et le lutétium peuvent être dosés au pH 10 et 370/460 nm entre 7–28 μg même en présence de 3 fois (rapport molaire) des autres lanthanides, sans interférence.

ZUSAMMENFASSUNG

Die fluorimetrische Bestimmung von Beryllium, von Lanthan und Lutetium in Gegenwart anderer Lanthaniden mit 1-Dicarboxymethylaminomethyl-2-hydroxy-3-naphthosäure (DHNA) wird beschrieben. Die Komplexe dieser Elemente bilden ein Metall–Liganden-Verhältnis von 1:1. Der Berylliumkomplex zeigt eine maximale Fluoreszenz beim pH 6.8 mit Maxima von 360 und 450 nm für die Anregung. Die Bestimmung von 0.1 μmol Beryllium wird in Gegenwart des Calcium–EDTA-Komplexes von 25 untersuchten Kationen nur von Aluminium bei mehr als 100 fachem und von Magnesium und Scandium bei mehr als 10 fachem molaren Überschuss gestört. Unter 15 Anionen verursacht ein mehr als 100 facher Überschuss an Phosphat, ein mehr als 50 facher an Arsenat oder Oxalat und ein mehr als 10 facher an Citrat, Fluorid und Tartrat zu kleine Ergebnisse. Lanthan und Lutetium können beim pH 10 und 370/460 nm im Bereich von 7–28 μg sogar in Gegenwart von 3 fachem Überschuss der anderen Lanthaniden ohne Störungen bestimmt werden.

REFERENCES

1 G. F. Kirkbright, T. S. West and C. Woodward, *Anal. Chem.*, 37 (1965) 137.
2 A. I. Cherkesov, *Dokl. Akad. Nauk SSSR*, 118 (1958) 309.
3 A. I. Cherkesov and T. S. Zhigalkina, *Tr. Astrakhansk. Tekhn. Inst. Rybn. Prom. i Khoz.*, 8 (1962) 25; *Anal. Abstr.*, (1964) 2096.
4 A. I. Cherkesov and T. S. Zhigalkina, *Zavodsk. Lab.*, 27 (1961) 658.
5 J. Körbl, F. Vydra and R. Přibil, *Talanta*, 1 (1958) 138.
6 D. H. Wilkins, *Talanta*, 4 (1960) 182.
7 G. F. Kirkbright, T. S. West and C. Woodward, *Talanta*, 12 (1965) 517.
8 K. A. Kraus and F. Nelson, *Proc. Intern. Conf. Peaceful Uses At. Energy, Geneva*, 7 (1955) 113.

9 B. BUDĚŠÍNSKÝ AND B. MENCLOVA, *Talanta*, 14 (1967) 688.
10 B. BUDĚŠÍNSKÝ AND K. HAAS, *Acta Chim. Acad. Sci. Hung.*, 39 (1963) 7.
11 B. BUDĚŠÍNSKÝ, *Z. Anal. Chem.*, 209 (1965) 379.
12 L. G. SILLÉN AND A. E. MARTELL, *Stability Constants of Metal-Ion Complexes*, Chem. Soc., Burlington House, London, 1964.
13 S. HIETANEN AND L. G. SILLÉN, *Acta Chem. Scand.*, 18 (1964) 1015.
14 G. BIEDERMANN AND L. CIAVATTA, *Acta Chem. Scand.*, 15 (1961) 1347.

Anal. Chim. Acta, 42 (1968) 455–465

Analytica Chimica Acta
Elsevier Publishing Company, Amsterdam
Printed in The Netherlands

A POTENTIOMETRIC STUDY OF THE WATER-SOLUBLE SILVER(I) COMPLEXES OF N,N'-BIS(2-HYDROXYETHYL)DITHIOOXAMIDE

PART III. DETERMINATION OF THE DIFFERENT SPECIES

L. C. VAN POUCKE AND M. A. HERMAN*
Department of General and Inorganic Chemistry, The University of Ghent, Ghent (Belgium)

(Received February 18th, 1968)

In previous papers[1,2] it was shown that silver(I) and N,N'-bis(2-hydroxyethyl)-dithiooxamide (HEDTO) form complexes with the general formula $B(AB)_n$ and $(AB)_n$, in which the metal ion is represented by A and the ligand by B. In these formulae, the number of ionizable hydrogen atoms still present in the complex molecule was not considered because the study was effected at constant pH value. In this paper, the values of n are determined and some information is given about the value of r, the number of hydrogen ions released by complex formation.

Determination of n

The extrapolation method of LEDEN[3] and FRONAEUS[4] was used for the determination of n; accordingly, a function of the stability constants and one variable was needed. Such functions can be obtained by two methods.

Method 1. In the previous paper[2] $\bar{p}$ and $\bar{q}$ were defined as follows:

$$\bar{p} = (C_A - A)/S = \sum_p \sum_q p K_{pq} A^p B^q / S \tag{1}$$

$$\bar{q} = (C_B - B)/S = \sum_p \sum_q q K_{pq} A^p B^q / S \tag{2}$$

with $S = \sum_p \sum_q K_{pq} A^p B^q$ and $K_{pq} = (A_p B_q)/(A)^p (B)^q$

As the complex formation can be represented by two different types of complexes $B(AB)_n$ and $(AB)_n$, eqns. (1) and (2) can be transformed as follows:

$$\bar{p} = \sum_n n K_{n,n+1} A^n B^{n+1}/S + \sum_n n K_{n,n} A^n B^n / S \tag{3}$$

$$\bar{q} = \sum_n (n+1) K_{n,n+1} A^n B^{n+1}/S + \sum_n n K_{n,n} A^n B^n / S \tag{4}$$

Subtracting eqn. (3) from eqn. (4) gives:

$$\bar{q} - \bar{p} = \sum_n K_{n,n+1} A^n B^{n+1}/S$$

From this

$$S_1 = (\bar{q} - \bar{p}) S/B = \sum_n K_{n,n+1} A^n B^n = \sum_n K_{n,n+1}\, u^n \tag{5}$$

with $u = A \cdot B$.

---

* Present address: Ruca, Antwerp (Belgium).

Equation (5) shows that S_1 satisfies the conditions for a LEDEN–FRONAEUS extrapolation.

The stability constants $K_{n,n}$ can be obtained from the function S_2

$$S_2 = S - S_1\mathrm{B} = \sum_n K_{n,n}\, u^n \tag{6}$$

Method 2. $C_\mathrm{A} - \mathrm{A}$ can be written as follows:

$$C_\mathrm{A} - \mathrm{A} = \sum_n nK_{n,n}\mathrm{A}^n\mathrm{B}^n + \mathrm{B}\sum_n nK_{n,n+1}\mathrm{A}^n\mathrm{B}^n \tag{7}$$

$$= \sum_n nK_{n,n}u^n + \mathrm{B}\sum_n nK_{n,n+1}\, u^n \tag{8}$$

$C_\mathrm{A} - \mathrm{A}$ as a function of B at a constant value of u gives a straight line. For a definite value of u,

$$\sum_n nK_{n,n}\, u^n \tag{9}$$

and

$$\sum_n nK_{n,n+1}\, u^n \tag{10}$$

are obtained from the intercept and the slope of this straight line. The reiteration of this operation for different values of u gives functions (9) and (10) as functions of u.

The application of the LEDEN–FRONAEUS extrapolation method to the functions (5), (6), (9) and (10) gives $n=1$, 2 and 3 for both types of complexes. The values of log K_{pq} obtained in this way are given in Table I.

TABLE I

VALUES OF log K_{pq} OBTAINED

	C_H = *0.01 M*	C_H = *0.05 M*
log K_{12}	9.95	9.98
log K_{23}	21.98	20.81
log K_{34}	31.37	—
log K_{11}	5.50	5.48
log K_{22}	16.08	15.91
log K_{33}	26.21	—

Because of the large experimental error, the values found for log K_{34} and log K_{33} at C_H = 0.05 *M* are not significant and are therefore not given here. From Table I it can be seen that the values for log $K_{n,n+1}$ and for log $K_{n,n}$ differ somewhat at different pH values; however, this variation is small and almost equals the experimental error. The small variation seems to indicate that in the general reaction equation:

$$p_t\mathrm{Ag}^+ + q_t\mathrm{H_2X} \rightleftarrows \mathrm{Ag}_{p_t}\mathrm{H}_{2q_t - r_t}X_{q_t} + r_t\mathrm{H}^+ \tag{11}$$

r_t has a value near 0. A method for the determination of r is described in the next paragraph in order to verify this interpretation.

Determination of r

Analogously to $\bar{p}$ and $\bar{q}$, $\bar{r}$ can be defined as follows:

$$\bar{r} = \frac{\text{concentration of H}^+ \text{ ions released by complex formation}}{\text{total concentration of the complexes}} = H_u/S$$

In the previous paper[2], it was noted that the change in the free energy of a solution containing H_2O, A, B, H, perchlorate and sodium ions can be given by the following equation:

$$dF = \mu_A da + \mu_B db + \mu_H dh + \mu_{ClO_4^-} dn_{ClO_4^-} + \mu_{Na^+} dn_{Na^+} + \mu dn \tag{12}$$

If h and b are kept constant, dF becomes:

$$dF = \mu_A da + \mu_{ClO_4^-} dn_{ClO_4^-} + \mu_{Na^+} dn_{Na^+} + \mu dn \tag{13}$$

A solution with volume V_0, containing a moles of A, b moles of B, h moles of mineral acid ($HClO_4$) and c moles of an indifferent electrolyte ($NaClO_4$), is diluted with 0.1 M sodium perchlorate. The values of h and c are chosen so that: $n_{NaClO_4} + n_{HClO_4} = 0.1\ V$. Therefore: $n_{ClO_4^-} = n_{NaClO_4} + n_{HClO_4} + n_{AgClO_4} = 0.1\ V + a$ and: $n_{Na^+} = c + 0.1(V - V_0)$.

Since for a dilute solution $n = kV$, eqn. (12) becomes:

$$dF = (\mu_A + \mu_{ClO_4^-}) da + (0.1 \mu_{ClO_4^-} + 0.1\, \mu_{Na^+} + k\mu) dV \tag{14}$$

dF is a total differential and, therefore, from eqn. (14), it is possible to write:

$$\left(\frac{\partial \mu_A}{\partial V}\right)_{a,h,b} + \left(\frac{\partial \mu_{ClO_4^-}}{\partial V}\right)_{a,h,b} = 0.1\left(\frac{\partial \mu_{ClO_4^-}}{\partial a}\right)_{V,h,b} + 0.1\left(\frac{\partial \mu_{Na^+}}{\partial a}\right)_{V,h,b} + k\left(\frac{\partial \mu}{\partial a}\right)_{V,h,b} \tag{15}$$

At constant ionic strength, eqn. (15) can be transformed to:

$$\left(\frac{\partial \ln A}{\partial V}\right)_{a,h,b} + \left(\frac{\partial \ln (ClO_4^-)}{\partial V}\right)_{a,h,b} = 0.1\left(\frac{\partial \ln (ClO_4^-)}{\partial a}\right)_{V,h,b} + 0.1\left(\frac{\partial \ln (Na^+)}{\partial a}\right)_{V,h,b} + k\left(\frac{\partial \ln \gamma_{H_2O}}{\partial a}\right)_{V,h,b} \tag{16}$$

From $(ClO_4^-) = 0.1 + C_A$ and $C_A \ll 0.1$ it follows that:

$$\left(\frac{\partial \ln (ClO_4^-)}{\partial V}\right)_{a,h,b} \cong 0$$

At a constant value of V, the concentration of sodium perchlorate is also constant:

$$\left(\frac{\partial \ln (Na^+)}{\partial a}\right)_{V,h,b} = 0$$

Taking into account eqn. (12) and (13) of the previous paper[2], the integration of eqn. (16) gives:

$$-\left[\int_0^a \left(\frac{\partial \ln A}{\partial V}\right)_{a,h,b} da\right]_{V,h,b} = N - N_0 - C_A$$

From eqn. (14) of the same paper it follows that:

$$\left[\int_0^a\left(\frac{\partial \ln \mathrm{A}}{\partial V}\right)_{a,b} \mathrm{d}a\right]_{V,b} - \left[\int_0^a\left(\frac{\partial \ln \mathrm{A}}{\partial V}\right)_{a,h,b}\right]_{V,h,b} = H_{\mathrm{u}}$$

The experimental methods were the same as described previously [1,2]. For constant values of b and h, a series of titrations was performed, each titration being for a definite value of a. The ln A values were plotted against V, and for a constant value of V, $\left(\frac{\partial \ln \mathrm{A}}{\partial V}\right)_{a,h,b}$ was determined.

Repetition of this determination for different values of a, gave $\left(\frac{\partial \ln \mathrm{A}}{\partial V}\right)_{a,h,b}$ as a function of a. A graphical integration gave the desired values for H_{u}.

The values of $\bar{r}$ obtained in this way are given in Table II.

TABLE II

VALUES OF $\bar{r}$ OBTAINED

a $(\cdot 10^7$ *mole*$)$	$\bar{r}$ *for* $C_B = 2.00 \cdot 10^{-4}$	$\bar{r}$ *for* $C_B = 1.00 \cdot 10^{-4}$
9.8	0.36	0.23
15.5	0.37	0.44
21.1	0.31	0.36
26.5	0.33	0.33
31.8	0.35	0.36
37.0	0.37	0.31
40.4	0.39	0.35
45.5	0.39	0.37

It appears that over the whole range, $\bar{r}$ is almost constant and equal to 0.35. A possible explanation is that r in the general reaction equation (11) can take the definite values of 0 and 1. Accordingly, the following complexes are present in the solution at $C_H = 0.01\,M$

$H_4AgX_2^+$ H_2AgX^+ H_3AgX_2 $HAgX$
$H_6Ag_2X_3^{2+}$ $H_4Ag_2X_2^{2+}$ $H_5Ag_2X_3^+$ $H_3Ag_2X_2^+$
$H_8Ag_3X_4^{3+}$ $H_6Ag_3X_3^{3+}$ $H_7Ag_3X_4^{2+}$ $H_5Ag_3X_3^{2+}$

DISCUSSION

The composition of the silver(I) complexes of HEDTO mentioned above agrees well with the composition of other metal rubeanates. Indeed, with dithiooxamide and N,N′-disubstituted derivatives, the following soluble complexes with the general formula $B(AB)_n$ have been found: $(PtB)B$ and $(CoB)_2B$ by Jacobs and Yoe[5], and $(PdB)B$ and $(PdB)_2B$ by Bobtelsky and Eisenstadter[6], who found also a complex of type $(AB)_n$:PbB. Another complex of this type is CuB found by Baker and Pflaum[7]. Besides these complexes, certain metal ions can form complexes of the type $A(AB)_n$. Thus, Baker and Pflaum[7] found $(CuB)Cu$ and Bobtelsky and Eisenstadter[6] found $(PdB)_2Pd$. In these papers, no mention is made about the number of ionizable hydrogen atoms still present in the complex molecule.

From the results of the present work it appears that rubeanic acid can form the following complexes in solution:

$H_jA_nB_{n+1}$, $H_jA_nB_n$ and in certain cases $H_jA_{n+1}B_n$;
the integer j varies with the pH.

For analytical use, two types of complexes can be distinguished: those with $n=1$ and those with $n>1$. In the former case, two or, at most, three complexes can be present, hence it seems relatively easy to find a region where one complex predominates. The only problem is then to keep j constant. This can be realised in acidic medium[8] or by using buffer solutions[8,9] if the buffer regions of the complexes are sufficiently separated. When $n>1$ as is the case here, more complexes exist and no region can be found where one complex predominates. Moreover, the different buffer regions overlap. Accordingly, analytical applications of complex rubeanates of the second type are very difficult to realise.

The authors are very grateful to Prof. Dr. Z. ECKHAUT for his kind interest and helpful discussions.

SUMMARY

Silver(I) and N,N′-bis(2-hydroxyethyl)dithiooxamide (H_2X) in acidic solutions, form a series of water-soluble polynuclear complexes. These complexes can be represented by two general formulae: $H_{2q}Ag_pX_q$ and $H_{2q-1}Ag_pX_q$ with $q=1,2,3$ and $p=q, q-1$.

RÉSUMÉ

L'ion argent donne avec le N,N′-bis(2-hydroxyethyl)dithiooxamide (H_2X) en milieu acide une série de complexes polynucléaires solubles dans l'eau. Ces complexes peuvent être représentés par les formules $H_{2q}Ag_pX_q$ et $H_{2q-1}Ag_pX_q$ dans lesquelles $q=1,2,3$ et $p=q, q-1$.

ZUSAMMENFASSUNG

Silber(I) gibt mit N,N′-Bis(2-hydroxyäthyl)dithiooxamid in sauren Lösungen eine Reihe von wasserlöslichen Komplexen deren Formeln dargestellt werden können durch $H_{2q}Ag_pX_q$ und $H_{2q-1}Ag_pX_q$ mit $q=1,2,3$ und $p=q, q-1$.

REFERENCES

1 L. C. VAN POUCKE, M. A. HERMAN AND Z. EECKHAUT, *Anal. Chim. Acta*, 40 (1968) 55.
2 L. C. VAN POUCKE AND M. A. HERMAN, *Anal. Chim. Acta*, 41 (1968) 1–7.
3 I. LEDEN, *Diss.*, Lund, 1943.
4 S. FRONAEUS, *Diss.*, Lund, 1948.
5 W. D. JACOBS AND J. H. YOE, *Anal. Chim. Acta*, 20 (1959) 332.
6 M. BOBTELSKY AND J. EISENSTADTER, *Anal. Chim. Acta*, 17 (1957) 579.
7 H. W. BAKER AND R. T. PFLAUM, *Proc. Iowa Acad. Sci.*, 68 (1961) 174.
8 A. GOEMINNE, M. A. HERMAN AND Z. EECKHAUT, *Anal. Chim. Acta*, 28 (1963) 512.
9 A. A. JANSSENS, G. L. VAN DE CAPELLE AND M. A. HERMAN, *Anal. Chim. Acta*, 31 (1964) 325.

Analytica Chimica Acta
Elsevier Publishing Company, Amsterdam
Printed in The Netherlands

STEPWISE FORMATION OF URANIUM(VI) COMPLEXES WITH SULPHONATED PHENOLIC COMPOUNDS

AMITAV BANERJEE AND ARUN K. DEY
Chemical Laboratories, University of Allahabad, Allahabad (India)
(Received January 2nd, 1968)

The presence of phenolic groups in organic compounds is mainly responsible for the formation of metallic complexes whereas the introduction of certain groups such as amino and nitroso influences the sensitivity of any colour reactions given. In the work described here, the following compounds were studied for their complex formation with uranium(VI): (*i*) disodium 2-naphthol-3,6-disulphonate (trivial name R-salt or Ferricon), and (*ii*) monopotassium 7-amino-1-naphthol-3,6-disulphonic acid (trivial name 2R-salt). These compounds react with metal ions to form coloured compounds in aqueous solution, hence most of the investigations of the complexes formed have been carried out spectrophotometrically. The complex formation of iron(III) with R-salt involves a 1:2 complex[1] with a stability constant of $10^{8.77}$; the interference of various ions with the colour formation has been discussed[2]. The composition and stability of the iron(III)–2R-salt chelate have been determined[3] and the vanadium(V)– 2R-salt chelate has also been studied[4].

However, it appears that no studies have been made on stepwise complex formation involving these salts. It was therefore of interest to study this problem by the Calvin–Bjerrum pH-titration technique[5,6] as used by IRVING AND ROSSOTTI[7]. The stepwise proton–ligand stability constants of the ligands as well as the stepwise metal–ligand stability constants of the uranyl complexes were determined. The computation methods described by IRVING AND ROSSOTTI[8] and SEN[9] were applied to determine these formation constants.

EXPERIMENTAL

Apparatus

A Leeds and Northrup pH meter was used with a glass-calomel electrode assembly. Checks were made with standard buffer solutions before each titration. Measurements were made at 25°.

Chemicals

Aqueous uranyl sulphate (Analar, B.D.H.) solutions were standardized by the usual methods[10]. A standard solution (0.02 *M*) was prepared by dilution.

Aqueous ligand solutions (0.02 *M*) of R-salt and 2R-salt (B.D.H. indicator grade) were prepared.

Sodium hydroxide (E. Merck) solutions were prepared in carbon dioxide-free water, and standardized by potentiometric titration against standard oxalic acid; the stock solution was suitably diluted. Sodium perchlorate (AnalaR, B.D.H.) solutions were standardized by the method of SILLÉN[11]. Perchloric acid (AnalaR, B.D.H.) solutions were standardized by potentiometric titration against standard alkali.

Twice-distilled water free from carbon dioxide was used for preparing solutions, for diluting stock solutions and for making up volumes.

Titration procedure

Mixtures containing: (A) acid (5 ml each of 0.1 *M* perchloric acid and 2.0 *M* sodium perchlorate), (B) ligand (mixture A and 25 ml of 0.02 *M* R-salt or 75 ml of 0.02 *M* 2R-salt), and (C) complex (mixture B and 5 ml of 0.02 *M* uranyl sulphate for the R-salt system, or 15 ml of 0.02 *M* uranyl sulphate for the 2R-salt system), were taken and the total volumes diluted to 100 ml. The ionic strength was 0.1 *M* sodium perchlorate. Mixtures A, B and C were separately titrated with standard (*ca.* 1.0 *M*) alkali solution by the potentiometric method. Three titration curves (Figs. 1 and 2) were obtained for each system.

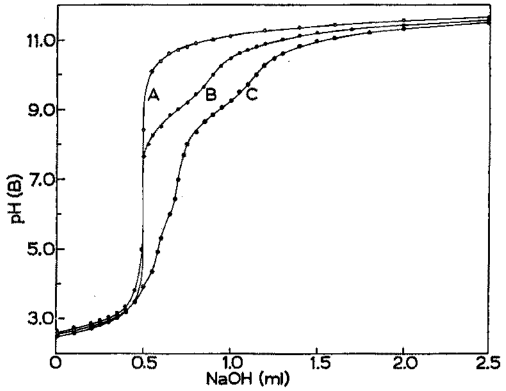

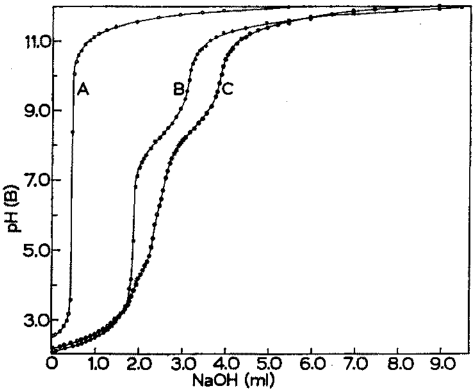

Fig. 1. Titration curves of uranyl–R-salt complex with 0.9524 *M* sodium hydroxide. (A) 0.0049 *M* perchloric acid; (B) 0.0050 *M* R-salt; (C) 0.0010 *M* uranyl sulphate.

Fig. 2. Titration curves of uranyl–2R-salt complex with 0.9804 *M* sodium hydroxide. (A) 0.0049 *M* perchloric acid; (B) 0.0150 *M* 2R-salt; (C) 0.0030 *M* uranyl sulphate.

Calculation

Proton–ligand stability constants. The association of protons (H) with the ligand (L) shorn of all dissociable protons, occurs in steps:

$$L + H \rightleftharpoons LH$$

$$LH + H \rightleftharpoons LH_2, \text{ etc.}$$

The average number of protons ($\bar{n}_A$) associated with a ligand molecule is defined as

$$\bar{n}_A = \frac{\text{total concentration of protons bound to ligand}}{\text{total concentration of ligand not bound to metal}}$$

Thus for a ligand with two dissociable protons,

$$\bar{n}_A = (C_{LH} + 2C_{LH_2})/(C_L + C_{LH} + C_{LH_2}) \qquad (1)$$

or

$$\bar{n}_A = (K_1^H C_H + 2K_1^H K_2^H C_H^2)/(1 + K_1^H C_H + K_1^H K_2^H C_H^2) \qquad (2)$$

where K_1^H and K_2^H are the first and second proton–ligand stability constants and C represents the concentrations. Rearrangement of eqn. (2) gives:

$$\bar{n}_A/(\bar{n}_A - 1)C_H + K_1^H = K_1^H K_2^H\,(2 - \bar{n}_A)C_H/(\bar{n}_A - 1) \qquad (3)$$

Since R-salt has only one dissociable proton, eqn. (3) simplifies to:

$$\log K_1^H = \log\{\bar{n}_A/(\bar{n}_A - 1)\} + \text{pH} \qquad (4)$$

The value of the protonation constant can be determined by substituting different values of $\bar{n}_A$ and corresponding pH values in eqn. (4) and then finding the average value.

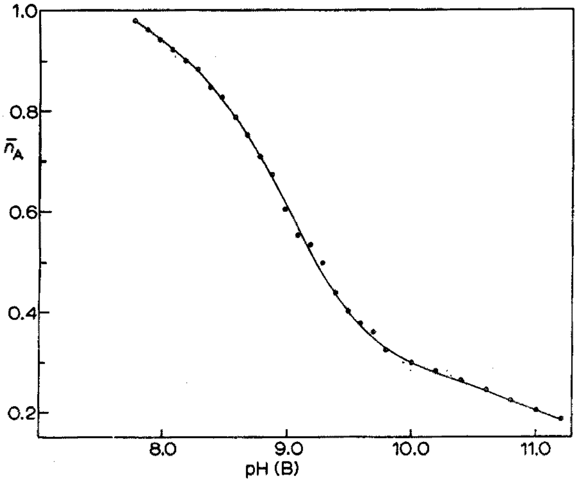

Fig. 3. Formation curve of proton–ligand system of R-salt.

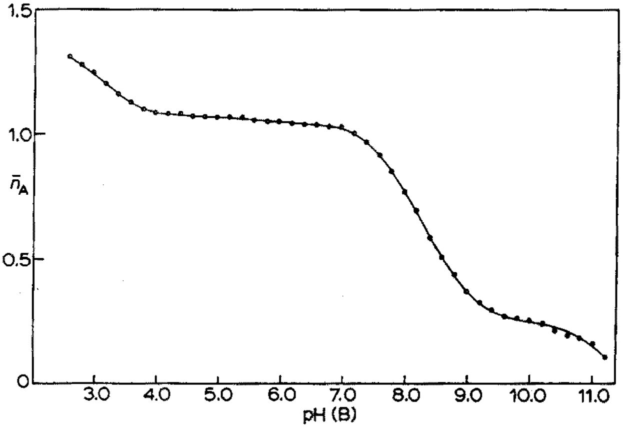

Fig. 4. Formation curve of proton–ligand system of 2R-salt.

In order to calculate the protonation constants by other methods, the formation curves were drawn (Figs. 3 and 4). Suitable computation methods[8] were then applied to determine the values of the protonation constants.

For the determination of the $\bar{n}_A$ values, eqn. (5) was used:

$$\bar{n}_A = \{yTC_L{}^0 + (v' - v'')\ (N^0 + E^0)/(V^0 + v')\}/TC_L{}^0 \tag{5}$$

where v' and v'' denote the volumes of alkali required in the acid (Curves A) and ligand (Curves B) titrations respectively, at a particular pH value, N^0 the normality of the alkali, E^0 and $TC_L{}^0$ the overall concentrations of the acid and the ligand in the titration mixtures, V^0 is the total volume of the mixtures and y is the number of dissociable protons.

Metal–ligand stability constants. For step-wise complex formation between a metal ion M and N ligands L, shorn of all ionisable hydrogen ions, the equilibria can be represented by

$$ML_{n-1} + L \rightleftharpoons ML_n \quad (n = 1,2,3,\ldots N)$$

The stepwise formation constants are given by:

$$K_n = C_{ML_n}/C_{ML_{n-1}}\, C_L \quad (n = 1,2,3,\ldots N)$$

where K_n is the nth metal–ligand stability constant.

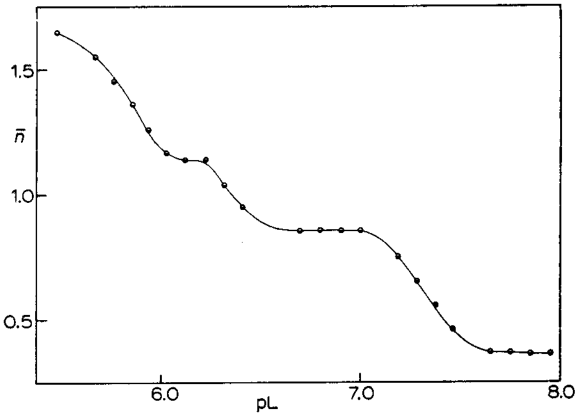

Fig. 5. Formation curve of metal–ligand system of uranyl–R-salt complex.

The formation constants were obtained from the analysis of the formation curves (Figs. 5 and 6) drawn between $\bar{n}$ and pL. The computation methods of IRVING AND ROSSOTTI[8] and SEN[9] were used. The value of $\bar{n}$, the average number of ligands attached per metal ion present in whatever form, is given by the following:

$$\bar{n} = (v''' - v'')\ [N^0 + E^0 + TC_L{}^0(y - \bar{n}_A)]/(V^0 + v'')\bar{n}_A\, TC_M{}^0 \tag{6}$$

where $TC_M{}^0$ denotes the total concentration of the metal present in the solution and v'' and v''' denote the volumes of alkali required in the cases of ligand and complex titrations respectively at the same pH. The other terms have their usual meanings.

Equation (6) can be simplified with the help of eqn. (5):

$$\bar{n}=(v'''-v'')\,(N^0+E^0)/(V^0+v')\,\bar{n}_A TC_M{}^0 \tag{7}$$

This equation was used to determine the values of $\bar{n}$.

The free ligand exponent (pL) was calculated from

$$\mathrm{pL}=\log_{10}\left[\frac{\sum_{n=0}^{n=j}\beta_n{}^{\mathrm{H}}\,(\mathrm{antilog}\ B)^{-n}}{(TC_L{}^0-\bar{n}\,TC_M{}^0)}\cdot\frac{V^0+v'''}{V^0}\right] \tag{8}$$

where $\beta_n{}^{\mathrm{H}}$ is the overall proton–ligand stability constant and B is the pH of the solution. The term $(V^0+v''')/V^0$ is the volume correction term, which was necessary for accuracy.

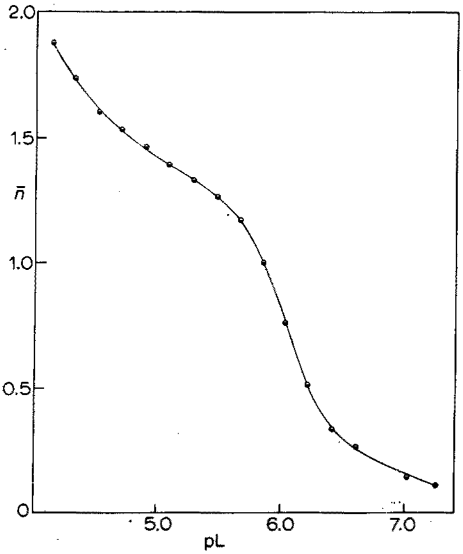

Fig. 6. Formation curve of metal–ligand system of uranyl–2R-salt complex.

RESULTS

Proton–ligand system

In the case of R-salt, the maximum value of $\bar{n}_A$ was found to be 1.0, thus only one proton is dissociated, as is also evident from the structure of this compound. The value of log $K_1{}^{\mathrm{H}}$ thus obtained is shown in Table I. Since R-salt has only one dissociable proton, the methods for determining the protonation constants are interpolation at half $\bar{n}_A$ values and the average value methods. The values by these methods are in agreement.

In the case of 2R-salt the formation curve extends upto $\bar{n}_A=1.5$, showing that LH and LH_2 are present, which is again evident from its structure. The protonation constants are shown in Table I. 2R-salt dissociates in two steps. The value of $K_1{}^{\mathrm{H}}/K_2{}^{\mathrm{H}}$ is greater than $10^{2.5}$ and therefore the interpolation at half $\bar{n}_A$ values method is applicable[8]. The value of log $K_1{}^{\mathrm{H}}$ was read directly from the formation curve (Fig. 4), but to obtain the value of log K_2^H, the equation log $K_1^H K_2^H = 2$ pH ($\bar{n}_A = 1.0$) was used, because the formation curve is incomplete at the upper region. The method of interpolation at various $\bar{n}_A$ values gave values agreeing with the results of the method of interpolation at half $\bar{n}_A$ values.

TABLE I

PROTONATION CONSTANTS OF R-SALT AND 2R-SALT

(Temperature 25°; μ = 0.1 M $NaClO_4$)

Method	*R-salt*	*2R-salt*		
	log K_1^H	*log K_1^H*	*log K_2^H*	*log β_2^{H}*[a]
Average value	9.22	—	—	—
Interpolation at half $\bar{n}_A$ values	9.24	8.60	2.50	11.10
Interpolation at various $\bar{n}_A$ values	—	8.48	2.48	10.96
Mean	9.23	8.54	2.49	11.03

[a] log K_1^H K_2^H.

TABLE II

FORMATION CONSTANTS OF THE URANYL R-SALT AND 2R-SALT COMPLEXES

(Temperature 25°; μ = 0.1 M $NaClO_4$)

Method	*R-salt complex*			*2R-salt complex*		
	log K_1	*log K_2*	*log β_2*[a]	*log K_1*	*log K_2*	*log β_2*[a]
Interpolation at half $\bar{n}$ values	7.41	5.74	13.15	6.23	4.79	11.02
Successive substitution	7.38	5.76	13.14	6.18	4.84	11.02
Least squares	7.48	5.61	13.09	6.17	4.98	11.15
Mean	7.42	5.70	13.12	6.19	4.87	11.06

[a] log K_1 K_2.

Metal–ligand system

The formation curves for the metal–ligand systems attain a maximum at $\bar{n} = 1.5$ in both cases, which indicates that 1:1 and 1:2 complexes are formed. The values of the formation constants are given in Table II. Since K_1/K_2 is less than $10^{2.5}$, the method of interpolation at half $\bar{n}$ values is not reliable, hence the values were subjected to the method of successive substitution[9]. The least squares method[8] was also applied. The values by all the methods were in good agreement.

DISCUSSION

The formation of complexes in solution is evident from the drop in the pH (proton liberation) when metal solution is added to the ligand solution (compare Curves B and C).

In the case of the uranyl–R-salt complex, the colour changes with pH. The ligand itself is yellow above pH 2.60. In the pH range 2.55–3.45, the mixture of uranyl ions and ligand remains yellow. However, at pH 3.9–4.9, an orange colour due to the ML complex appears and deepens; this orange colour persists up to pH *ca.* 5.30 where $\bar{n} \approx 1.0$. ML_2 has a reddish-orange colour and this colour persists up to pH *ca.* 6.0 where $\bar{n} \approx 1.5$. Beyond 6.45, the complex decomposes, so that the yellow colour of the ligand predominates and a turbidity appears because of pronounced hydrolysis of the metal ion. The uranyl–2R-salt chelate has the same yellow colour as the reagent over the whole pH range.

The authors are grateful to the Council of Scientific and Industrial Research, New Delhi, for a research grant and the award of a fellowship to one of them (A.B.).

SUMMARY

The metal complexes of uranium(VI) with disodium 2-naphthol-3,6-disulphonate and 7-amino-1-naphthol-3,6-disulphonic acid were studied by the established potentiometric techniques of BJERRUM and IRVING AND ROSSOTTI. The step-wise protonation constants of the ligands and the step-wise stability constants of the uranyl complexes were determined in 0.1 *M* sodium perchlorate media at 25°.

RÉSUMÉ

On a examiné les complexes métalliques de l'uranium(VI) avec 2-naphtol-3, 6-disulfonate disodique et 7-amino-1-naphtol-3,6-disulfonate disodique à l'aide des techniques potentiométriques de BJERRUM, ET IRVING ET ROSSOTTI. Les constantes de "protonation" des ligands et les constantes de stabilité des complexes d'uranyle sont déterminées en milieu perchlorate de sodium 0.1 *M* à 25°.

ZUSAMMENFASSUNG

Es wurden die Metallkomplexe von Uran(VI) mit Dinatrium-2-naphthol-3, 6-disulfonat und 7-Amino-1-naphthol-3,6-disulfonsäure potentiometrisch untersucht. Die einzelnen Protonisierungskonstanten der Liganden und der Stabilitätskonstanten der Uranylkomplexe wurden in 0.1 *M* Natriumperchlorat bei 25° bestimmt.

REFERENCES

1 S. K. BANERJI, *Z. Anorg. Chem.*, 315 (1962) 229.
2 S. N. SINHA AND A. K. DEY, *Chim. Anal. (Paris)*, 45 (1963) 224.
3 R. L. SETH AND A. K. DEY, *Z. Anal. Chem.*, 194(4) (1963) 271.
4 B. V. AGARWALA AND A. K. DEY, *Mikrochim. Acta*, in press.
5 J. BJERRUM, *Metal Amine Formation in Aqueous Solution*, P. Haase and Son, Copenhagen, 1941.
6 M. CALVIN AND K. W. WILSON, *J. Am. Chem. Soc.*, 67 (1945) 2003.
7 H. IRVING AND H. S. ROSSOTTI, *J. Chem. Soc.*, (1954) 2904.
8 H. IRVING AND H. S. ROSSOTTI, *J. Chem. Soc.*, (1953) 3397.
9 B. SEN, *Anal. Chim. Acta*, 27 (1962) 515.
10 A. I. VOGEL, *A Text Book of Quantitative Inorganic Analysis*, 3rd Edn., Longmans, London, 1961, Ch.5.
11 L. G. SILLÉN, *Some Laboratory Methods*, KTH, Stockholm, 1959.

Analytica Chimica Acta
Elsevier Publishing Company, Amsterdam
Printed in The Netherlands

DETERMINATION OF MICROGRAM AMOUNTS OF THE SIX PLATINUM-GROUP METALS IN IRON AND STONY METEORITES*

J. G. SEN GUPTA
Geological Survey of Canada, Ottawa, Ontario (Canada)

(Received January 24th, 1968)

The chemical determination of the 6 closely associated platinum metals in iron and stony meteorites has always been a very difficult problem because of the complexities involved in separating the platinum metals from the other elements and from each other. NODDACK AND NODDACK[1] were the first to study by arc and X-ray spectroscopic methods the abundances of all the 6 platinum-group metals in iron meteorites, but with the exception of finding a very faint trace of platinum, they failed to detect the other metals of the group in stony meteorites. HAWLEY[2] reported the determination of platinum by fire assay in some 19 iron, 9 stony and one stony–iron meteorites, but in all cases the "platinum" determined was actually a "mixture of platinum, palladium, rhodium and iridium". During more recent years, emission spectrography[3], neutron activation [4–12] and chemical [13–15] methods have been used for the determination of one or more of these elements in meteorites.

In this work, the determinations of osmium, ruthenium, palladium and platinum have been made with more sensitive and selective reagents than those described in a previous paper[13]. The absolute abundances of the 6 platinum metals in 5 stony, and 3 iron, meteorites have been determined and the results are compared with available published data on the same, or similar, meteorites.

The feasibility of quantitative recovery of the platinum metals from materials similar to iron meteorites by perchloric acid decomposition and subsequent chemical separation, as used in this study, was tested by means of iron–copper–nickel buttons prepared by the fire assay method from synthetic mixture of salts incorporating traces of the 6 platinum metals. The results of this study[13,14] showed quantitative recovery of the platinum metals from such materials. Though a similar perchloric acid decomposition method was used in the present study for the stony meteorites, the post-decomposition treatment to separate silica and recover the platinum metals is different. Only the salient features of the apparatus and the experimental procedures which differ from those previously published will be included here.

EXPERIMENTAL

Apparatus

Spectrophotometric measurements were made either in 1-cm borosilicate glass

---

* Presented to the Division of Analytical Chemistry, 152nd National Meeting, American Chemical Society, New York, N.Y., September 1966.

or in 5-cm silica cells with a Beckman Model B spectrophotometer. A Radiometer Universal (No. 22) pH meter was used for all pH measurements.

For separation of the base metals from the platinum metals, two Dowex 50W-X8 cation-exchange resin columns as described previously[15] were used.

Reagents

Standard solutions of platinum metals. A standard solution of platinum(IV) was prepared by dissolving accurately weighed Specpure metal (Johnson, Matthey and Mallory Co.) in aqua regia followed by removal of nitrous oxides by repeated evaporation with hydrochloric acid.

For preparation of standard solutions of osmium(IV), ruthenium(III), rhodium-(III) and iridium(IV), the chloroammonium salt (Specpure, Johnson, Matthey and Mallory Co.) of each element was dissolved in 0.12 *N* hydrochloric acid and the solution standardized by evaporating an aliquot to dryness in a small porcelain crucible, reducing the chloride in a current of hydrogen at 600° and weighing the metal.

The dilute solutions of the platinum metals used in preparing the standard curves were freshly prepared from concentrated stock solutions just before use.

Procedure

Decomposition of the meteorite. An accurately weighed amount of the meteorite (4–7 g for iron and 15–20 g for stony meteorites), was transferred to a 1-l round-bottom distillation flask connected to a 300-ml trap for perchloric acid vapour, and then through a water condenser to two receivers (30 ml capacity) in series[15], and attacked by 70% perchloric acid; the osmium and ruthenium tetroxides were collected in chilled 3% hydrogen peroxide solution in the receivers[13].

Separation of osmium from ruthenium and its spectrophotometric determination by thiourea. The hydrogen peroxide solution of the osmium and ruthenium tetroxides was quickly transferred to a chilled 1-l distillation flask and a thermometer inserted through a ground-glass joint. Water (25 ml) was added to the trap and 10 ml and 5 ml, respectively, of freshly prepared 5% thiourea in 1:1 ethanol–hydrochloric acid were added to the two receivers. The chilled distillation flask was substituted for the one in which the sample was decomposed and osmium tetroxide was distilled by boiling the solution at 105–110° with 5 ml of concentrated sulfuric acid and 30 ml of 30% hydrogen peroxide solution for 30 min. The trap was then boiled for 25 min with 15 ml of 70% perchloric acid. Mild suction was applied to the end of the receivers throughout these distillation operations. The osmium–thiourea color complex was fully developed by immersing the two receivers *in situ* in hot water baths (85°) for 15 min. The rose-red solution was transferred to a 25-ml volumetric flask, 1:1 ethanol–hydrochloric acid solution being used for rinsing and for diluting to volume. The absorbance of the solution was measured in a 5-cm cell at 480 nm against 1:1 ethanol–hydrochloric acid solution as the blank. The standard curve for osmium was prepared by taking 0, 10, 15, 25, 50 and 100 µg of osmium as ammonium chloroosmate in the trap, distilling with 20 ml of 70% perchloric acid for 25 min and collecting and determining the osmium tetroxide as above.

Recovery of ruthenium and its spectrophotometric determination with 1,4-diphenyl-3-thiosemicarbazide. The usefulness of 1,4-diphenyl-3-thiosemicarbazide as a colorimetric reagent for determination of microgram amounts of ruthenium in meteorites was demonstrated by HARA AND SANDELL[16] who used a different method of decomposition of meteorites. They did not determine osmium, and used a tin(II) chloride–hydrochloric acid solution as the absorbant for ruthenium tetroxide. In the present method, osmium is separated from ruthenium by distillation with sulfuric acid and hydrogen peroxide. The final volume of the solution left in the flask and containing the ruthenium is too large for the sodium bismuthate oxidation used by HARA AND SANDELL[16] to be effective in separating the ruthenium as tetroxide. Oxidation by sodium bromate and sulfuric acid[13] proved to be satisfactory. As this latter method produced considerable bromine during the reaction, the tin(II) chloride–hydrochloric acid absorbing solution for ruthenium tetroxide could not be employed and a chilled 6 *N* hydrochloric acid solution containing 3% hydrogen peroxide was substituted.

In the final procedure, 20, 20 and 10 ml, respectively, of cold 3% hydrogen peroxide in 6 *N* hydrochloric acid solution were placed in the trap, the first and the second receivers, and the solution in the distillation flask was gently boiled under suction until the hydrogen peroxide was completely decomposed. Concentrated sulfuric acid (10 ml) and 20 ml of 10% sodium bromate solution were added to the distillation flask and the solution was boiled at 110° for 1 h. The absorbing solutions were rinsed into a 150-ml Erlenmeyer flask with a total volume of 20 ml of 6 *N* hydrochloric acid. The solution was heated on the steam bath until both the decomposition of hydrogen peroxide and the expulsion of bromine were complete. If the ruthenium content was less than 60 μg, the whole solution was used for the spectrophotometric procedure; for more than 60 μg an aliquot was taken. The solution was cooled to room temperature, 3 ml of a freshly prepared saturated solution of 1,4-diphenyl-3-thiosemicarbazide in methanol was mixed with it and the flask was heated at 100° for 12 min in a bath of boiling water. The flask was then cooled under running water and the solution rinsed into a 125-ml separatory funnel with 20 ml of 6 *N* hydrochloric acid. Reagent-grade chloroform (5 ml) was then added and the solution was vigorously shaken for 1 min. The chloroform layer was transferred to a 1-cm cell and the absorbance was measured at 560 nm against a chloroform blank. The standard curve was prepared by distilling 0, 5, 10, 20, 40 and 60 μg of ruthenium (as ammonium chlororuthenate) and developing and extracting the color complex as previously described.

Recovery and determination of palladium, platinum, rhodium and iridium. The recovery of the 4 platinum metals (Pd, Pt, Rh and Ir) and other common metals from the perchloric acid solution, separation of the platinum metals from the base metals by ion exchange, and selective spectrophotometric determination of palladium by arsenazo III in presence of platinum, rhodium and iridium have been described previously[15]. After the spectrophotometric measurement, the colored solution of palladium–arsenazo III was combined with the main portion and the whole evaporated to dryness on the steam bath. Organic matter was destroyed by heating with fuming nitric acid and 30% hydrogen peroxide. Platinum and palladium were separated from rhodium and iridium by solvent extraction of their diethyldithiocarbamate complexes in the presence of potassium iodide which complexed the latter two elements; palladium was separated from platinum by chloroform extraction of its colored complex with *p*-nitrosodimethylaniline[17]. For the determination of platinum the solution was evaporated to dryness in the presence of sodium chloride, the organic matter destroyed by heating with nitric and perchloric acids and the nitric acid expelled by evaporation with hydrochloric acid. The platinum was brought into solution by boiling with hydrochloric

TABLE I

THE PLATINUM METALS (p.p.m.) IN SOME STONY METEORITES

	Enstatite chondrite		*Olivine-bronzite chondrites*				*Olivine-hypersthene chondrites*						
	Abee		*Belly River*	*Allegan*	*Plainview*	*Forest City*	*Bruderheim*		*Peace River*		*Benton*	*Mocs*	*Holbrook*
Ru	1.00^{k}	0.97^{h}	1.18^{k}	1.1^{d}	1.1^{e}	0.95^{d}	n.d.	0.715^{d}	n.d.^{k}	·	0.50^{k}	0.73^{d}	0.75^{d}
	1.03^{k}		1.20^{k}										0.06^{g}
Rh	0.25^{k}	·	0.36^{k}	·	·	0.21^{f}	0.25^{k}	·	0.30^{k}	·	0.48^{k}	·	0.15^{f}
	0.25^{k}		0.40^{k}						0.31^{k}				0.064^{g}
Pd	0.44^{k}	1.0^{a}	0.77^{k}	1.5^{a}	·	·	0.50^{k}	1.0^{a}	0.41^{k}	0.89^{a}	0.42^{k}	0.84^{a}	0.44^{g}
	0.46^{k}	0.79^{h}	0.80^{k}						0.44^{k}				
Os	0.59^{k}	0.586^{i}	0.72^{k}	1.04^{d}	·	0.85^{d}	0.53^{k}	0.67^{d}	0.54^{k}	·	0.34^{k}	0.56^{c}	1.24^{d}
	0.59^{k}	0.78^{h}	0.72^{k}						0.54^{k}			0.89^{d}	0.16^{g}
Ir	0.10^{k}	0.083^{b}	0.95^{k}	·	0.5^{b}	0.54^{b}	0.40^{k}	0.435^{b}	0.60^{k}	·	1.50^{k}	·	0.24^{g}
	0.11^{k}	0.32^{h}	1.00^{k}						0.62^{k}				
Pt	0.70^{k}	$1.3^{b,h}$	0.80^{k}	·	1.6^{b}	1.75^{b}	0.60^{k}	0.9^{b}	0.55^{k}	·	0.80^{k}	·	0.44^{g}
	0.75^{k}		0.75^{k}						0.52^{k}				

[a] GREENLAND[4]. [b] BAEDECKER AND EHMANN[5]. [c] MORGAN AND LOVERING[6]. [d] BATE AND HUIZENGA[7]. [e] HARA AND SANDELL[26] (chemical). [f] SCHINDEWOLF AND WAHLGREN[8]. [g] MASON AND WIIK[25] (spectrographic). [h] CROCKET *et al.* [27]. [i] MORGAN AND LOVERING[28]. [k] This work. n.d. = Looked for, not detected. Neutron activation, except where otherwise stated.

TABLE II

THE PLATINUM METALS (p.p.m.) IN SOME IRON METEORITES

	Medium octahedrites							*Fine octahedrites*		*Nickel-rich ataxites*		
	Annaheim (Ni = 8.0%)		*Henbury (Ni = 7.5%)*			*Toluca (Ni = 8.6%)*		*Madoc (Ni = 8.0%)*	*Gibeon (Ni = 8.0%)*	*Klondike (Skookum, Ni = 18.23%)*	*Piňon (Ni = 16.5%)*	*San Cristobal (Ni = 25.6%)*
Ru	6.2^{h}	·	5.0^{b}	6.0^{c}	·	5.3^{c}	·	11.0^{h}	·	33.5^{h}	·	·
	6.4^{h}							12.0^{h}		34.8^{h}		
Rh	2.3^{h}	·	2.7^{b}	1.3^{c}	·	1.1^{c}	·	4.0^{h}	·	5.1^{h}	·	·
	2.0^{h}							4.2^{h}		5.5^{h}		
Pd	5.2^{h}	·	1.7^{b}	3.9^{c}	2.0^{d}	4.0^{c}	4.72^{d}	2.7^{h}	3.5^{e}	13.4^{h}	9.88^{d}	13.8^{e}
	5.5^{h}				2.1^{e}		3.0^{e}	2.4^{h}		13.0^{h}		
Os	3.5^{h}	·	13.5^{b}	·	2.25^{f}	·	2.54^{f}	5.0^{h}	2.52^{f}	17.4^{h}	28.3^{g}	·
	3.8^{h}							5.2^{h}		17.3^{h}		
Ir	1.6^{h}	3.5^{a}	4.7^{b}	2.3^{c}	14^{a}	2.05^{c}	·	3.0^{h}	·	13.4^{h}	·	·
	1.8^{h}							3.1^{h}		12.8^{h}		
Pt	3.5^{h}	·	9.4^{b}	5.7^{c}	·	6.55^{c}	·	6.0^{h}	·	24.0^{h}	·	·
	3.2^{h}							6.1^{h}		23.0^{h}		

[a] COBB[9], neutron activation. [b] SEN GUPTA AND BEAMISH[13], chemical. [c] NICHIPORUK AND BROWN[3], spectrographic. [d] GOLDBERG *et al.*[10], neutron activation. [e] SMALES *et al.*[11], neutron activation. [f] HERR *et al.*[12], neutron activation. [g] HEY[24]. [h] This work.

acid and hydrogen peroxide and was finally determined by reacting with tin(II) chloride, extracting the yellow color complex with tributyl phosphate in *n*-hexane and measuring it spectrophotometrically at 350 nm[18].

The organic matter from the rhodium and iridium fraction was destroyed by evaporation with nitric acid and hydrogen peroxide, and the salts converted to chlorides by evaporation with hydrochloric acid. Rhodium was separated from iridium in 1 *N* hydrochloric acid by reduction with copper powder which precipitated rhodium but not iridium[19]. For the determination of rhodium(III), the rhodium–copper precipitate was filtered and dissolved by heating with aqua regia, and any unattacked material was brought into solution by chlorination. From the solution, the copper(II) was first separated on a small Dowex 50W-X8 cation-exchange resin column at pH 1.5 and the rhodium(III) chloride was heated on the steam bath with 10 ml of 10% tin(II) chloride solution in 2 *N* hydrochloric acid for 1 h and then cooled to room temperature[20]. For iron meteorites the total solution was diluted to 25 ml with 2 *N* hydrochloric acid and the spectrophotometric measurement was made in a 5-cm cell at 475 nm; for stony meteorites the total volume was made to 10 ml after development of color and measurement was made in a 1-cm cell.

After separation of copper at pH 1.5 by the small ion-exchange column, iridium was oxidized to iridium(IV) by heating with nitric acid, and the determination finished spectrophotometrically by a modified tin(II) chloride–hydrobromic acid reaction as described by MARKS AND BEAMISH[21].

RESULTS AND DISCUSSION

The platinum-group metals were determined in 5 stony meteorites (Abee, Belly River, Bruderheim, Peace River and Benton) and 3 iron meteorites (Annaheim, Madoc and Klondike) by the proposed method. The results of this study are given in Tables I and II for the stony and iron meteorites, respectively. The duplicate values given in Tables I and II represent separate determinations. Other known determinations of the platinum metals in these meteorites are included in Tables I and II for comparison. Where similar analytical data for these particular meteorites are not available, mean values for other meteorites of the same class have been quoted from the more recent papers. The classification of stony meteorites in Table I as enstatite, olivine-bronzite and olivine-hypersthene chondrites is based on the presence of peculiar structures known as chondrules and also from the values of the ratios of 100 MgO/MgO + FeO, as suggested by PRIOR[22] and MASON[23]. Iron meteorites of Table II are classified according to their structure, which roughly parallels the nickel content. The nickel contents of the Annaheim, Madoc and Klondike meteorites (*cf.* Table II) were determined by the dimethylglyoxime method. The nickel contents of the other iron meteorites of Table II were taken from HEY[24]. In Table I, stony meteorites of the same class, and in Table II iron meteorites of identical structure and approximately similar nickel content, have been compared on the basis of the platinum-group metals data, obtained by different methods.

In the discussion which follows, the data for platinum metals in meteorites under a particular classification are compared in the order in which they appear in Tables I and II. In Table I the present data for the platinum metals in Abee are comparable to the neutron activation data in most cases. GREENLAND's palladium values[4]

(Table I) in general are very high, as he himself admitted. Because no other published data for the platinum-group metals content of Belly River are available in the literature, the new data are compared with other olivine-bronzite chondrites such as Allegan, Plainview and Forest City for which some neutron activation data are available (*cf.* Table I). The present values for ruthenium, rhodium, osmium and iridium in the Belly River sample are comparable to those obtained by the neutron activation method for these other members of this class of meteorites. The neutron activation data for palladium in Allegan and platinum in Plainview and Forest City are slightly higher than those of Belly River.

Among the olivine-hypersthene chondrites studied here, only palladium in Peace River and 5 platinum-group metals in Bruderheim (*cf.* Table I) have also been determined by the neutron activation method. Mocs and Holbrook, for which some published data are available, are included for comparison. Repeated efforts failed to detect any ruthenium in Bruderheim and Peace River, although BATE AND HUIZENGA[7] found 0.715 p.p.m. in Bruderheim; these authors also found 0.75 p.p.m. of ruthenium in Holbrook whereas only 0.06 p.p.m. ruthenium was reported for the same meteorite by MASON AND WIIK[25] (cupellation followed by spectrographic determination). Excepting palladium, the agreement between this work and the neutron activation data available for osmium, iridium, and platinum is satisfactory. The spectrographic value for palladium in Holbrook is close to the values found in the present work for Bruderheim, Peace River and Benton, and the neutron activation value for osmium in Mocs given by MORGAN AND LOVERING[6] is almost identical with the present values in Bruderheim and Peace River. The rhodium value of SCHINDEWOLF AND WAHLGREN[8] for Holbrook is close to the present value for Bruderheim; it is, however, slightly lower than those for Peace River and Benton.

Only the iridium value of Annaheim, obtained by the neutron activation method[9], is available for comparison (Table II) and the new analytical data for Annaheim, which is a medium octahedrite, are compared also with those of Henbury and Toluca, iron meteorites of similar structure. Similarly, Madoc (fine octahedrite) is compared with Gibeon, and Klondike (nickel-rich ataxite) with Piñon and San Cristobal. The new ruthenium, rhodium, palladium and iridium values for Annaheim are comparable to those obtained for Henbury and Toluca by spectrographic[3] and neutron activation[9–12] methods. The osmium value for Annaheim is also similar to that for Toluca but the platinum content is slightly lower than those of Henbury and Toluca. Although the iridium value for Annaheim obtained by COBB[9] is comparable to the present value, COBB's value for Henbury is much higher; the spectrographic data agree with the chemical data. Henbury, which was previously analyzed by SEN GUPTA AND BEAMISH[13] by the perchloric acid method but with different colorimetric methods for some elements, shows remarkable agreement between different methods in most cases, except for osmium, where the chemical value was found to be higher than the neutron activation value of HERR *et al.*[12]. However, the osmium values of SEN GUPTA AND BEAMISH[13] for Canon Diablo (coarse octahedrite) and Casas Grandes (medium octahedrite) agree with those of HERR *et al.*[12] in the same meteorites. It is possible that the discrepancies in the osmium and iridium values in Henbury can be attributed to the mislabelling problem as pointed out by HEY[24] in his compilation of trace element data in meteorites.

The only palladium and osmium data available in the literature are for some fine octahedrites and nickel-rich ataxites. The palladium contents of Madoc and Gibeon are comparable. Klondike has a very high nickel content, and its content of platinum-group metals is also very high; no nickel-rich ataxite having a similar nickel content and values for the platinum-group metals determined by other methods could be found in the literature and Piñon and San Cristobal, whose nickel contents are close to that of Klondike were, therefore, selected for comparison. The palladium contents of these two meteorites were found to be similar to that of Klondike; both Klondike and Piñon have high osmium contents.

The author wishes to express his thanks to Dr. J. A. MAXWELL for encouragement and Dr. K. R. DAWSON for supplying the meteorite samples.

SUMMARY

Microgram amounts of the 6 platinum-group metals in 5 stony and 3 iron meteorites were determined spectrophotometrically after perchloric acid decomposition and ion-exchange separation. The accuracy of the determinations of osmium, ruthenium and platinum was improved by the use of more sensitive procedures; arsenazo III was used for the determination of palladium in presence of platinum, rhodium and iridium. The data for platinum-group metals thus obtained are compared with published data obtained by neutron activation and spectrographic methods for the same meteorites or for other meteorites of the same class. With a few exceptions, the agreement between the new data and published data is satisfactory.

RÉSUMÉ

On a effectué le dosage de six métaux du groupe du platine (à l'état de traces) dans cinq météorites pierreux et trois météorites ferreux, par spectrophotométrie après décomposition à l'acide perchlorique et séparation par échange d'ions. L'exactitude du dosage de l'osmium, du ruthénium et du platine est améliorée en utilisant des procédés plus sensibles; on utilise l'arsènazo III pour le dosage du palladium en présence de platine, rhodium et iridium. Les résultats obtenus correspondent généralement bien à ceux fournis par les méthodes spectrographiques et par activation neutronique.

ZUSAMMENFASSUNG

Mikrogramme der 6 Platinmetalle in fünf steinigen und drei eisernen Meteoriten wurden spektralphotometrisch bestimmt, nachdem die Proben in Perchlorsäure gelöst und an einem Ionenaustauscher getrennt waren. Die Genauigkeit der Bestimmungen von Osmium, Ruthenium und Platin wurden durch die Verwendung empfindlicherer Verfahren verbessert. Für die Bestimmung des Palladiums in Gegenwart von Platin, Rhodium und Iridium wurde Arsenazo III verwendet. Die Ergebnisse wurden mit publizierten verglichen, die mit Hilfe der Neutronenaktivierungsanalyse und spektrographischer Methoden für die selben Meteoriten und für andere Meteoriten derselben Klasse erhalten wurden. Mit wenigen Ausnahmen ist die Übereinstimmung befriedigend.

REFERENCES

1 I. Noddack and W. Noddack, *Naturwissenschaften*, Heft 35, 18 (1930) 757.
2 F. G. Hawley, *Popular Astronomy*, 47 (1939) 439.
3 W. Nichiporuk and H. Brown, *J. Geophys. Res.*, 70 (1965) 459.
4 L. Greenland, *Geochim. Cosmochim. Acta*, 31 (1967) 849.
5 P. A. Baedecker and W. D. Ehmann, *Geochim. Cosmochim. Acta*, 29 (1965) 329.
6 J. W. Morgan and J. F. Lovering, *Science*, 144 (1964) 835.
7 G. L. Bate and J. R. Huizenga, *Geochim. Cosmochim. Acta*, 27 (1963) 345.
8 U. Schindewolf and M. Wahlgren, *Geochim. Cosmochim. Acta*, 18 (1960) 36.
9 J. C. Cobb, *J. Geophys. Res.*, 72 (1967) 1329.
10 E. Goldberg, A. Uchiyama and H. Brown, *Geochim. Cosmochim. Acta*, 2 (1951) 1.
11 A. A. Smales, D. Mapper and K. F. Fouché, *Geochim. Cosmochim. Acta*, 31 (1967) 673.
12 W. Herr, W. Hoffmeister and J. Langhoff, *Z. Naturforsch.*, 15A (1960) 99.
13 J. G. Sen Gupta and F. E. Beamish, *Am. Mineralogist*, 48 (1963) 379.
14 J. G. Sen Gupta and F. E. Beamish, *Anal. Chem.*, 34 (1962) 1761.
15 J. G. Sen Gupta, *Anal. Chem.*, 39 (1967) 18.
16 T. Hara and E. B. Sandell, *Anal. Chim. Acta*, 23 (1960) 65.
17 J. H. Yoe and J. J. Kirkland, *Anal. Chem.*, 26 (1954) 1935.
18 G. H. Faye and W. R. Inman, *Anal. Chem.*, 33 (1961) 278.
19 G. G. Tertipis and F. E. Beamish, *Anal. Chem.*, 32 (1960) 486.
20 E. B. Sandell, *Colorimetric Determination of Traces of Metals*, 3rd Edn., Interscience, New York, 1959, pp. 773–774.
21 A. G. Marks and F. E. Beamish, *Anal. Chem.*, 30 (1958) 1464.
22 G. T. Prior, *Mineral. Mag.*, 18 (1916) 26.
23 B. Mason, *J. Geophys. Res.*, 65 (1960) 2965.
24 M. H. Hey, *Catalogue of Meteorites*, The British Museum (Natural History), London, 1966.
25 B. Mason and H. B. Wiik, *Geochim. Cosmochim. Acta*, 21 (1961) 276.
26 T. Hara and E. B. Sandell, *Geochim. Cosmochim. Acta*, 21 (1960) 145.
27 J. H. Crocket, R. R. Keays and S. Hsieh, *Geochim. Cosmochim. Acta*, 31 (1967) 1615.
28 J. W. Morgan and J. G. Lovering, *Geochim. Cosmochim. Acta*, 31 (1967) 1893.

Analytica Chimica Acta
Elsevier Publishing Company, Amsterdam
Printed in The Netherlands

DIVERSES METHODES D'ANALYSE DES ALLIAGES D'ETAIN ET DE SAMARIUM

A. PERCHERON
Laboratoire des Terres Rares, C.N.R.S., Bellevue (France)

M. PINTA
Laboratoire de Spectrographie, O.R.S.T.O.M., Bondy (France)

(Reçu le 2 janvier, 1968)

Les alliages d'étain et de samarium, par la structure de ces deux éléments semblent avoir des propriétés physiques, en particulier électriques et magnétiques très intéressantes.

Leur comportement au cours de l'élaboration, leur très forte chaleur de réaction, nous a incité à faire une étude thermodynamique. Tout d'abord, nous avons été amené à établir leur diagramme de phases et par conséquent à mettre au point des méthodes d'analyse. En effet, un des constituants, le samarium, étant très volatil, la composition finale de l'alliage peut différer des teneurs initiales des éléments. La gamme des teneurs envisagées est de 0 à 100% de samarium par rapport à l'étain.

Aucun travail sur l'analyse des terres rares en présence d'étain ou inversement n'a été réalisé à notre connaissance. Nous avons étudié les trois méthodes suivantes: analyse chimique, fluorescence-X et spectrographie d'arc, afin de comparer et de contrôler les résultats obtenus. Nous pensons pouvoir transposer ces méthodes à l'analyse d'autres alliages de terres rares avec l'étain qui sont de plus en plus étudiés actuellement.

ANALYSE CHIMIQUE

De nombreuses méthodes de dosage de chacun des éléments ont été expérimentées afin de déterminer leur précision, leur sensibilité et leur spécificité. Seules, sont décrites celles remplissant ces trois conditions. Les essais ont été effectués sur des mélanges synthétiques de solutions mères obtenues par dissolution dans l'acide chlorhydrique *M*, d'oxyde de samarium d'une part et d'étain métallique d'autre part.

Dosage du samarium

Gravimétrie par précipitation de l'oxalate[1]. On précipite le samarium par l'acide oxalique à pH 1. En effet, dans ces conditions l'oxalate de samarium est très peu soluble[2] et l'étain forme des oxalates complexes très stables et très solubles[3].

Mode opératoire. On porte à l'ébullition la solution contenant environ 2 g Sm/l. A 250 ml de cette solution on ajoute 60 ml d'une solution saturée d'acide oxalique en agitant. Le magma gélatineux se transforme rapidement en précipité cristallin.

On laisse reposer pendant 8 h et après avoir lavé 5 ou 6 fois avec une solution à 2% d'acide oxalique et 1% d'acide chlorhydrique concentré, on filtre. On sèche le filtre à l'étuve directement en creuset de platine; l'oxalate passe à l'état d'oxyde par calcination.

L'erreur est inférieure ou égale à 0.1% (Tableau I).

Dosage compleximétrique. L'acide éthylène diaminetétracétique (EDTA) donne avec les cations des terres rares des complexes très stables. On dose[4] en retour l'excès d'EDTA à pH 8–8.5 par la sulfate de manganèse en présence de noir ériochrome T comme indicateur. La solution d'EDTA est étalonnée[5] à l'aide d'une solution de zinc.

TABLEAU I

RÉSULTATS DE L'ANALYSE DU SAMARIUM PAR PRÉCIPITATION OXALIQUE

Composition du mélange à analyser		
Sm (g)	*Sn (g)*	*Sm dosé (g)*
0.4743	0	0.4742
0.4672	0.1100	0.4668
0.4203	0.3025	0.4197
0.3927	0.2488	0.3923
0.3553	0.2604	0.3549
0.4699	0.1978	0.4697

TABLEAU II

RÉSULTATS DE L'ANALYSE DU SAMARIUM PAR LA MÉTHODE COMPLEXIMÉTRIQUE

Composition du mélange à analyser		
Sn (mg)	*Sm (mg)*	*Sm dosé (mg)*
0	96	95.4
44.4	94	93.8
36	64.6	64.5
60	64.6	64.5
69	79.8	79
24	39.84	39.8

Mode opératoire. L'étain pouvant gêner, il est éliminé en attaquant l'alliage par l'acide nitrique concentré (voir p. 491). La solution à doser est diluée à 100 ml et on ajoute un excès d'EDTA de façon à complexer le samarium. On ajoute 100 mg d'acide ascorbique, quelques gouttes de noir ériochrome T et on ajuste le pH à 8–8.5. On titre avec la solution de sulfate de manganèse jusqu'au virage au rouge.

L'erreur est généralement inférieure ou égale à 0.2% (Tableau II). Le dosage direct[6] par l'EDTA en présence d'indicateur mixte est moins précis. L'erreur est inférieure à 0.5%.

Dosage de l'étain

Plusieurs méthodes dont la précipitation par le cupferron[7] et la précipitation sous forme d'hydroxyde[8], bien que très précises et reproductibles, ont dû être éliminées car elles n'étaient pas spécifiques.

Gravimétrie. Nous avons constaté au cours des essais de dissolution des métaux que l'attaque de l'étain par l'acide nitrique concentré (54%) conduit à l'acide α ou β stannique, insoluble en milieu nitrique concentré ou dilué, et qui par calcination conduit à l'oxyde SnO_2. Cette oxydation permet une très bonne séparation du samarium et un dosage précis et reproductible.

L'erreur est inférieure ou égale à 0.1% (Tableau III).

Le dosage par l'acide phénylarsénique[9] est également spécifique et aussi précis que le précédent, mais beaucoup plus long.

Mode opératoire. 0.1 g d'échantillon environ est dissous dans l'acide chlorhydrique concentré. La solution est amenée à 200 ml et ajustée à pH 0.6. L'étain est précipité à chaud par addition de 35 ml de solution aqueuse saturée d'acide phénylarsénique. On filtre immédiatement et on lave jusqu'à élimination des chlorures. La calcination à 1075–1100° conduit à l'oxyde (Tableau IV).

TABLEAU III

RÉSULTATS DE L'ANALYSE DE L'ÉTAIN PAR GRAVIMÉTRIE

Composition du mélange à analyser		
Sm (g)	*Sn (g)*	*Sn dosé (g)*
0.055	0.2805	0.2807
0.100	0.3913	0.3918
0.0234	0.2394	0.2393
0.296	0.3216	0.3220
0.188	0.3580	0.3576

TABLEAU IV

RÉSULTATS DE L'ANALYSE DE L'ÉTAIN PAR PRÉCIPITATION PAR L'ACIDE PHÉNYLARSÉNIQUE

Composition du mélange à analyser		
Sm (g)	*Sn (g)*	*Sn dosé (g)*
0.0537	0.1330	0.1327
0	0.1944	0.1940
0.0476	0.1220	0.1215
0.0310	0.1076	0.1072

Volumétrie. De bons résultats ont également été obtenus par volumétrie. Dans la plupart des méthodes[10–15] on réduit d'abord l'étain(IV) à l'état stanneux. On titre ensuite l'étain(II) par un oxydant approprié.

La méthode préconisée par DANNENMULLER[10] conduit le plus rapidement aux résultats les plus satisfaisants. Le mode opératoire est le suivant: 0.5 g à 1 g d'échantillon est dissous par 60 ml d'acide chlorhydrique et quelques millilitres d'eau oxygénée. Après l'attaque, on ajoute 60 ml d'acide chlorhydrique, 100 ml d'eau et 2 g de nickel en limaille fine. On porte à l'ébullition doucement pendant 30 min. Avant dissolution complète du nickel et jusqu'à la fin du titrage on maintient une atmosphère de gaz carbonique sur la liqueur. La fin de la réduction est indiquée par la disparition presque complète du nickel. On refroidit et on titre avec une solution de bromate de potassium après addition d'1 ml d'empois d'amidon et de quelques millitres d'iodure de potassium.

L'erreur est inférieure ou égale à 0.1%.

Les méthodes d'analyse chimique retenues sont précises et reproductibles, elles donnent des résultats à 0.1% près. Elles sont satisfaisantes sur ce point, mais elles exigent une quantité assez importante de produit 0.1 g à 1 g et elles sont longues.

FLUORESCENCE-X

Les inconvénients de l'analyse chimique, précédemment cités, nous ont conduits à étudier le dosage du samarium et de l'étain dans leurs alliages par fluorescence-X.

Principe et conditions générales

L'intensité I_i mesurée d'une radiation de fluorescence émise par un élément E_i est liée à la concentration C_i% de cet élément dans une solution solide ou liquide par la relation:

$$I_i = kC_i/\Sigma_j(\mu_e+\mu_f)_jC_j$$

où k est une constante de proportionnalité, C_j la concentration de l'élément E_j, (μ_e) et (μ_f) les coefficients massiques d'absorption relatifs à l'élément E_j pour les longueurs d'onde d'excitation et de fluorescence de l'élément E_j.

L'intensité d'une radiation de fluorescence-X émise par un élément donné sera rapportée à une intensité d'une radiation de référence correspondant à une concentration connue de cet élément. On est donc amené à tracer au préalable des courbes d'étalonnage $I = \mathrm{f}\ (c\%)$ pour chaque élément à partir d'échantillons étalons, puis ensuite à comparer pour un échantillon inconnu l'intensité mesurée à celles indiquées sur la courbe.

L'analyse pourrait être effectuée sur des échantillons massifs, mais des effets de matrice importants risqueraient de fausser les résultats: granulométrie, dimension, finition de la surface et influence des autres éléments contenus dans l'échantillon.

On opère donc sur des solutions aqueuses à 10 g/l. La solution aqueuse représente une matrice uniforme où les ions dissous n'ont pratiquement plus d'influence mutuelle.

On utilise un spectromètre à fluorescence-X Philips PW 1540.05, constitué par quatre éléments principaux:

(*a*) un générateur haute tension de 1000 W alimentant le tube à rayons-X à anticathode de tungstène;

(*b*) un porte échantillon dont la fenêtre délimite la zone irradiée;

(*c*) le spectromètre comprenant des fentes de collimation, un cristal analyseur du rayonnement de fluorescence émis par l'échantillon et un compteur d'impulsions;

(*d*) un ensemble électronique permettant le comptage des impulsions.

Le Tableau V permet de voir qu'il n'y a pas d'impossibilités à doser ces deux éléments en présence.

TABLEAU V

CARACTÉRISTIQUES DU SPECTRE DE RAYONS-X DE L'ÉTAIN ET DU SAMARIUM

Elément	*Série*	*X raie (unité x)*	*Discontinuité d'absorption (unité x)*	*Potentiel d'excitation (volts)*
Sn	K	$\alpha_1 = 489.57$	434.339	29.1
	L	$\alpha_1 = 3600$	2771.5, 2976.3, 3149.5	4.46
Sm	K	309	264.09	46.8
	L	2199	1595.4, 1699.1, 1840.8	6.75

TABLEAU VI

ANALYSE PAR FLUORESCENCE-X, COURBE D'ÉTALONNAGE DE L'ÉTAIN

Quantités relatives (%)												
	Sn	100	90	80	70	60	50	40	30	20	10	0
	Sm	0	10	20	30	40	50	60	70	80	90	100
Nombre de coups/sec[a]		2108	2075	1834	1485	1310	1091	843	601	420	210	11

[a] Moyenne de 10 comptages, durée d'un comptage: 64 sec.
Sensibilité de la baie de comptage: 8.
Constante de temps: 4.
Facteur de multiplication: 1.

Etablissement des courbes d'étalonnage

Etain. La raie choisie pour le dosage est la raie Lα1. Le numéro atomique de l'étain et la longueur d'onde de la raie étudiée conduisent à utiliser le fluorure de lithium comme cristal analyseur et le compteur à flux gazeux comme détecteur. Pour éviter l'absorption du rayonnement de fluorescence par l'air, les parties du spectromètre correspondant au passage des rayons-X depuis l'échantillon jusqu'au compteur seront maintenues sous un vide primaire. Afin d'éliminer au maximum le fond continu, on effectue une discrimination. La courbe d'étalonnage est définie Tableau VI. Le fond continu est mesuré sur la matrice, soit la solution de samarium pur.

Nous obtenons une variation linéaire de l'intensité de la raie émise en fonction de la concentration: $Y = ax + b$. A partir des résultats expérimentaux x et y, on calcule a et b. L'erreur d'estimation est: $y - Y = \pm 1.5\%$.

L'écart type d'estimation est: $\sigma_D = \{\Sigma(y-Y)^2/(n-2)\}^{\frac{1}{2}} = 0.6$, le n étant nombre de résultats.

La limite de sensibilité est de 0.5%.

Samarium. Les conditions opératoires sont les suivantes:
Raie de dosage: raie Lα1 (goniomètre à 66°18).
Cristal analyseur: LiF.
Compteur à scintillation (850 V).
Semi-vide.
Excitation: 30 kw–20 mA.
Sensibilité de la baie de comptage: 16.
Constante de temps: 4.
Facteur de multiplication: 1.
La courbe d'étalonnage est définie Tableau VII.

Analyse proprement dite

L'échantillon à analyser est dissous dans l'acide chlorhydrique 0.1 *M*. Puis on ajuste la solution de façon à obtenir une concentration de 10 g/l, pour être dans les mêmes conditions que les solutions étalons.

Après avoir déterminé l'ordre de grandeur des concentrations respectives de samarium et d'étain dans l'échantillon, on établit au voisinage de ces grandeurs une

TABLEAU VII

ANALYSE PAR FLUORESCENCE-X, COURBE D'ÉTALONNAGE DU SAMARIUM[a]

Quantités relatives (%)	Sm	100	90	80	70	60	50	40	30	20	10	0
	Sn	0	10	20	30	40	50	60	70	80	90	100
Nombre de coups/sec		11331	10200	9295	8325	7465	6449	5425	4330	3135	2014	743

[a] Erreur absolue: ±1.2%.
Ecart type d'estimation $\sigma_D = 0.43$.
Limite de sensibilité: 0.05%

TABLEAU VIII

COURBE D'ÉTALONNAGE DU SAMARIUM ENTRE 0 ET 20%

Nombre de coups/sec	2841	2533	1797	1521	1246	1001	693
% Sm	20	15	10	7.5	5	2.5	0

TABLEAU IX

ANALYSE DE SOLUTIONS SYNTHÉTIQUES PAR FLUORESCENCE-X

Pourcentage de Sm dans la solution à analyser	*Sm (%)*	*Sn (%)*
5	4.9	94.8
15	14.8	85.6
25	25	74

TABLEAU X

ANALYSE DE DIVERS ALLIAGES PAR FLUORESCENCE-X

Pourcentage de Sm avant l'élaboration de l'alliage	*Sn*[a] *(poids en g/l)*	*Sm*[a] *(poids en g/l)*	*% Sn*	*% Sm*
70 (1)	3.45	5.45	39	61
68	3.2	5.15	38	62
46	5.45	3.05	64	36
30	7.3	2.05	78	22
70 (2)	3.65	4.6	44	56
46	5.2	2.8	65	35
10	6.9	0.4	94.5	5.5
80	2.25	5.5	32	68
95	0.9	8.35	8	92

[a] Les résultats obtenus sont par défaut car il y a oxydation de l'alliage.

courbe d'étalonnage avec des concentrations plus rapprochées ce qui permet une évaluation plus précise sur la courbe (voir Tableau VIII).

Le nombre de coups par seconde enregistré pour l'échantillon est de 901. D'après la courbe d'étalonnage on en déduit une teneur en samarium de 1.95%.

Les analyses (voir Tableaux IX et X) permettent de vérifier la perte assez importante de samarium au cours de l'élaboration par volatilisation. Cette perte varie suivant le traitement thermique subi par l'alliage.

L'analyse par fluorescence-X, bien que moins précise que l'analyse chimique, permet des manipulations très rapides et sur de faibles quantités. Par exemple, elle a permis d'analyser des résidus d'essai de volatilité de l'ordre d'une dizaine de milligrammes.

SPECTROGRAPHIE D'ARC

Nous avons envisagé l'analyse par spectrographie d'arc pour les faibles teneurs du samarium dans l'étain et inversement. Cependant, la prise d'essai très faible nécessaire à cette méthode nous a incité à l'utiliser, après dilution, pour les fortes teneurs.

Principe général

Dans une source d'excitation donnée, l'intensité d'une raie spectrale est fonction du nombre N d'atomes présents suivant la loi $I = kN^m$, k et m sont des constantes qui dépendent de l'élément, de la raie et des conditions d'excitation; N est proportionnel à la concentration C de l'élément: $I = k'C^m$.

Dans des conditions d'excitation données, les intensités des raies des éléments constituant un milieu complexe ont entre elles une relation qui ne dépend que de leur concentration. Le rapport des intensités de deux raies émises par un seul ou par deux éléments différents peut varier largement avec le mode d'excitation. On doit dans la mesure du possible utiliser des conditions d'excitation reproductibles.

Afin d'éviter les erreurs provenant en particulier des fluctuations de la source, on utilise la méthode de l'étalon interne[16]: mesure du rapport de deux raies spectrales appartenant l'une à l'élément dosé, l'autre à un étalon bien choisi et de concentration connue.

On détermine log I_x/I_E qui est fonction de la concentration, I_E et I_x étant les intensités respectives des raies de l'étalon E et de l'élément à doser x, C_x étant sa concentration.

$$\log (I_x/I_E) = m \log C_x + \text{constante}$$

La précision du dosage dépend de la pente de cette courbe, elle est d'autant plus grande que la pente est plus forte.

La sensibilité et la précision de la méthode des étalons internes sont fonction des conditions d'excitation, de la nature de l'élément pris comme étalon et des raies choisies.

L'étalon interne doit satisfaire à certaines conditions et notamment: les vitesses de volatilisation de l'élément analysé et de l'étalon interne doivent être analogues, les raies étudiées doivent avoir des longueurs d'onde et des potentiels d'excitation voisins.

Lorsqu'une émulsion photographique est impressionnée par un flux énergétique de valeur relative I pendant un temps t, le noircissement résultant mesuré par sa densité optique D est lié à I par la relation: $D=\gamma \log It$, $It=E$. E est l'exposition et γ est le contraste.

Pratiquement, cette courbe de la densité en fonction de log E, appelée courbe caractéristique, est rectiligne entre deux valeurs de log E.

Pour une longueur d'onde donnée, la pente de la partie rectiligne de la caractéristique est γ. On comparera plusieurs caractéristiques dans leur région rectiligne. Pour déterminer le rapport d'intensité des deux raies choisies, on construit leurs courbes caractéristiques. Pour cela, on fait varier l'exposition E à l'aide d'un secteur à échelons que l'on place devant la fente d'entrée du spectrographe.

Les courbes caractéristiques de la raie de l'élément dosé d'intensité I_X et de la raie de l'étalon interne I_E sont représentées figure 1.

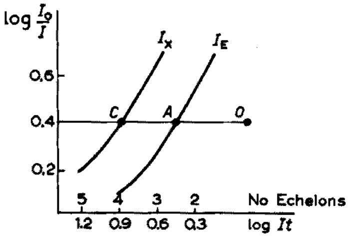

Fig. 1. Courbes caractéristiques d'un couple de raies d'analyse.

En négligeant le fond spectral, ce qui est possible dans le cas présent, on a:

$$\log (I_X/I_E) = \log I_X - \log I_E = \overline{AC}$$

La courbe d'étalonnage est obtenue en construisant cette grandeur en fonction de la concentration.

Détermination des conditions opératoires

Nous utilisons un spectrographe Jarrel-Ash, modèle 7130-3.4 mètres dont le réseau plan est à 590 traits/mm. On opère dans le premier ordre.

La source d'excitation est un arc continu en atmosphère contrôlée.

Etain. Choix de l'étalon interne. Après plusieurs essais, compte tenu des conditions exposées plus haut, nous avons choisi finalement le samarium, sa vitesse de volatilisation étant très voisine de celle de l'étain; ces deux éléments étant sous forme d'oxydes (Fig. 1).

Choix des raies. Nous avons recherché les raies les plus sensibles et dont l'intensité convient au problème envisagé:

Sn I 3262.328 Å	Intensité 400
Sm II 3661.350 Å	Intensité 100

Choix de l'atmosphère contrôlée. Un courant de gaz carbonique donne de meilleurs résultats que l'air ou l'argon. Dans l'air, il y a formation de cyanogène dont les bandes moléculaires se superposent avec le spectre étudié. L'argon absorbe le rayonnement émis, ce qui diminue trop l'intensité des raies.

On opère dans une cloche en quartz avec un débit de 1.5 l/min avec un passage de 30 sec avant l'allumage de l'arc.

Dans le Tableau XI, sont indiquées les autres conditions opératoires.

Dilution de l'échantillon. Le sulfate de potassium est utilisé comme tampon spectral.

(*a*) Entre 0 et 50% d'etain, on effectue un prémélange A dans le rapport 1/1 de l'échantillon et de l'étalon interne (Sm_2O_3). Le mélange spectrographié à la composition suivante: 1.5 mg du mélange A, 23.5 mg de K_2SO_4, 25 mg de graphite.

(*b*) Entre 50 et 100% d'étain, le prémélange B est dans le rapport 1/4 de l'échantillon et de l'étalon interne. Le mélange spectrographié à la composition suivante: 1 mg de mélange B, 24 mg de K_2SO_4, 25 mg de graphite.

TABLEAU XI

CONDITIONS OPÉRATOIRES D'ANALYSE DE L'ÉTAIN PAR SPECTROGRAPHIE D'ARC

Arc continu anodique Jarrel-Ash	
Type d'électrodes	graphite (Péchiney) (a) anode: diamètre de 6 mm, cratère de 4 mm de profondeur et 3 mm de diamètre (b) cathode: diamètre de 6 mm, conique à son extrémité
Entrodes	2 mm
Source d'excitation	250 V—10 A
Flambage	0
Temps de pose	30 sec
Fente d'entrée	20 μ de largeur; 15 mm de hauteur
Secteur à échelons	tel que log $(I_1/I_2) = 0.2$
Longueur d'ondes photographiées	2800 à 3800 Å 1er ordre
Emulsion photographique	Spectroguil lente
Révélateur Multiflex Guilleminot	4 min à 21°
Gamme de concentrations	0 à 100%
Dilution	50 fois entre 0 et 50% 75 fois entre 50 et 100%

Remarques: La quantité de samarium varie d'un échantillon à l'autre. Toutefois, nous déterminons la quantité d'étain par rapport à celle de samarium en remarquant que l'on n'a, en fait, que deux constituants, samarium et étain, leur somme étant

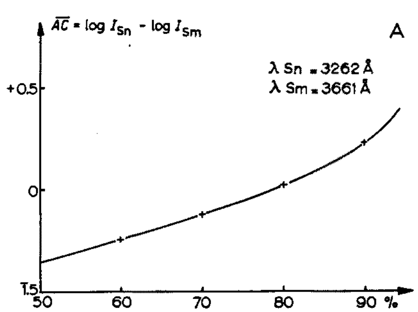

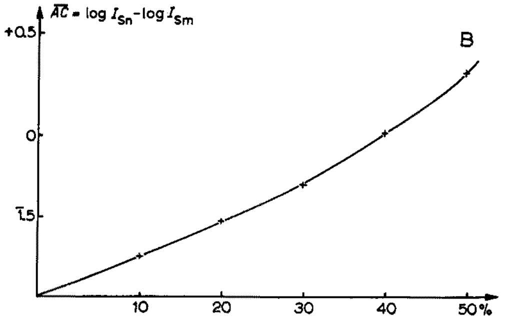

Fig. 2A. Spectrographie d'arc. Courbe d'étalonnage de l'étain dans le samarium entre 50 et 100% Sn.

Fig. 2B. Spectrographie d'arc. Courbe d'étalonnage de l'etain dans le samarium entre 0 et 50% Sn.

constante. La détermination du rapport étain–samarium est bien un dosage d'étain.

Le mélange par broyage doit être fait avec beaucoup de soins afin d'obtenir une bonne homogénéité.

Courbe d'étalonnage. Nous disposons pour déterminer cette courbe d'une gamme de concentrations étalons. Ce sont des mélanges d'oxyde de samarium et d'oxyde d'étain. Pour chaque concentration nous déterminons la valeur $\overline{AC}$. Soient $\overline{AC}$ =f (concentration) les courbes d'étalonnage (voir Figs. 2A et 2B).

En faisant varier les conditions opératoires, temps de pose, prise d'essai de l'échantillon, raies d'analyse, nous obtenons les courbes d'étalonnage pour des concentrations plus faibles. La limite de sensibilité est de 100 p.p.m.

Dosage du samarium. Nous avons procédé à une étude semblable à celle de l'étain pour le samarium. Les conditions opératoires sont résumées dans le Tableau XII. La courbe d'étalonnage (Fig. 3) est obtenue pour les concentrations variant de 0 à 100%. La limite de sensibilité est de 100 p.p.m.

TABLEAU XII

CONDITIONS OPÉRATOIRES D'ANALYSE DU SAMARIUM PAR SPECTROGRAPHIE D'ARC

Gamme de concentrations	0 à 100%
Préparation de l'échantillon	5 mg de mélange à analyser 1 mg La_2O_3 20 mg K_2SO_4 26 mg de graphite
Etalon interne	lanthane (oxyde de..)
Type d'électrodes	Voir Tableau XI
Arc continu anodique	Jarrel-Ash
Entrodes	2 mm
Source d'excitation	250 V—10 A
Flambage	0
Atmosphère contrôlée de CO_2	
Fente d'entrée	20 μ de largeur, 15 mm de hauteur
Secteur à échelons	Voir Tableau XI
Temps de pose	30 sec
Longueur d'ondes photographiées	2800 à 3800 Å
Raies d'analyse	Sm II 3321.284 Å $I = 50$ La II 3265.67 Å $I = 300$
Emulsion photographique	Spectroguil lente
Révélateur multiflex	4 min à 21°

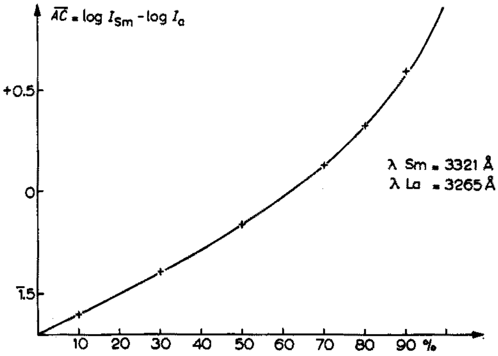

Fig. 3. Spectrographie d'arc. Courbe d'étalonnage du samarium dans l'étain.

Analyse proprement dite

Nous avons analysé les alliages en reportant la valeur de $\overline{AC}$ déduite des caractéristiques sur les courbes d'étalonnage. Les alliages sont dissous dans l'acide chlorhydrique, on effectue ensuite une coprécipitation sous forme d'hydroxydes. Par calcination, on obtient le mélange d'oxydes. Les résultats obtenus (Tableau XIII) permettent de vérifier la perte de samarium par volatilisation au cours de l'élaboration.

Pour que les résultats soient valables, il faut faire au moins trois essais en prenant soin de recommencer en même temps l'émission de trois étalons afin de vérifier les courbes d'étalonnage.

Précision. Pour l'étain, l'erreur absolue est de ±1% et l'écart type $\sigma=0.6$.

Pour le samarium, l'erreur absolue est de 2%, et l'écart type $\sigma=0.8$.

TABLEAU XIII

ANALYSE DES ALLIAGES PAR SPECTROGRAPHIE D'ARC

Pourcentage de Sm avant élaboration	*Valeur analytique Sm %*	*Valeur analytique Sn %*
5	2	97
16	11	90
50	41	59

COMPARAISON DES RÉSULTATS OBTENUS

Echantillons synthétiques

Les échantillons synthétiques sont préparés à partir de solutions étalons chlorhydrique à 10 g/l. Pour l'analyse chimique, le samarium est précipité sous forme d'oxalate, l'étain par l'acide phénylarsénique. L'analyse par fluorescence-X est faite directement sur la solution. Pour la spectrographie, les hydroxydes de samarium et d'étain sont coprécipités par l'ammoniaque en présence de chlorure d'ammonium et calcinés afin d'obtenir le mélange d'oxydes (Tableau XIV).

Alliages

Pour l'analyse chimique, les alliages sont attaqués à l'acide nitrique concentré: on dose ainsi l'étain. Le samarium est dosé dans le filtrat par précipitation oxalique.

TABLEAU XIV

COMPARAISON DES ANALYSES DU SAMARIUM DANS DES MÉLANGES SYNTHÉTIQUES

Pourcentage des samarium dans les mélanges	*Analyse chimique*	*Fluorescence-X*	*Arc*
25	25.05	25	24.5
20	19.9	19.8	19.5
15	15.1	14.8	15.5
10	9.86	9.7	9.8
5	4.89	4.9	4.8

Pour la fluorescence-X, on procède à la dissolution de l'alliage dans l'acide chlorhydrique au 1/10.

L'alliage est oxydé par chauffage à 800° à l'air pour l'analyse par spectrographie d'arc ou dissous et traité comme les échantillons synthétiques (Tableau XV).

TABLEAU XV

COMPARAISON DES ANALYSES DE DIVERS ALLIAGES PAR LES TROIS MÉTHODES

Quantités avant élaboration	*Valeurs analytiques*		
	Analyse chimique	*Fluorescence-X*	*Arc*
5% Sm	2.1	1.95	2
95% Sn	97.6	98	97
30% Sm	25.2	26	24.8
70% Sn	74.6	74	74.8
46% Sm	34.5	35	34
54% Sn	65.3	65	66
70% Sm	61.4	61	62
30% Sn	38.5	39	38.7
95% Sm	91.6	92	91
5% Sn	7.8	8	8.5

TABLEAU XVI

CARACTÉRISTIQUES ANALYTIQUES DES MÉTHODES

Caractéristiques	*Analyse chimique*	*Fluorescence-X*	*Spectrographie d'arc*
Précision	0.1%–0.5%	1.5%	2% Sm dans Sn 1.5% Sn dans Sm
Sensibilité	Peu sensible	500 p.p.m. Sm 5000 p.p.m. Sn	100 p.p.m. Sn 100 p.p.m. Sm
Ecart type	0.1	0.6 Sn 0.4 Sm	0.6 Sn 0.8 Sm
Temps d'exécution	Long	Rapide	Long

CONCLUSION

Bien que les résultats obtenus par les différentes méthodes se recoupent et se vérifient, elles présentent chacune des caractéristiques que nous avons soulignées dans le Tableau XVI.

L'analyse chimique paraît être la méthode la plus précise dans un certain domaine de concentrations, mais sa sensibilité est assez faible et son temps d'exécution est long. Elle permettra par exemple de déterminer les proportions exactes d'un alliage autour d'un composé défini ou d'un eutectique. Elle n'est pas utilisable pour les faibles concentrations des deux constituants. Dans ces domaines, la fluorescence-X peut apporter de précieux renseignements. D'autre part, sa rapidité d'exécution et la faible quantité de produit nécessaire à sa réalisation la font utiliser pour les analyses courantes et la vérification de l'homogénéité des alliages.

L'analyse par spectrographie d'arc est beaucoup plus sensible que les deux autres méthodes et elle sera choisie pour les faibles teneurs des deux constituants; par exemple, dans l'étude des extrémités du diagramme de phases, détermination de la limite de solubilité et variation des paramètres. Dans le domaine des fortes concentrations, elle permettra aussi de contrôler les résultats obtenus par les autres méthodes.

Nous nous proposons d'appliquer les méthodes précédentes à tous les alliages étain–terres rares. Leurs caractéristiques pourront légèrement varier suivant l'élément terre rare considéré, mais à quelques exceptions près, il est fort probable qu'elles seront utilisables.

RÉSUMÉ

Diverses méthodes d'analyse des alliages étain–samarium sont étudiées: analyse chimique, fluorescence-X, spectrographie d'arc. Nous comparons leurs caractéristiques ainsi que les résultats obtenus. La similitude du comportement des terres rares peut permettre l'extension de ces méthodes aux autres alliages terres rares–étain.

SUMMARY

Several methods of analysis for tin–samarium alloys are studied: chemical analysis, X-ray fluorescence and arc spectrography. Their characteristics and the results obtained are compared. The chemical methods are most precise but are insensitive and tedious. X-Ray fluorescence is suitable for routine work and for control of alloy homogeneity. Arc spectrography is by far the most sensitive method The methods can be applied to alloys of other rare earths with tin.

ZUSAMMENFASSUNG

Verschiedene Analysenmethoden für Zinn–Samarium-Legierungen werden untersucht: Chemische Analyse, Röntgenfluoreszenz- und optische Spektralanalyse. Die Merkmale der Methoden und die erhaltenen Ergebnisse werden verglichen. Die chemischen Methoden sind am genauesten, aber unempfindlich und mühsam. Die Röntgenfluoreszenzanalyse ist für Routineuntersuchungen und zur Kontrolle der Legierungshomogenität geeignet. Die Spektralanalyse ist am empfindlichsten. Die Methoden können ebenso für Zinn-Legierungen mit anderen Seltenen Erden angewendet werden.

BIBLIOGRAPHIE

1 I. M. KOLTHOFF, *Treatise on Analytical Chemistry*, Philips-Elving.
2 L. A. SARVER ET P. H. M. BRINTON, *J. Am. Chem. Soc.*, 49 (1927) 943, 958.
3 P. KARSTEN ET H. L. KIES, *Rec. Trav. Chim.*, 67 (1948) 753.
4 G. W. C. MILNER ET J. W. EDWARDS, *Anal. Chim. Acta*, 18 (1958) 513.
5 H. FLASHKA ET F. SADEK, *Z. Anal. Chem.*, 156 (1957) 23.

6 G. Brunisholz et R. Cahen, *Helv. Chim. Acta*, 34 (1956).
7 A. Pinkus et J. Claessens, *Bull. Soc. Chim. Belges*, 31 (1927) 413.
8 R. Thery, *Chim. Anal. (Paris)*, 32 (1950) 19.
9 J. S. Knapper, K. A. Graig et G. C. Chandlee, *J. Am. Chem. Soc.*, 55 (1933) 3945.
10 M. Dannenmuller, *Rev. Met. (Paris)*, 6 (1941).
11 W. F. Hillebrand et G. E. F. Lundell, *Applied Inorganic Analysis*, J. Wiley, 1953.
12 M. L. Malaprade, *Bull. Soc. Chim. France*, 18 (1951) 739
13 J. A. Sherer, *J. Res. Natl. Bur. Std.*, 21 (1938) 95.
14 C. C. Miller et L. R. Currie, *Analyst*, 73 (1948) 377.
15 H. J. G. Challes et J. T. Jones, *Analyst*, 82 (1957) 658.
16 M. Pinta, *Recherche et dosage des éléments traces*, Dunod, 1962.

Analytica Chimica Acta
Elsevier Publishing Company, Amsterdam
Printed in The Netherlands

THE SOLVENT EXTRACTION OF METAL COMPLEXES OF PYRIDINE-2-ALDEHYDE-2′-PYRIDYLHYDRAZONE

M. A. QUDDUS AND C. F. BELL
Department of Chemistry, Brunel University, London, W3 (England)

(Received January 25th, 1968)

Studies have been reported recently of the extraction into immiscible organic solvents of metals as their complexes with terdentate ligands such as 1-(2-pyridylazo)-2-naphthol[1] (PAN) and 1-(thiazolylazo)-2-naphthol[2]. These ligands are used widely as indicators in compleximetric titrations and as selective reagents for metals.

The extraction behaviour of their metal complexes is interpreted in terms of the ionization of the acidic hydroxyl group of the ligand, HA, to give anions A^- which chelate with the metal ion to form an uncharged extractable species. In the simple case of a dipositive metal ion, M^{2+}, which can show 6 coordination, the extracted species is MA_2.

The chelating properties of other types of terdentate ligands have also been described. Among these is pyridine-2-aldehyde-2′-pyridylhydrazone (PAPHY)[3-5]. Chelation to the metal involves the nitrogens of the two pyridine rings and the terminal nitrogen of the pyridylhydrazine group. This enhances the acidity of the hydrogen of the imino-group. A dipositive metal ion, with coordination number 6, forms a complex ion $M(PAPHY)_2^{2+}$. On increasing the pH, this successively loses two protons to give $M(PAPY)_2$, an uncharged complex. A dipositive metal ion, with coordination number 4, gives a mono complex, $M(PAPHY)^{2+}$, which deprotonates to $M(PAPY)^+$. Solvent extraction of such a metal is possible if this ion associates with, or the fourth coordination position is occupied by, a suitable anion to form a neutral ternary complex. An important difference between the behaviour of PAPHY as a ligand compared with those mentioned previously is that deprotonation occurs after instead of before chelation.

Possible applications of substituted hydrazones as selective analytical reagents have been discussed[6]. Although the analytical significance of the formation of neutral complexes by the deprotonation of metal–PAPHY complex ions has been pointed out[4], no systematic study of the factors involved in their solvent extraction has been reported. A study of the extraction of various metals by solutions of PAPHY in chloroform is described in this paper.

EXPERIMENTAL

Apparatus

Optica Recording and Unicam SP 600 spectrophotometers were used with 1-cm silica cells. A Vibron pH meter No. 39 A (E.I.L., Richmond, Surrey) was used with a screened glass electrode and a calomel electrode.

A scintillation counter with a NaI(Tl) crystal (Dynatron Radio, Maidenhead) and a Rotatest horizontal rotator (Luckhams, Raynes Park, London) were also employed.

Reagents

A.R. chemicals were used throughout.

Pyridine-2-aldehyde-2'-pyridylhydrazone (m.p. 178–179° uncorrected; Aldrich Chemical Co, Milwaukee). The m.p. was identical with that of the reaction product of pyridine-2-aldehyde and 2-pyridylhydrazine after recrystallization from ethanol.

Buffers. The following mixtures were used, their respective pH ranges being given in brackets. Hydrochloric acid–sodium acetate (2.5–4.0); acetic acid–sodium acetate (4.0–6.0); potassium dihydrogen phosphate–sodium hydroxide (6.0–8.0); borax–hydrochloric acid (8.0–9.0); and borax–sodium hydroxide (9.0–11.0). All were purified by extraction with PAPHY in chloroform followed by washing with several portions of pure chloroform.

Zinc-65. $t_{\frac{1}{2}} = 245$ d, $\gamma = 0.51$ and 1.11 MeV with a specific activity of 1 mC/$2.6 \cdot 10^{-5}$ mmole was supplied by the Radiochemical Centre, Amersham.

Extraction of metals by PAPHY in chloroform

The aqueous phase (10 ml) containing a known quantity of metal, presaturated with chloroform, buffered to the required pH and of ionic strength 0.1, was shaken for 1 h with 10 ml of PAPHY in chloroform, presaturated with water, in stoppered 50-ml Pyrex tubes at 20±2°. In all cases, an excess of PAPHY over the metal present was used. Except for palladium(II), equilibrium was reached within a few minutes; for palladium, the rate appeared to be pH-dependent. The absorbance, A_1, of the chloroform extract was measured at the wavelength for maximum absorbance. The pH of the aqueous phase was measured immediately after equilibration.

Equilibration and measurements of absorbance were repeated at least twice and the average of the three absorbance values was taken in calculating D, the distribution ratio. Since the volumes of the two phases were equal, $D = A_1/(A_0 - A_1)$, where A_0 = absorbance for 100% extraction. A_0 was taken as the sum of the absorbances measured after successive extractions of the same aqueous phase containing a known quantity of metal with several aliquots of PAPHY in chloroform. At a high pH, the absorbance of the second extract was generally very low and near to zero. No independent measurement of the concentration of metal left in the aqueous phase was made, hence very high and very low values of D may be in error.

The variation of D with $[\text{PAPHY}]_0$ at constant pH, and with pH at constant $[\text{PAPHY}]_0$, was examined for each metal. The effect of various anions was also studied in the case of palladium(II) and copper(II).

The dependence of the absorbance of the chloroform phase on the concentration of metal extracted was determined at the pH of maximum (≃100%) extraction. Subsequent distribution studies were carried out with initial concentrations of metal chosen such that, even for 100% extraction, the absorbance of the organic extract was within the range for which Beer's law was obeyed.

The distribution of ^{65}Zn was measured by equilibrating for 2 h, 10-ml volumes of aqueous buffer containing radiotracer (0.15 μg/l) and PAPHY in chloroform; 2-ml aliquots were transferred from each phase to 5-ml polythene vials for counting.

D was given directly as the ratio of the count in the organic phase to that in the aqueous phase.

Job's method of continuous variations

The variant of Job's method adapted for extractable species in a two-phase system[7] was used. The experimental procedure was essentially that used in the extraction studies. For each metal, ten 2-phase mixtures were prepared in which the sum of the molar concentrations of PAPHY and metal salt was constant but their ratio was varied as in the conventional Job method[8]. The volumes of both phases were equal and the pH of the aqueous solution was adjusted for maximum extraction. After equilibration, the absorbance of the chloroform extract was measured at λ_{max}.

DISTRIBUTION EQUILIBRIA

Pyridine-2-aldehyde-2′-pyridylhydrazone exists in aqueous solution as HL, H_2L^+, H_3L^{2+} and L^-. The pk values reported previously[9] and this spectrophotometric study show that protonation is significant only when the pH is less than 6. L^- is formed in significant amounts only in very strongly alkaline solution.

In the following treatment, the distribution equilibria are discussed in terms of the neutral PAPHY molecule (HL) coordinating as a terdentate ligand. Complexing between metal ions and anionic buffer components or hydroxyl ions will affect the extraction and additional terms must then be included in the distribution equations.

Metals of coordination number 6

Reaction with PAPHY (HL) proceeds according to:

$$M^{2+} + HL \xrightleftharpoons{\beta_1} M(HL)^{2+}$$

$$M^{2+} + 2\,HL \xrightleftharpoons{\beta_2} M(HL)_2^{2+}$$

$$\beta_1 = [M(HL)^{2+}]/[M^{2+}][HL] \tag{1}$$

$$\beta_2 = [M(HL)_2^{2+}]/[M^{2+}][HL]^2 \tag{2}$$

Step-wise deprotonation occurs according to:

$$M(HL)_2^{2+} \xrightleftharpoons{k_1} M(HL)L^+ + H^+$$

$$M(HL)L^+ \xrightleftharpoons{k_2} ML_2 + H^+$$

where

$$k_1 = [M(HL)L^+][H^+]/[M(HL)_2^{2+}] \tag{3}$$

$$k_2 = [ML_2][H^+]/[M(HL)L^+] \tag{4}$$

If insufficient ligand is present to form the bis-complex, deprotonation of $M(HL)^{2+}$ may take place.

$$M(HL)^{2+} \underset{}{\overset{k_3}{\rightleftharpoons}} ML^+ + H^+$$

where

$$k_3 = [ML^+][H^+]/[M(HL)^{2+}] \tag{5}$$

The neutral complex, ML_2, partitions according to

$$P_{ML_2} = [ML_2]_0/[ML_2] \tag{6}$$

and the ligand according to

$$P_{HL} = [HL]_0/[HL] \tag{7}$$

At the concentration of metal salt used, 10^{-5} *M* or below, it is assumed that no polynuclear species is formed.

Then

$$D = \frac{\Sigma[M]_0}{\Sigma[M]} = \frac{[ML_2]_0}{[M^{2+}]+[M(HL)^{2+}]+[ML^+]+[M(HL)_2{}^{2+}]+[M(HL)L^+]+[ML_2]} \tag{8}$$

Substituting eqns. (1)–(7) in eqn. (8):

$$D = \frac{P_{ML_2}k_1k_2\beta_2[HL]_0{}^2}{P_{HL}{}^2[H^+]^2\left\{1+\dfrac{\beta_1[HL]_0}{P_{HL}}+\dfrac{\beta_1k_3[HL]_0}{P_{HL}[H^+]}+\dfrac{\beta_2[HL]_0{}^2}{P_{HL}{}^2}+\dfrac{k_1\beta_2[HL]_0{}^2}{P_{HL}{}^2[H^+]}+\dfrac{k_1k_2\beta_2[HL]_0{}^2}{P_{HL}{}^2[H^+]^2}\right\}} \tag{9}$$

Considering, in turn, one species in the denominator of eqn. (8) to predominate in the aqueous phase, the relationship of D with $[HL]_0$ or $[H^+]$ can be seen. When M^{2+} predominates,

$$D = P_{ML_2}\cdot k_1k_2\beta_2[HL]_0{}^2/P_{HL}{}^2\cdot[H^+]^2 = K\cdot[HL]_0{}^2/[H^+]^2 \tag{10}$$

where K is an extraction constant. Separate plots of $\log_{10}D$ against $\log_{10}[HL]_0$ and against pH will be linear with a slope of 2.

When $M(HL)^{2+}$ predominates, $\log_{10}D$ will vary with $\log_{10}[HL]_0$ and $2\cdot$pH; for $M(HL)L^+$, $\log_{10}D$ will be independent of $[HL]_0$ and vary with pH; for ML_2, D reduces to P_{ML_2}.

Metals of coordination number 4

The formation of an extractable species, MLX, where X^- is a monovalent anion, can be represented by

$$ML^+ + X^- \rightleftharpoons MLX$$

Using $k_4 = [MLX]/[ML^+][X^-]$ and $P_{MLX} = [MLX]_0/[MLX]$

$$\begin{aligned} D &= [MLX]_0/\{[M^{2+}]+[M(HL)^{2+}]+[ML^+]+[MLX]\} \\ &= \frac{P_{MLX}\cdot k_3k_4[X^-]\beta_1[HL]_0}{[H^+]P_{HL}\left\{1+\dfrac{\beta_1[HL]_0}{P_{HL}}+\dfrac{k_3\beta_1[HL]_0}{P_{HL}[H^+]}+\dfrac{k_3k_4[X^-]\beta_1[HL]_0}{[H^+]P_{HL}}\right\}} \end{aligned} \tag{11}$$

When M^{2+} predominates in the aqueous phase and X^- is the conjugate base of the strong acid, HX, eqn. (11) reduces to

$$D = P_{MLX}\cdot k_3k_4[X^-]\beta_1[HL]_0/[H^+]P_{HL} \tag{12}$$

and plots of $\log_{10}D$ against $\log_{10}[HL]_0$ (at constant $[X^-]$ and pH), $\log_{10}[X^-]$ (at constant $[HL]_0$ and pH) and pH (at constant $[X^-]$ and $[HL]_0$) will all be linear and of slope 1.

When HX is a weak acid, $[X^-] = [HX]K_{HX}/[H^+]$

and

$$D = P_{MLX}k_3k_4\beta_1K_{HX}[HL]_0[HX]/[H^+]^2 \cdot P_{HL} \tag{13}$$

The plot of $\log_{10}D$ against pH (for constant [HX] and $[HL]_0$) will have a slope of 2.

RESULTS

Metals of coordination number 6

Nickel. Job plots show that a 1:2 complex is extracted at pH 7.45 from acetate solution. No simple whole number ratio of metal to ligand was found when phosphate buffer was used. The masking action of phosphate buffers near this pH has been noted before[10]. Other buffers, *e.g.* citrate and tartrate, were avoided for the same reason. It proved simplest to adjust the pH to the range 6.0–8.0 and maintain constant ionic strength by means of 0.1 *M* sodium acetate and perchloric acid solutions.

The plot of $\log_{10}D$ against pH (Fig. 1) has a slope of 2. The plot of $\log_{10}D$ against $\log_{10}[\mathrm{PAPHY}]_0$ (Fig. 2) at pH 7.51 has a slope of 2 for low concentrations of PAPHY. With increase in $[\mathrm{PAPHY}]_0$, the extraction increases and finally, becomes close to 100%, but the slope becomes less. The same trend is apparent for extraction at pH 6.55, but in this case a limiting value of 78% extraction is reached. For low values of $[\mathrm{PAPHY}]_0$, the metal is present in the aqueous phase as the hydrated ion. With increasing $[\mathrm{PAPHY}]_0$, more PAPHY partitions into the aqueous phase and successively $\mathrm{Ni(PAPHY)^{2+}}$ and $\mathrm{Ni(PAPHY)_2^{2+}}$ are formed. When all the metal is in the form of the bis-complex, further increase in $[\mathrm{PAPHY}]_0$ has no effect on *D*

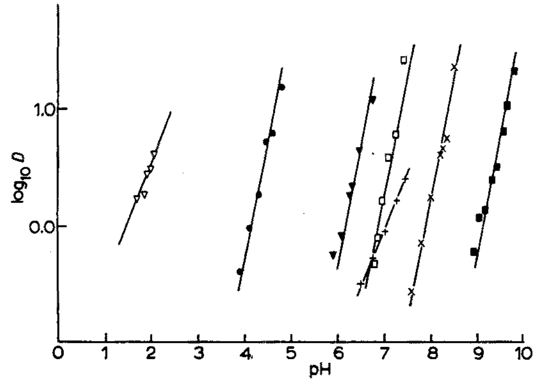

Fig. 1. ▽ Pd(II), 4 µg/ml, HCl/KCl solution; ● Fe(II), 0.5 µg/ml, acetate buffer; ▼ Ni(II), 1 µg/ml, acetate solution; □ Zn(II), 1 µg/ml, acetate solution; + Cu(II), 0.5 µg/ml, phosphate buffer; × Cd(II), 1 µg/ml, borate buffer; ■ Mn(II), 0.5 µg/ml, borate buffer. In the extraction of Mn(II), $2.5 \cdot 10^{-3}$ *M* PAPHY in chloroform was used; in all other cases, the concentration was $5 \cdot 10^{-4}$ *M*.

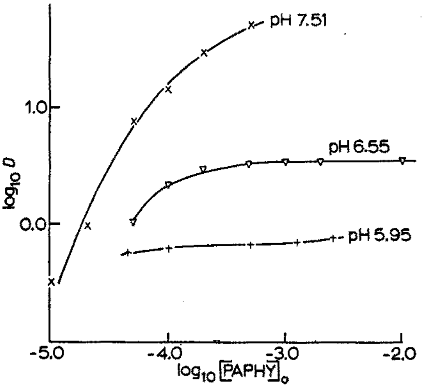

Fig. 2. Variation of $\log_{10}D$ with $\log_{10}[\mathrm{PAPHY}]_0$ for nickel(II) (1 µg/ml) extracted from acetate solutions.

and its magnitude is determined solely by the extent to which $Ni(PAPHY)_2^{2+}$ deprotonates, *i.e.* on the pH.

Zinc. Job plots show that a 1:2 complex is extracted at pH 7.45 from acetate solution. Again, when phosphate was present, no simple whole number molar ratio of metal to ligand was observed. Distribution behaviour studied spectrophotometrically confirms that zinc reacts with two molecules of PAPHY and two protons are released in forming the extractable species from acetate solution (Fig. 1). Although the results for Job plots when a phosphate buffer was used, were anomalous, distribution studies with ^{65}Zn show a similar variation of $\log_{10}D$ with $\log_{10}[PAPHY]_0$ (Fig. 3) to that observed with nickel in acetate solution.

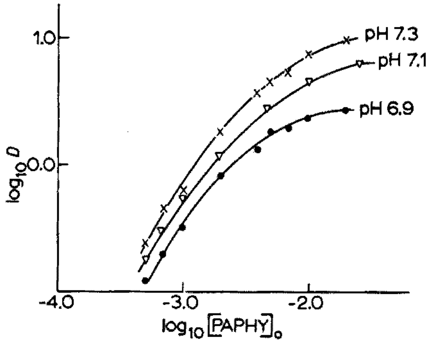

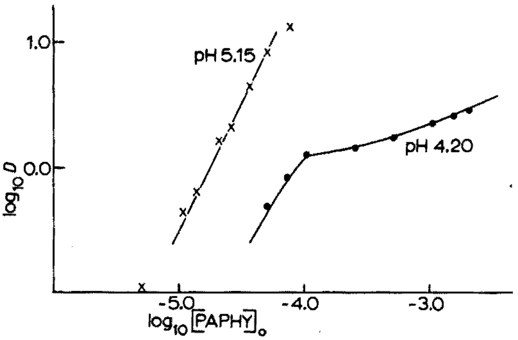

Fig. 3. Variation of $\log_{10}D$ with $\log_{10}[PAPHY]_0$ for $^{65}Zn(II)$ extracted from phosphate buffers.

Fig. 4. Variation of $\log_{10}D$ with $\log_{10}[PAPHY]_0$ for iron(II) (0.5 μg/ml) extracted from acetate buffers.

Cadmium. Job plots show that a 1:2 complex is extracted at pH 9.0 from borate solution. The plot of $\log_{10}D$ against pH has a slope of 2 (Fig. 1); against $\log_{10}[PAPHY]_0$, the slope of the plot is 2 at pH 8.40 (borate buffer), but approximates to 1 at pH 7.69 (phosphate buffer). This suggests that $Cd(PAPHY)^{2+}$ is the main ion present at the lower pH for the concentrations used.

Iron. Job plots show that a 1:2 complex is extracted at pH 5.15 from acetate solution. The plot of $\log_{10}D$ against pH has a slope of 2 (Fig. 1); against $\log_{10}[PAPHY]_0$, similar behaviour to that shown by nickel and zinc was found (Fig. 4) although for the range of concentrations studied, $\log_{10}D$ did not become completely independent of $\log_{10}[PAPHY]_0$ at pH 4.20.

Manganese. Job plots show that a 1:2 complex is extracted at pH 10.20. The spectrophotometric data show that $\log_{10}D$ varies with 2 $\log_{10}[PAPHY]_0$ at pH 10.15 and 9.14, and with 2 pH (Fig. 1).

For all these metals, eqn. (10) is obeyed for some experimental conditions. When $\log_{10}D = 0$, it becomes

$$\log_{10}K + 2\,\mathrm{pH} + 2\log_{10}[PAPHY]_0 = 0.$$

$\log_{10}K$ values calculated from this are given in Table I together with values for $\log_{10}k_2'$ where k_2' is the dissociation constant of $M(HL)L^+$ corrected to zero ionic strength (taken from GREEN *et al.*[9]).

The larger negative values for $\log_{10}K$ observed for the extraction of nickel and zinc from borate and phosphate buffers compared with those from acetate solution show that in the former cases, the formation of water-soluble complexes reduces the extraction. $\mathrm{Log}_{10}K$ values for the extraction of nickel, zinc and iron from acetate solution and cadmium from borate solution show a good linear correlation with Lions' $\log_{10}k_2'$ values (Fig. 5). This supports the assumption that the essential prerequisite for extraction is deprotonation to form ML_2 in the aqueous phase.

TABLE I

EXTRACTION CONSTANTS FOR METAL–PAPHY COMPLEXES

Metal	*pH*	*$\log_{10}K$*	*$\log_{10}k_2'$*
Ni	8.01	−6.82[b]	
	7.51	−5.60[a]	−8.50
Zn	8.20	−7.32[b]	
	7.3	−8.32[p]	
	6.97	−6.82[a]	−8.85
Fe	5.15	−0.78[a]	−6.57
Cd	8.4	−9.12[b]	−10.22
Mn	10.12	−13.74[b]	

[a] Acetate.
[b] Borate.
[p] Phosphate

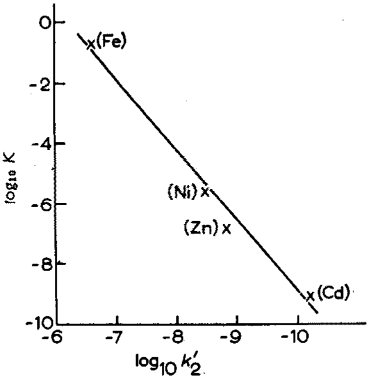

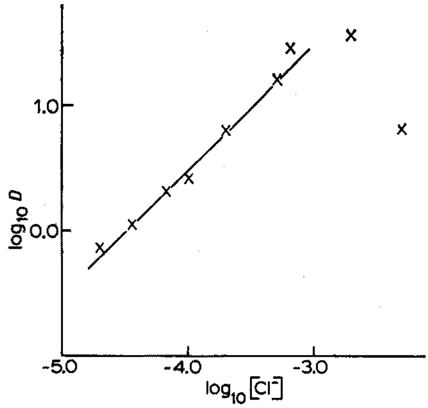

Fig. 5. Correlation of extraction constants ($\log_{10}K$) of Ni(II), Zn(II), Fe(II) and Cd(II) with $\log_{10}k_2'$ values[9].

Fig. 6. Variation of $\log_{10}D$ with $\log_{10}[Cl^-]$ for palladium(II) (4 µg/ml) extracted from acetate buffers at pH 4.02 by 10^{-3} M PAPHY in chloroform.

Metals of coordination number 4

Palladium. Plots of $\log_{10}D$ against $\log_{10}[\mathrm{PAPHY}]_0$ and pH have slopes of 1. For added chloride, the plot of $\log_{10}D$ against $\log_{10}[Cl^-]$ (Fig. 6) is initially linear with a slope of 1; increase in chloride concentration leads to a maximum for D and then a sharp decrease. The complex extracted is therefore Pd(PAPY)Cl; a complex of this composition is precipitated from aqueous solution at low pH[11]. At high chloride concentration, the competitive complexing with chloride ion reduces the amount of palladium extracted.

$$D = \Sigma[\mathrm{Pd}]_o/\Sigma[\mathrm{Pd}]$$

$$= \frac{[\mathrm{Pd(PAPY)Cl}_o]}{\{[\mathrm{Pd}^{2+}]+[\mathrm{Pd(PAPHY)}^{2+}]+[\mathrm{Pd(PAPY)}^{+}]+[\mathrm{Pd(PAPY)Cl}]+\sum_{1}^{n}[\mathrm{PdCl}_n{}^{2-n}]\}}$$

For low values of chloride and when palladium(II) predominates, this reduces to eqn. (12) where $\mathrm{MLX} = \mathrm{Pd(PAPY)Cl}$ and $\mathrm{X}^- = \mathrm{Cl}^-$.

A marked variation with pH was noted in the rate of attainment of distribution equilibrium. Below pH 4.2, the absorbance of the chloroform extract reached a maximum value in less than 10 min. It then decreased on shaking for longer periods, the metal being apparently back-extracted slowly into the aqueous phase. At higher pH values, the absorbance increased much more slowly with time of shaking; at pH 6.5, the absorbance reached a maximum value only after shaking for 2 h. This behaviour may be associated with slow hydrolysis of palladium chlorocomplexes but was not investigated further.

Copper. Job plots at pH 8.77, showed that λ_{max} for the chloroform extract varied with the metal:ligand ratio. With excess of ligand, λ_{max} was between 480 and 483 nm; with excess of metal, λ_{max} was at 510 nm. Job plots were made in the absence and presence of chloride ion in the aqueous phase. The results are shown in Figs. 7 and 8. In the presence of chloride ion and when excess of PAPHY is present, a bis-complex (λ_{max} 480 nm) predominates in the chlorofom extract; when excess of metal is present, a 1:1 complex (λ_{max} 510 nm) is formed as well. Analysis of the solid left after evaporation of the solvent showed that chlorine was present in the species extracted. Job plots of data on solutions without chloride ion show the bis-complex is dominant but the shift of λ_{max} to 510 nm for systems deficient in PAPHY shows that a 1:1 complex is also formed in these.

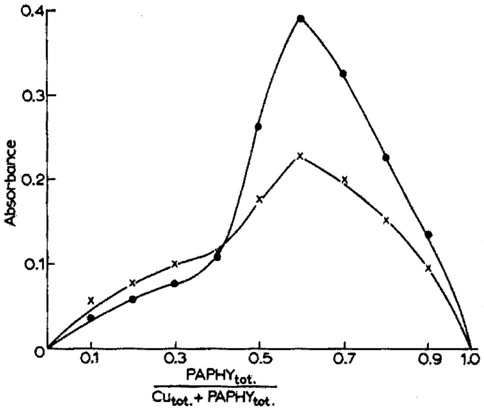

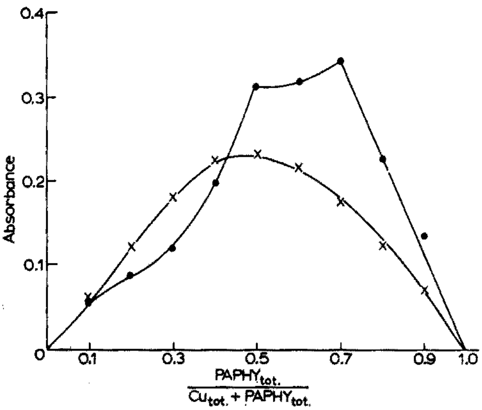

Fig. 7. Absorbance of chloroform extract as a function of the mole fraction of PAPHY in a chloride-free system. × 510 nm; ● 470 nm.

Fig. 8. Absorbance of chloroform extract as a function of the mole fraction of PAPHY with chloride added. × 510 nm; ● 470 nm.

The plot of $\log_{10}D$ against pH has a slope of 1; $\log_{10}D$ against $\log_{10}[\text{PAPHY}]_0$ is linear with slope close to 1 (0.9). In all distribution experiments, excess of PAPHY was present. The results indicate that a 1:1 complex is extracted and one proton is lost in the extraction.

Both mono- and bis-complexes of PAPHY with copper have already been reported[12]. Cu(PAPY)Cl has been made and its reaction with sodium hydroxide caused partial conversion to Cu(PAPY)OH. With no other ligand present, copper(II) reacts with two moles of PAPHY to form Cu(PAPHY)_2^{2+} which deprotonates to Cu(PAPY)_2 [5]. Cu(PAPY)OH is believed[6] to be formed in the potentiometric titration of Cu/PAPHY mixtures in dioxane/water.

The extraction of an analogous complex, Cu(PAN)OH, has been suggested[1] from a study of the distribution of copper(II) between aqueous solutions and PAN in carbon tetrachloride. As the authors noted, it is difficult to reconcile this formulation with the observed dependence of $\log_{10}D$ on pH (instead of 2·pH); this dependence was attributed to the unusually large value of the stability constant of the mono-complex. NAVRÁTIL[2], in his work on the copper complex of 1-(thiazolylazo)-2-naphthol, commented that neither he nor BETTERIDGE *et al.*[1] had used the complete range of concentrations possible for studying the dependence of *D* on pH.

In the case of Cu(PAPHY)^{2+}, the complex is again very stable and a readily ionised hydrogen is involved ($\log_{10}\beta_1 = 11.6$, $pk_1' = 5.96$[9]); Cu(PAPY)^+ is undoubtedly formed in weakly acidic solutions. Since it was established that chloride ion, when present, is co-extracted, it appears from distribution studies that the species extracted is Cu(PAPY)X where X^- is Cl^-, ClO_4^- or some other anion of a strong acid. When excess of PAPHY is present in the organic phase, the mono-complex is converted to the bis-complex and it is the absorbance of this which is measured in the distribution experiments.

CONCLUSIONS

The values given for the extinction coefficients in Table II show that PAPHY is a highly sensitive reagent for several metals. Comparison with the extinction coefficients for aqueous solutions of metal–PAPHY complexes[13] shows the significant increase in sensitivity obtained by measuring the absorbance after the extraction of the coloured complex into chloroform. The chief disadvantage is that most of the neutral complexes studied have their wavelengths of maximum absorbance at *ca.* 470 nm, so that it is not possible to identify the extracted metal by measuring

TABLE II

MOLAR ABSORBANCES OF BIS-PAPHY COMPLEXES IN CHLOROFORM SOLUTION

Metal	ε_{max} ($\cdot 10^{-4}$)	λ_{max} (nm)	*Metal*	ε_{max} ($\cdot 10^{-4}$)	λ_{max} (nm)
Zn	7.06	470	Ni	3.38	470
Cd	7.98	470	Mn	5.71	470
Fe	5.00	405	Pd	1.56	560
Cu	6.28	480			

the absorption spectrum. However, the extracted complexes of iron and palladium have wavelengths of maximum absorbance characteristic of the metal concerned.

The extraction behaviour of PAPHY complexes follows the same pattern as that observed in familiar systems involving 8-hydroxyquinoline and PAN[14]. Plots of percentage extraction against pH are typically sigmoid, extraction being low at low pH and rising rapidly to virtually 100% as the pH is increased. There is then usually a range of pH within which extraction is complete, but a further increase in pH reduces the extent of extraction due to the formation of water-soluble complexes.

PAPHY is a more selective reagent than 8-hydroxyquinoline or other bidentate ligands. Only when the bis-complexes of PAPHY with divalent metals are fully deprotonated are zero-charged extractable species formed; deprotonated bis-complexes with trivalent metals are cationic and will not be extracted (it is conceivable that $M(III)(PAPY)_2^+$ could form part of an extractable ion-pair but this was not observed for the Co(III) complex). In the complexes of 8-hydroxyquinoline, it is often found that the coordination number of the metal ion and its charge are simultaneously satisfied with the result that extractable complexes are formed for divalent and trivalent metals.

The imino-hydrogen in PAPHY is so feebly acidic that complex formation in the aqueous phase except at very high pH values must be between metal ions and PAPHY molecules to form complex cations. The deprotonation of these determines the degree of formation of an uncharged species and hence D. Complexing of the metal in the aqueous phase may, in some circumstances, be complete (for example, when the concentration of PAPHY in the organic phase is high) but not all of it can be extracted because the pH is not high enough to complete the deprotonation.

For two metals present at the same concentration in the aqueous phase, the ratio of extraction constants must be greater than 10^4 for quantitative separation[14]. Figure 1 shows that iron(II) can be quantitatively separated from the other metal ions listed provided that a suitable buffer is chosen.

The low $pH_{\frac{1}{2}}$ value for palladium(II) reflects the high stability and marked acidity of the mono-PAPHY complex. Provided that there is another ligand present which can occupy the fourth coordination position and produce an uncharged complex, PAPHY is a very selective reagent for the extractive analysis of palladium. Since this work was completed, CAMERON AND GIBSON[15] have reported that potassium tetrachloropalladate(II) in aqueous solution at pH 3.1 reacts with PAPHY to give a complex of composition Pd(PAPY)Cl. These authors describe a procedure for palladium which exploits the extraction of this complex into *o*-dichlorobenzene.

The work carried out so far on palladium and copper illustrates how the extraction of a ternary complex depends on the nature of the second ligand and points the way to one means of improving selectivity in extraction procedures using a terdentate ligand.

We wish gratefully to acknowledge the help of B.D.H. Limited, Poole, England, in supporting this work by a financial grant.

SUMMARY

The distribution behaviour of the complexes formed between the terdentate ligand, pyridine-2-aldehyde-2′-pyridylhydrazone, and Zn(II), Cd(II), Fe(II), Cu(II), Ni(II), Mn(II) and Pd(II) has been studied between aqueous buffer and chloroform. Results are interpreted in terms of the complexes in the aqueous solution and the loss of a proton from each coordinated ligand to form an uncharged, extractable species. The suitability of PAPHY as a spectrophotometric reagent used in conjunction with a solvent extraction procedure is discussed.

RÉSUMÉ

On a examiné le partage des complexes formés entre pyridine-2-aldéhyde-2′-pyridylhydrazone ("terdentate ligand") et les métaux: Zn(II), Cd(II), Fe(II), Cu(II), Ni(II), Mn(II) et Pd(II) en milieu eau tampon–chloroforme. Les résultats sont exprimés en complexes dans la solution aqueuse et la perte d'un proton de chaque ligand coordiné pour former une particule non chargée extractible. On envisage la possibilité d'utiliser ce réactif (PAPHY) comme réactif spectrophotométrique avec extraction dans un solvant.

ZUSAMMENFASSUNG

Das Verteilungsverhalten der Komplexe zwischen dem 3-zähnigen Liganden Pyridin-2-aldehyd-2′-pyridylhydrazon (PAPHY) und Zn(II), Cd(II), Fe(II), Cu(II), Ni(II), Mn(II) und Pd(II) zwischen einem wässrigen Puffer und Chloroform wurde untersucht. Die Ergebnisse wurden interpretiert als Funktion der Komplexe in der wässrigen Lösung und des Verlustes eines Protons von jedem koordinierten Liganden, um ein ungeladenes, extrahierbares Teilchen zu bilden. Die Eignung von PAPHY als spektralphotometrisches Reagenz in Verbindung mit einer Flüssigextraktion wird diskutiert.

REFERENCES

1 D. Betteridge, Q. Fernando and H. Freiser, *Anal. Chem.*, 35 (1963) 294.
2 O. Navrátil, *Collection Czech. Chem. Commun.*, 29 (1964) 2490.
3 F. Lions and K. V. Martin, *J. Am. Chem. Soc.*, 80 (1958) 3858.
4 J. F. Geldard and F. Lions, *J. Am. Chem. Soc.*, 84 (1962) 2262.
5 J. F. Geldard and F. Lions, *Inorg. Chem.*, 2 (1963) 270.
6 M. L. Heit and D. E. Ryan, *Anal. Chim. Acta*, 32 (1965) 448.
7 H. Irving and T. B. Pierce, *J. Chem. Soc.*, (1959) 2565.
8 P. Job, *Ann. Chim. (Paris)*, 9 (1928) 113.
9 R. W. Green, P. S. Hallman and F. Lions, *Inorg. Chem.*, 3 (1964) 376.
10 J. Fresco and H. Freiser, *Anal. Chem.*, 36 (1964) 631.
11 C. F. Bell and D. R. Rose, *Talanta*, 12 (1965) 696.
12 J. F. Geldard and F. Lions, *Inorg. Chem.*, 4 (1965) 414.
13 A. J. Cameron, N. A. Gibson and R. Roper, *Anal. Chim. Acta*, 29 (1963) 73.
14 G. K. Schweitzer, *Anal. Chim. Acta*, 30 (1964) 68.
J. Starý, *The Solvent Extraction of Metal Chelates*, Pergamon Press, Oxford, 1964, p. 18.
15 A. J. Cameron and N. A. Gibson, *Anal. Chim. Acta*, 40 (1968) 413.

Analytica Chimica Acta
Elsevier Publishing Company, Amsterdam
Printed in The Netherlands

COMPUTER TECHNIQUES FOR THREE-DIMENSIONAL ANALYSIS IN ATOMIC-ABSORPTION FLAME PHOTOMETRY*

J. L. MALAKOFF, J. RAMÍREZ-MUÑOZ AND W. Z. SCOTT
Beckman Instruments, Inc., 2500 Harbor Boulevard, Fullerton, Calif. (U.S.A.)

(Received March 20th, 1968)

A first approach to the application of computer techniques to the field of atomic-absorption flame photometry has recently been published[1]. All computer procedures referred to previously[1] leading to the preparation of automatic plots of analytical results, were confined to *two-variable systems, i.e.*, to chemical-instrumental systems in which all variables (composition variables and parameters) were fixed in order to be able to measure the values of one variable as a function of the values of another. Two-dimensional plots were obtained for calibration curves and flame profiles.

It is now shown that composite three-dimensional graphs can be plotted by the introduction of a third variable. The three-dimensional representation not only gives a complete picture of the phenomenon studied at increasing values of the two independent variables, but also helps to choose particular situations of instrumental settings for best performance. Of particular interest is:

Appropriate value of the free variable to attain *maximum sensitivity* for a particular concentration or set of concentrations.

Appropriate value of the free variable to attain a *linear response*, even if under these circumstances the maximum sensitivity is not achieved. The obtaining of a linear response is imperative if mono-addition or multi-addition techniques are to be used in the evaluation of concentrations in unknown solutions.

The computer techniques used to represent and to study some typical cases are described, and some examples of three-dimensional representation are included.

Variations of absorbance are studied as a function of analyte concentration and a second independent variable. For example, the second independent variable becomes height of selection zone, concentration of interfering components, feed rate, slit width, or pressure of combustion gases. A three-dimensional Cartesian representation of the experimental space would have absorbance readings along the X-axis, analyte concentration along the Z-axis, and the various independent variables along the Y-axis. The following standard notation will be used for most of the experiments described:

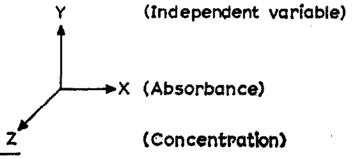

---

* Presented at the 18th Pittsburgh Conference on Analytical Chemistry and Applied Spectroscopy, March 1967.

The ability to process large volumes of data, to perform curve fitting and smoothing manipulations of the data, and to allow the experimenter to coordinate the effects of these manipulations, requires the techniques of graphical data processing. A system involving a cathode-ray tube display scope on-line to a digital computer is utilized in this work.

An IBM 2250 remote scope was used on-line to an IBM 360/Mod 40 computer. This allows direct communication with the computer as various decisions are based on the graphic display of the results on the scope. It is possible to delete data points, restore data points, fit smooth curves to the data, rotate and adjust the three-dimensional axes, look at multiple sets of data, etc. For permanent recording of any display on the scope, the CalComp Digital Plotter is utilized. Since the computer operates in a multi-processing environment, the scope operation occurs simultaneously with normal scientific and commercial data processing.

EXPERIMENTAL

Instrumentation

The following instruments were used:

For computer and plotting techniques. (*a*) IBM 360, Model 40, 256K, three-disk, six-tape system. In the previous paper[1] an IBM 1410, 40K, six-tape system was used. (*b*) CalComp Digital Plotter, Model 565, off-line via CalComp Model 470 tape system. (*c*) IBM 2250 Model I Remote Display Scope.

For flame photometry techniques. Beckman Model 979 atomic-absorption spectrophotometer equipped with a 10-in Beckman potentiometer recorder and used with a Beckman laminar flow burner (air–acetylene flame), a Beckman laminar flow burner (nitrous oxide–acetylene flame), and a Techtron laminar flow burner (air–acetylene flame).

Operating conditions for each of the analytes mentioned in this paper have been described in *Flame Notes**.

Solutions

Sample solutions. These were prepared with distilled water, background solution (acid solutions, solutions containing releasers) or organic solvents.

Standard solutions. Solutions were obtained by dilution of stock solutions with distilled water, background solution or organic solvents.

Blanks were prepared according to the solvent utilized for samples and standards.

Analytical systems studied

The three-dimensional analysis was applied to the correlation of:

(1) Absorbance (The instruments are prepared to read per cent absorption, thus the per cent absorption values are transformed into absorbance values.)

(2) Concentration (Analyte concentration in the solutions aspirated by the instrument.)

(3) Another variable parameter, which is chosen as required.

Some examples that were studied are shown in Table I.

---

* Obtainable from Beckman Instruments, Inc., Fullerton, Calif. 92634, U.S.A.

TABLE I

ANALYTICAL SYSTEMS STUDIED

Case	*Z Variable*[a]	*X Variable*[b]	*Y Variable*
1	Analyte concentration	Absorbance	Height of the burner
2	Analyte concentration	Absorbance	Slit width
3	Analyte concentration	Absorbance	Fuel gas pressure
4	Analyte concentration	Absorbance	Support gas pressure
5	Analyte concentration	Absorbance	Interfering component concentration
6	Analyte concentration	Absorbance	Interference ratio
7	Analyte concentration	Noise level	Height of the burner
8	Analyte concentration	Fluctuational concentration limit (p.p.m.)[2]	Height of the burner
9	Analyte concentration	Percentual concentration limit (p.p.m.)[2]	Height of the burner
10	Fuel pressure	Absorbance[c]	Interfering component concentration
11	Fuel pressure	Absorbance[c]	Interference ratio
12	Analyte concentration	Absorbance[c]	Addition concentration (releaser, protector, counter-ionization agent)
13	Analyte concentration	Absorbance[c]	Feed rate

[a] Fixed variable.
[b] Variable calculated from the instrument readings.
[c] Absorbance at fixed concentration of the analyte.

CASE STUDIES

Flame profiles (Case 1)

Flame profiles have been widely used in atomic absorption for the study of analyte atom distribution along the flame at different conditions: different flames with the same burner (lean, rich flames), influence of acids, influence of releasers, influence of concomitant interfering metallic elements, comparisons of flames of different nature (air–acetylene and nitrous oxide–acetylene flames), comparison of different burners (turbulent and laminar flow burners), and even comparison of the position of the emitting and absorbing zones for the same analyte in the same flame[1].

The three-dimensional plot makes it possible to study the complete picture of the atom distribution at the necessary concentrations to cover most of the reading scale (depending upon the analyte's percentual sensitivity). The position of the maxima of percentual sensitivity for best response can be determined under given instrumental parameters, and a useful guide for linearity tests at different heights is also possible. The three-dimensional plot has also made it possible to explain the behavior of analytes generating concave, curved calibration graphs when other authors reported convex calibration graphs, or *vice versa*. In some cases, clear transition points of sharp linearity have been found.

Optimization curves (Cases 2, 3 and 4)

In these cases, the variations of readings (actually the corresponding absorbance values) according to the variation of an instrumental parameter (slit width or pressure of the gases) are followed at given analyte concentrations. By looking at the maxima of the curves (and in some cases, the maximum of the surface), it is possible to determine the optimization parameters.

Interference curves (Cases 5 and 6)

The interferences can be referred to as either absolute concentration of the interfering component or relative concentration. (The interference ratio equals concentration of the interfering component divided by concentration of the analyte.) The three-dimensional plot gives the general variation of the absorbance values along the analyte concentration range. Asymptotic curves or surfaces indicate saturation values which are very useful in deciding the magnitude of buffering in buffer addition techniques.

Sensitivity curves (Cases 7, 8 and 9)

It is interesting (Case 7) to study the variation of noise level (peak-to-peak noise) at different heights over the chosen analyte concentration range. This type of plotting also allows representation of the variation of the concentration limits (fluctuational and percentual) under the same conditions, which will give an idea of the variation of the fluctuational and percentual sensitivity[2] respectively, with height and concentration. The plot effectively substitutes a clear picture for long and tiring tables of numerical values.

Fuel gas curves (Cases 10 and 11)

The magnitude of the interference effects for a given analyte concentration will depend on the concentration of the interfering component (an absolute or relative concentration or an interference ratio) and on the flame conditions. Flame conditions can be varied by varying the fuel gas pressure.

Counter-interference curves (Case 12)

The plots make it possible to watch the results obtained when the concentration of counter-interferences are changed. At a given analyte concentration, the results represent those for the interference ratio (interfering component at constant concentration).

Feed rate curves (Case 13)

This is a derivation of Case 4, if the variation of support gas pressure does change the feed rate (sample solution intake).

Other cases

Many other cases might be included, for there are many different combinations possible from the variables involved in the multi-variable system which atomic absorption represents. Among them, variation of lamp current has also been studied in a similar way as Cases 2, 3 and 4.

COMPUTER RESULTS

The following graphs were taken from the scope and generated on the plotter.

Each represents a surface generated from the experimental input data by the engineer on the scope. The flame profile graphs have burner elevation on the Y-axis, absorbance on the X-axis and element concentration on the Z-axis.

Figure 1 shows a flame profile of iron evaluated in a methyl isobutyl ketone system, plus ethanol. The axes are in their standard positions. Figure 2 represents the same system as shown in Fig. 1, except that the axes are now removed from the surface area and the plot has been rotated; actually the Z-axis has been rotated counter-clockwise. Figure 3 again represents the same system, but this time, it varies from Fig. 2 by the elongation of the Y-axis. Figure 4 shows the same system, but differs from Fig. 3 by the rotation of the Z-axis clockwise.

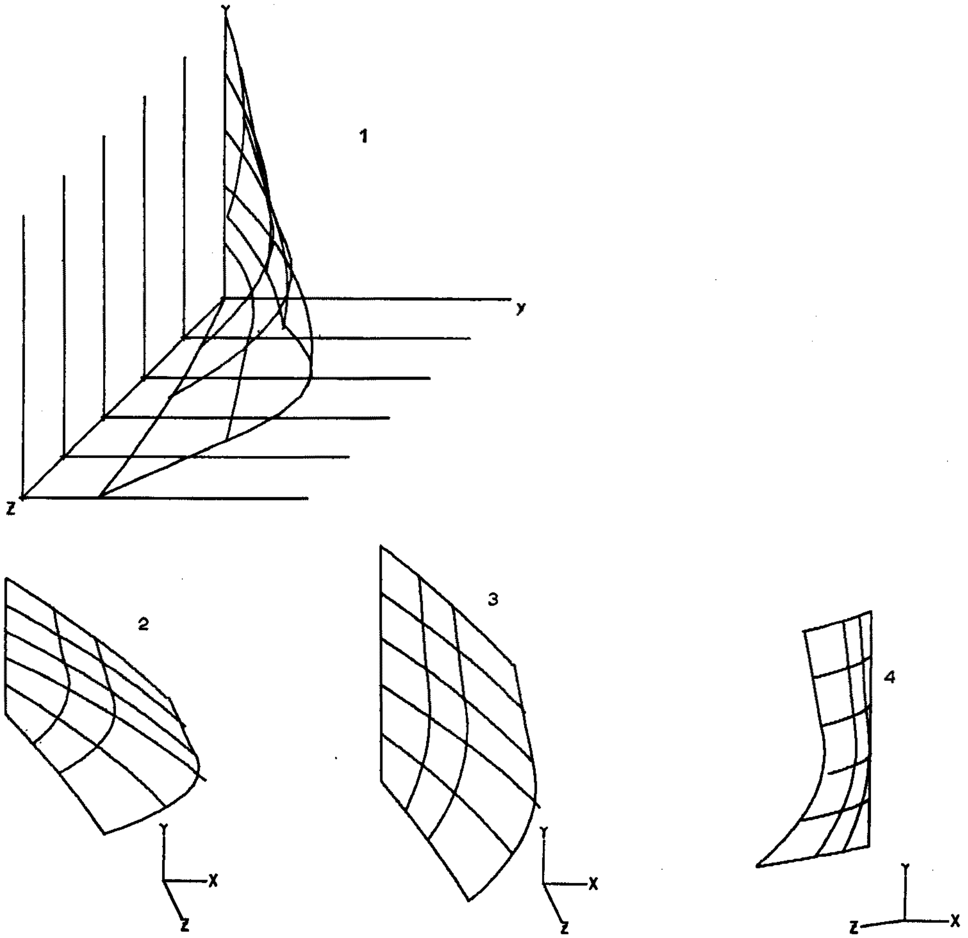

Figs. 1–4. Iron. Normal flame profile. Methyl isobutyl ketone system plus ethanol. (X) absorbance. (Y) burner elevation (inches). (Z) concentration (p.p.m.).

The remaining graphs are each of a different system, as described below. The particular display on the scope for a good view of each individual surface varies as shown in each figure.

Figure 5 shows a flame profile of iron in a methyl isobutyl ketone system without ethanol. A flame profile of rhodium is shown in Fig. 6. Figure 7 shows lamp current variations plotted against absorbance and concentration of europium. Figure 8 shows feed rate variations plotted against absorbance and concentration

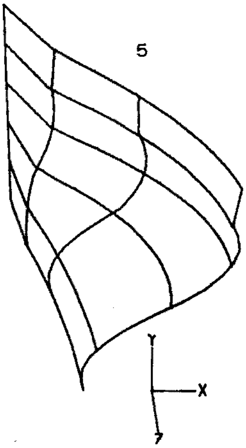

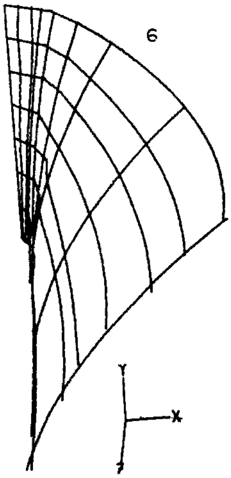

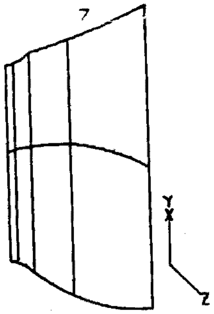

Fig. 5. Iron. Normal flame profile. Methyl isobutyl ketone system without ethanol. X,Y,Z as in Fig. 1.

Fig. 6. Rhodium. Normal flame profile. X,Y,Z as in Fig. 1.

Fig. 7. Europium. Lamp current variations. (X) absorbance. (Y) lamp current (mA). (Z) concentration (p.p.m.).

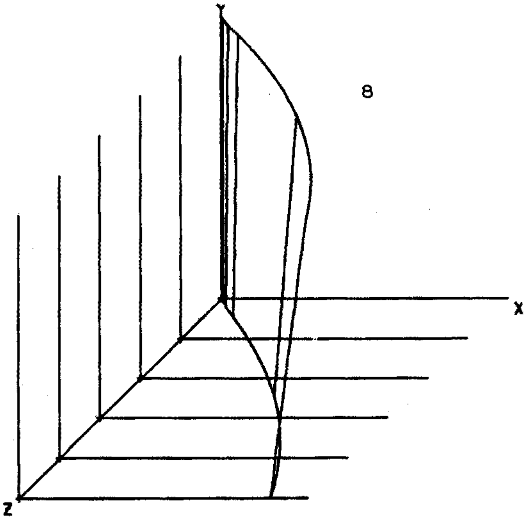

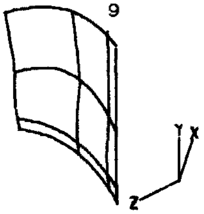

Fig. 8. Titanium. Feed rate variations. (X) absorbance. (Y) feed rate (ml/min). (Z) concentration (p.p.m.).

Fig. 9. Neodymium. Slit width variations. (X) absorbance. (Y) slit width (mm). (Z) concentration (p.p.m.).

of titanium. Figure 9 shows slit-width variations *versus* absorbance and concentration of neodymium.

While these are not all the systems mentioned, they are good examples of some typical cases.

CONCLUSION

Flame methods in atomic-absorption work can be augmented and enhanced by computer techniques for data reduction and mathematical analysis. Three-dimensional graphic display (on the scope and the plotter) of experimental results allows for both a realistic and comprehensive approach to atomic-absorption analysis. The quickly established results are reliable, easily interpreted and extremely useful. These procedures have and will continue to widen our insight into flame methods in atomic-absorption analysis, and have the advantage that creative experimentation is not hindered by routine data reduction chores.

SUMMARY

Flame methods, specifically in atomic-absorption work, have been augmented and enhanced by computer techniques for data reduction and mathematical analysis. Three-dimensional graphic display of experimental results allows for both a realistic and comprehensive approach to atomic-absorption analysis. The computer procedures and the mathematical techniques are described. Their coordination establishes quick, reliable, easily interpreted and useful results. The various equipment used is also described. The use of the remote scope (basically a cathode-ray tube) for immediate on-line display of three-dimensional data representation is explored. Several typical problems and their resulting solutions are presented in detail. Variations of absorbance are studied as a function of analyte concentration and a second variable: height of selection zone, concentration of interferent components, feed rate, slit width, or pressure of combustion gases. Variations of absorbance values are closely related to variations of percentual sensitivity.

ZUSAMMENFASSUNG

Die Flammenmethoden, besonders bei der Flammenabsorptionsanalyse wurden vermehrt und verbessert durch Anwendung einer Computertechnik zur Verminderung der Daten und mathematischen Analyse. Dreidimensionale graphische Darstellungen der experimentellen Ergebnisse gestatten sowohl eine realistische als auch umfassende Näherung. Das Computer-Verfahren und die mathematischen Techniken werden beschreiben. Ihre Zusammenfassung ermöglicht schnelle, zuverlässige, leicht zu interpretierende und brauchbare Ergebnisse. Die verschiedenen Anordnungen, die verwendet wurden, werden ebenfalls beschrieben. Verschiedene typische Probleme und ihre Ergebnisse werden im einzelnen angegeben.

RÉSUMÉ

Des méthodes de photométrie de flamme, en particulier pour l'absorption atomique ont été développées en utilisant des techniques "computer" pour la réduction des valeurs et l'analyse mathématique, avec graphique tridimensionnel. On décrit procédés "computer" et techniques mathématiques. Leur coordination fournit des résultats rapides, sûrs, faciles à interpréter et utiles. On décrit également les divers équipements. Plusieurs problèmes typiques et leurs solutions sont présentés en détail.

REFERENCES

1 J. Ramírez-Muñoz, J. L. Malakoff and C. P. Aime, *Anal. Chim. Acta*, 36 (1966) 328.
2 J. Ramírez-Muñoz, *Talanta*, 13 (1966) 87.

Anal. Chim. Acta, 42 (1968) 515–522

Analytica Chimica Acta
Elsevier Publishing Company, Amsterdam
Printed in The Netherlands

SOME INTERFERENCE EFFECTS OCCURRING IN THE HYDROGEN/ARGON/ENTRAINED-AIR FLAME

R. SMITH, C. M. STAFFORD AND J. D. WINEFORDNER
Department of Chemistry, University of Florida, Gainesville, Fla. 32601 (U.S.A.)

(Received April 5th, 1968)

Several authors have recently examined the so-called "cool" flames with respect to their use in flame methods of analysis. These flames are usually hydrogen/oxygen or hydrogen/entrained-air flames in which the combustible gas is diluted with an inert gas such as nitrogen or argon. ZACHA AND WINEFORDNER[1] have used the hydrogen/argon/entrained-air (H_2/A) flame in the flame emission determination of 14 elements and have obtained limits of detection which were better than, or as good as, those obtained with a hydrogen/oxygen flame (H_2/O_2). The results were attributed to the low background noise associated with the H_2/A flame and also to possible chemiluminescence with certain elements. DAGNALL *et al.*[2] have used a hydrogen flame diluted with nitrogen to observe the molecular band emission of S_2 in a determination of sulphur. ALKEMADE[3] has made quantum efficiency measurements of the atomic fluorescence of sodium in hydrogen flames and has found that deactivation of the excited sodium atoms is very much reduced when argon is mixed with the flame gases. As a result, the H_2/A flame has been used considerably in atomic fluorescence spectrometry and is probably the most suitable type of flame for general use with this technique. Background emission in the ultraviolet and visible is almost exclusively restricted to the wavelength range 2800–3500 Å and the background noise is considerably lower than that of a H_2/O_2 flame[1] over a wide range of wavelengths.

Temperature measurements[4] on hydrogen/argon/oxygen laminar flames indicate flame temperatures of the order of 1850°K (gas flows were H_2 1.72 l min^{-1}, O_2 0.50 l min^{-1}, A 3.45 l min^{-1}), and it is very possible that the thermal temperature of the H_2/A flame is of this order. DE GALAN AND WINEFORDNER[5] have measured the rotational, vibrational, and electronic temperatures of several turbulent flames; however, their results chiefly indicate the lack of thermal equilibrium in the H_2/A flame, and the thermal temperature of this flame must not be assumed from their results. They suggested a possible flame temperature of 2100°K. The potential usefulness of the H_2/A and other "cool" flames in analytical chemistry has prompted the study of the interelement effects reported here. The significant differences between these flames and typical flames currently used in analysis also justify such an investigation.

In this study, we have examined the interference of several anionic and cationic species on the flame emission from calcium, measured at the 4227 Å resonance line. The interferences were measured at various heights in the flame and comparisons were made with the H_2/O_2 turbulent flame. Calcium was chosen as a suitable element for this investigation for several reasons:

(*a*) The interference effects for calcium determinations in other flames are well documented in the literature and their mechanisms are fairly well understood. Therefore, comparisons and generalizations are much easier to make.

(*b*) The results of this investigation are almost certainly applicable to the determination of calcium by atomic absorption and atomic fluorescence because measurements were carried out at the calcium resonance line.

(*c*) The study of equilibrium in turbulent flames[5] indicated that chemiluminescence effects would be low for elements (*e.g.* calcium) having comparatively low ionization potentials. Flame emission measurements[1] also indicated that calcium does not exhibit significant chemiluminescence in the H_2/A flame. Therefore, the types of interference can be characterized more easily in the absence of chemiluminescence effects which may complicate the interpretation of the results.

EXPERIMENTAL

Apparatus

A versatile flame spectrometer was constructed which was capable of use for flame emission, atomic absorption, or atomic fluorescence in conjunction with either AC or DC amplification systems. A Czerny-Turner monochromator, described elsewhere[1], was used in conjunction with a 1.5-in diameter lens of 4 in focal length situated at a distance of 8 in from the flame and the entrance slit. The entrance slit of the monochromator was fitted with an optical stop which restricted the field of view to a section of the flame 3–4 mm in height. This was essential for the interference/height studies described below. The detector system consisted of an RCA 1P28 photomultiplier operated at 650 V together with an Aminco electrometer[6] and a Sargent recorder[1] used without damping.

A Beckman, medium-bore, total-consumption aspirator burner was mounted on a calibrated carrier with vertical travel which could be used to raise or lower the burner over a range of 130 mm with an accuracy of ± 0.5 mm or better. The position on the scale which corresponded to zero height above the burner tip was found by removing the focussing lens and the monochromator cover, and directing the beam of a low powered gas laser through the restricted entrance slit, such that an image of the beam appeared in the center of the back mirror of the monochromator. This ensured the laser beam was horizontal. The burner jack was then raised until the tip of the burner just entered the very narrow (*ca.* 1 mm) laser beam. Repeated determinations in this manner gave the location of the zero height to within 1 mm.

Procedure

Varying molar excesses of foreign ions were investigated with respect to their effect on the emission intensity of 10^{-4} M (4 p.p.m. Ca) calcium chloride solution. The signal was measured at the calcium resonance line 4227 Å in order that the results might have some significance for atomic fluorescence as well as flame emission spectrometry. Slit widths of 0.25 mm were used for the H_2/A flame and 0.10 mm for the H_2/O_2 flame. Flow rates for the flame gas constituents were: H_2 6.2 l min^{-1}, A 3.0 l min^{-1} for the H_2/A flame; and H_2 6.2 l min^{-1}, O_2 3.0 l min^{-1} for the hydrogen/oxygen flame. These were not necessarily the optimum flow rates for the calcium determination, but were chosen to give a flame of convenient size for the interference/

height studies. The overall height of the luminous portion of the H_2/A flame was 130 mm, that of the H_2/O_2 flame was 100 mm.

Calcium stock solutions were made up from calcium carbonate dissolved in dilute hydrochloric acid, evaporated to dryness, and made up to volume with deionized, distilled water. Interferent stock solutions were made up directly from metal chlorides (RbCl, NaCl, and CsCl), sodium salts (NaH_2PO_4, $Na_2H_2P_2O_7$, NaF, NaBr, NaI, Na acetate, Na oxalate, Na_2H_2EDTA and $NaClO_4$) or free acids (citric, tartaric, hydrochloric, sulphuric, and nitric).

RESULTS AND DISCUSSION

In any interference study of this nature, the choice of standard always presents some difficulty. In the past, many apparent inconsistencies in the interference results quoted by different authors can be traced to the fact that different compounds were used as the reference standard. Calcium chloride was chosen as the reference standard for this investigation, mainly because of its widespread use in earlier studies for interference effects in other types of flame. Calcium chloride was also a convenient reference standard in that there was no additional interference caused by excesses of chloride (as HCl), nor was there any interference from sodium (as NaCl). Therefore, any measured interference was entirely due to the other cation or anion which was added. The choice of foreign cations and anions made for this study was based upon the characteristic interference effects of these species on the emission of calcium in other flames.

Ionization interferences

If there is any significant concentration of ionized calcium atoms existing in the flame, the addition of an element having a lower ionization potential will reduce the concentration of calcium ions present. Consequently, there will be an increase in the concentration of calcium atoms and a corresponding increase in the measured signal. Addition of up to five-fold molar excesses of sodium chloride and cesium chloride resulted in no enhancement of the calcium emission at any height in either the H_2/A or H_2/O_2 flames. The absence of detectable ionization effects can be attributed to two sources:

(*a*) There is only a small concentration of ionized calcium in the H_2/A flame. No signal could be detected in the 3934 Å region which is characteristic of Ca^+ emission. However, some emission due to Ca^+ was observed in the H_2/O_2 flame.

(*b*) The lack of equilibrium conditions existing in the turbulent flames[5] used, would also minimize any effect of alkali metal ionization on the calcium ion population.

Spectral interferences

Rubidium gave rise to a spectral interference (Fig. 3) on the calcium emission at 4227 Å, with our monochromator, because of the existence of low intensity rubidium resonance lines at 4202 Å and 4216 Å. The interference due to rubidium was about 50% less in the H_2/O_2 flame than in the cooler H_2/A flame. For both flames, the degree of interference increased with height in the flame, but this effect was most marked for the H_2/A flame.

The degree of interference of rubidium in the two flames is a complex relationship depending on the relative emission of calcium and rubidium with flame temperature. However, the most important factor in the comparison is the relative concentrations of free calcium atoms in the two flames. In the H_2/O_2 flame, the ratio of the Ca 4227 Å atom line to the CaOH 5541 Å molecular band is approximately 3 times greater than in the H_2/A flame. In other words, the calcium atom/calcium hydroxide or oxide *ratio* is critically dependent on flame temperature and hence spectral interferences such as rubidium have the greatest influence in the cool H_2/A flame. Furthermore, the existence of a higher population of rubidium ions in the H_2/O_2 flame will also tend to reduce this particular spectral interference. A more complex spectral interference could be expected from the strontium ion line at 4216 Å.

Interferences associated with compound formation

When total consumption aspirator burners are used in flame spectrometry, it is very difficult to distinguish between interferences caused by formation of refractory compounds and interferences caused by involatile compounds. In the former instance, the interference is due to slow or incomplete dissociation of the metal compound in the gas phase (*i.e.*, a chemical process), whereas the latter type of interference refers to the physical change involved in volatilization. Invariably, the two processes occur together, and can only be distinguished under more controlled conditions, such as when laminar flames are used.

In nearly all cases of compound formation interference, the degree of interference decreased with height of measurement in the flame, as a result of the kinetically controlled vaporization or dissociation. With laminar flames, thermodynamic equilibrium considerations will be expected to become important. The effects of the anions examined are discussed below in various groups.

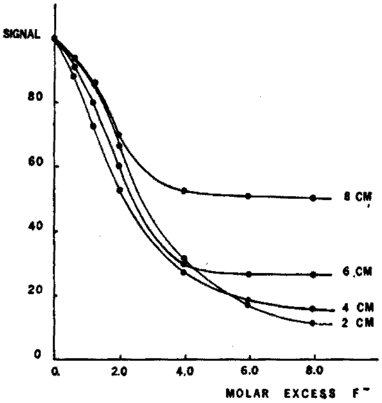

Fig. 1. Effect of increasing concentrations of fluoride on the relative flame emission signal of calcium at 4227 Å in the H_2/A flame. Measurements were made at 2, 4, 6 and 8 cm above the burner tip.

(a) Halogen compounds. As stated above, the addition of excess chloride (as HCl or NaCl) has no effect on the emission signal of calcium chloride. Additions of excess fluoride, bromide, or iodide result in a depression of the calcium emission. The effects of these anions at 4.0 cm above the burner tip are summarized in Figs. 2a

and 2b for both the H_2/A and H_2/O_2 flames. In both flames, CaI_2 and $CaBr_2$ give well defined changes in the slopes of the interference curves, corresponding to a 1:2 stoichiometric ratio. The bromide and iodide show decreased interference for greater heights of observation in both types of flame. The interference is decreased by about 5% per cm over the range 3–7 cm. The fluoride (Fig. 2) does not show a distinct change in slope in either flame when measured at 4.0 cm, although a distinct change can be observed when measured at 6.0 cm in the H_2/A flame, becoming more obvious (Fig. 1) as the height of measurement is increased to 8.0 cm. The break in the curve corresponds to a 1:2 stoichiometric ratio for this last height of measurement. Interpretations of the interference caused by the calcium halogen salts in non-equilibrium flames are complicated by the necessity of establishing a reaction mechanism for their decomposition to atomic calcium. In a true equilibrium flame, this is unnecessary. The dissociation energies and melting and boiling points[9] for the anhydrous halides are given in Table I. Interference caused by the presence of fluoride can be directly related to the low volatility of calcium fluoride as well as to its higher dissociation energy. Depression of the signal caused by the presence of iodide or bromide, however, can not be directly related to the dissociation energies of their calcium salts and appears to be contradictory to their relative volatilities, as expressed by their melting and boiling temperatures. The most likely explanation of the signal depressions caused by the halides is that the fluoride reduces the signal for the

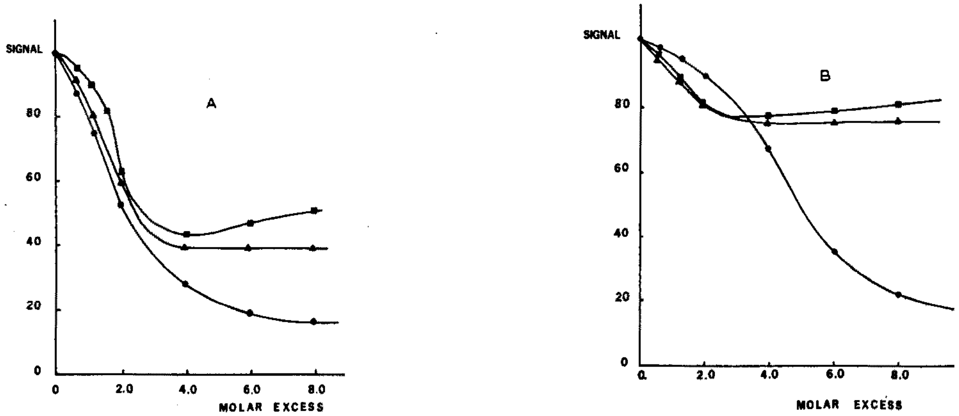

Figs. 2a and 2b. Effect of increasing concentrations of halide anions on the relative emission signal of calcium at 4227 Å in (a) the H_2/A flame, (b) the H_2/O_2 flame. ● fluoride, ▲ iodide, ■ bromide. Data obtained at a height of 4 cm above the burner tip.

TABLE I

Compound	*Dissoc. energy*[a] *(eV)*[8]	*Melting point (°)*[9]	*Boiling point (°)*[9]
CaF_2	3.15	1360	2500
$CaCl_2$	2.76	772	1600
$CaBr_2$	2.9	730	812
CaI_2	2.8	740	1100

[a] Dissociation energies are quoted for the diatomic molecules CaX.

reasons listed above, and that the bromide and iodide are more susceptible to hydrolysis than is the chloride:

$$CaX_2 + 2\,H_2O \rightarrow Ca(OH)_2 + 2\,HX$$

(b) Oxyanions. The presence of oxyanions such as sulphate, nitrate, phosphate, and pyrophosphate causes a depression of the calcium signal (Figs. 3a and 3b). The presence of perchlorate results in an enhancement. The perchlorate enhancement has been attributed[10] to explosive decomposition of either calcium or sodium perchlorates in the flame, resulting in a more efficient dispersion process of solid particles of the analyte. The evaporation of calcium chloride in the cooler H_2/A flame is slower than in the H_2/O_2 flame; the perchlorate enhancement is, therefore, greater in the cooler flame. The depressive effects of the sulphate and nitrate can be attributed to their mode of decomposition to calcium atoms; that is, they decompose initially to calcium oxide. Calcium sulphate is considerably less volatile than the nitrate and also has a higher thermal stability. Again, the interference effects of these two anions are greater in the H_2/A flame. In this latter flame, the sulphate shows a well defined change in slope at a stoichiometric ratio of 1:1; the nitrate interference exhibits a gradual depression with increasing anion excess. The degree of interference of both of these anions is practically independent of the height of measurement in the H_2/A flame although in the H_2/O_2 flame, the degree of interference is reduced at greater heights of observation.

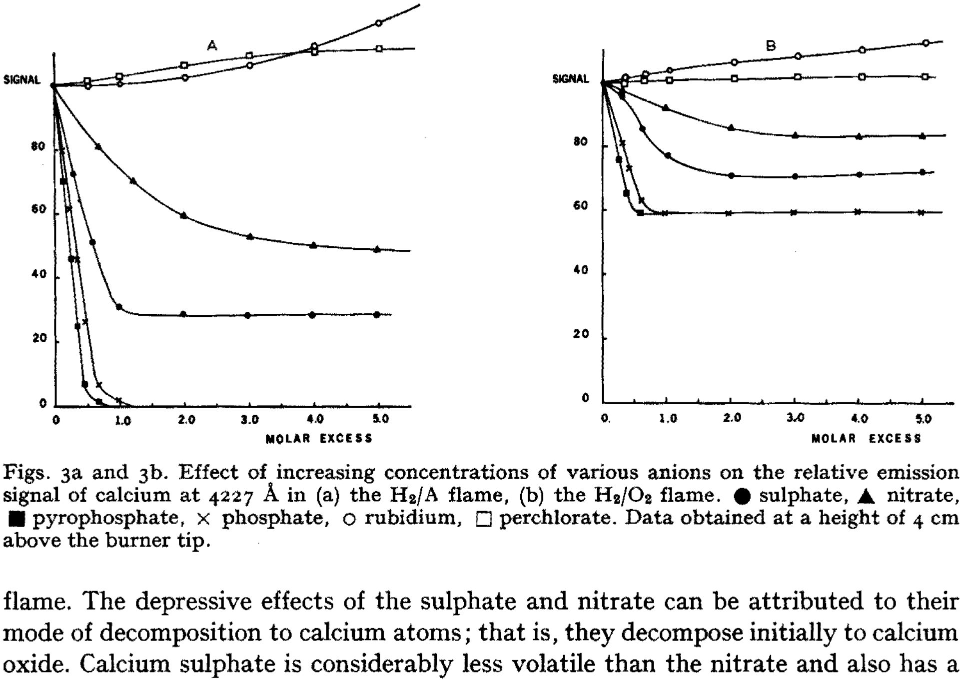

Figs. 3a and 3b. Effect of increasing concentrations of various anions on the relative emission signal of calcium at 4227 Å in (a) the H_2/A flame, (b) the H_2/O_2 flame. ● sulphate, ▲ nitrate, ■ pyrophosphate, × phosphate, ○ rubidium, □ perchlorate. Data obtained at a height of 4 cm above the burner tip.

The interference of phosphate on the determination of calcium has received considerable attention in the literature and the proposed mechanisms have been well summarized by HERRMANN AND ALKEMADE[7] and ELWELL AND GIDLEY[11]. Both pyrophosphate and phosphate show well defined changes in the slope of the interference plot (Figs. 3a and 3b) at stoichiometric ratios of calcium to anion of 2:1 and 3:2, respectively. The presence of excess amounts of these anions reduces the calcium emission signal to zero in the H_2/A flame. In the H_2/O_2 flame, the interference decreases with increased heights of observation in a similar manner to that described by HERRMANN AND ALKEMADE[7]. The interferences of both phosphate and pyrophosphate are attributed solely to the low volatilities of their calcium salts[12].

(c) Carboxylic acids. The effects of the organic anions: acetate, citrate, tartrate are similar and all give a negative interference (Figs. 4a and 4b) which is much greater in the H_2/A flame than the H_2/O_2 flame. The magnitude of the interference is approximately the same as that encountered in the presence of nitrate, and is typical of a thermally unstable salt[9] which decomposes at a comparatively low temperature to calcium oxide*. Of course, for equilibrium flames any interference will be independent of the mechanism of decomposition. The carboxylic acid salts most probably decompose to the oxide by way of the carbonate and some differences may be expected between their degrees of interference in hydrogen and hydrocarbon flames. In the latter, the presence of a considerable partial pressure of carbon dioxide may retard the decomposition of the intermediate carbonate and give rise to greater interference.

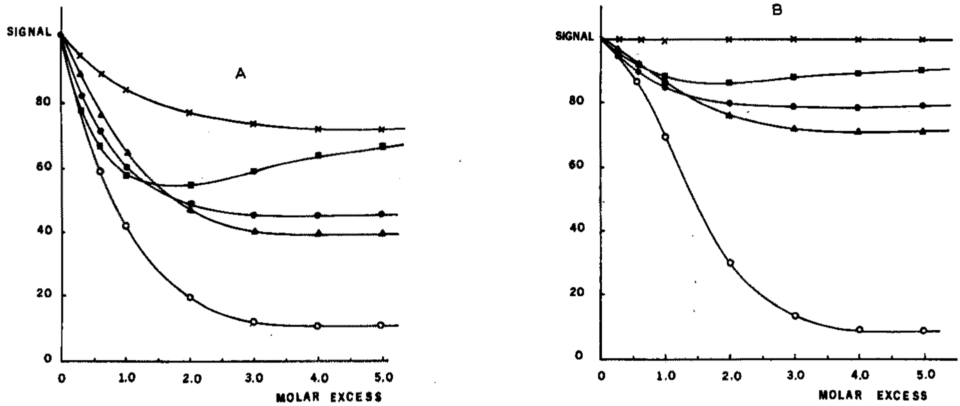

Figs. 4a and 4b. Effect of increasing concentrations of organic carboxylate anions on the relative emission signal of calcium at 4227 Å in (a) the H_2/A flame, (b) the H_2/O_2 flame. ● citrate and tartrate, ▲ acetate, ○ oxalate, × EDTA (pH 10), EDTA (pH 4). Data obtained at a height of 4 cm above the burner tip.

Oxalate has a much greater effect on the depression of the calcium signal than any other organic acid, despite the fact that calcium oxalate also decomposes at a comparatively low temperature[9] (Figs. 4a and 4b). This is an apparently anomalous behavior for which we are hesitant to offer an explanation.

Ethylenediaminetetraacetic acid (EDTA) has found use as a protecting agent[7] in flame methods of analysis. A large excess of this chelating agent forms complexes with many of the cations present in the analyte, and the complexes then decompose rapidly in the flame, thus eliminating many cationic interferences. By calculation, it can be shown that at a pH of 4.0 calcium does not form an EDTA complex although complex formation is complete at a pH of 10 even for very low concentrations of metal and ligand. The results for the interference of EDTA on the

---

* *cf.* nitrate interference.

calcium emission, in the H_2/A flame (Figs. 4a and 4b) show a distinct difference, depending on the pH of the solution. The depression caused by EDTA at the lower pH could arise from the formation of a calcium/EDTA salt, as opposed to a complex. The magnitude of this interference is typically that of a carboxylic acid. There was no interference from EDTA at a pH of 4 or a pH of 10 when a H_2/O_2 flame was used, and measurements were made 6.0 cm above the burner. When measurements were made 4.0 cm above the burner, only the solution at a pH of 4 showed any interference in the H_2/O_2 flame (Fig. 4b). However, it is reasonable to expect that EDTA would not function as a protecting agent for calcium in the presence of interfering anions and some cations at the lower pH value.

CONCLUSIONS

The results of the examination of interferences for the flame emission spectrometry of calcium, described here, clearly demonstrate a serious limitation to the use of cool flames for analytical purposes. The use of the H_2/A flame in conjunction with a total-consumption burner accentuates any interference effects (spectral or volatilization) which are found with the hotter H_2/O_2 flame. Many anions show a reduced degree of interference with greater heights of observation; this would appear to be a function of the residence time of the evaporating particles in the flame. Improvements in the use of H_2/A flames could, therefore, be made by using a chamber aspirator and laminar flow type of burner, resulting in the formation of smaller droplets and possibly reduced rise velocity. Further improvements suggested by the results of this study would be the use of a suitable releasing agent (such as EDTA at an appropriate acidity), together with a high concentration of sodium or ammonium perchlorate. This would combine enhanced selectivity with an improvement in sensitivity and would enable the effective use of total-consumption burners. Finally, it must be pointed out that determinations of calcium by flame methods of analysis are particularly prone to interference effects, and it is quite possible that H_2/A flames could be used for the analysis of other elements without any modifications of technique.

One of the authors (R.S.) thanks the National Science Foundation Science Development Grant of the University of Florida for financial support in the form of a post-doctorate research fellowship. This work was supported in part by AFOSR (SRC)-OAR, U.S.A.F. Grant No. AF-AFOSR-1033-67.

SUMMARY

An examination was made of the effects of various cations and anions on the determinations of calcium (4227 Å) by flame emission using turbulent hydrogen/argon/entrained-air and hydrogen/oxygen flames. The effects of height of observation and mechanisms of interference are discussed for Cs^+, Rb^+, F^-, Br^-, I^-, NO_3^-, ClO_4^-, SO_4^{2-}, PO_4^{3-}, $P_2O_7^{4-}$, acetate, oxalate, citrate, tartrate and EDTA. Ionization interferences were not detected in the hydrogen/argon/entrained-air flame, but all other types of interference were more serious with this flame than with the hydrogen/oxygen flame. The study also suggests some methods by which the effects of the interferences may be overcome.

RÉSUMÉ

On a examiné l'influence de divers cations et anions (Cs^+, Rb^+, F^-, Br^-, I^-, NO_3^-, ClO_4^-, SO_4^{2-}, PO_4^{3-}, $P_2O_7^{4-}$, acétate, oxalate, citrate, tartrate et EDTA), sur le dosage du calcium (4227 Å) par émission de flamme en utilisant les flammes hydrogène/argon/air et hydrogène/oxygène. Les interférences d'ionisation n'ont pas été détectées dans la flamme hydrogène/argon/air, mais tous les autres types d'interférences sont plus sérieux avec cette flamme qu'avec la flamme hydrogène/oxygène. On propose quelques moyens permettant d'éviter les interférences.

ZUSAMMENFASSUNG

Die Einflüsse zahlreicher Kationen und Anionen auf die Bestimmungen von Calcium (4227 Å) durch Flammenemission unter Verwendung einer turbulenten Wasserstoff–Argon–Luft- und Wasserstoff–Sauerstoff-Flamme wurden untersucht. Die Störungen folgender Ionen werden diskutiert: Cs^+, Rb^+, F^-, Br^-, I^-, NO_3^-, ClO_4^-, SO_4^{2-}, PO_4^{3-}, $P_2O_7^{4-}$, Acetat, Oxalat, Citrat, Tartrat und ÄDTA. Störungen durch Ionisation wurden in der Wasserstoff–Argon–Luft-Flamme nicht nachgewiesen, aber alle anderen Arten von Störungen waren in dieser Flamme ernsthafter als in der Wasserstoff–Sauerstoff-Flamme. Es werden einige Methoden vorgeschlagen, bei denen diese Einflüsse vermieden werden können.

REFERENCES

1 K. ZACHA AND J. D. WINEFORDNER, *Anal. Chem.*, 38 (1966) 1539.
2 R. M. DAGNALL, K. C. THOMPSON AND T. S. WEST, *Analyst*, 92 (1967) 506.
3 C. T. J. ALKEMADE, in E. R. LIPPINCOTT AND M. MARGOSHES, *Proc. Colloq. Spect. Intern. X*, Spartan Books, Washington, 1963, p. 143.
4 H. P. HOOYMAYERS, *Ph.D. Thesis*, University of Utrecht, 1966.
5 L. DE GALAN AND J. D. WINEFORDNER, *J. Quant. Spectry. Radiative Transfer*, 7 (1964) 703.
6 J. M. MANSFIELD, J. D. WINEFORDNER AND C. VEILLON, *Anal. Chem.*, 37 (1965) 1049.
7 R. HERRMANN AND C. T. J. ALKEMADE, *Chemical Analysis by Flame Photometry*, 2nd Edn., translated by P. T. GILBERT, J. Wiley (Interscience), 1963.
8 G. HERZBERG, *Spectra of Diatomic Molecules*, 2nd Edn., Van Nostrand, 1950.
9 *Handbook of Chemistry and Physics*, 45th Edn., Chemical Rubber Co., Cleveland, Ohio, 1963.
10 J. H. GIBSON, W. E. L. GROSSMAN AND W. D. COOKE, *Intern. Colloq. Spectroscopy*, University of Maryland, 1962.
11 W. T. ELWELL AND J. A. F. GIDLEY, *Atomic Absorption Spectrophotometry*, 2nd Edn., Pergamon Press, 1966.
12 R. SMITH AND J. D. WINEFORDNER, *Spectroscopy Letters*, in press.

Analytica Chimica Acta
Elsevier Publishing Company, Amsterdam
Printed in The Netherlands

SHORT COMMUNICATIONS

The adsorption of trace elements in sea water on various container surfaces*

The trace element analysis of sea water can be complicated by the fact that serious losses of trace elements can occur by adsorption onto the walls of the containers used for storing the sea water samples. MURPHY AND RILEY[1] observed that phosphate ions in sea water were strongly adsorbed onto polyethylene and polyvinyl chloride surfaces, while HASSENTEUFEL *et al.*[2] found that phosphate adsorption onto Pyrex glass surfaces was only slight. HUMMEL[3] reported that sea water stored in polyethylene bottles lost over 75% of its content of gold in three weeks and KOCZY[4] noted a similar decrease in the uranium content of sea water stored in glass bottles. SCHUTZ AND TUREKIAN, using radioactive tracers, concluded that no significant adsorption of selenium, silver, cobalt, cesium, zinc, chromium and antimony occurred when sea water was stored in Pyrex glass bottles for periods of up to 6 months[5]. STRICKLAND AND PARSONS[6] reported the slow deposition of iron onto both polyethylene and glass container surfaces. HØGDAHL[14] studied the adsorption–desorption properties of rare-earth elements in sea water using radioactive tracers of yttrium and found that over 50% of the yttrium was adsorbed onto polypropylene surfaces from sea water stored at pH's greater than 7.4, but observed no adsorption at pH's below 3.4. HØGDAHL also reported that all of the adsorbed yttrium could be desorbed by the addition of 0.5 ml of concentrated HCl to 200 ml of sea water, which had been stored at a pH of 8.2. WEST *et al.*[8] extensively studied the adsorption behavior of silver under a variety of conditions and reported losses of about 7–10% onto silica glass and polypropylene surfaces from 0.1 *M* NaCl solutions at a pH of 4.6 after contact times of up to 248 h. RILEY[7] has suggested several reasons for the adsorptive properties of glass and plastic surfaces. Since these materials are supercooled liquids, they possess high adsorption energies due to their distorted and broken bonds. This leads to the adsorption of ions from solution and to the formation of bonds between the surface and the adsorbed ions. Glass can act both as an anion and cation exchanger while surfaces of plastics under the influence of oxygen, heat or light may become degraded with the formation of carboxyl or carbonyl groups which may show adsorptive properties. Also, catalysts, fillers and plasticizers present in plastics may present active sites for adsorption.

This present study was initiated to determine the optimum conditions for storing sea water and describes the adsorption behavior of the eleven trace elements Sc, Fe, Zn, Co, Sr, Rb, Ag, In, Sb, Cs and U in sea water samples stored in polyethylene bottles, in Pyrex glass bottles and in polyethylene bottles containing sufficient hydrochloric acid to lower the pH of the sea water to about 1.5.

Experimental

Radioactive tracers of the elements of interest were separately added to 3000-ml samples of unfiltered sea water. These tracers were contained in dilute hydrochlor-

---

* This paper is based on work performed under United States Atomic Energy Commission Contract AT(45-1)-1830.

ic or nitric acid, and when necessary the pH of the spiked sea water was adjusted to its original pH of 8.0 by the addition of dilute sodium hydroxide. Aliquots (200 ml) were immediately poured into a series of 250-ml polyethylene bottles, Pyrex glass bottles, and polyethylene bottles containing 1 ml of concentrated hydrochloric acid to lower the pH of the spiked sea water to about 1.5. The polyethylene bottles were immediately counted in a 9-in diameter by 9-in thick NaI(Tl) well crystal to determine the initial counting rate of the radioactive tracers. After several predetermined periods of storage, the contents from one of each type of container were poured into new 250-ml polyethylene bottles which were then counted in the NaI(Tl) well crystal to determine the amount of tracer lost by adsorption onto the walls of the original containers. This procedure was used with the radioactive tracers ^{46}Sc, ^{59}Fe, ^{60}Co, ^{65}Zn, ^{85}Sr, ^{86}Rb, ^{110}Ag, ^{114}In, ^{124}Sb and ^{134}Cs. The specific activities of these tracers were sufficiently high to insure that the amount of stable element added with the tracers did not exceed the concentration of these elements already present in sea water. Thus, precipitations and other complications induced by exceeding the solubility products of these elements were minimized.

For the uranium adsorption studies, ^{235}U tracer was added to 600 ml of unfiltered sea water and the pH adjusted to 8.0 as described above. The sea water was then divided into 200-ml aliquots which were placed in a 250-ml polyethylene bottle, a Pyrex glass bottle and a polyethylene bottle containing 1 ml of concentrated hydrochloric acid to lower the pH to about 1.5. The uranium concentration was initially and then periodically measured after several storage periods by removing 5-ml aliquots from each container and determining the uranium by neutron activation analysis. The uranium concentration in the sea water was increased from about 3 p.p.b. to about 120 p.p.b. by the addition of the ^{235}U tracer and this may have altered the uranium behavior.

Results and discussion

The behavior of these tracers in sea water stored in the various containers is presented in Fig. 1. It is evident that serious losses of indium, scandium, iron, silver, uranium and cobalt can occur by their adsorption onto container surfaces. Indium was lost most rapidly, with greater than 90% adsorbed onto polyethylene surfaces after about 20 days of storage. However, when the pH of the sea water was lowered to about 1.5 with hydrochloric acid, the adsorption onto polyethylene was completely eliminated. Indium was slowly adsorbed from sea water onto Pyrex glass surfaces, with about a 20% loss after 75 days of storage. The behavior of iron was quite similar to that of indium. After 55 days, more than 90% of the iron was adsorbed onto polyethylene surfaces; again, however, the addition of the hydrochloric acid completely prevented this adsorption. After 55 days nearly 70% of the iron was adsorbed onto Pyrex glass surfaces. The behavior of scandium was similar to that of indium and iron except that the addition of the hydrochloric acid was only partially effective, allowing about 35% of the scandium to become adsorbed after 60 days. After 50 days about 20% of the uranium was lost to Pyrex glass surfaces and about 10% to polyethylene surfaces even with the addition of hydrochloric acid to the sea water. The uranium adsorption studies are being continued beyond 50 days to determine its subsequent behavior. About 20% of the silver was adsorbed onto the polyethylene surface after about 10 days and remained at that level throughout the experiment. Insignificant

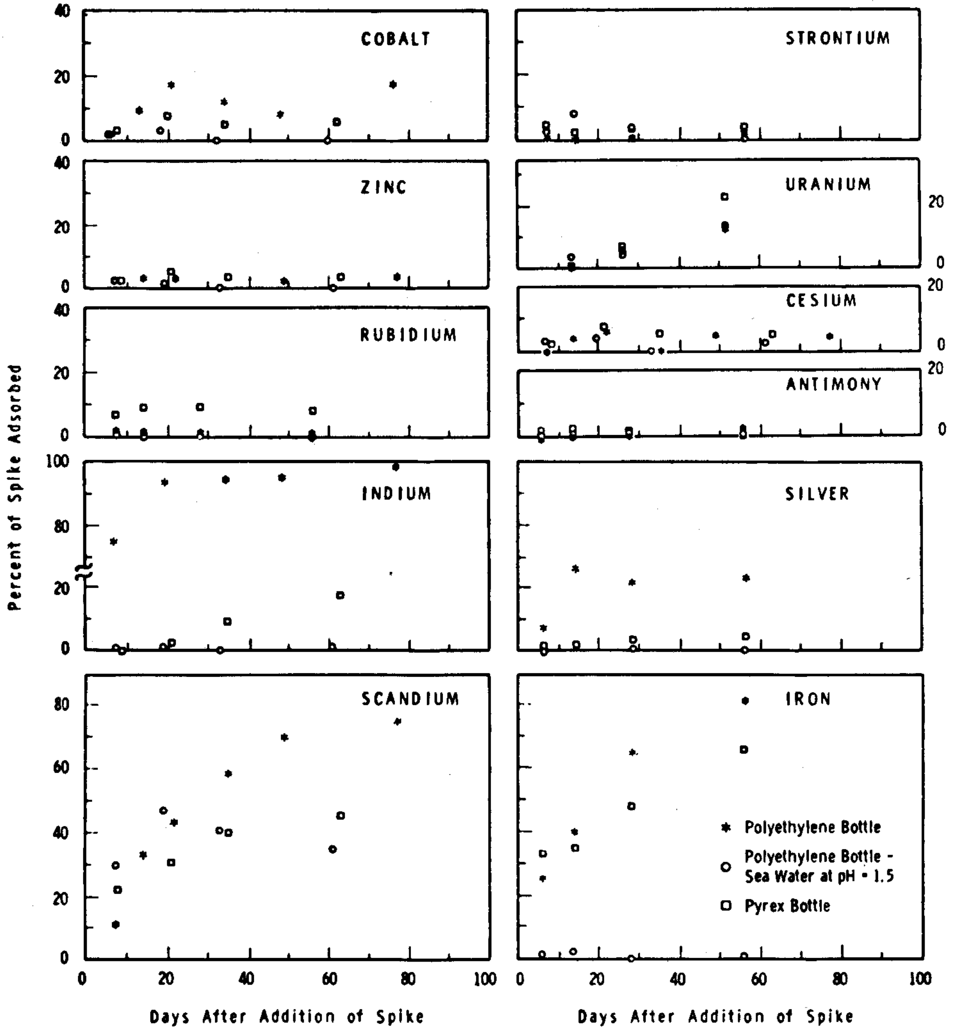

Fig. 1. The adsorption of trace elements in sea water onto various container surfaces.

silver adsorption occurred on Pyrex glass surfaces and on polyethylene surfaces when the sea water was acidified with hydrochloric acid. About 10–20% of the cobalt was lost on polyethylene after about 10 days. However, the adsorption onto polyethylene was prevented by the addition of the hydrochloric acid. About 5–10% of the cobalt was lost on the Pyrex glass surfaces after about 20 days and remained constant at that level throughout the experiment. About 10% of the rubidium was lost on the Pyrex glass surfaces after about 10 days and remained constant at that level. However, no adsorption occurred for rubidium in sea water stored in polyethylene containers. Negligible adsorption of zinc, cesium, strontium and antimony on all container surfaces was observed for storage periods of up to 75 days.

All of the radioactive tracers were added to the sea water samples in a soluble form. The ^{110m}Ag was added as Ag^+, while the forms reported[8] to exist in sea water are $AgCl_2^-$ and $AgCl_3^{2-}$. The ^{235}U tracer was added as uranyl ion, while the uranium in sea water exists[8] as the carbonate complex, $UO_2(CO_2)_3^{4-}$. Iron is reported to exist in sea water mainly as colloidal iron(III) hydroxide and iron(III) phosphate[9], but the ^{59}Fe tracer was added as iron(III) chloride. The ^{124}Sb tracer was added as Sb^{3+}; however, the chemical form of antimony in sea water is unknown, but should parallel the chemistry of arsenic which is reported[8] to exist as $HAsO_4^{2-}$, $H_2AsO_4^-$, H_3AsO_4 and H_3AsO_3. The Cs, Rb, Sr, Zn, Co, Sc and In were added as Cs^+, Rb^+, Sr^{2+}, Zn^{2+}, Co^{2+}, Sc^{3+} and In^{3+}, respectively and these are probably the principal forms in which these elements exist in sea water.

It appears that the optimum conditions for storing sea water consist of immediately acidifying the sea water to a pH of about 1.5 and storing the samples in polyethylene bottles. Most polyethylene is very pure except for traces of iron (*ca.* 10 p.p.m.), whereas Pyrex glass contains relatively high impurity levels of many elements and could present some contamination problems[10]. It is recommended that the polyethylene bottles be well rinsed before use with purified hydrochloric or nitric acid to remove traces of iron or other materials on the surface of the bottles.

Freezing the acidified sea water samples may retard the adsorption of scandium and uranium onto polyethylene surfaces. Freezing has been used effectively to preserve sea water samples for analyses of nitrate and nitrite[11], reactive phosphate[12] and silicate[13]. However, the effect of this procedure on trace elements has not been determined.

Environmental & Radiological Sciences Department, D. E. Robertson
Pacific Northwest Laboratory,
Battelle Memorial Institute, Richland, Wash. (U.S.A.)

1 J. Murphy and J. P. Riley, *Anal. Chim. Acta*, 14 (1956) 318.
2 W. Hassenteufel, R. Jagitsch and F. F. Koczy, *Limnol. Oceanog.*, 8 (1963) 152.
3 R. W. Hummel, *Analyst*, 82 (1957) 483.
4 G. Koczy, *Oesterr. Akad. Wiss. Math. Naturw. Kl., Sitzber., Abt. IIa*, 158 (1950) 113.
5 D. F. Schutz and K. K. Turekian, *Geochim. Cosmochim. Acta*, 29 (1965) 259.
6 J. D. H. Strickland and T. R. Parsons, A Manual of Sea Water Analysis, *Fisheries Res. Board Can., Bull. No. 125*, 2nd Edn., 1965, p. 96.
7 J. P. Riley, in J. P. Riley and G. Skirrow, *Chemical Oceanography*, Vol. 2, Academic Press, London and New York, 1965, p. 303.
8 E. D. Goldberg, in M. N. Hill, *The Sea*, Vol. 2, Interscience Publishers, New York and London, 1963, p. 4–5.
9 J. P. Riley, in J. P. Riley and G. Skirrow, *Chemical Oceanography*, Vol. 2, Academic Press, London and New York, 1965, p. 378.
10 D. E. Robertson, *Anal. Chem.*, 40 (1968) 1067.
11 R. R. Proctor, *Limnol. Oceanog.*, 7 (1962) 479.
12 A. W. Collier and K. T. Marvin, *Fisheries Bull. U.S.*, 84 (1953) 71.
13 J. D. H. Strickland and T. R. Parsons, A Manual of Sea Water Analysis, *Fisheries Res. Board Can., Bull. No. 125*, 1960, p. 185.
14 O. Høgdahl, *Semi-annual Progrress Report No. 7*, Central Institute for Industrial Research, Oslo, Norway, Oct. 30, 1965,
15 F. K. West, P. W. West and F. A. Iddings, *Anal. Chim. Acta*, 37 (1967) 112.

(Received March 25th, 1968)

Heats of transitions and kinetic study of liquid crystals by differential thermal analysis

Recent investigations in these laboratories concerning the applications of differential thermal analysis (DTA) have led us to apply this technique to the study of liquid crystal transitions. Several papers have appeared in which the application of DTA to the determination of liquid crystal phase transitions is discussed[1-3]. Because of the sensitivity and reliability of this technique and because thermodynamic data are rare for liquid crystals, initial attention was given to the study of the *p-n*-alkoxybenzoic acid series which exhibits liquid crystal behavior. The detection of the solid-nematic and nematic-isotropic transitions for *p-n*-butoxybenzoic acid, the determination of their respective enthalpy and entropy changes and the initial kinetic study of these transitions are reported in this communication.

Reagents

p-n-Butoxybenzoic acid (K and K Laboratory, New York) was recrystallized twice from glacial acetic acid, ethanol and finally benzene.

Certified reagent-grade *p*-aminobenzoic acid (Fisher Scientific Co.) was twice recrystallized from benzene–methanol (10:1) and chloroform–methanol (10:1). M.p. 187.6–188.0°.

o-Chlorobenzoic acid (Eastman White Label) was twice recrystallized from benzene–heptane (1:5) and pure carbon tetrachloride. M.p. 139.2–140.0°.

Procedure A. Determination of ΔH

Thermograms were obtained with samples contained in an open 4-mm glass tube in the calorimeter cell of a DuPont Model 900 Differential Thermal Analyzer. Samples of 2–4 mg were weighed directly into the tubes and placed into the sample reservoir of the calorimeter cell. The cell was enclosed and flushed three times with dry nitrogen to prevent decomposition of the sample during the heating process. Samples were heated at a rate of 5°/min from room temperature to 200°.

The difference in temperature (ΔT) between reference and samples was measured at a sensitivity of 0.5°/in. The reference was a glass tube containing glass beads. After completion of the run, the calorimeter cell containing the sample was cooled to room temperature with dry ice and acetone mixture while the system was flushed with dry nitrogen to prevent condensation of moisture on the cell and its contents. The above procedure was repeated on this same sample.

Thermograms of *p-n*-butoxybenzoic acid were determined by the above procedure.

The instrument was calibrated for the determination of ΔH values by calculating a calibration coefficient from the thermograms (procedure outlined above) of *o*-chlorobenzoic acid (ΔH_f = 39.3 cal/g; m.p. 140.2°) and *p*-aminobenzoic acid (ΔH_f = 36.5 cal/g; m.p. 188.5°). The areas of the melting point transition peaks were found by drawing a line from the point where the thermogram departs from the base line to the point where it returns. The enclosed area was measured by means of a planimeter. The calibration coefficient, mcal/°-min, was calculated for both substances from the following equation:

$$E = \Delta HMa/A(\Delta T_s)T_s$$

where E = calibration coefficient; ΔH = ΔH of fusion, mcal/mg; A = peak area, sq. in; ΔT_s = Y-axis sensitivity setting, °/in; T_s = X-axis sensitivity setting, °/in; M = sample mass, mg; a = heating rate, °/min.

An average calibration coefficient was obtained with the two above standard materials whose melting points bracket the transition temperatures of *p-n*-butoxybenzoic acid. The ΔH of transition was then obtained by substitution into the above equation.

Procedure B. Determination of transition temperatures

Thermograms were obtained with the sample in a glass capillary placed in the standard micro-cell of the Differential Thermal Analyzer. A glass capillary filled with glass beads was employed as the reference. The sample was heated from room temperature to 200° at a rate of 20°/min. As described in procedure A above, two thermograms were obtained from a single sample: first from a fresh sample and a second after cooling to room temperature.

The transition temperature was assumed to correspond with the extrapolated onset temperature where this temperature is defined as the temperature corresponding to the intersection of extrapolations of the base line and the longest straight line section of the low temperature side of the peak.

Results and discussion

Since the initial thermograms of the first peak were found not to be reproducible, giving broad and unsymmetrical peaks due to poor heat transfer and unpredictable collapse of sample, the following discussion applies only to the second thermograms of procedure A and B.

Owing to the design of the calorimeter cell it was found that the extrapolated onset temperature obtained from procedure A does not generally correspond to the true transition temperature. Procedure B however, which utilizes the standard cell, does yield a true transition temperature.

Figure 1 is a typical thermogram of *p-n*-butoxybenzoic acid obtained by procedure B. The extrapolated onset temperatures were determined and gave values of 148° and 165° corresponding to the solid-nematic and nematic-isotropic transitions respectively. This is in good agreement with the values of 147° and 160° reported by JONES[4].

Figure 2 is a typical thermogram of *p-n*-butoxybenzoic acid obtained using the calorimeter cell (procedure A). This thermogram was used to determine the ΔH of transitions because procedure B gave non-reproducible values. ΔH and ΔS for the solid-nematic transition were found to be 24.2 ± 0.3 cal/g and 0.0575 ± 0.0007 cal/g-°K, respectively, and for the nematic-isotropic transition, 4.0 ± 1 cal/g and 0.0092 ± 0.003 cal/g-°K, respectively. These values are indeed consistent with current theories concerning the energy requirements for the individual phase transitions[5].

The kinetics of transition were studied by the method of SPEROS AND WOODHOUSE[6,7]. Both the solid-nematic and nematic-isotropic transitions exhibit an exponential dependence of dH/dt on time preceding their linear behavior (Fig. 3). The logarithmic region for the solid-nematic transition is greater than the corresponding region for the nematic-isotropic case. The ratio of the slopes of the linear regions for the solid-nematic to nematic-isotropic transitions is less than that calculated on the basis of ΔH values and the total time required for these transitions to take place. This suggests that the extent of reorientation for the nematic-isotropic transition is less than that required for the preceding transition.

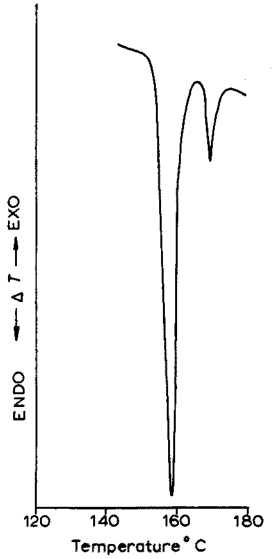

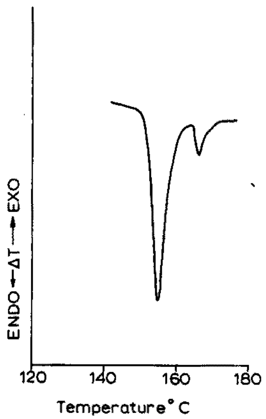

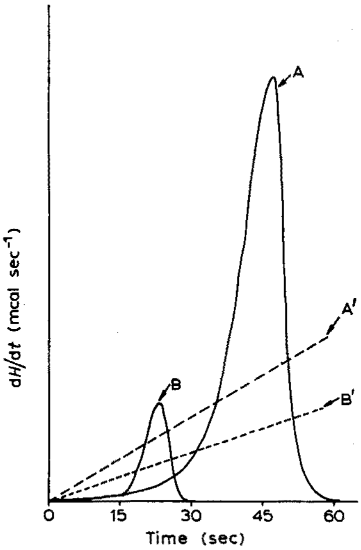

Fig. 1. Typical thermogram of *p*-*n*-butoxybenzoic acid (procedure B).

Fig. 2. Typical thermogram of *p*-*n*-butoxybenzoic acid (procedure A).

Fig. 3. Dependence of dH/dt on time.

Extension of this work to other mesomorphic compounds should help to elucidate the cause of the aforementioned behavior. Other members of the *p*-*n*-alkoxybenzoic acid series are being studied in addition to a number of cholesterol esters which exhibit similar behavior.

Department of Chemistry, ANGELO V. SANTORO
Hunter College, The City University of New York,
New York, N.Y. 10021 (U.S.A.)

Department of Chemistry, GERALD I. SPIELHOLTZ
Herbert H. Lehman College, The City University of New York,
Bronx, N.Y. 10468 (U.S.A.)

1 E. M. BARRAL, II, R. S. PORTER AND J. F. JOHNSON, *J. Phys. Chem.*, 70 (1966) 385.
2 E. M. BARRAL, II, R. S. PORTER AND J. F. JOHNSON, *J. Phys. Chem.*, 68 (1964) 2810.
3 H. MARTIN AND F. H. MULLER, *Kolloid-Z.*, 187 (1963) 107.
4 B. JONES, *J. Chem. Soc.*, (1935) 1874.
5 G. W. GRAY, *Molecular Structure and the Properties of Liquid Crystals*, Academic Press, London, 1962, pp. 66–79.
6 D. M. SPEROS AND R. L. WOODHOUSE, *Nature*, (1963) 1261.
7 D. M. SPEROS AND R. L. WOODHOUSE, *J. Phys. Chem.*, 67 (1963) 2164.

(Received March 25th, 1968)

Zur Analyse von Cer(IV)-phosphaten und Cer(IV)-phosphat-sulfaten

Phosphate des vierwertigen Cers werden in zunehmendem Masse als anorganische Kationenaustauscher verwendet[1-6]. Die in Mineralsäuren ohne komplexbildende Anionen schwerlöslichen Verbindungen bilden neben amorphen Produkten unter geeigneten Bedingungen sehr gut ausgebildete kristalline Phasen, in denen Phosphatgruppen durch Sulfatgruppen ersetzt werden können. Solche Stoffe haben noch bei pH 2 eine Austauschkapazität für Natrium von rund 1 mVal/g[4,7]. Damit geben sie ideale Möglichkeiten zum systematischen Studium der Austauschereigenschaften als Funktion der chemischen Zusammensetzung und der Kristallstruktur[4,7].

Bei der in diesem Zusammenhang vorgenommenen Überprüfung der bisher für diese Stoffe vorgeschlagenen Analysenmethoden wurden wir zu Modifikationen bzw. Ersatz der vorgeschlagenen Verfahren[1-3] durch andere veranlasst, die nach unseren Erfahrungen eine schnelle und sichere Bestimmung der Bestandteile ermöglichen.

Die bei weitem eleganteste Methode zur Bestimmung des vierwertigen Cers ist seine Reduktion mit Arsen(III) und Rücktitration des überschüssigen Reduktionsmittels mit Cer(IV) in schwefelsaurer Lösung. Ebenfalls in schwefelsaurer Lösung ist die photometrische Bestimmung von Phosphat nach dem Vanadat–Molybdat-Verfahren möglich[8-10]. Hierbei wird zur Ausschaltung der Eigenabsorption durch das Cer(IV) die gelbe Aufschlusslösung mit Natriumazid versetzt und dadurch das Cer(IV) zum dreiwertigen reduziert.

Für die Bestimmung von Sulfat in den sulfathaltigen Cer(IV)-phosphat-sulfaten [4,7,11] hat sich deren thermische Zersetzung in Anlehnung an das von GROTE UND KREKELER empfohlene Verfahren sehr bewährt[12-17]. Die dabei entstehenden Schwefeloxide werden in Wasserstoffperoxid absorbiert und die entstehende saure Lösung acidimetrisch titriert.

Bestimmung des Cer(IV)

150–300 mg Cer(IV)-phosphat werden mit 40 ml 20 *N* Schwefelsäure versetzt. Hierzu werden in der Kälte 15 ml 0.1 *N* Arsen(III)-Masslösung (0.025 Mol As_2O_3 + 0.17 Mol NaOH pro Liter Lösung) sowie ein Tropfen 0.01 *M* OsO_4-Lösung gegeben und unter Rühren zum Sieden erhitzt. Da sich reines kristallines Cer(IV)-phosphat in Gegenwart von Arsen(III) deutlich langsamer auflöst, wird die Reaktion durch Zusatz von *ca.* 1 ml 85%iger Phosphorsäure beschleunigt. Gleichzeitig bewirkt dieser Zusatz einen schärferen Indikatorumschlag bei der Rücktitration des überschüssigen Arsen(III). In jedem Fall ist der Aufschluss nach längstens 2 Stunden beendet. Ein Titerverlust der Arsen(III)-Lösung wird dabei nicht beobachtet. Manchmal bleibt eine weisse Trübung bestehen, die wahrscheinlich aus Cer(III)-sulfat besteht, das unter den angegebenen Bedingungen nur wenig löslich ist[18], oder aus schwerlöslichen Cer(III)-sulfatphosphaten[19,20].

Der Überschuss des As(III) wird nach Abkühlen und Verdünnen der Lösung mit Wasser auf *ca.* 150 ml unter Zusatz von Ferroin und OsO_4 mit Cer(IV)-Masslösung titriert[21]. Analysenergebnisse an Cer(IV)-phosphaten bekannter Zusammensetzung zeigt Tabelle I.

Bestimmung des Phosphatgehaltes

120–180 mg Cer(IV)-phosphat werden in 50 ml heisser 20 *N* Schwefelsäure gelöst. Die klare Lösung wird nach Abkühlen in einen 500 ml-Messkolben überführt, mit 5 ml 1 *M* Natriumazid-Lösung versetzt und mit Wasser aufgefüllt. Hiervon werden 10 ml in einen 100 ml-Messkolben pipettiert, wobei dieses Mengenverhältnis zur Konstanthaltung des Säuregrades in den Aliquoten einzuhalten ist. Nach Zusatz von 25 ml VM-Lösung (Bereitung s. unten) und Auffüllen mit Wasser auf 100 ml wird die Extinktion der Lösung nach halbstündigem Stehen bei 25° bei 400 nm gegen Wasser als Vergleich gemessen.

Bereitung der VM-Lösung. 0.75 g Ammoniumvanadat und 16.7 g Ammoniummolybdat in heissem Wasser lösen, nach Abkühlen 32 ml konz. Schwefelsäure zusetzen und mit Wasser auf 1 Liter auffüllen. Die Lösung ist unbegrenzt haltbar.

Analysenergebnisse an Cer(IV)-phosphaten bekannter Zusammensetzung zeigt Tabelle II.

TABELLE I

OXIDIMETRISCHE RÜCKTITRATION VON CER(IV) MIT ARSEN(III)

(Mittelwerte aus 6 Einzelbestimmungen)

Vorgegeben mg Ce	*Gefunden mg Ce*	*Abweichung des Mittelw.* (%)
50.28	50.35	+0.1
90.50	90.31	−0.2
130.7	130.3	−0.3

TABELLE II

PHOTOMETRISCHE PHOSPHATBESTIMMUNG IN CER(IV)-PHOSPHAT

(Mittelwert aus 5 Einzelbestimmungen)

Vorgegeben mg PO_4	*Gefunden mg PO_4*	*Abweichung des Mittelw.* (%)
19.43	19.45	+0.1
58.29	58.31	+0.0
97.15	97.38	+0.2

Sulfatbestimmung in sulfathaltigen Cer(IV)-phosphaten

Zur Sulfatbestimmung in sulfathaltigen Cer(IV)-phosphaten eignet sich das von GROTE UND KREKELER für die Schwefelbestimmung in organischen Verbindungen vorgeschlagene Verfahren[12-17]. Wir haben unsere Zersetzungsapparatur folgendermassen bemessen: Verbrennungsrohr aus Quarz, 100 cm lang, *ca.* 2 cm lichte Weite. Der Röhrenofen mit einer maximalen Arbeitstemperatur von 1300° kann über eine weite Strecke des Rohres verschoben werden. 100–200 mg Cer(IV)-phosphat werden in einem unglasierten Porzellanschiffchen im Verbrennungsrohr innerhalb von 20 min auf 1200° erhitzt. Die entstandenen Schwefeloxide werden mit einem schwachen Luftstrom in das mit Glasperlen gefüllte Absorptionsgefäss gesaugt und hier in 60 ml 3%-igem H_2O_2 absorbiert. Die durch die Apparatur gesogene Luft wird vorher mit konz. Schwefelsäure und 2 *N* Natriumhydroxidlösung gewaschen. Das Gasabsorptionsgefäss ist durch einen Kugelschliff mit dem Quarzrohr verbunden. Die Zersetzungsreaktion ist nach *ca.* 60 min beendet. Danach werden die an den Wänden des Quarzrohres adsorbierten Schwefeloxide durch Erhitzen mit einem Bunsenbrenner in das Absorptionsgefäss getrieben. Die acidimetrische Titration erfolgt mit 0.04 *N* Natriumhydroxidlösung gegen Tashiro-Indikator oder mit potentiometrischer Endpunktsanzeige.

Als Beispiel für die Reproduzierbarkeit der Methode sind in der Tabelle III die Analysenergebnisse eines sulfathaltigen Cer(IV)-phosphats zusammengestellt.

TABELLE III

SULFATBESTIMMUNG IN SULFATHALTIGEM CER(IV)-PHOSPHAT

Sulfatgehalt (%)	*Abweichung vom Mittelwert (%)*
8.91	—1.1
9.15	+1.6
9.02	+0.1
8.88	−1.4
8.95	−0.7
9.06	+0.6
9.08	+0.8
9.01 Mittelwert	

Wir danken der DECHEMA Deutsche Gesellschaft für chemisches Apparatewesen für die Gewährung eines Paul Duden-Stipendiums und der Deutschen Forschungsgemeinschaft für die Förderung der Arbeit.

Institut für anorganische Chemie, Universität
Frankfurt a. Main, Robert-Mayer-Strasse 7–9
(Deutsche Bundesrepublik)

K.-H. KÖNIG
E. MEYN
G. ECKSTEIN

1 D. R. VISSERS, *Ph.D. Thesis*, University of Wisconsin, Madison, 1959.
2 W. A. CILLEY, *Ph.D. Thesis*, University of Wisconsin, Madison, 1963.
3 G. G. ROCCO, I. R. WEINER UND I. P. CALI, *Report AFCRL-64-1018*, 1964.
4 K.-H. KÖNIG UND E. MEYN, *J. Inorg. & Nucl. Chem.*, 29 (1967) 1153.
5 E. M. LARSEN UND W. A. CILLEY, *J. Inorg. & Nucl. Chem.*, 30 (1968) 287.
6 G. ALBERTI, U. CONSTANTINO, F. DI GREGORIO, P. GALLI UND E. TORRACCA, *J. Inorg. & Nucl. Chem.*, 30 (1968) 295.
7 G. ECKSTEIN, *Diplomarbeit*, Frankfurt/M., 1968.
8 I. M. KOLTHOFF UND P. J. ELVING, *Treatise on Analytical Chemistry*, Part II, Vol. 5, Interscience, New York, 1961, p. 351–353.
9 M. DE SESA UND L. ROGERS, *Anal. Chem.*, 26 (1954) 1381.
10 E. MEYN, *Diplomarbeit*, Frankfurt/M., 1964.
11 K.-H. KÖNIG UND E. MEYN, *J. Inorg. & Nucl. Chem.*, 29 (1967) 1519.
12 W. GROTE UND H. KREKELER, *Z. Anal. Chem.*, 98 (1934) 463.
13 W. GROTE UND H. KREKELER, *Angew. Chem.*, 46 (1933) 106.
14 L. T. HALLET UND J. W. KUIPERS, *Ind. Eng. Chem., Anal. Ed.*, 12 (1940) 360.
15 R. N. WALTER, *Anal. Chem.*, 22 (1950) 1332.
16 ANONYM, *DIN 51768*.
17 W. LANGE, *Glueckauf*, 78 (1942) 651.
18 F. WIRTH, *Z. Anorg. Chem.*, 76 (1912) 174.
19 A. I. UL'YANOV, T. I. KAZAKOVA UND E. YA. RUMYANTSEVA, *Izv. Akad. Nauk SSSR, Otd. Khim. Nauk*, 1962, p. 1910.
20 N. N. MIRONOV UND A. YA. KAREV, *Tr. Khim. i Khim. Tekhnol.*, 4 (1961) 731.
21 K. GLEU, *Z. Anal. Chem.*, 95 (1933) 305.

(Eingegangen den 15. Januar, 1968)

Acides hétéropolymolybdiques mesurés dans l'ultraviolet

Acide phosphomolybdique

La solution de phosphate (P $\leqslant$ 6 μg), acidifiée par l'acide perchlorique (acidité du milieu: 0.78 *M*) est additionnée de molybdate de sodium (concentration du milieu: 0.02 *M*).

Les rapports s'établissent comme suit: $[P^-]/[MoO_4{}^{2-}] = 1/2 \cdot 10^6$ et $[H^+]/[MoO_4{}^{2-}] = 40$, environ[1]; le pH du milieu (8 ml) s'établit à 0.6 environ[2]. Après extraction par 4 ml d'éther, à 2 ml d'extrait (centrifugé) sont ajoutés 5 ml d'alcool absolu et de l'eau pour diluer à 10 ml; mesures photométriques en cuves de quartz (1 cm), ouverture 50 μ, à 220 nm.

La courbe d'absorption de l'acide phosphomolybdique cristallisé, en solution aqueuse (Fig. 1) (le coefficient d'extinction moléculaire ε, chiffré par son log, étant exprimé par rapport au molybdène), indique que la densité optique augmente avec la longueur d'onde décroissante; l'éther présente à 220 nm une densité optique faible (A = 0.3 à 220 nm)*. La courbe (Fig. 2) exprime l'optimum d'acidité; la densité optique est une fonction linéaire de la quantité phosphore en essai, jusqu'à 3 μg P environ, au minimum. Le coefficient d'extinction moléculaire, dans ce domaine de teneurs de phosphore, calculé à l'aide de cette droite et par rapport au phosphore, s'établit à $15 \cdot 10^4$: exprimé à l'aide des valeurs extraites de la courbe d'absorption (Fig. 1), identique d'ailleurs aux courbes publiées d'autre part[1,3,4,15], il s'élève à $7.8 \cdot 10^4$: l'acide phosphomolybdique formé extemporanément par voie analytique paraît présenter une forme optiquement plus active que l'acide cristallisé. L'éther, outre sa faible densité optique, n'extrait pas d'acides molybdiques du milieu**; il n'en est pas de même de l'acétate d'isobutyle[5,6], l'acétate *n*-butylique[7–9], l'alcool isobutylique [10–14], l'alcool *n*-butylique[15,16], les acétates d'amyle et d'isoamyle[17]*** dont la densité

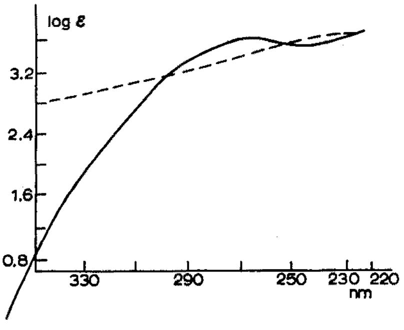

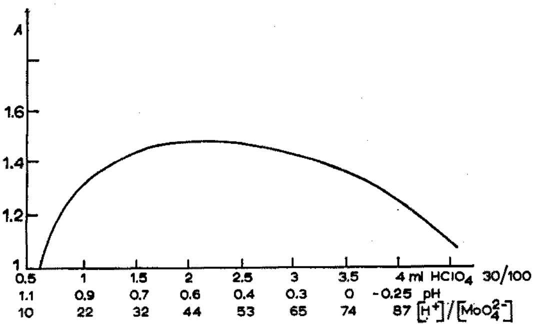

Fig. 1. Courbe de log ε en fonction de λ. (——) aSiW, aPW, aBW; (– – –) aPMo, aSiMo.

Fig. 2. Phosphomolybdate: A en fonction de l'acidité. $\lambda = 220$; $c = 1$; $O = 50\,\mu$.

---

* Mesures de densité optique faites au moyen du spectrophotomètre U.V., M. JEAN ET R. CONSTANT. Celle-ci est dans ce cas particulier mesurée à l'aide du liquide dilué dans l'alcool absolu et l'eau, dans les conditions des essais ci-dessus.

** Il s'agit de l'acide molybdique lui-même, ou de ses produits de polymérisation (en particulier l'acide tétramolybdique).

*** Les indications de la littérature se rapportent à ces solvants, employés soit seuls, soit en mélange avec différents autres solvants: chloroforme, benzène, éther etc.

optique est trop élevée à 220 nm (respectivement $A = 0.3$ à 260 nm; 1.8 à 244 nm; 0.4 à 220 nm; 1.2 à 240 nm; 1.96 à 255 nm, acétate d'isoamyle)*, et qui extraient les acides molybdiques, d'où une densité optique importante du témoin (exempt de phosphore). Par exemple $A = 1.4$ à 260 nm du témoin avec l'alcool isobutylique comme solvant*. La présence de fer (et autres éléments) dans le milieu où est formé l'acide phosphomolybdique modifie l'extractibilité par les solvants de celui-ci, et il n'est, par exemple, pas extrait par l'acétate de butyle[1].

Acide arseniomolybdique

L'arseniate disodique (As < 15 μg) forme aisément, en milieu perchlorique, l'acide arseniomolybdique avec le molybdate de sodium ($[MoO_4^{2-}] = 0.02\ M$): les rapports de concentration sont les suivants: $[H^+]/[MoO_4^{2-}] = 50$ environ; $[As]/[MoO_4^{2-}] = 1/10^5$. L'extraction est faite par l'éther dont une fraction, séparée centrifugation, est traitée comme indiqué ci-dessus. Mesures à 220 nm. Le coefficient d'extinction moléculaire est environ: $3.3 \cdot 10^4$.

Acide silicomolybdique

Il est obtenu du métasilicate $SiO_3Na_2 \cdot 5\ H_2O$[18] ou du fluosilicate SiF_6Na_2 (Si $\leqslant$ 5 μg), en milieu perchlorique (acidité du milieu 0.10 à 0.15 M), au moyen du molybdate de sodium (concentration du milieu 0.055 M); les rapports s'établissent à $[Si^-]/[MoO_4^{2-}] = 1/3 \cdot 10^5$ et $[H^+]/[MoO_4^{2-}] = 7$ ou 2 environ, avec pH 0.9 à 1.5 selon l'acidité des milieux réalisés.

Selon la courbe d'absorption (Fig. 1) de l'acide silicomolybdique cristallisé, en solution aqueuse, la densité optique augmente aux plus basses longueurs d'onde. Un solvant extractif de l'acide silicomolybdique est choisi parmi les solvants de faible absorption aux basses longueurs d'onde, donc à l'exclusion des alcools et esters tels que isobutylique, amylique ou isoamylique[19-22]. L'alcool isopropylique, cependant soluble dans le milieu aqueux, facilite la formation de l'acide silicotungstique, mais augmente la densité optique du milieu[18].

Le dibutylcarbitol extrait, du milieu perchlorique (pH 0.9-1), l'acide silicomolybdique. Le coefficient d'extinction exprimé par rapport au silicium atteint, dans l'ordre de grandeur des teneurs visées, $6 \cdot 10^4$ à 235 nm. En milieu perchlorique 0.12 M (pH 1.3 à 1.5) l'acide silicotungstique est extrait seul. Après formation de l'acide silicomolybdique en milieu perchlorique, l'acidification sulfurique supplémentaire à 0.54 M confère un coefficient d'extinction moléculaire du même ordre de grandeur.

L'acétate d'éthyle, en milieux de pH 0.9 à 1.5, n'extrait pas les acides silicomolybdique et molybdiques; après formation de l'acide silicomolybdique en milieu perchlorique, l'acidité étant portée à 5.4 M par addition d'acide sulfurique, l'acétate d'éthyle extrait l'acide silicomolybdique[23,24], et le coefficient d'extinction moléculaire est, à 245 nm, du même ordre que précédemment.

L'extraction est faite par 3, 5 ou 4 ml de solvant, du milieu aqueux atteignant 7 à 10 ml, dont 2 ml sont prélevés après centrifugation; ils sont dilués par 5 ml d'alcool absolu et de l'eau pour compléter à 10 ml; ce liquide est mesuré au spectrophotomètre. La quantité de silicium en essai, jusqu'à 5 μg Si au moins, est liée à la densité optique par une fonction linéaire. Calculé au moyen des valeurs de la courbe d'absorption

---

* Mesures dans les conditions de la note de la p. 543.

(Fig. 1), le coefficient d'extinction n'atteint que $1.5 \cdot 10^4$ environ à 220 nm; dans ce cas l'on a mesuré l'absorption de l'acide α-silicomolybdique en solution aqueuse, alors que dans le travail précédent il s'agissait de la forme β.

En conclusion, la nature du milieu à analyser étant réservée, le microdosage du phosphore, de l'arsenic et du silicium serait possible dans l'ultraviolet à l'état d'hétéropolyacides molybdiques, séparés par des solvants appropriés.

Centre d'Etudes Nucléaires de Saclay,
Gif-sur-Yvette (France)

M. JEAN

1 Z. F. SHAKHOVA ET E. N. DOROKHOVA, *Zh. Neorgan. Khim.*, 10 (1965) 2060.
2 S. R. CROUCH ET H. V. MALMSTADT, *Anal. Chem.*, 39 (1967) 1084.
3 S. DUBOIS ET P. SOUCHAY, *Ann. Chim. (Paris)*, 3 (1948) 105 (12 ser.).
4 B. E. REZNIK ET L. P. TSYGANOK, *Zh. Neorgan. Khim.*, 10 (1965) 1914.
5 J. PAUL, *Mikrochim. Acta*, (1965) 830 et 836.
6 J. PAUL, *Anal. Chim. Acta*, 35 (1966) 200.
7 R. B. HESLOP ET E. F. PEARSON, *Anal. Chim. Acta*, 39 (1967) 209.
8 TADASHI HAYAMI ET KATSUHIKO HONJO, *Japan Analyst*, 15 (1966) 816.
9 P. PAKALNS, *Anal. Chim. Acta*, 40 (1968) 1.
10 G. B. SLOANE-STANLEY ET ANAHIB KHEIR ELDIN, *Biochem. J.*, 85 (1961) 40 P.
11 C. H. LUEK ET D. F. BOLTZ, *Anal. Chem.*, 28 (1956) 1168.
12 C. H. LUEK ET D. F. BOLTZ, *Anal. Chem.*, 30 (1958) 183.
13 H. M. THEAKSTON ET W. R. BANDI, *Anal. Chem.*, 38 (1966) 1764.
14 F. UMLAND ET G. WÜNSCH, *Z. Anal. Chem.*, 213 (1966) 186.
15 C. WADELIN ET M. G. MELLON, *Anal. Chem.*, 11 (1953) 1668.
16 V. DJURKIN ET G. F. KIRKBRIGHT, *Analyst*, 91 (1966) 89.
17 W. J. KIRSTEN, *Microchem. J.*, 12 (1967) 307.
18 H. E. GARRETT ET A. J. WALKER, *Analyst*, 89 (1964) 642.
19 Z. F. SHAKHOVA, E. N. DOROKHOVA ET N. K. CHUYAN, *Zh. Analit. Khim.*, 21 (1966) 707.
20 L. TRUDELL ET D. F. BOLTZ, *Anal. Chem.*, 35 (1963) 2122.
21 P. PAKALNS ET W. W. FLYNN, *Anal. Chim. Acta*, 38 (1967) 403.
22 P. PAKALNS, *Anal. Chim. Acta*, 40 (1968) 328.
23 J. PAUL ET W. F. R. POVER, *Anal. Chim. Acta*, 22 (1960) 185.
24 D. R. SCHINK, *Anal. Chem.*, 37 (1965) 764.

(Reçu le 22 janvier, 1968)

Acides hétéropolytungstiques mesurés dans l'ultraviolet

Les hétéropolyacides tungstiques ne sont pas employés pour le dosage des éléments constituant leur atome central, au même titre que les dérivés molybdiques, en raison de l'insolubilisation des polyacides tungstiques résultant de l'acidification.

En bref, l'acidification d'une solution de tungstate de sodium (à pH 8 environ), aboutit successivement aux formes solubles du paratungstate A: $(HW_6O_{21})^{5-}$, vers pH 5.2; puis du ψ-métatungstate (que l'on écrira: $(H_3W_6O_{21})^{3-}$, sans entrer dans la discussion de sa structure); cette forme est stable vers pH 4 à 3 environ; à pH < 2, le trioxyde hydraté précipite. Le métatungstate lui-même, dont la formation est lente, n'intervient vraisemblablement pas[1,2]. L'utilisation des tungstates devrait donc se situer dans des zones de pH telles qu'il n'y ait pas précipitation d'acide tungstique.

La formation de l'acide hétéropolytungstique visé intervient antérieurement à la formation des formes polytungstiques, et non après[1].

L'intérêt analytique de l'acide borotungstique avait été envisagé, en raison de la sensibilité élevée dans l'ultraviolet, analogue à celle propre aux hétéropolyacides, et que semble annoncer la courbe 1 (l'acide boromolybdique n'existe en effet pas).

Acide phosphotungstique

Le phosphore ($\leqslant$ 12 μg P) à l'état de phosphate est traité en milieu perchlorique (0.045 *M*) par le tungstate de sodium (0.022 *M*) dans le rapport $[H^+]/[WO_4^{2-}] = 2$ environ; le milieu résultant est à pH $\leqslant$ 2; la précipitation d'acide tungstique n'apparait pas. Le rapport $[P]/[WO_4^{2-}] = 1/4 \cdot 10^4$ environ. L'acide phosphotungstique est extrait au moyen d'alcool *n*-amylique[3] (3 ml), après centrifugation, il est prélevé de la phase organique (2 ml) que l'on additionne d'alcool absolu (5 ml) et d'eau (pour 10 ml); mesures en cuves de 1 cm (quartz), ouverture 50 μ; la longueur d'onde est 265 à 270 nm, selon le maximum indiqué par les courbes d'absorption (Fig. 1)*. L'alcool *n*-amylique lui-même présente, dans les mêmes conditions de dilution, une densité optique de 0.05, à 265 à 270 nm; elle s'abaisse d'ailleurs uniformément avec la longueur d'onde croissante. Dans les conditions précisées ci-dessus, l'alcool *n*-amylique n'extrait pas d'acides tungstiques. La densité optique est une fonction linéaire de la quantité de phosphore en essai, jusqu'à 8 μg P environ, au minimum.

Calculé au moyen de la quantité de phosphore en solution mesurée, le coefficient d'extinction moléculaire ε s'établit à $4 \cdot 10^4$ à 265–270 nm; à partir de la courbe** obtenue au moyen de l'acide phosphotungstique cristallisé, il s'élève approximativement à la même valeur. On remarque que la mesure sous la forme du phosphotungstate de bismuth–thiourée[6] donnant une coloration jaune sensible, pourrait offrir une augmentation de la sensibilité, si ce n'est que la longueur d'onde à l'optimum de densité optique (320–324 nm) entraîne inversement une diminution de sensibilité: par exemple, la densité optique n'est que 0.4 à 320 nm pour 7.65 μg P; elle a la valeur 0.09 si la mesure porte sur la dilution hydroalcoolique de la phase organique (à comparer avec 0.99 à $\lambda = 265$ à 270 nm (Fig. 2)); ce résultat indique toutefois la réalité de la formation du phosphotungstate de bismuth–thiourée. Si, en vue de tenter de former directement le complexe bismuthique lors de la réaction du phosphate sur le tungstate, l'on introduit non de l'acide perchlorique, mais une solution de bismuth perchlorique de même acidité, la formation de l'acide phosphotungstique est inhibée, alors que celle de l'acide phosphomolybdique a bien lieu dans les mêmes conditions, en la présence même du bismuth[7]. Ainsi, le bismuth n'est pas combiné à l'acide phosphotungstique[8], lui-même moins aisément réductible que l'acide phosphomolybdique.

Les réducteurs utilisés pour ce dernier sont, en général, sans effet sur les acides tungstique et phosphotungstique, et seul le Ti^{3+} en milieu acide, les acides ascorbique et l'hydroquinone en milieu peu acide, réduisent les tungstates, mais sans action préférentielle sur l'acide phosphotungstique; celui-ci et le tungstate sont réduits également. L'acide phosphotungstique formé analytiquement, doit donc être séparé selon indiqué ci-dessus, et la phase organique séparée est réduite par le Ti^{3+}; les

---

* Cette courbe établie à l'aide de l'acide phosphotungstique cristallisé, est sensiblement identique à celles publiées antérieurement[1,2,4,5] et vaut également pour les acides silico- et borotungstiques.

** Figure 1 de la précédente communication concernant les derivés molybdiques.

sensibilités obtenues par mesure des colorations bleues résultantes sont très inférieures à celles que l'on observe par mesure directe dans l'ultraviolet.

L'acide arséniotungstique est formé selon les mêmes lois. Il est extractible par l'acétate d'éthyle; la sensibilité du dosage correspondrait toutefois à un coefficient d'absorption moléculaire de l'ordre du cinquième seulement de celui valant pour le phosphore.

L'acide silicotungstique dont la formation analytique exige un milieu relativement acide, et se trouve donc limitée par la polymérisation et la précipitation des acides tungstiques (pH 1.6), doit être extrait immédiatement par l'alcool *n*-amylique après mise en présence des réactifs. Pour 0.8 mg Si au maximum, sous forme de solution de métasilicate de sodium $SiO_3Na_2 \cdot 5H_2O$, l'acidité perchlorique est $[H^+] = 0.2$ M, et la concentration en tungstate de sodium $[WO_4^{2-}] = 0.05$ M, avec le rapport minimum: $Si/WO_4^{2-} = 1/12$. Après extraction, la phase organique centrifugée est mesurée (cuves de 1 cm quartz, ouverture 50 μ, $\lambda = 263$*), par rapport à l'eau.

La différence de densité optique, sensiblement linéaire en fonction de la quantité de silicium en oeuvre, atteint seulement 0.24 pour 0.8 mg Si; l'acide silicotungstique n'est donc formé qu'en très faible quantité, par la voie analytique.

L'acide borotungstique est formé et isolé difficilement, l'acide ψ-métatungstique paraissant se former par polymérisation de l'acide tungstique d'une part, et par rétrogradation de l'acide borotungstique d'abord formé d'autre part; ce dernier doit donc être extrait rapidement**.

Les doses mises en oeuvre vont jusqu'à 160 μg de bore en essai, sous forme d'acide borique. Pour chaque essai, il doit être mené parallèlement un témoin exempt de bore, et la différence de densité optique est déterminée. L'étude des acides borotungstiques fait l'objet d'un travail de SOUCHAY[9]. Les conditions de formation analytique de l'acide borotungstique sont: acidité perchlorique $[H] = 0.17$ M environ, concentration maximale en acide borique $[B^-] = 0.0022$ M; concentration en tungstate de sodium: $[WO_4^{2-}] = 0.05$ M; le milieu résultant est à pH 1.2 environ. Le solvant ne doit évidemment pas présenter de fonctions alcool libres; l'acétate d'éthyle, dans les conditions de l'essai, a une densité optique de 0.5 à 255 nm. Des solvants autres, les uns: acétate de méthyle, formiates de méthyle, d'éthyle, sont trop solubles dans l'eau, les autres: acétates de propyle, de butyle, n'extraient que pas ou peu, et ont des densités optiques trop élevées. Le mélange réactionnel étant formé, après 15 à 20 sec au plus, est additionné de 3.5 ml d'acétate d'éthyle (préalablement lavé et saturé d'eau); après agitation et décantation, recueil de la phase organique que l'on centrifuge, et l'on mesure la densité optique du témoin et de l'essai (cuves de 1 cm quartz, cuve témoin eau, ouverture 50 μ, $\lambda = 255$ nm***).

La différence de densité optique entre témoin et essai est sensiblement linéaire en fonction de la quantité de bore, mais, relativement faible, s'établit par exemple à 0.12 seulement pour 160 μg de bore, trop petite pour présenter quelque intérêt; résultant de la valeur log $\varepsilon = 3.6$ donnée par courbe (Fig. 1), le coefficient s'élèverait à

---

* Selon la courbe établie à l'aide de l'acide silicotungstique cristallisé et conforme aux données en référence 1 et 2.

** Des tentatives en vue de complexer sélectivement l'acide borotungstique par des substances à fonctions amine ou amino-acides, ou par formation de complexes métal-bore[6], et ainsi de le fixer, n'ont pas abouti.

*** Selon la courbe déterminée au moyen de l'acide synthétisé par la méthode de NIKITINA[10].

environ $4 \cdot 10^4$. De cette différence, il résulte que la formation analytique de l'acide borotungstique est très incomplète; elle parait limitée par la polymérisation de l'acide ψ-métatungstique et CAMPBELL arrive à une telle conclusion[11].

En définitive, seule la mesure dans l'U.V. de l'acide phosphotungstique pourrait présenter quelque intérêt pratique.

Centre d'Etudes Nucléaires de Saclay,
Gif-sur-Yvette (France)

M. JEAN

1 P. SOUCHAY, *Ann. Chim. (Paris)*, 18 (1943) 61, 73, 169.
2 O. GLEMSER, W. HOLZNAGEL, M. HÖLTJE ET E. SCHWARZMANN, *Z. Naturforsch.*, 20 (1965) 725.
3 W. A. JACOBS, *J. Biol. Chem.*, 12 (1912) 429.
4 S. DUBOIS ET P. SOUCHAY, *Ann. Chim. (Paris)*, 3 (1948) 105 (12° ser.).
5 AKIRA OUCHI, HIROSHI MATSUMOTO ET YUKICHI YOSHINO, *Nippon Kagaku Zasshi*, 83 (1962) 955.
6 M. JEAN, *Ann. Chim. (Paris)*, 3 (1948) 470 (12° ser.).
7 M. JEAN, *Anal. Chim. Acta*, 31 (1964) 24.
8 S. A. MALIK ET T. J. R. WEAKLEY, *Chem. Commun.*, (1967) 1094.
9 P. SOUCHAY, *Ann. Chim. (Paris)*, 20 (1945) 96 (12° ser.).
10 E. A. NIKITINA ET O. N. SOKOLOVA, *Zh. Obshch. Khim.*, 27 (1951) 1.
11 R. H. CAMPBELL, *Thèse*, Purdue University, July 1959.

(Reçu le 22 janvier, 1968)

Atomization with heated air for sensitivity enhancement in atomic absorption spectrophotometry

NAKANO AND TAKADA[1] have pointed out that the sensitivity of atomic absorption spectrophotometry for magnesium can be doubled if the air used for atomization of the sample is heated to 100°. RAWSON[2] has studied the use of hot air and coal gas at an atomizer temperature of 55° in the determination of zinc, copper, manganese and calcium and has claimed useful increases in sensitivity. However, the scope of this enhancement technique for other elements does not appear to have been studied. We have investigated the increase in sensitivity obtained by using air at 100° instead of at 20° for 14 elements, both in aqueous and 90% acetone[3] media. When appropriate, the *n*-amyl methyl ketone (AMK) solutions of the pyrollidine dithiocarbamate complexes (APDC) have also been examined.

A Techtron AA-4 atomic absorption spectrophotometer was used in the investigation; the settings for the hollow-cathode lamps, burner and spectrophotometer were those recommended by the manufacturer. Hot air for the atomizer was supplied from a preheater which consisted of a 7-m helix of 6.3-mm bore stainless steel tubing wrapped with a 300-W heating tape and contained in an insulated box. The heat input was controlled by a variable transformer. The temperature of the air passing to the atomizer was measured by means of a thermistor and associated bridge circuit. The concentrations of the solutions of the various elements were adjusted so that they lay within the linear region of the calibration curve in all the solvents at both 20° and 100°.

It was found (Table I) that the use of heated air in the atomizer enhances the

TABLE I

ATOMIC ABSORPTION ENHANCEMENT FACTORS

Element	*Fuel gas*	*Solvent enhancement*[a]		*Thermal enhancement*[b]			*Total enhancement*[c]	
		90% Acetone	*APDC in AMK*	*Aqueous*	*90% Acetone*	*APDC in AMK*	*90% Acetone*	*APDC in AMK*
Cadmium	Coal gas	3.7	2.3	1.4	1.4	1.5	5.2	3.5
Calcium	Acetylene	0.5	—	1.3	1.6	—	2.6	—
Chromium	Acetylene	3.3	—	2.6	0.5	—	1.6	—
Cobalt	Coal gas	2.7	1.8	1.3	1.8	2.3	4.9	4.1
Copper	Coal gas	3.8	2.3	2.1	1.9	1.8	7.2	4.1
Iron	Coal gas	3.7	2.3	2.0	2.5	2.0	9.2	4.6
Lead	Coal gas	1.6	2.4	1.4	1.8	1.6	2.9	3.8
Magnesium	Acetylene	2.5	—	2.3	3.0	—	7.5	—
Manganese	Acetylene	3.0	—	1.0	1.1	—	3.3	—
Nickel	Coal gas	3.1	1.8	1.7	2.0	1.9	6.2	3.4
Silver	Coal gas	5.3	2.9	1.2	1.5	2.1	7.9	6.1
Strontium	Acetylene	1.1	—	1.5	1.0	—	1.1	—
Tin	Acetylene	1.6	1.0	1.6	1.8	1.4	2.9	1.4
Zinc	Coal gas	3.0	2.0	1.5	1.5	1.4	4.5	2.8

[a] Absorbance in selected solvent/absorbance in aqueous medium.
[b] Absorbance at 100°/absorbance at 20° in same solvent.
[c] Absorbance at 100° in chosen solvent/absorbance at 20° in aqueous medium.

absorption with most elements, in favourable instances by up to 3-fold. When heated air is used in conjunction with organic solvents, the sensitivity over aqueous media is increased up to 9-fold. Unfortunately, because of the use of different spectrophotometers, it is not possible to compare the enhancement found in the present work with that obtained by RAWSON[2].

The enhancement obtained by using heated air is probably caused partly by the greater efficiency of atomization, and partly by the greater flame temperature. However, other factors are almost certainly operative.

Department of Oceanography,
The University, Liverpool 3 (Great Britain)

J. P. RILEY
D. TAYLOR

1 K. NAKANO AND T. TAKADA, *Nippon Kagaku Zasshi*, 88 (1967) 109.
2 R. A. G. RAWSON, *Analyst*, 91 (1966) 630.
3 J. P. RILEY AND D. TAYLOR, *Anal. Chim. Acta*, 40 (1968) 479.

(Received April 17th, 1968)

BOOK REVIEW

Progress in Nuclear Resonance Spectroscopy, Vol. 3, Edited by J. W. EMSLEY, J. FEENEY AND L. H. SUTCLIFFE. Pergamon Press, Oxford, 1967, vi + 419 pp., price 140 s.

This volume contains six separate articles dealing with spectral analysis (62 pp.), the isotope shift (24 pp.), nuclear spin relaxation studies of molecules on surfaces (42 pp.), relaxation processes in systems of two non-identical spins (30 pp.), microdynamic behaviour of liquids as studied by NMR relaxation times (72 pp.) and finally solvent effects and nuclear magnetic resonance (172 pp.).

The chapters are naturally written for the NMR specialists although the analyst will find the first and last chapter of some considerable use. It will be seen, from the number of pages devoted to each topic, that nearly half the book is devoted to solvent effects. The reference list for each chapter is extensive.

E. F. MOONEY (Birmingham)

Anal. Chim. Acta, 42 (1968) 550

ANOUNCEMENT

PRELIMINARY ANNOUNCEMENT OF 1969 PITTSBURGH CONFERENCE

The Twentieth Pittsburgh Conference on Analytical Chemistry and Applied Spectroscopy, Inc., will be held in Cleveland, Ohio, U.S.A., March 2–7, 1969. The headquarters for the meeting will be the Cleveland Convention Center. An estimated 300 papers on all phases of Analytical Chemistry and Spectroscopy will be presented. Symposia on the following subjects are now being arranged.

1. Analytical techniques on the horizon,
2. SSP award symposium on emission spectroscopy,
3. Computer interfacing with analysis,
4. Spectroscopic analysis of glasses and oxides,
5. Spark source mass spectroscopy,
6. Analysis – food and agricultural chemicals,
7. Coblentz symposium on infrared spectroscopy,
8. Specific ion electrodes,
9. Nuclear magnetic resonance in solids.

Papers are not restricted to the symposium subjects and original papers on all phases of analytical chemistry and spectroscopy are invited. Authors who wish to present papers at the 1969 Pittsburgh Conference should submit three copies of a 150 word abstract and include the names and addresses of the authors, and the name of the laboratory in which the work was done. Abstracts should be sent to: WILLIAM M. HICKAM, Westinghouse Research Laboratories, Pittsburgh, Pa. 15235, U.S.A. The final date for receipt of abstracts is October 15, 1968.

In addition to the program of technical papers, there will be an exhibition of the newest analytical instrumentation. More than 200 companies will display instruments, chemicals, and equipment. A complete program of activities for wives and lady attendees at the Conference is also being planned for the 1969 Pittsburgh Conference.

1969 Pittsburgh Conference Chairman G. L. CARLSON and Exposition Chairman W. G. FATELEY, Carnegie-Mellon University, Mellon Institute, Pittsburgh, Pa. 15213, U.S.A.

Anal. Chim. Acta, 42 (1968) 550

ANALYTICA CHIMICA ACTA VOL. 42 (1968)
AUTHOR INDEX

ANALYTICA CHIMICA ACTA VOL. 42 (1968)

SUBJECT INDEX

VOL. 42 NO. 3 ANALYTICA CHIMICA ACTA SEPTEMBER 1968

CONTENTS

(continued on page 4 of cover)

(contents, continued from page 3 of cover)

Short communications
